THÈSE EN COTUTELLE PRÉSENTÉE

POUR OBTENIR LE GRADE DE

DOCTEUR DEL'UNIVERSITE DE BORDEAUX

ET DE L'UNIVERSITÉ DE CATANIA

ÉCOLE DOCTORALE DES SCIENCES DE LA VIE ET DE LA SANTÉ

SPÉCIALITÉ-NEUROSCIENCES

PAR TOMMASO DALLA TOR

LA SIGNALISATION DU RECEPTEUR CANNABINOÏDE DE TYPE-1 ET SON ROLE DANS LA REGULATION DE LA DYNAMIQUE DU LACTATE CEREBRAL CHEZ LA SOURIS EN LIBRE MOUVEMENT

Sous la direction de Giovanni Marsicano et de Filippo Drago

Soutenue le 18/02/2026

Membres du jury :

M. Riccardo Brambilla	University of Pavia	Examinateur
M. Marco Riva	University of Milano	Examinateur
M. Roberto Ciccocioppo	University of Camerino	Examinateur
M. Manuel Guzman	University of Madrid	Rapporteur
M. Edgar Soria-Gómez	Achucarro Basque Center for Neuroscience	Rapporteur

DEPARTMENT OF DOCTORAL SCHOOL OF HEALTH AND LIFE SCIENCES
PH.D. SCHOOL IN NEUROSCIENCE

Tommaso Dalla Tor

CANNABINOID TYPE-1 RECEPTOR SIGNALLING AND ITS ROLE IN REGULATING BRAIN LACTATE DYNAMICS IN FREELY MOVING MICE

Tutor: Giovanni Marsicano
Co-Tutor: Filippo Drago

Date of defence: 18/02/2026

Members of jury:

M. Riccardo Brambilla	University of Pavia	Examinateur
M. Marco Riva	University of Milano	Examinateur
M. Roberto Ciccocioppo	University of Camerino	Examinateur
M. Manuel Guzman	University of Madrid	Rapporteur
M. Edgar Soria-Gómez	Achucarro Basque Center for Neuroscience	Rapporteur

Academic Year 2025/2026

ABSTRACT

The brain is one of the most active metabolic organs in the body. Despite accounting for only ~2% of total body weight, it consumes up to 20% of the body's energy. This energy is primarily derived from glucose metabolism, which produces both ATP and lactate. In the central nervous system (CNS), astrocytes are the main source of lactate, generated mostly via aerobic glycolysis. Neurons, in contrast, rely largely on oxidative phosphorylation for ATP production and preferentially utilize lactate as an energy substrate in a process known as the astrocyte-to-neuron lactate shuttle (ANLS). Beyond its metabolic role, lactate also functions as a key signalling molecule involved in neuronal plasticity, memory, and behavioural regulation. However, the mechanisms controlling lactate production and release in the brain remain poorly understood.

Recent findings have implicated the cannabinoid receptor type 1 (CB1R) in the regulation of astrocytic metabolism. Persistent activation of astroglial mitochondrial CB1Rs (mtCB1Rs) for 24 hours has been shown to suppress lactate production. In contrast, our recent work reveals that transient (5 minutes) stimulation of CB1Rs in astrocytes triggers a transient increase in lactate levels. While these effects have been observed *in vitro*, the impact of CB1R activation on brain lactate dynamics *in vivo* has yet to be directly examined.

In this thesis, we address this gap using fiber photometry (FP) and eLACCO2.1, a genetically encoded fluorescent biosensor for extracellular lactate. We successfully established a protocol to monitor lactate dynamics in freely moving mice and validated the responsiveness of the sensor to exogenous lactate administration. Our *in vivo* experiments revealed that lactate levels are modulated not only by cannabinoid exposure but also by behavioural state, particularly locomotor activity. Specifically, we observed brain region-specific patterns in lactate fluctuations during periods of immobility and following Δ^9-THC administration, suggesting that CB1R activation alters the timing and dynamics of lactate regulation in a circuit-dependent manner.

In parallel, we investigated the intracellular signalling mechanisms underlying CB1R-dependent regulation of lactate in cultured astrocytes, with a particular focus on the switch between the transient and persistent effects induced by WIN55 stimulation. Using the broad PKC inhibitor Go 6983, we found that PKC activity is required for both the transient lactate increase and the later suppression induced by CB1R stimulation. Blocking PKC abolished both

effects, indicating that it serves as a critical molecular switch within the CB1R-lactate signalling axis. Interestingly, a progressive accumulation of lactate was observed when PKC was inhibited in the presence of CB1R activation. Control experiments with PKC inhibition alone did not show changes in baseline lactate levels, although technical limitations prevented full quantification.

Together, these findings establish a new *in vivo* method for studying lactate dynamics in freely moving mice, demonstrate that Δ^9-THC alters brain lactate dynamics specifically during periods of immobility, suggesting that CB1R signalling reshapes neurometabolic responses in relation to behavioural state and brain region, and uncover a previously not fully characterized role for PKC in astrocyte metabolic regulation. This work advances our understanding of the complex interplay between cannabinoid signalling, astrocyte function and behaviour, and sets the stage for future studies into the neurometabolic consequences of CB1R activity.

RÉSUMÉ

Le cerveau est l'un des organes les plus actifs sur le plan métabolique. Bien qu'il ne représente qu'environ 2 % du poids corporel total, il consomme jusqu'à 20 % de l'énergie de l'organisme. Cette demande énergétique est principalement satisfaite par le métabolisme du glucose, qui produit à la fois de l'ATP et du lactate. Dans le système nerveux central (SNC), les astrocytes constituent la principale source de lactate, généré majoritairement via la glycolyse aérobie. Les neurones, en revanche, dépendent largement de la phosphorylation oxydative pour la production d'ATP et utilisent préférentiellement le lactate comme substrat énergétique dans un processus connu sous le nom de navette lactate astrocyte-neurone (ANLS). Au-delà de son rôle métabolique, le lactate agit également comme une molécule de signalisation essentielle impliquée dans la plasticité neuronale, la mémoire et la régulation du comportement. Pourtant, les mécanismes qui contrôlent la production et la libération de lactate dans le cerveau restent mal compris.

Des travaux récents ont mis en évidence le rôle du récepteur cannabinoïde de type 1 (CB1R) dans la régulation du métabolisme astrocytaire. Une activation persistante des CB1Rs mitochondriaux (mtCB1Rs) astrogliaux pendant 24 heures entraîne une diminution de la production de lactate. En revanche, nos travaux récents ont montré qu'une stimulation brève (5 minutes) des CB1Rs dans les astrocytes induit une augmentation transitoire des niveaux de lactate. Bien que ces effets aient été observés in vitro, l'impact de l'activation des CB1Rs sur les dynamiques de lactate cérébral in vivo n'a pas encore été examiné de manière directe.

Dans ce travail de thèse, nous avons abordé cette question en utilisant la fibre photométrie (FP) et eLACCO2.1, un biosenseur fluorescent génétiquement codé, permettant la détection du lactate extracellulaire. Nous avons établi un protocole permettant de mesurer les dynamiques du lactate chez des souris libres de leurs mouvements et validé la sensibilité du capteur à l'administration de lactate exogène. Nos expériences in vivo ont révélé que les niveaux de lactate sont modulés non seulement par l'exposition aux cannabinoïdes, mais également par l'état comportemental, en particulier l'activité locomotrice. Plus précisément, nous avons observé des fluctuations spécifiques à certaines régions cérébrales lors des phases d'immobilité et après l'administration de Δ^9-THC, suggérant que l'activation des CB1Rs modifie la temporalité et la dynamique de la régulation du lactate de manière dépendante du circuit neuronal.

Parallèlement, nous avons étudié les mécanismes de signalisation intracellulaire impliqués dans la régulation du lactate dépendante des CB1Rs dans des astrocytes en culture, en nous concentrant particulièrement sur la transition entre les effets transitoires et persistants induits par la stimulation au WIN55. En utilisant l'inhibiteur large spectre de la PKC, Go 6983, nous avons montré que l'activité de la PKC est indispensable tant pour l'augmentation transitoire du lactate que pour la suppression prolongée induite par l'activation des CB1Rs. Le blocage de la PKC a aboli ces deux effets, indiquant que cette kinase joue un rôle de commutateur moléculaire essentiel dans l'axe de signalisation CB1R–lactate. Fait intéressant, une accumulation progressive de lactate a été observée lorsque la PKC était inhibée en présence de l'activation des CB1Rs. Les expériences de contrôle avec inhibition de la PKC seule n'ont pas montré de modifications des niveaux basaux de lactate, bien que des limitations techniques aient empêché une quantification complète.

Ensemble, ces résultats établissent une nouvelle méthode in vivo pour l'étude des dynamiques du lactate chez l'animal en mouvement libre, montrent que le Δ^9-THC modifie les dynamiques de lactate cérébral spécifiquement pendant les phases d'immobilité, et mettent en lumière un rôle encore mal caractérisé de la PKC dans la régulation métabolique astrocytaire. Ce travail enrichit notre compréhension des interactions complexes entre la signalisation cannabinoïde, la fonction des astrocytes et le comportement locomoteur, et ouvre la voie à de futures recherches sur les conséquences neurométaboliques de l'activité des CB1Rs.

LIST OF PUBLICATIONS

1. Mariani, Y., Dalla-Tor, T., Garavaldi, T., Julio-Kalajzić, F., Gisquet, D., Gomez-Sotres, P., Cannich, A., Gambino, G., Drago, F., Serrat, R., Hurel, I., Chaouloff, F., Pouvreau, S., Bellocchio, L., Marsicano, G., & Covelo, A. (2025). Astroglial CB1 Reveal Sex-Specific Synaptic Effects of Amphetamine. Glia, 73(8), 1673. https://doi.org/10.1002/GLIA.70026

2. Fernandez Moncada I., Eraso-Pichot A., Dalla Tor T., Fortunato-Marsol B., & Marsicano G., (2023). An enquiry to the role of CB1 receptors in neurodegeneration. Neurobiology of Disease. Aug:184:106235. https://doi:10.1016/j.nbd.2023.106235

3. Fernández-Moncada, I., Lavanco, G., Fundazuri, U. B., Bollmohr, N., Mountadem, S., Dalla Tor, T., Hachaguer, P., Julio-Kalajzic, F., Gisquet, D., Serrat, R., Bellocchio, L., Cannich, A., Fortunato-Marsol, B., Nasu, Y., Campbell, R. E., Drago, F., Cannizzaro, C., Ferreira, G., Bouzier-Sore, A. K., … Marsicano, G. (2024). A lactate-dependent shift of glycolysis mediates synaptic and cognitive processes in male mice. Nature Communications, 15(1). https://doi.org/10.1038/S41467-024-51008-2

4. Gómez-Sotres, P., Skupio, U., Dalla Tor, T., Julio-Kalajzic, F., Cannich, A., Gisquet, D., Bonilla-Del Rio, I., Drago, F., Puente, N., Grandes, P., Bellocchio, L., Busquets-Garcia, A., Bains, J. S., & Marsicano, G. (2024). Olfactory bulb astrocytes link social transmission of stress to cognitive adaptation in male mice. Nature Communications, 15(1). https://doi.org/10.1038/S41467-024-51416-4

5. Gómez-Sotres, P, Welte J., Dalla Tor T., Rodrigues S. R., Marsicano G. (2025). Handbook of Endocannabinoid Function in the Central Nervous System. Chapter 5: Cannabinoid modulation of brain mitochondria. Handbook of Endocannabinoid Function in the Central Nervous System. https://doi.org/10.1016/B978-0-443-13908-6.00008-6. In press.

6. Eraso-Pichot A., Baraibar AM., Olivera-Pinto A., Dalla Tor T., Garavaldi T., Fernández-Moncada I., Kedziora M., Bellocchio L., Serrat R., Beriain S., Matias I., Cannich A., Mato S., Marsicano G. Specialized cannabinergic astrocytes mediate endocannabinoid functions in mice. In submission.

ABBREVIATIONS

2-AG: 2-Arachidonoylglycerol

AA: Arachidonic Acid

AC: Adenylate Cyclase

ACAT-1: Acetyl-CoA Acetyltransferase 1

AcAc: Acetoacetate

ADP: Adenosine Diphosphate

AEA: Anandamide (N-arachidonoylethanolamide)

AMPK: AMP-Activated Protein Kinase

ANLS: Astrocyte-Neuron Lactate Shuttle

ATP: Adenosine Triphosphate

BBB: Blood Brain Barrier

BDNF: Brain-Derived Neurotrophic Factor

BHB: β-Hydroxybutyrate

Ca^{2+}: Calcium Ion

CBD: Cannabidiol

CCK+: Cholecystokinin-positive neurons

CNS: Central Nervous System

COX-2: Cyclooxygenase-2

CPT-1: Carnitine Palmitoyltransferase 1

cAMP: Cyclic Adenosine Monophosphate

Cyt c: Cytochrome c

CUD: Cannabis Use Disorder

DAG: Diacylglycerol

DAGLα/β: Diacylglycerol Lipase alpha/beta

ECS: Endocannabinoid System

ETC: Electron Transport Chain

ER: Endoplasmic Reticulum

FAO: Fatty Acid Oxidation

FABPs: Fatty Acid Binding Proteins

FAAH: Fatty Acid Amide Hydrolase

FBS: Fetal Bovine Serum

FP: Prostaglandin F2α Receptor (FP receptor)

G-6-P: Glucose-6-Phosphate

GDE1: Glycerophosphodiester Phosphodiesterase 1

GLUTs: Glucose Transporters

GPCRs: G Protein-Coupled Receptors

GPR55: G Protein-Coupled Receptor 55

GSH: Reduced Glutathione

GSSG: Oxidized Glutathione (Glutathione Disulphide)

H2O2: Hydrogen Peroxide

HBP: Hexosamine Biosynthetic Pathway

HCAR1: Hydroxycarboxylic Acid Receptor 1 (GPR81)

HDACs: Histone Deacetylases

HIF-1α: Hypoxia-Inducible Factor 1-alpha

HK: Hexokinase

IP3: Inositol 1,4,5-trisphosphate

ISH: In Situ Hybridization

K^{+}: Potassium Ion

LTP: Long-Term Potentiation

MAGL: Monoacylglycerol Lipase

MAPK: Mitogen-Activated Protein Kinase

MCU: Mitochondrial Calcium Uniporter

MCT: Monocarboxylate Transporter

MRC: Mitochondrial respiratory chain

MERCs: Mitochondria–Endoplasmic Reticulum Contacts

mtCB1R: Mitochondrial Cannabinoid Receptor Type 1

NAAA: N-Acylethanolamine Acid Amidase

NADH: Nicotinamide Adenine Dinucleotide (reduced form)

NADPH: Nicotinamide Adenine Dinucleotide Phosphate (reduced form)

Na^+: Sodium Ion

NAPE-PLC: N-acyl-phosphatidylethanolamine-specific Phospholipase C

NAPE-PLD: N-acyl-phosphatidylethanolamine-specific Phospholipase D

NVU: Neurovascular Unit

O_2: Molecular Oxygen

PDH: Pyruvate Dehydrogenase

PDKs: Pyruvate Dehydrogenase Kinases

PFK-1: Phosphofructokinase-1

PIP2: Phosphatidylinositol 4,5-bisphosphate

PK: Pyruvate Kinase

PLC: Phospholipase C

PLCβ: Phospholipase C beta

pmCB1R: Plasma Membrane Cannabinoid Receptor Type 1

PPP: Pentose Phosphate Pathway

ROS: Reactive Oxygen Species

SCN: Suprachiasmatic Nucleus

SCOT: Succinyl-CoA:3-Ketoacid CoA Transferase

SGLTs: Sodium-Glucose Linked Transporters

SNr: Substantia Nigra pars Reticulata

TCA: Tricarboxylic Acid Cycle (Krebs Cycle)

TRPM8: Transient Receptor Potential Melastatin 8

TRPVs: Transient Receptor Potential Vanilloid Channels

Veh: Vehicle

VRAC: Volume-Regulated Anion Channel

α-KG: Alpha-Ketoglutarate

Δ^9-THC: Delta-9-Tetrahydrocannabinoli

Δ^9-THCA: Delta-9-Tetrahydrocannabinolic Acid

INDEX

ABSTRACT III

RÉSUMÉ V

LIST OF PUBLICATIONS VII

ABBREVIATIONS VIII

INTRODUCTION 1

1. Brain energy metabolism: an overview 2

1.1. Glucose metabolism 3

1.2. Metabolic compartmentalization 13

2. Astrocytes 14

2.1. Astrocytic regulation of extracellular environment 16

2.2. Astrocyte-mediated synaptic signalling 18

2.3. Neurovascular coupling and cerebral blood flow regulation 19

2.4. Astrocytes and brain bioenergetics 20

2.5. Astrocyte functions are coordinated by specific signalling systems 24

3. Brief overview of the endocannabinoid system 25

3.1. ECS ligands: cannabinoids 27

3.2. Cannabinoid receptors 33

3.3. CB1R modulation of brain function & behaviour 36

OBJECTIVES 45

MATERIALS AND METHODS 47

1. Animals 48

In vitro 48

2. Primary mixed cortical brain cell cultures 48

3. HEK293T cultures 49

4. Drug preparation and administration 49

5. Fluorescence imaging 49
In vivo 50
6. Adeno-associated viruses (AAV) 50
7. Surgery for viral injection and optic fiber implantation 51
8. Pharmacological treatment of mice 51
9. Behavioural analyses 52
Locomotion and fiber photometry recordings 52
Δ^9-THC-induced tetrad assay 53
10. Histology 54
Mice perfusion 54
Double immunofluorescence 54
11. Statistical analysis 54
RESULTS 57
PART 1 - A lactate-dependent shift of glycolysis mediates synaptic and cognitive processes in male mice 58
PART 2 – Unpublished data: In vivo imaging of CB1-dependent modulation of brain metabolism 119
Chapter I. Development of a reliable protocol for *in vivo* lactate measurement using eLacco2.1 in freely moving mice. 120
Chapter II. Investigation of the impact of locomotion on brain lactate levels across different brain regions. 123
Chapter III. Contribution of lactate to the locomotor effects of cannabinoids. 131
Chapter IV. Exploration of the molecular mechanisms underlying CB1R-dependent lactate modulation in cultured astrocytes. 133
DISCUSSION 135
Chapter I. Development of a reliable protocol for *in vivo* lactate measurements using eLacco2.1 in freely moving mice. 136
Chapter II. Investigation of the impact of locomotion on brain lactate levels across different brain regions. 137

Chapter III. Contribution of lactate to the locomotor effects of cannabinoids. 141

Chapter IV. Exploration of the molecular mechanisms underlying CB1R-dependent lactate modulation in cultured astrocytes. 142

REFERENCES 146

List of figures

Figure 1. Compartmental glucose dynamics in the neuropil. 5
Figure 2. Simplified overview of the major metabolic pathways in the brain. 6
Figure 3. Schematic representation of the MRC and OXPHOS. 11
Figure 4. Astrocytic modulation of neurotransmission and synaptic plasticity. 17
Figure 5. Illustration of the ANLS model. 22
Figure 6. Schematic representation of endocannabinoid signalling across tripartite synapse. 27
Figure 7. Example of the 4 different classes of cannabinoids. 28
Figure 8. Distribution of CB1 receptors expression in the CNS of adult mice. 34
Figure 9: CB1 activation in astrocytes modulates Ca^{2+} dynamics, ROS production and glucose metabolism affecting neuronal functioning. 42
Figure M1. Addgene full sequence map for pAAV-CAG-eLACCO2.1. 50
Figure M2. Schematic representation of setup of a generic rodent in vivo FP experiment. 53
Figure R1. In vitro Determination of eLACCO2.1 isosbestic point. 121
Figure R2. FP recording of eLACCO2.1 signal in freely moving mice. 122
Figure R3. CAG promoter-mediated expression of eLACCO2.1 in the hippocampus. 123
Figure R4. Representative trace of FP eLACCO2.1 recordings in a freely moving mouse. . 124
Figure R5. Hippocampal lactate levels before and during immobility in vehicle or Δ⁹-THC treated mice. 126
Figure R6. Striatal lactate levels before and during immobility in vehicle or Δ⁹-THC treated mice. 128
Figure R7. SNr lactate levels before and during immobility in veh or Δ⁹-THC treated mice. 130
Figure R8. Lactate treatments did not rescue the hypo-locomotive effect of Δ⁹-THC. 132
Figure R9. PKC inhibition abolishes both transient and persistent effects of CB1R activation on astrocytic lactate levels. 134

INTRODUCTION

1. Brain energy metabolism: an overview

The brain is widely regarded as one of the most important and complex organs in the body. Despite representing only 2% of the total body weight, the brain requires a big amount of energy in order to perform its physiological functions. Indeed, the brain accounts for approximately 20% of the body's total oxygen (O_2) consumption and about 25% of its total glucose utilization (Bélanger et al., 2011; Magistretti & Allaman, 2013). This high metabolic demand likely arises from the brain complex structural organization, composed of heterogeneous cell populations organized into highly intricate signalling networks, whose activity modulate a vast array of functions that regulates diverse bodily functions (Bullmore & Sporns, 2012; Suárez et al., 2020).

Interestingly, unlike other high-energy-demanding tissues such as muscle or liver, the brain has minimal energy reserves, which are insufficient to sustain normal functions for extended periods of time in absence of the continuous blood-borne energy supply (Barros et al., 2007; Bélanger et al., 2011; Mergenthaler et al., 2013; S. Zhang et al., 2021). As a result, the brain is extremely sensitive to energy deprivation, a vulnerability that becomes evident during conditions such as hypoxia or hypoglycaemia, which rapidly disrupt neural function and can lead to coma (Brownlee et al., 2020; Cryer, 2007). These observations underscore the critical importance of a continuous and stable supply of energy substrates, particularly O_2 and glucose, to meet the substantial metabolic demands of the brain (Madrer et al., 2025).

This supply is tightly regulated by specialized barrier structures at the blood–neural interfaces, most notably the blood–brain barrier (BBB) (Abbott et al., 2010; Alahmari, 2021). The BBB enables precise regulation of ions and metabolites diffusion while also serving as a protective barrier against pathogens and toxins. This regulation is achieved through the formation of a tightly controlled neurovascular unit (NVU), composed of endothelial cells, pericytes, and astrocytes. These cellular components work together to maintain the chemical stability of the neural environment, ensuring proper brain function (Abbott, 2013; Alahmari, 2021). Its selective permeability allows the controlled passage of specific metabolites, ions, and hormones necessary for brain function, while restricting the entry of others. For instance, glutamate, an abundant amino acid in the bloodstream, is largely excluded from entering the brain, while a unidirectional efflux mechanism facilitates its transport from the brain to the blood (Bai & Zhou, 2017; Daneman & Prat, 2015; Leibowitz et al., 2012). Consequently, since the brain lacks direct access to circulating glutamate and other peripheral metabolites, it must synthesize these compounds *de novo*. This local biosynthesis primarily relies on glucose as a carbon source,

although alternative fuels such as lipids might also contribute (Schousboe et al., 2014; Weber & Barros, 2015). To meet the dual demands of continuous energy supply and localized *de novo* synthesis of signalling molecules and metabolic intermediates, the brain has developed intricate intercellular metabolic networks. These networks coordinate the compartmentalization and distribution of metabolic tasks among different cell types to ensure adequate availability of both energy and biosynthetic substrates (Weber & Barros, 2015).

In the following sections of this introduction, I will first examine in detail how glucose is utilized in the brain, followed by an overview of its principal metabolic pathways. Then, I will explore the cellular and compartmental specialization of the brain, with a particular focus on the dynamic interplay between astrocytes and neurons in regulating metabolic processes, supporting brain function, and influencing behaviour.

1.1. Glucose metabolism

Brain energy metabolism functions as a highly dynamic and tightly regulated network that maintains a precise balance between energy production and consumption via a series of interconnected molecular pathways. As previously mentioned, glucose is an obligatory energy substrate for the brain, and ~25% of total body glucose consumption is dedicated to fulfilling its energetic requirements. (Bélanger et al., 2011). Of note, and under certain conditions, the brain can utilize alternative energy sources, such as ketone bodies during development or in times of starvation, and lactate during intense physical exertion. (Magistretti & Allaman, 2013; Nehlig, 2004; Van Hall et al., 2009).

Glucose metabolism supplies the energy necessary for normal brain function by generating adenosine triphosphate (ATP), the fundamental energy currency of all cells, and as well the synthesis of key neurotransmitters and other metabolites necessary for signalling. Therefore, strict regulation of glucose metabolism is imperative for sustaining brain physiology. Disruptions in this metabolic balance have been implicated in a range of diseases, affecting not only brain function but also systemic homeostasis (Madrer et al., 2025).

1.1.1. Glucose transporters

Once transported from the bloodstream across the BBB, glucose enters brain cells via two primary transporter families: facilitative glucose transporters (GLUTs) and sodium-dependent glucose transporters (SGLTs) (Devraj et al., 2011; Koepsell, 2020). GLUTs belong to the SLC2A family of sodium-independent facilitative hexose transporters, which comprises 14 members: GLUT1-GLUT14, numbered according to their order of discovery (Pragallapati &

Manyam, 2019). However, in the brain the most relevant are GLUT1, GLUT3 and GLUT4. GLUT1, encoded by the SLC2A1 gene, is predominantly expressed in astrocytes, oligodendrocytes and endothelial cells of the BBB. Of note, GLUT1 expression is regulated at both the transcriptional and post-transcriptional levels in response to circulating glucose concentrations (Benarroch, 2014). The localization of GLUT1 in both endothelial cells and astrocytes facilitates the delivery of blood-borne glucose into the brain (Fig. 1). Indeed, more than 90% of the total glucose transport across the BBB is mediated by GLUT1, making it the main route for glucose entry in the brain parenchyma (Boado et al., 1999). Consistent with its localization, GLUT1 primarily mediates glucose uptake into astrocytes, supporting both metabolic and antioxidant functions that are essential for maintaining neuronal health (Pragallapati & Manyam, 2019). Given its critical role in mediating glucose transport across the BBB, GLUT1 deficiency in the brain can result in severe neurological impairments. One such condition is GLUT1 Deficiency Syndrome, a rare genetic disorder first described by De Vivo et al. in 1991. It results from loss-of-function mutations in the GLUT1 SLC2A1 gene and its clinical manifestations include developmental encephalopathy characterized by infantile-onset refractory epilepsy with important seizures, developmental delay, cognitive impairment, and motor abnormalities such as spasticity, ataxia, dystonia, and epilepsy. Additional features may include acquired microcephaly and hypotonia (De Vivo et al., 1991).

GLUT3 instead is the primary glucose transporter in neurons (Fig. 1) (Nagamatsu et al., 1992). Between all the GLUTs, GLUT3 is the one that uptakes glucose with higher affinity (I. A. Simpson et al., 2007). It is encoded by the SLC2A3 gene (Kayanos et al., 1988) and is predominantly expressed in grey matter, with much lower expression in white matter. This distribution suggests that GLUT3 plays a key role in supplying glucose to regions of high metabolic activity. (Haber et al., 1993). It is located primarily on axons and dendrites where it ensures a continuous and efficient supply to neurons even under conditions of glucose shortage due to its high affinity for glucose (Liang et al., 2018).

While GLUT1 and GLUT3 are constitutively expressed at cell membranes, GLUT4, best known as the insulin-responsive glucose transporter, is translocated to the membrane in response to insulin signalling (McNay & Pearson-Leary, 2019; Pearson-Leary & McNay, 2016). It plays a significant role in cognitive and memory-related functions, including hippocampal memory processing and is thought to support GLUT3 during periods of elevated neuronal activity or metabolic demand, such as during learning, memory formation, or

sustained synaptic transmission (Albaik et al., 2024; McNay & Pearson-Leary, 2019; Pearson-Leary & McNay, 2016).

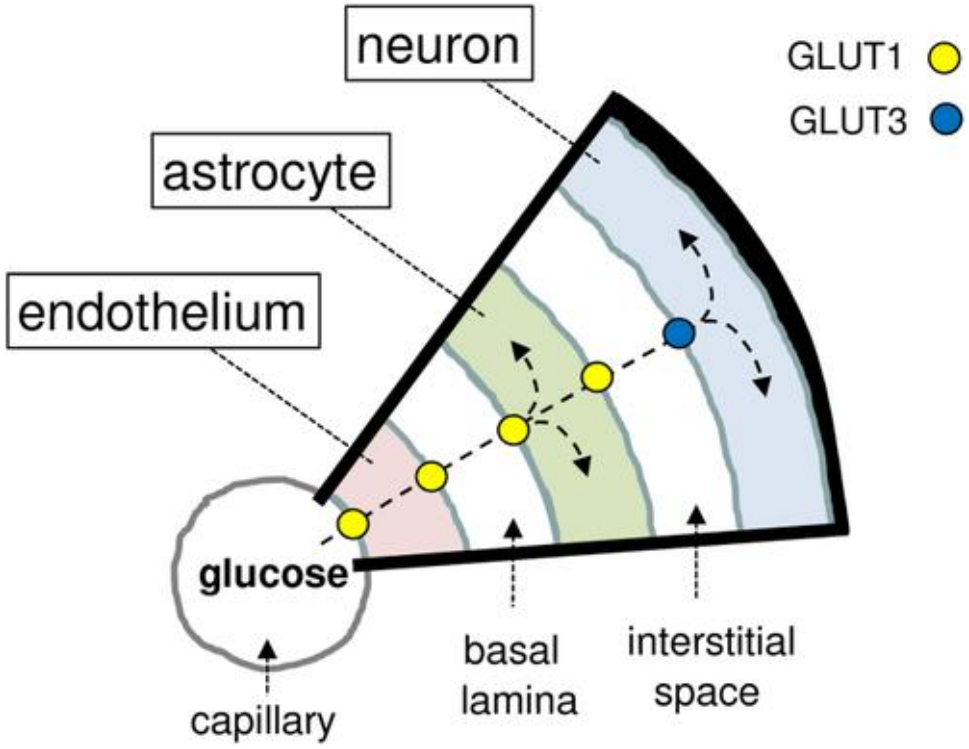

Figure 1. Compartmentalized glucose dynamics in the neuropil.
Glucose crosses the capillary endothelium via the facilitative glucose transporter GLUT1 and then enters astrocytes also via GLUT1. Astrocytes metabolize some glucose and export the remaining fraction to be internalized via GLUT3 and metabolized by neurons. The driving force for the flux of glucose into the brain is glucose metabolism. Figure from (Barros et al., 2017).

Beyond GLUT transporters, endothelial cells at the BBB also express SGLTs, which mediate glucose uptake by coupling it to the inward sodium gradient, enabling transport against the glucose concentration gradient. SGLT1 and SGLT2 are detected in select regions of the CNS, including the brainstem, where they are thought to contribute to glucose sensing and the regulation of systemic energy balance. In contrast, SGLT3 does not function as a classical glucose transporter, instead, it acts as a glucose sensor, modulating neuronal excitability in response to extracellular glucose levels (Mei et al., 2024; Wright & Loo, 2020).

1.1.2. Major metabolic fates of glucose

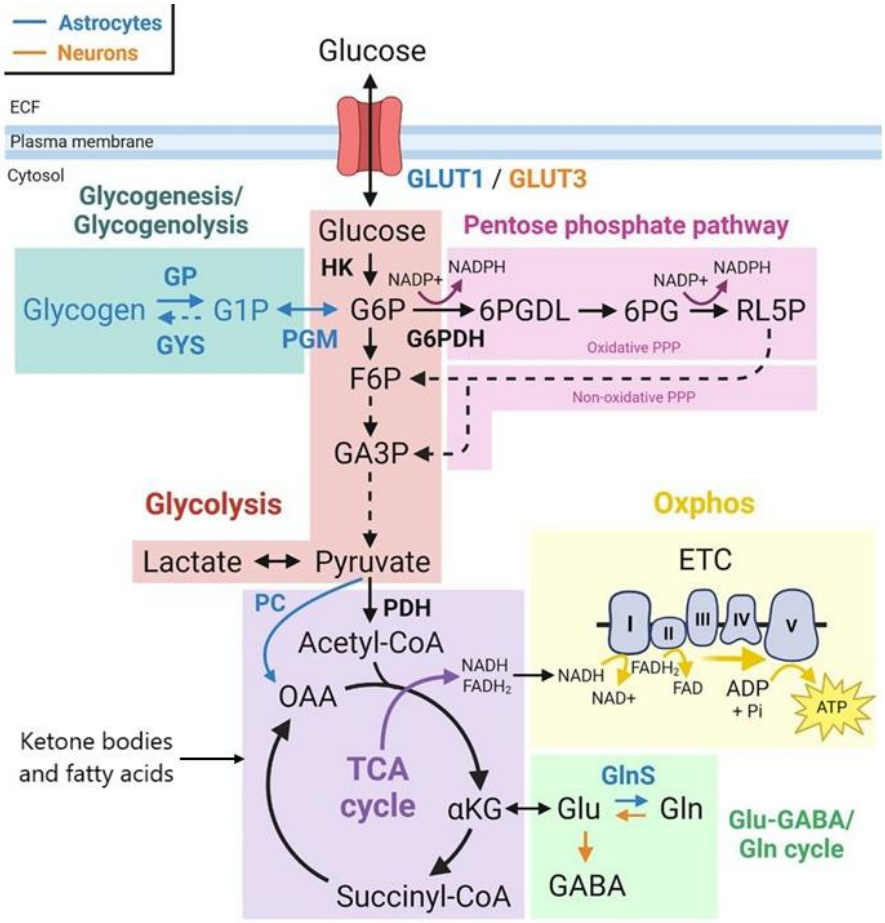

Figure 2. Simplified overview of the major metabolic pathways in the brain.
This diagram illustrates glucose metabolism through glycolysis, the PPP, the TCA cycle, and glycogen synthesis. It also highlights alternative fuel source such as ketone bodies and fatty acids. Figure adapted from (Neal et al., 2024).

The substantial energy demands of brain functions are sustained by a network of tightly regulated metabolic pathways that ensure a continuous supply of ATP and biosynthetic precursors. Core components of this network include glycolysis, mitochondrial respiration, the pentose phosphate pathway (PPP) and glycogenesis (Fig. 2). Mitochondrial respiration encompasses both the activity of the tricarboxylic acid (TCA) cycle and the electron transport chain (ETC), driving a large part of ATP production within neurons and glial cells. These pathways not only generate the energy required for neuronal signalling and maintenance but also produce critical intermediates for neurotransmitter synthesis, antioxidant defence, and cellular repair. Understanding the organization and regulation of these metabolic routes is essential for elucidating how the brain sustains its complex functions and responds to physiological challenges (Bélanger et al., 2011; Mergenthaler et al., 2013; Rae et al., 2024). Furthermore, a brief overview of lipid, amino acid, and ketone body metabolism is provided below.

Glycolysis

Glucose can be metabolized in the glycolytic pathway, which in the presence of oxygen is in most cases followed by oxidative phosphorylation. Glycolysis occurs in the cytoplasm of both neurons and glial cells and plays a central role in energy production by converting glucose into pyruvate in an oxygen-independent manner (Madrer et al., 2025).

The glycolytic pathway consists of ten sequential enzymatic reactions that convert one molecule of glucose into two molecules of pyruvate, alongside the generation of two molecules of NADH, two hydrogen ions, two water molecules, and a net gain of two ATP molecules. Glycolysis proceeds through two phases: a preparatory phase, which consists in five reactions in which ATP is consumed, and a payoff phase, other five reactions in which ATP is produced (Tanner et al., 2018). Three crucial enzymes serve as major regulatory checkpoints in glycolysis: hexokinase (HK), phosphofructokinase-1 (PFK-1), and pyruvate kinase (PK) (X. Zhang et al., 2021). In the first step of glycolysis, HK catalyses the phosphorylation of glucose using one molecule of ATP in order to produce glucose-6-phosphate (G-6-P) (Massa et al., 2011). G-6-P may then proceed through glycolysis, enter into the PPP, or used to synthesize glycogen. Between the three main regulatory enzymes, PFK-1 is considered as the crucial one. It catalyses the conversion of fructose 6-phosphate to fructose 1,6-bisphosphate, consuming one more ATP molecule. The final irreversible step of glycolysis is catalysed by PK, which converts phosphoenolpyruvate to pyruvate, generating two molecules of ATP. Pyruvate produced at the end of glycolysis follows distinct metabolic fates: it can enter the mitochondria to fuel the TCA cycle for oxidative ATP production or, particularly in astrocytes, be carboxylated to oxaloacetate, supporting anaplerotic flux and biosynthetic pathways (J. Rose et al., 2020; Y. M. Zhang et al., 2023). When required for redox balance, pyruvate can be reduced to lactate using NADH produced earlier in glycolysis despite the normal oxygen tension, a phenomenon known as aerobic glycolysis (Y. M. Zhang et al., 2023).

Glycolytic ATP production is closely linked to the cellular bioenergetic state and becomes especially important in situations demanding immediate energy availability, such as intense or acute neuronal activation (X. Zhang et al., 2021). Beyond its role in ATP production, glycolysis generates metabolic intermediates that feed several biosynthetic and catabolic pathways, including the TCA cycle, the PPP, the hexosamine biosynthesis pathway (HBP), fatty acid oxidation (FAO) and glycogen synthesis (Kierans & Taylor, 2024; H. Wang et al., 2024).

The Pentose Phosphate Pathway

The PPP is a glucose-oxidizing metabolic route that operates in parallel to glycolysis. It serves two major functions: the generation of ribose 5-phosphate for nucleotide synthesis, and the production of nicotinamide adenine dinucleotide phosphate (NADPH), which is essential for maintaining redox homeostasis and supporting various biosynthetic processes such as the synthesis of fatty acids, cholesterol, proline, deoxyribonucleotides, and tetrahydrofolate. In addition to its antioxidant role, NADPH is consumed by specific oxidases (NOXes) to promote the controlled generation of reactive oxygen species (ROS) and reactive nitrogen species (RNS), whose levels modulate cell signalling and innate immune responses (TeSlaa et al., 2023).

The PPP consists of two interconnected branches: the oxidative (oxPPP) and the non-oxidative (non-oxPPP) arms. The oxPPP begins with glucose-6-phosphate, which is also a substrate of glycolysis, and its irreversibly conversion into ribulose 5-phosphate, yielding two molecules of NADPH per glucose-6-phosphate. In contrast, the non-oxPPP comprises the interconversion of ribulose 5-phosphate into ribose 5-phosphate, and a series of reversible reactions that consume the latter metabolite to produce the glycolytic intermediates fructose 6-phosphate and glyceraldehyde 3-phosphate, enabling metabolic flexibility based on cellular needs (Patra & Hay, 2014).

In the brain, the PPP plays a crucial role in sustaining the function of both neurons and glial cells. One of its key contributions is the regeneration of NADPH, which serves as a cofactor for glutathione reductase in converting oxidized glutathione (GSSG) back to its reduced form (GSH), the major cellular antioxidant. Neurons, which have limited antioxidant capacity, rely on NADPH to sustain their GSH levels and protect themselves from oxidative damage (TeSlaa et al., 2023; Tu et al., 2019). This is a critical aspect of cellular wellbeing, as the accumulation of oxidative damage is proposed to be a key factor in the aetiology of neurodegenerative disorders. While glycolysis remains the primary glucose pathway in neurons under normal conditions, the PPP becomes critically important under conditions of oxidative stress or high biosynthetic demand. Astrocytes, in contrast, exhibit a higher PPP flux capacity, contributing not only to antioxidant defence but also to metabolic support of neurons through the production of NADPH and biosynthetic precursors. The dynamic balance between glycolysis and PPP activity in brain cells reflects the need to simultaneously manage high metabolic demand, redox stability, and cellular maintenance. Accordingly, the dysregulation of the PPP in brain cells has

been implicated in aging and the pathophysiology of disorders such as Alzheimer's disease, Parkinson's disease, and stroke (Bonvento & Bolaños, 2021; Herrero-Mendez et al., 2009).

Glycogenesis

Although the brain lacks substantial energy reserves, it retains a limited capacity to store glucose as glycogen through a process known as glycogenesis. Glycogen is primarily stored in astrocytes within both grey and white matter, where it serves as a critical energy buffer. Under conditions of increased energy demand, glycogen is mobilized by glycogen phosphorylase to produce G-6-P, which enters glycolysis to generate ATP (Nadeau et al., 2018). Beyond its role as an energy reserve, glycogen also contributes to neurotransmitter synthesis and signalling. Glycogen-derived lactate can fuel neuronal metabolism, while glycogen breakdown supports glutamate uptake and glutamine synthesis, both essential for maintaining synaptic transmission (Gibbs, 2016). The importance of brain glycogen is further underscored by evidence showing that inhibition of glycogen synthesis impairs long-term potentiation (LTP) and memory formation (Duran et al., 2013).

1.1.3. Glucose oxidation by mitochondria

In the presence of oxygen, pyruvate generated by glycolysis is transported into mitochondria via the mitochondrial pyruvate carrier (MPC), where, at the level of the mitochondrial matrix, it undergoes decarboxylation to form acetyl-CoA (Fernie et al., 2004). Acetyl-CoA then combines with oxaloacetate to form citrate, initiating the tricarboxylic acid (TCA) cycle, also known as Krebs cycle. Through a series of eight enzymatic reactions, the acetyl group is oxidized, and electrons are transferred to specific carriers, namely NADH and $FADH_2$, while regenerating oxaloacetate to sustain continued cycle activity. The reducing equivalents generated by TCA cycle activity – primarily carried by NADH and $FADH_2$ - are essential substrates for the mitochondrial ETC to drive ATP synthesis. Electrons from NADH and $FADH_2$ enter the ETC via a series of four protein complexes embedded in the inner mitochondrial membrane: NADH:ubiquinone oxidoreductase (Complex I), succinate dehydrogenase (Complex II), ubiquinol–cytochrome c oxidoreductase (Complex III), and cytochrome c oxidase (Complex IV) (Nolfi-Donegan et al., 2020). NADH and $FADH_2$ generated from the TCA cycle donate their electrons to complex I and complex II, respectively. These electrons reduce coenzyme Q (ubiquinone) to ubiquinol, which then transfers electrons to Complex III. Then, complex III passes the electrons to cytochrome c (Cyt c), which in turn delivers them to Complex IV. Finally, Complex IV transfers the electrons to O_2, the terminal electron acceptor, resulting in the formation of H_2O. As electrons move through the ETC,

Complexes I, III, and IV actively pump protons from the mitochondrial matrix into the intermembrane space, generating an electrochemical gradient. This proton gradient is used by the ATP synthase (Complex V) to condense ADP and inorganic phosphate to produce ATP, in a process known as OXPHOS (Fig. 3). The reoxidation of NADH and $FADH_2$ during this process not only drives ATP production but also enables the TCA cycle to proceed continuously. (Arnold & Finley, 2023). The OXPHOS can yield ~31 ATP molecules per molecule of glucose, making it significantly more efficient than glycolysis. Consequently, in the presence of oxygen, most cells preferentially rely on this pathway for energy production (Fernie et al., 2004; H. Liu et al., 2025; Magistretti & Allaman, 2013).The availability of oxygen, essential for OXPHOS, normally suppresses glycolysis, in a phenomenon known as the Pasteur effect. In well-oxygenated cells such as neurons, the Pasteur effect ensures preferential use of mitochondrial respiration over glycolysis, thereby maximizing ATP yield and supporting high-energy demands. (Barros et al., 2021). The TCA cycle also provides metabolic flexibility by processing alternative substrates such as amino acids and fatty acids (FA). Moreover, several of its intermediates are critical precursors for anabolic processes, including amino acid and nucleotide synthesis, as well as gluconeogenesis. Consequently, not all pyruvate entering the TCA cycle is directed toward ATP production only (Arnold & Finley, 2023).

In addition to driving ATP synthesis, OXPHOS is associated with the production of mitochondrial ROS, a process closely linked to the structural organization of the mitochondrial respiratory complex (MRC). Mitochondrial Complex I, a primary source of ROS, can function either as an individual complex or as part of higher-order assemblies known as supercomplexes, formed with Complexes III and IV (Lenaz et al., 2016). The incorporation of Complex I into supercomplexes enhances the efficiency of electron transfer within the ETC, thereby minimizing electron leakage and reducing ROS generation (Lopez-Fabuel et al., 2016). Mitochondria are the main source of intracellular ROS, and accordingly, these organelles are particularly susceptible to oxidative stress. When ROS production exceeds the capacity of antioxidant defences, it can disrupt mitochondrial dynamics (including fission and fusion), interfere with cell cycle kinases regulation, and activate innate immune responses. These disruptions contribute to cellular dysfunction and may play a role in the pathogenesis of neurodegenerative diseases (Knott et al., 2008; M. T. Lin & Beal, 2006).

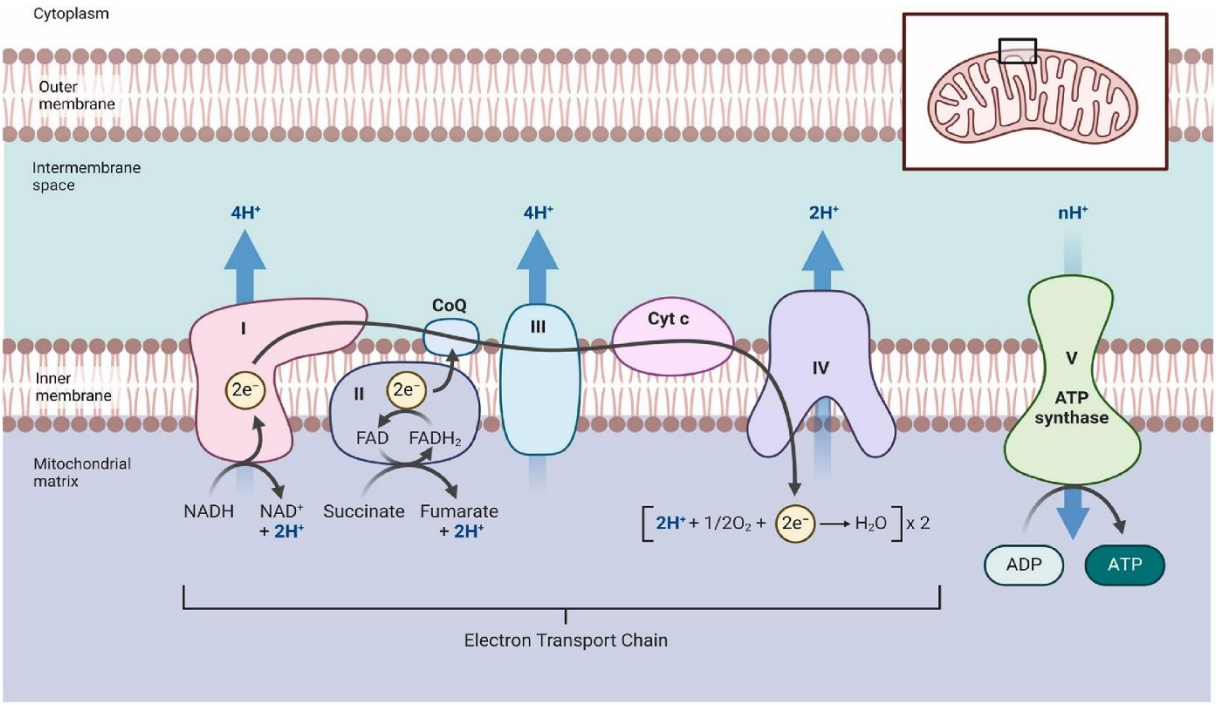

Figure 3. Schematic representation of the MRC and OXPHOS.
This figure illustrates the electron flow through complexes I-IV, proton translocation across the inner mitochondrial membrane and ATP synthesis via complex V. Figure from (T. Wang & Zhang, 2024).

1.1.4. Alternative fuels for mitochondrial function

Although glucose is the primary energy source of the brain, it is not the only substrate capable of fuelling neural activity. Under specific physiological or pathological conditions, such as fasting, prolonged exercise, starvation, or ketogenic diets, the brain is capable of using alternative substrates, including fatty acids (via fatty acid oxidation, FAO) and ketone bodies. These pathways provide metabolic flexibility, particularly during periods of glucose scarcity, and contribute to the maintain brain energy homeostasis and adapt to energetic stress (Clarke & Sokoloff, 1999; García-Rodríguez & Giménez-Cassina, 2021; Szrok-Jurga et al., 2023).

Lipids play essential structural roles in the brain, contributing to neuronal membranes and myelin sheaths. In addition to these functions, early studies have shown that FAO can meet up to 20% of the brain's energy requirements, predominantly within astrocytes (Ebert et al., 2003). FAO begins with the activation of fatty acids to fatty acyl-CoA, which is then transported into mitochondria via the carnitine shuttle, a system dependent on the carrier molecule L-carnitine. This transport involves more than two dozen enzymes and proteins, with carnitine palmitoyltransferase I (CPT-1) acting as the rate-limiting enzyme of the pathway (Houten et al., 2016). Within the mitochondrial matrix, fatty acyl-CoA undergoes β-oxidation, yielding NADH, $FADH_2$, and acetyl-CoA, which fuel the TCA cycle and the mitochondrial ETC for ATP production. Although FAO is highly energy-efficient, producing up to 106 ATP molecules

per palmitate compared to ~36 from glucose, it requires substantially more oxygen (31 moles vs. 6 per glucose), making it less favorable in the oxygen-limited environment of the brain. Additionally, FAO generates considerable amounts of ROS, particularly superoxide, contributing to oxidative stress. As a result, while FAO can support brain metabolism during energy crises, glucose remains the preferred substrate due to its lower oxygen requirement and reduced ROS burden. Notably, recent evidence suggests that astrocytic FAO may serve a signalling function by maintaining the mitochondrial respiratory chain in a disassembled yet ROS-permissive state, which appears to support cognitive performance through redox-dependent mechanisms (Morant-Ferrando et al., 2023).

In parallel, ketone bodies, primarily β-hydroxybutyrate (BHB) and acetoacetate (AcAc), serve as alternative energy substrates during periods of carbohydrate depletion. Their oxidation (ketolysis) in the brain is facilitated by the concerted activity of BHB dehydrogenase and succinyl-CoA:3-oxoacid-CoA transferase (SCOT) to produce AcAc-CoA, which then is cleaved into two molecules of Acetyl-CoA via a thiolase reaction catalysed by the mitochondrial acetyl-CoA acetyltransferase 1 (ACAT-1). The utilization of ketone bodies becomes significant during prolonged fasting, starvation, or chronic ketogenic diet, when hepatic production of ketones increases and glucose availability declines (Lamanna et al., 2009). Beyond their role in energy production, ketone bodies, particularly BHB, also act as signalling molecules, influencing gene expression, epigenetic regulation, and pathways related to memory, aging, and neuroprotection (García-Rodríguez & Giménez-Cassina, 2021; Saito et al., 2022).

1.1.5. Main biosynthetic pathways

Beyond energy production, brain metabolism supports a variety of biosynthetic processes essential for neural development, signalling, and homeostasis. Two key biosynthetic domains in the brain involve amino acid and lipid metabolism, both of which contribute to neurotransmitter synthesis, membrane structure, and the regulation of cellular function.

Amino acids are indispensable for multiple brain-specific metabolic pathways, serving not only as protein building blocks but also as neurotransmitters and metabolic intermediates. The synthesis and degradation of several key neurotransmitters, including glutamate, γ-aminobutyric acid (GABA), dopamine, and serotonin, are directly linked to amino acid availability (Bak et al., 2006; Kölker et al., 2018). For example, the biosynthesis of L-glutamate and GABA consumes α-ketoglutarate (α-KG), an intermediate of the TCA cycle. In a similar

context, the glycolytic intermediate 3-phosphoglycerate serves as the precursor for L-serine. This L-amino acid plays a particularly important role in brain metabolism, as it serves not only as a precursor for glycine and D-serine, co-agonists of NMDA receptors involved in synaptic plasticity but also contributes to the synthesis of sphingolipids and phosphatidylserine, essential components of neuronal membranes. While L-serine is synthesized primarily by astrocytes, it is taken up and utilized by neurons, highlighting one of the many critical aspects of neuron-glia metabolic cooperation (Furuya, 2008; Kölker et al., 2018). Additionally, amino acids such as alanine and aspartate are involved in key regulatory functions. Both are formed through transamination reactions that participate in the urea cycle and pyrimidine biosynthesis, while simultaneously generating intermediates like pyruvate and oxaloacetate. These intermediates feed into gluconeogenesis and help maintain energy balance in the brain (Chandel, 2021).

In parallel, lipid biosynthesis is equally vital for brain structure and function. The brain is one of the most lipid-rich organs in the body, with lipids making up nearly half of its dry weight. These lipids are not only structural components of cellular membranes and myelin sheets but also participate in signal transduction and membrane trafficking. Among them, cholesterol is particularly important; although it is largely excluded from systemic circulation due to the BBB, it is synthesized *de novo* in the adult brain primarily by astrocytes (D. Yang et al., 2022). Cholesterol is essential for synaptogenesis, membrane fluidity, and myelin formation. Its synthesis originates from acetyl-CoA through the mevalonate pathway, a multistep process regulated by key enzymes such as HMG-CoA reductase. In addition to cholesterol, other lipids such as phospholipids and sphingolipids play critical roles in neuronal membrane integrity and signalling. Fatty acid synthesis also occurs locally in glial cells, contributing to membrane remodelling and the formation of lipid-based signalling molecules. Dysregulation of brain lipid metabolism has been implicated in several neurodevelopmental and neurodegenerative disorders, including Alzheimer's disease, where altered cholesterol homeostasis is thought to affect amyloid processing and synaptic function (Pfrieger, 2003; J. Zhang & Liu, 2015).

1.2. Metabolic compartmentalization

The brain's cellular architecture is highly specialized, with neurons and glial cells working together to support functions such as synaptic signalling, metabolic coupling, blood flow regulation, axonal insulation and immune surveillance. A large share of the brain energy budget is devoted to ATP production, primarily to fuel the Na^+/K^+ ATPase, and to a lesser extent the Ca^{2+} ATPase, which are engaged to restore ion gradients dissipated during electrical activity such as postsynaptic currents, but also during recycling of synaptic vesicles and

neurotransmitters (Pulido & Ryan, 2021; Rangaraju et al., 2014). Regions dense in synapses, dendrites, and axon terminals are among the most energy-demanding, with synaptic activity alone accounting for up to 80% of the total metabolic cost of neuronal network function. Neurons are responsible for approximately 80% of total energy consumption in the brain, while glial cells account for the remaining 20% (Harris et al., 2012). Glial cells, however, exhibit notable metabolic flexibility. While they primarily metabolize glucose, they can also utilize alternative substrates such as lactate, pyruvate, glutamate and amino acids to support a wide range of functions (Zielke et al., 2009). In particular, glia contributes to brain lipid homeostasis and ATP generation through FAO and amino acid metabolism (Afridi et al., 2022; Mallick et al., 2024). This adaptability is essential for maintaining neural homeostasis, and its disruption may be linked to neurodegenerative disease.

Neurons depend primarily on OXPHOS for energy production and exhibit a higher rate of mitochondrial respiration than glial cells. Despite this, neurons are not avid glucose consumers but rather they preferentially use lactate, supplied largely by glia cells, to fuel oxidative metabolism (Bolaños et al., 2010; Bouzier-Sore et al., 2006; Magistretti & Allaman, 2018). This preference is linked to their inherently low glycolytic activity, which results from the continual proteasomal degradation of PFKFB3, a key glycolytic regulator (Herrero-Mendez et al., 2009). As a result, neurons are limited in their ability to upregulate glycolysis during metabolic stress, making them vulnerable to OXPHOS inhibition. Indeed, forced overexpression of PFKFB3 in neurons induces oxidative stress and apoptosis, indicating that excessive glycolytic activity is detrimental to neuronal survival (Herrero-Mendez et al., 2009; Jimenez-Blasco et al., 2024). The distinct bioenergetic and redox profiles of neurons and glia cells are critical for maintaining correct neurotransmission and neuronal viability. These differences are partially attributed to mitochondrial organization: neurons display higher levels of mitochondrial Complex I and increased SC assembly, which enhances OXPHOS efficiency (Lopez-Fabuel et al., 2016). Accordingly, neurons depend on lactate for ATP production while directing glucose toward the PPP, which supports antioxidant defences through regeneration of GSH (Bolaños et al., 2010).

2. Astrocytes

Astrocytes are the most abundant type of glial cells within the CNS, accounting for approximately 30% of all cells in the mammalian brain (Brazhe et al., 2023; Herculano-Houzel, 2014). The term “astrocyte” encompasses different cells with a great heterogeneous morphology. Indeed, astrocytes were first classified based on morphological characteristics and

location. Therefore, two main types of astrocytes have been defined in literature. White matter astrocytes, named “fibrous astrocytes”, characterized by unbranched, long and thin processes that envelop nodes of Ranvier, helping to maintain ion balance and local homeostasis. The second type is grey matter astrocytes, named “protoplasmic astrocytes” and characterized by many branching processes that occupy a huge volume and enclose synapses. These structures allow them to enwrap synapses and blood vessels, contributing to synaptic modulation, neurotransmitter recycling, and BBB maintenance (Miller & Raff, 1984; Oberheim et al., 2012). In addition, two more specialized types of astrocytes in the central nervous system have been described: Müller cells, that are situated in the retina, and a cerebellum-specific type of astrocyte, the Bergmann glia, (Khakh & Deneen, 2019; Oberheim et al., 2012). This morphology and density-based classification has been significantly expanded by recent transcriptomic studies, which reveal a high degree of molecular heterogeneity and functional specialization among astrocytes, both across and within distinct brain regions (de Ceglia et al., 2023; Doyle et al., 2008; Holt, 2023; O’dea et al., 2025; Yeh et al., 2009).

Once considered to be only passive support cells, astrocytes are now considered as active participants in CNS function, playing essential roles in synaptic plasticity, homeostatic regulation, and behavioural control (Perea et al., 2009; Verkhratsky et al., 2021). In this context, astrocyte malfunction is linked to the pathophysiology of various neurological disorders (Perea et al., 2009; Verkhratsky et al., 2021; Won et al., 2025). Neuronal activity modulates diverse astrocyte activities, including for example intracellular Ca^{2+} dynamics, cAMP signalling or specific metabolic processes, which in turn promote and shape diverse aspects of brain function (Allen et al., 2022; Guerra-Gomes et al., 2018; Khakh & Deneen, 2019; Theparambil et al., 2024; Verkhratsky et al., 2021; Zhou et al., 2019). Among others, astrocytes actively shape synaptic transmission via the release of a variety of signalling molecules (Fig 4.). For instance, neuronal-evoked Ca^{2+} signalling in astrocytes promotes gliotransmission, a process whereby these cells release molecules with neurotransmitter-like functions (gliotransmitters), such as glutamate or D-serine. Similarly, and likely with a different spatio-temporal pattern than gliotransmission, astrocytes can also release other types of signalling molecules like hydrogen peroxide (H_2O_2), peptides like brain-derived neurotrophic factor (BDNF) and its precursor proBDNF, or metabolites like lactate which act on specific receptors (Lauritzen et al., 2014; Won et al., 2025). Notably, astrocytes also play essential roles in supporting neuronal metabolism, BBB integrity, regulating neurotransmitter homeostasis, modulating neuroimmune responses, promoting the clearance of metabolic waste and maintenance of ion and water

balance (Bélanger et al., 2011; Bugiani et al., 2021; Verkhratsky & Nedergaard, 2018; Zimmer et al., 2024).

The following paragraphs will outline the principal functions of astrocytes in the CNS, offering a comprehensive overview of their critical roles in brain metabolism and overall physiology.

2.1. Astrocytic regulation of extracellular environment

Astrocytes play a pivotal role in modulating neuronal excitability, particularly during periods of heightened synaptic activity. One of their primary functions is the maintenance of extracellular environment, including the control of diverse ions levels, like K^+, and the uptake/recycling of neurotransmitters.

Efficient astrocyte-mediated K^+ clearance is essential for preventing pathological neuronal hyperexcitability and ensuring stable network oscillations (Bellot-Saez et al., 2017; Rupareliya et al., 2023). Astrocytes use several mechanisms to control extracellular K^+ levels. Inwardly rectifying K^+ channels, particularly Kir4.1 - highly expressed in astrocytes' membranes - enable passive uptake of K^+ during neuronal activity. The Na^+/K^+ ATPase further contributes to active K^+ transport into astrocytes. Additionally, spatial buffering via gap junctions, formed by connexins such as Cx43, allows redistribution of excess K^+ throughout the astrocytic network. Other transporters, such as NKCC1, may also play a role during intense stimulation by supporting ion and volume regulation (Barros, 2022; MacAulay, 2020).

Astrocytes are central to the uptake, release, and metabolism of neurotransmitters, exerting tight control over synaptic signalling and neuronal responsiveness (Perea et al., 2009). They modulate key neurotransmitters including glutamate, GABA, adenosine, and monoamines, thereby exerting a tight control over synaptic signalling and neuronal responsiveness (Perea et al., 2009). Among these, glutamate clearance is particularly critical, as excessive extracellular glutamate can lead to excitotoxicity and neuronal damage. Astrocytes express high-affinity transporters such as EAAT1/GLAST and EAAT2/GLT-1, which remove the majority of glutamate from the synaptic cleft. (Rose et al., 2018; Schousboe, 2020). Genetic deletion or dysfunction of these transporters leads to pathological glutamate accumulation, resulting in neuronal hyperexcitability, seizures, and neurodegeneration (Pajarillo et al., 2019).

Inhibitory neurotransmission is similarly regulated by astrocytes, primarily through GABA uptake mediated by GABA transporters GAT-1 and GAT-3, the latter being predominantly localized in astrocytic membranes, while GAT-1 is almost equally present in both (Andersen et al., 2023). This astrocytic uptake modulates extracellular GABA concentrations, shapes inhibitory tone, and contributes to neurotransmitter recycling (Andersen, 2025; Andersen et al., 2023; Perea et al., 2016).

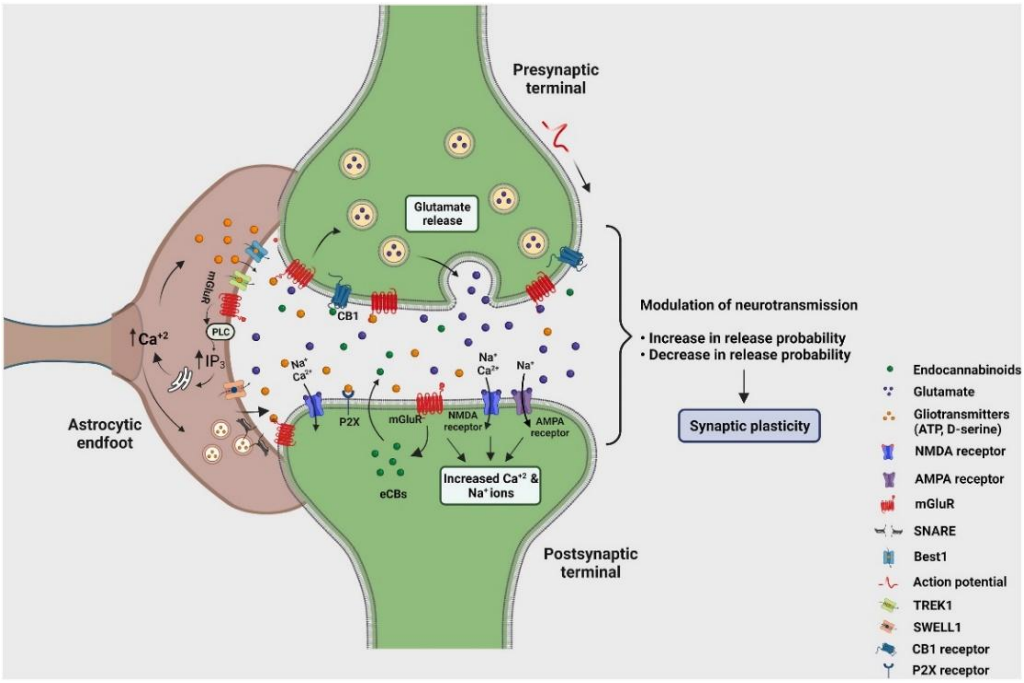

Figure 4. Astrocytic modulation of neurotransmission and synaptic plasticity.
Neuronal activity triggers neurotransmitter release, which activates postsynaptic receptors (mGluR, NMDA, AMPA) to regulate synaptic plasticity. These neurotransmitters also stimulate astrocytic receptors, like mGluRs, raising intracellular Ca^{2+} via the PLC–IP_3 pathway. Elevated Ca^{2+} drives gliotransmitter release through vesicular and channel-mediated mechanisms. These gliotransmitters act on pre- and postsynaptic targets, modulating synaptic vesicle release and plasticity. SWELL1-mediated released gliotransmitters and endocannabinoids released by mGlu1 activation also affects synaptic transmission. This highlights the central role of astrocytes in dynamic synaptic regulation. Figure from (Rupareliya et al., 2023).

A key integrative mechanism for both glutamatergic and GABAergic systems is the glutamate/GABA-glutamine cycle. In this cycle, astrocytes convert glutamate taken up from the synaptic cleft into glutamine via the enzyme glutamine synthetase, which is exclusively expressed in astrocytes. Glutamine is then shuttled back to neurons, where it is reconverted into either glutamate or GABA, depending on the neuronal subtype. This astrocyte-neuron coupling ensures a continuous supply of neurotransmitter precursors while preventing excitotoxic or inhibitory spill over. Thus, through a coordinated set of transporter and enzymatic functions, astrocytes not only maintain extracellular neurotransmitter homeostasis but also enable the metabolic recycling necessary for sustained synaptic transmission (Andersen, 2025).

2.2. Astrocyte-mediated synaptic signalling

Astrocytes can directly influence brain function via the controlled release of gliotransmitters, which are signalling molecules that fine-tune synaptic function and neural network dynamics (Araque et al., 1999; Lei et al., 2024; Savtchouk & Volterra, 2018). This signalling process known as gliotransmission has been demonstrated across various brain regions in rodents and humans and is now recognized as a critical process in modulating brain function (Miguel-Quesada et al., 2023; Won et al., 2025). Gliotransmission is engaged when astrocytes sense synaptic activity via metabotropic and ionotropic receptors including those for glutamate, GABA, endocannabinoids (eCBs), among others. This detection triggers intracellular Ca^{2+} signalling, largely mediated by the IP3R2 pathway, which vary depending on the type of neurotransmitter and the frequency of neuronal activity involved. Notably, these Ca^{2+} signals can propagate across astrocytic networks via gap junctions, enabling the coordination of activity across distant synapses (Giaume et al., 2021; Savtchouk & Volterra, 2018). In response, astrocytes release gliotransmitters, such as glutamate, GABA, ATP, and D-serine, that act either on pre- or post-synaptic neuronal receptors (Fig. 4) (Araque et al., 2014). Importantly, the frequency and duration of neuronal activity can influence both the type and effect of gliotransmitter release from a single astrocyte, leading to context-dependent, even opposing, synaptic outcomes (Covelo & Araque, 2018). The release of gliotransmitters occurs through diverse mechanisms, including vesicular exocytosis, transporter activity, and channel-mediated pathways, enabling astrocytes to directly modulate neuronal excitability and synaptic function (Araque et al., 1999; Haydon & Carmignoto, 2006; Verkhratsky & Nedergaard, 2018). Recent findings suggest that a specific subpopulation of astrocytes in the hippocampus may possess synaptic-like vesicular machinery for glutamate release (de Ceglia et al., 2023; Harada et al., 2016). Also, the SWELL1 channel, a subunit of the volume-regulated anion channel (VRAC), has been identified as a mediator of glutamate and GABA release from astrocytes (Yang et al., 2023). This capacity for bidirectional communication between astrocytes and neurons via gliotransmission promoted the concept of the 'tripartite synapse', a functional unit composed of presynaptic and postsynaptic neuronal terminals along with surrounding astrocytic processes, which has become a foundational model for understanding how glial cells integrate into the core mechanisms of brain function (Araque et al., 2014). Accordingly, astrocyte gliotransmitter release regulates synaptic plasticity (LTP and LTD), neurotransmitter release, and memory consolidation (Escalada et al., 2024; Navarrete et al., 2012; Panatier et al., 2011; Perea et al., 2009). Growing evidence further supports that gliotransmission, through bidirectional

communication with synapses, is essential for the regulation of complex behaviours such as learning and memory, emotional states including depression-like behaviour and addiction, fear processing, sleep-wake cycles, feeding behaviour, and circadian rhythm control (Kofuji & Araque, 2021; Mariani et al., 2025; Murat & García-Cáceres, 2021). Moreover, recent in vivo studies have shown that astrocytic Ca^{2+} signalling can enhance inhibitory circuit activity, thereby modulating sensory processing and limiting excessive excitation (Miguel-Quesada et al., 2023; Rupareliya et al., 2023). In this context, it is important to note that the dysregulation of astrocytic Ca^{2+} dynamics and gliotransmitter release is proposed to be implicated in the pathogenesis of several CNS disorders (Cheong & Lee, 2025; Lei et al., 2024).

2.3. Neurovascular coupling and cerebral blood flow regulation

Given the fact that neurons have a little store of glycogen, brain depends on systemic circulation for its glucose and oxygen requirements. Thus, local increases in cerebral blood flow are essential to meet the heightened metabolic demands that accompany neuronal activity (Brazhe et al., 2023; Macvicar & Newman, 2015). The neurovascular unit (NVU) is a fundamental concept in order to understand CNS physiology. It is a structure made up of neurons, blood vessels, astrocytes, pericytes and microglia, which form contact with each other and regulate essential processes in the CNS (Lia et al., 2023; Rupareliya et al., 2023). Astrocytes make direct contact with blood vessels via specialized structures called endfeet, and they are well positioned to influence cerebral blood flow and neurovascular coupling (Brazhe et al., 2023). Thus, astrocytes play an important position in coordinating the neuronal demand with the supply of energy substrates. This is achieved by the ability of astrocytes to control the vascular tone (Cohen-Salmon et al., 2025; Jha & Morrison, 2020; Macvicar & Newman, 2015; Marina et al., 2020). When cerebral blood flow is reduced, astrocytes respond via Ca^{2+}-dependent signalling pathways, activating sympathetic control circuits that increase both cerebral perfusion and heart rate (Attwell et al., 2010; Koehler et al., 2009; Macvicar & Newman, 2015; Marina et al., 2020). They detect synaptic activity at tripartite synapses and translate this into vascular responses by modulating capillary tone releasing different vasoactive molecules such as prostaglandins, NO, and arachidonic acid, thereby ensuring that regions with heightened neuronal demand receive adequate oxygen and nutrients. (Lecrux et al., 2019; C. Y. Liu et al., 2018).

In addition to regulating blood flow, astrocytes play a crucial role in the formation, maintenance, and dynamic modulation of the BBB. Through their perivascular endfeet, astrocytes provide structural support and influence the functional properties of endothelial cells, thereby shaping the transport of molecules between the bloodstream and the brain parenchyma.

They modulate BBB permeability by regulating enzyme activity in cerebral endothelial cells, such as enhancing alkaline phosphatase and Na^+/K^+-ATPase function, and by modifying transporter systems. For instance, astrocytes can increase the transport capacity of neutral amino acids and upregulate glucose transporter activity, reinforcing the barrier's ability to meet the metabolic demands of the CNS. (Ando et al., 2018; Gradisnik & Velnar, 2023).

2.4. Astrocytes and brain bioenergetics

Astrocytes traditionally account for only 5–15% of the brain energy budget. However, experimental evidence shows that they take up a disproportionately high amount of glucose compared to their energy demands. In the resting brain, astrocytes are responsible for approximately 50% of glucose uptake, a proportion that increases during functional activation, surpassing neuronal glucose uptake under stimulated conditions (Chuquet et al., 2010). Remarkably, astrocytes release up to 85% of the glucose they consume as lactate. Neuronal activity further enhances both glucose uptake and lactate production in astrocytes (Magistretti & Pellerin, 1999). These observations underpin the concept of neuro-metabolic coupling, specifically the astrocyte to neuron lactate shuttle (ANLS) model which will be further discussed in the next sections (Bonvento & Bolaños, 2021). Astrocytes rely less on OXPHOS than neurons, a difference linked to elevated expression of pyruvate dehydrogenase kinases (PDKs) and reduced activity of the pyruvate dehydrogenase (PDH) complex (Kumar Jha et al., 2012). Structurally, astrocytic mitochondria exhibit lower assembly of respiratory SCs and a higher proportion of free Complex I, which diminishes respiratory efficiency and elevates mitochondrial ROS production (Lopez-Fabuel et al., 2016). This de-active form of Complex I favours direct electron transfer to oxygen, promoting superoxide generation. Importantly, mitochondrial ROS in astrocytes plays a physiological role by activating hypoxia-inducible factor 1α (HIF-1α), thus promoting the synthesis of several glycolytic enzymes (Almeida et al., 2004; Jimenez-Blasco et al., 2020), while also modulating the PPP and maintaining basal activity of the antioxidant transcription factor NRF2 (Vicente-Gutierrez et al., 2019). Beyond glucose metabolism, astrocytes are key sites for FAO and cholesterol synthesis, two processes that contribute to redox balance, membrane homeostasis, and synaptic support (Eraso-Pichot et al., 2018; Morant-Ferrando et al., 2023).

2.4.1. Lactate shuttling: mechanistic insight into neuron–astrocyte metabolic coupling

Whereas neurons are cells that fully oxidize glucose through mitochondrial respiration, astrocytes are less oxidative and instead partially oxidize glucose. In this metabolic process,

known as aerobic glycolysis, astrocytes preferentially convert glucose into lactate even in the presence of oxygen, resulting in the production of only 2 ATP molecules per metabolized glucose (Y. M. Zhang et al., 2023). Although this process is energetically less efficient, substantial evidence indicate that astrocytes are net lactate producers (Brooks, 2018; Chatton et al., 2016; Magistretti & Allaman, 2018; Vaccari-Cardoso et al., 2022). One molecular mechanism underlying this distinct astrocytic metabolic profile involves the regulation of PDH complex, which is highly phosphorylated in these cells thereby reducing its activity and favouring aerobic glycolysis. In addition, the mitochondrial ETC in astrocytes exhibits a distinct structural organization compared to that of neurons. Astrocytes contain higher levels of free complex I, and consequently fewer mitochondrial SCs, which are critical for maximizing electron flux efficiency and ATP production (Lopez-Fabuel et al., 2016). Furthermore, the monocarboxylate transporters (MCTs), responsible for lactate transport across the membrane, as well as LDH expression, change significantly between neurons and astrocytes (Magistretti & Allaman, 2015; Simpson et al., 2007). These clear metabolic differences between neurons and astrocytes provide strong support for the ANLS model, which proposes that astrocyte-derived lactate is transported to neurons, where it is oxidized as an additional energy substrate (Fig. 5) (Magistretti & Pellerin, 1999). This theory reinforces the idea that glucose metabolism in the brain is functionally compartmentalized: astrocytes mainly convert glucose into lactate and store glycogen, whereas neurons primarily utilize glucose and lactate for mitochondrial ATP production (Barros & Weber, 2018; Jolivet et al., 2009). According to the ANLS model, astrocytes release lactate during periods of high neuronal activity or energy demand to support neuronal oxidative metabolism (Magistretti & Allaman, 2018). The classical ANLS mechanism proposes that synaptic transmission elevates extracellular glutamate levels, which are rapidly taken up by astrocytes through sodium-dependent glutamate transporters. This uptake triggers activation of the Na^+/K^+ ATPase, leading to increased ATP consumption and thereby stimulating glucose uptake and glycolysis. The resulting lactate is released into the extracellular space and taken up by neurons, where it fuels ATP production through OXPHOS (Barros & Deitmer, 2010; Bonvento & Bolaños, 2021; Pellerin et al., 2007). In addition to glutamate, other neuronal signals, such as extracellular potassium (K^+), ammonium (NH_4^+), and activation of cannabinoid type-1 receptor (CB1R), have also been shown to stimulate astrocytic lactate release (Fernández-Moncada, Lavanco, et al., 2024; Lerchundi et al., 2015; Sotelo-Hitschfeld

et al., 2015). The mechanisms by which CB1R modulates lactate dynamics will be discussed in greater detail in the following sections of this thesis.

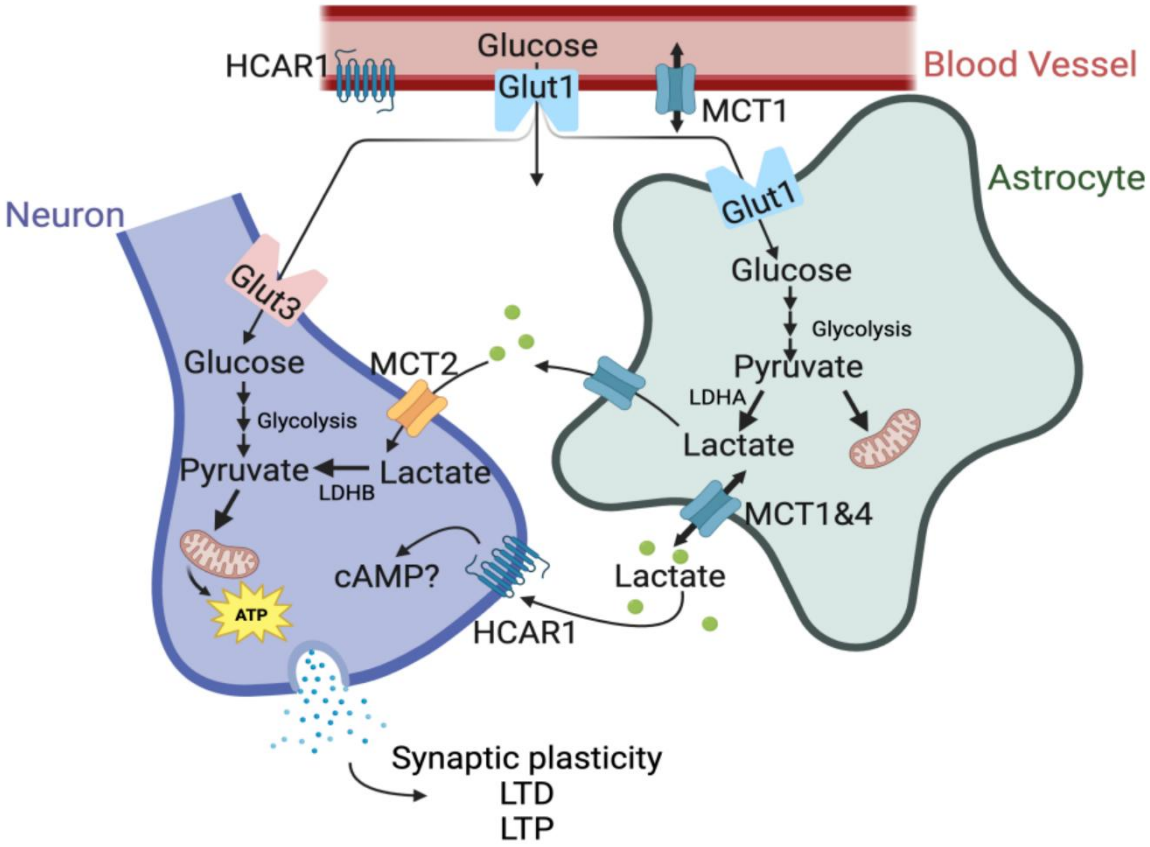

Figure 5. Illustration of the ANLS model.
During neuronal activity, glutamate is released into the synaptic cleft, and subsequently glucose from blood vessels is taken up by astrocytes and metabolized to pyruvate via glycolysis. Pyruvate is then converted into lactate by LDHA and released through MCT1/4 transporters. Neurons take up lactate via MCT2 and use it aerobically to meet energy demands and maintain homeostasis. Figure adapted from (Wu et al., 2023)

Over the past few decades, this shift in understanding has led neuroscientists to reconsider lactate not merely as a metabolic by-product, but as a key signalling molecule in the brain. Emerging evidence now shows that lactate plays an essential role in neurobiological processes such as memory formation and consolidation (Magistretti & Allaman, 2018; Newman et al., 2011; Suzuki et al., 2011; Tadi et al., 2015; Y. Zhang et al., 2016).

While the ANLS is strongly supported by a substantial body of evidence and remains the most widely accepted model, some studies have challenged this view, proposing alternative interpretations of lactate flux dynamics in the brain (Díaz-García et al., 2017; Dienel, 2017). Therefore, additional experimental studies are needed to further validate the ANLS and potentially reconcile the conflicting findings both supporting and challenging this model.

2.4.2. Lactate production and transport

Transport of lactate across cell membranes is mediated by the MCT family, which comprises 14 isoforms with varying substrate affinities and tissue distributions. These transporters facilitate the bidirectional movement of lactate and other monocarboxylates such as pyruvate and ketone bodies across cell membranes, depending on concentration gradients and cellular context (Morris & Felmlee, 2008). Within the CNS, three specific isoforms, MCT1, MCT2, and MCT4, exhibit distinct regional and cell-type specific distributions (Eid et al., 2018). MCT1 is primarily expressed in endothelial cells of the BBB and in glial cells, mainly astrocytes (Pierre & Pellerin, 2005). Due to its strategic localization, MCT1 plays a key role in the bidirectional transport of L-lactate across cellular membranes. The direction of this transport, either influx or efflux, is determined by the concentration gradients of lactate and protons across the membrane (Halestrap & Price, 1999; Vijay & Morris, 2014). MCT2 shares approximately 60% sequence identity with MCT1 but is predominantly localized to synaptic regions (Pierre & Pellerin, 2005; Vijay & Morris, 2014). Recognized as the primary neuronal transporter for extracellular lactate uptake, MCT2 exhibits a significantly higher affinity for monocarboxylate substrates compared to MCT1 (Descalzi et al., 2019). Lastly, MCT4, despite having the lowest substrate affinity among the three isoforms, possesses a high transport capacity. It is predominantly expressed in glycolytic tissues, including astrocytes, and is thought to facilitate lactate efflux to prevent intracellular accumulation. This export is essential for maintaining glycolytic flux, as excessive intracellular lactate would otherwise inhibit glycolysis (Ueno et al., 2023; Vijay & Morris, 2014).

2.4.3. Beyond metabolism: lactate as a signalling molecule

Lactate, in addition to its role as an energy substrate for neuronal activity, is increasingly recognized as a key signalling molecule involved in multiple aspects of brain function. Its production by astrocytes has been implicated in long-term memory formation and cognitive function. This is supported by evidence showing that disruption of lactate production in astrocytes, or interference with MCTs involved in the ANLS, impairs LTP and memory consolidation (Alberini et al., 2017; Suzuki et al., 2011). As potential underlying mechanism, lactate promotes plasticity gene expression by increased intracellular levels of NADH, contributing to redox regulation, and leading to the potentiation of NMDAR signalling in neurons (Brooks, 2009; Margineanu et al., 2018; J. Yang et al., 2014). Moreover, lactate in the intercellular space serves as a signalling molecule binding to the lactate receptor hydroxycarboxylic acid receptor 1 (HCAR1) or GPR81 (Lauritzen et al., 2014), and potentially

other G-protein-coupled receptors (GPCRs), in neurons, endothelial cells and glial cells, resulting in inhibition of adenylyl cyclase and indicating then its involvement in neurotransmission, neurovascular coupling, and brain metabolism (Bergersen, 2014). Key signalling pathways activated by lactate include those that involve AMP-activated protein kinase (AMPK), HIF-1α, and the modulation of histone deacetylases (HDACs). These pathways influence gene expression, mitochondrial function, and overall cellular metabolism (J. Zhou et al., 2024). Importantly, several studies have suggested a neuroprotective role of elevated lactate levels in the brain, supported by its ability to prevent excitotoxicity through a coordinated cellular pathway that involves ATP production and release and activation of P2Y receptors and ATP-sensitive K^+ channels (Jourdain et al., 2016; Margineanu et al., 2018).

2.5. Astrocyte functions are coordinated by specific signalling systems

These regulatory functions highlight astrocytes not only as passive supporters but as dynamic integrators of synaptic activity, bridging metabolic, vascular and electrical signalling in the CNS. They maintain extracellular ion homeostasis, clear neurotransmitters such as glutamate and GABA from the synaptic cleft, and release gliotransmitters that modulate synaptic transmission and plasticity (Valles et al., 2023; Verkhratsky et al., 2021). Through the ANLS, they provide neurons with lactate to support neuronal oxidative metabolism, while also contributing to antioxidant defence and pH regulation (Magistretti & Allaman, 2018; Verkhratsky & Nedergaard, 2018) . In addition, astrocytes influence cerebral blood flow via vasoactive signalling, coordinate metabolic coupling between neurons and the vasculature, and participate in the structural remodelling of synapses (Verkhratsky & Nedergaard, 2018; Zimmer et al., 2024). The diversity of these roles is matched by the complexity of their regulation, which involves numerous signalling systems, including purinergic, glutamatergic, GABAergic, adrenergic, and cholinergic pathways, as well as hormonal and peptide modulators. Astrocytes express specific receptors for each of these signalling systems, through which they mediate essential functions (Akther & Hirase, 2022). For instance, purinergic signalling, mediated by ATP and adenosine, modulates astrocytic Ca^{2+} dynamics, gliotransmitter release, and neurovascular coupling (Akther & Hirase, 2022; Pelligrino et al., 2011). Glutamatergic and GABAergic inputs provide astrocytes with direct readouts of synaptic activity, enabling them to adjust neurotransmitter clearance and metabolic support accordingly (Akther & Hirase, 2022; Magistretti & Allaman, 2018). Cholinergic signalling further modulates astrocyte excitability and influences plasticity-related processes (Araque et al., 2014; Takata et al., 2011). Together,

these systems and others, provide a rich regulatory framework that allows astrocytes to integrate diverse neural and systemic signals.

Among the neuromodulatory networks influencing astrocyte physiology, the endocannabinoid system (ECS) has emerged as a key player capable of integrating synaptic activity with metabolic and vascular responses, thereby providing a critical link between neuronal signalling and the broader homeostatic functions of the brain (Lu & Mackie, 2021). The following sections will examine the ECS in detail, with a particular focus on how activation of the cannabinoid type 1 receptor can modulate brain energy metabolism.

3. Brief overview of the endocannabinoid system

The ECS has emerged over the past 30 years as one of the most important neuromodulatory networks in the mammalian brain (Lu & Mackie, 2021). Its discovery was initially triggered by the isolation of the primary psychoactive compound of *Cannabis sativa*, (–)-trans-Δ^9-tetrahydrocannabinol (Δ^9-THC) (Mechoulam & Gaoni, 1965), which paved the way for the identification of cannabinoid-binding receptors (CBRs) in the 1990s (Matsuda et al., 1990; Munro et al., 1993). These findings were followed by the description of endogenous ligands for these cannabinoid receptors, the so-called endocannabinoids (eCBs). Among others, these discoveries helped to define the core components of the ECS: two main receptors, cannabinoid type-1 (CB1R) and type-2 (CB2R) receptors, their endogenous ligands, and the enzymes responsible for eCB synthesis and degradation (Iannotti et al., 2016; Lu & Mackie, 2021; Martinez Ramirez et al., 2023).

The ECS is now recognized as one of the most extensive neuro-modulatory systems of the mammalian brain (Busquets-García et al., 2022; Gorzkiewicz & Szemraj, 2018), regulating a broad array of physiological processes including nociception, motor coordination, thermoregulation, sleep, synaptic plasticity, learning and memory, emotional behaviour, stress responses, appetite, immune modulation, metabolism, and reproductive function (Meccariello et al., 2020). Within the CNS, it is especially critical for diverse cognitive functions such as emotional regulation and memory formation (Campolongo & Trezza, 2012; Lowe et al., 2021; Marsicano & Lafenêtre, 2009).

Both CB1R and CB2R are members of the GPCR superfamily, characterized by seven transmembrane domains, and are primarily coupled to Gi/o proteins. Upon activation, these receptors inhibit adenylyl cyclase (AC), reduce activity of voltage-gated calcium (Ca^{2+}) channels, and activate inward-rectifying K^+ channels and MAP kinase pathways, though

responses vary by cell type (Battista et al., 2012; Iannotti et al., 2016; R. Pertwee, 2010). CB1R is the main signalling hub of the brain ECS and are predominantly expressed in presynaptic membranes throughout the brain, where they modulate neurotransmitter release. On the other hand, CB2Rs are more associated with peripheral immune cells, though they are increasingly recognized in microglia and other CNS immune populations, especially during pathological conditions (Atwood & MacKie, 2010; Herkenham et al., 1990; Lu & Mackie, 2021).

Unlike classical neurotransmitters, which are synthesized to be stored in synaptic vesicles, the eCBs are produced on demand, typically in response to postsynaptic depolarization or activation of GPCRs (Lu & Mackie, 2021). The two primary eCBs are arachidonoyl ethanolamide (anandamide, AEA) and 2-arachidonoylglycerol (2-AG), both lipid-derived molecules originating from membrane phospholipids (Devane et al., 1992; Mechoulam et al., 1995). While CB1R and CB2R remain the primary targets of eCBs, many of these lipids also modulate the activity of other proteins, including peroxisome proliferator-activated receptors (PPARs) and transient receptor potential (TRP) channels, especially the acylethanolamides (Howlett, 2002; Lu & Mackie, 2021).

Classically, endocannabinoids are considered to work as retrograde messengers. They are synthesized and released from postsynaptic neurons in response to depolarization and bind presynaptic CB1Rs to suppress both excitatory and inhibitory neurotransmitter release (Heifets & Castillo, 2009). This mechanism is now a well-established example of retrograde synaptic signalling. However, accumulating evidence has expanded our understanding of CB1R distribution, revealing that these receptors are also expressed post-synaptically, as well as on intracellular organelles such as mitochondria and endosomes, where they modulate metabolic and signalling events (Fig. 6) (Fernández-Moncada, Rodrigues, et al., 2024; Lutz, 2020). For instance, the mitochondria-associated CB1R (mtCB1R) found in different brain cell types, have been shown to play critical roles in controlling intracellular Ca^{2+} signalling, synaptic transmission and brain bioenergetics (Eraso-Pichot et al., 2023; Fernández-Moncada, Lavanco, et al., 2024; Hebert-Chatelain et al., 2016; Jimenez-Blasco et al., 2020; Serrat et al., 2021).

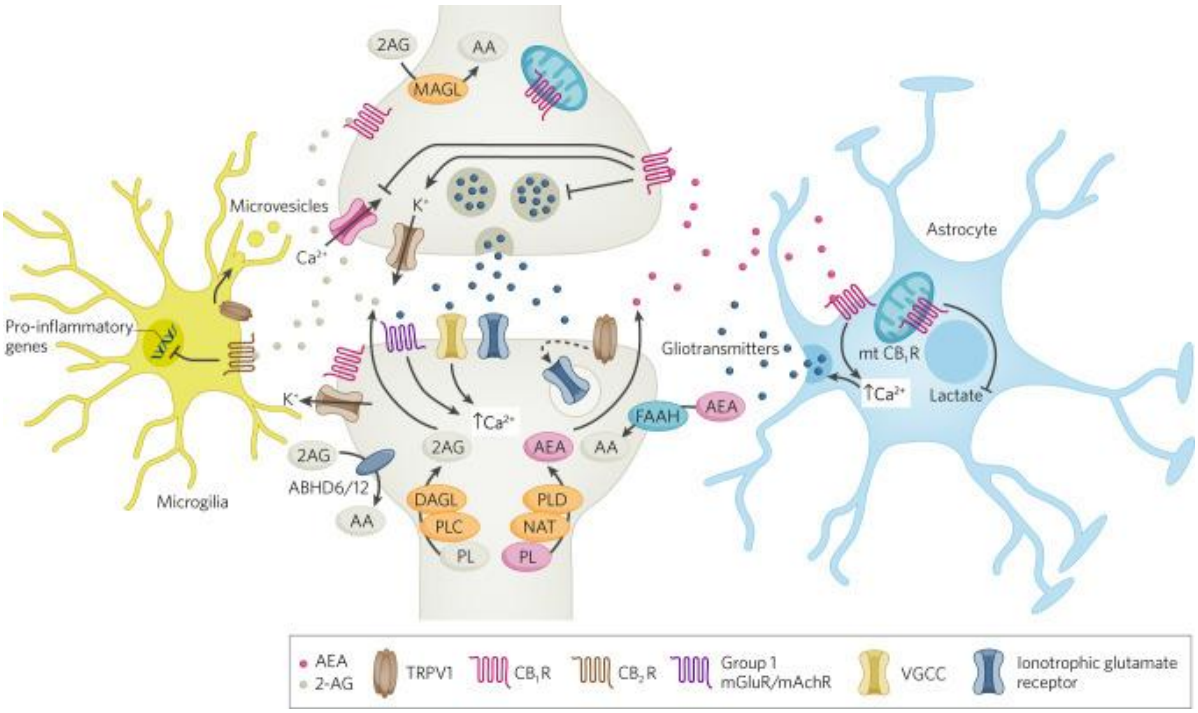

Figure 6. Schematic representation of endocannabinoid signalling across tripartite synapse.
eCBs are synthesized in the postsynaptic neuron in response to elevated intracellular Ca^{2+} and act retrogradely on presynaptic CB1Rs to suppress neurotransmitter release. AEA can also activate postsynaptic TRPV1 receptors, triggering long-term depression (LTD) via glutamate receptor internalization. Astrocytic CB1Rs modulate intracellular Ca^{2+} levels, promoting gliotransmitter release and influencing nearby synapses. In microglia, CB2 receptor activation regulates cytokine release. Additionally, mitochondrial CB1Rs contribute to intracellular metabolic regulation. Figure from (Scheyer et al., 2022).

Importantly, CBR1s are also expressed in glial cells, particularly astrocytes. Early studies highlighted a significant role for astrocytic CB1Rs in modulating synaptic transmission and influencing behavioural responses (Eraso-Pichot et al., 2023; Fernández-Moncada & Marsicano, 2023; Metna-Laurent & Marsicano, 2015). These findings expand the classical neuron-centric view of the ECS and suggest that astrocyte-specific endocannabinoid signalling may be critical for regulating CNS homeostasis and plasticity.

3.1. ECS ligands: cannabinoids

Several classes of cannabinoids have been identified over the years, and they are commonly categorized based on their pharmacological properties, molecular structure, or origin (Fig. 7). These include:

- eCBs**,** such as 2-AG and AEA.
- Phytocannabinoids, naturally occurring compounds found in *Cannabis sativa*, such as Δ^9-THC and cannabidiol (CBD).

- Synthetic cannabinoids**,** such as indole-derived compounds like WIN55,212-2 and bicyclic cannabinoids like CP55,940.
- Antagonists and inverse agonists, including highly selective CB1R antagonists like AM251.

(Adel & Alexander, 2021; Devane et al., 1992; D'mbra et al., 1992; Morales & Reggio, 2021; Rock & Parker, 2021; Stella, 2023).

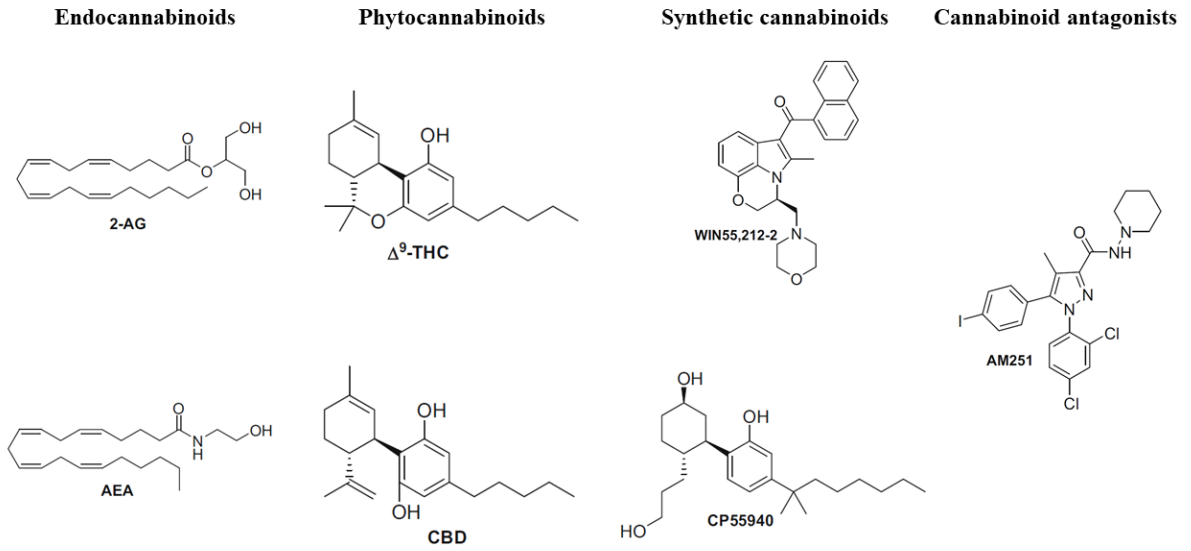

Figure 7. Example of the 4 different classes of cannabinoids.
Picture adapted from (Morales & Reggio, 2021).

Interestingly, although a lot of agonists are slightly selective between CB1 and CB2 receptors, cannabinoid antagonists tend to be highly selective, with some demonstrating over 1000-fold preference for one receptor subtype over the other (Howlett & Abood, 2017).

3.1.1. Endocannabinoids

eCBs are endogenous lipidic molecules that act as agonists for CB1R and CB2R (Simankowicz & Stępniewska, 2025; Wilson & Nicoll, 2001). These molecules are eicosanoids derived from arachidonic acid (AA) and other polyunsaturated fatty acids (Morales & Reggio, 2021). Among them, AEA and 2-AG were the first discovered eCBs and are the most abundant endogenous ligand of the brain ECS in mammals (Martinez Ramirez et al., 2023; Wilson & Nicoll, 2001). Several other endocannabinoid-like compounds have since been identified, including 2-arachidonyl glycerol ether (noladin ether or 2-AGE), N-arachidonoyl dopamine (NADA), palmitoylethanolamide (PEA), virodhamine, and oleamide (Bisogno et al., 2000; Hanus et al., 2001; Iannotti et al., 2016; Porter et al., 2002). Currently, AEA and 2-AG remain the best-characterized in terms of biosynthesis, metabolism, and pharmacology. Although AEA was

identified first due to its CB1R activation properties, earning its name from the Sanskrit word ananda (bliss) (Devane et al., 1992), substantial evidence now suggests that 2-AG may serve as the more potent endogenous ligand for CB1Rs, particularly in central synapses (Katona & Freund, 2008; Nikas et al., 2024).

Unlike classical neurotransmitters, eCBs are not pre-packaged in vesicles. These molecules are derived from hydrophobic membrane lipid precursors, and synthesized on demand in response to physiological stimuli, such as GPCR activation or membrane depolarization (Eraso-Pichot et al., 2023; Gorzkiewicz & Szemraj, 2018; Lu & Mackie, 2021). Once synthesized, eCBs are rapidly released and typically act in a paracrine manner, although autocrine signalling has also been described (Bacci et al., 2004; Piomelli, 2003).

Despite their structural similarity, AEA and 2-AG are generated and degraded by distinct enzymatic pathways and display different affinities and efficacies at cannabinoid receptors. For instance, 2-AG acts as a full agonist with high affinity for both CB1R and CB2R, whereas AEA is a partial and biased agonist, showing moderate affinity for CB1R and low affinity for CB2R (Howlett, 2002; Simankowicz & Stępniewska, 2025). In the striatum, a region essential for motor and cognitive function and rich in CB1Rs expression and, AEA selectively inhibits excitatory (glutamatergic) synapses, whereas 2-AG preferentially modulates inhibitory (GABAergic) synapses (Maccarrone et al., 2008). Moreover, the distribution and concentration of AEA and 2-AG vary across brain regions (Bisogno et al., 1999; Lemtiri-Chlieh & Levine, 2022). Notably, 2-AG also serves as a principal source of AA for prostaglandin synthesis in tissues such as the brain, liver, and lungs; indicating broader physiological roles beyond classical endocannabinoid signalling, including inflammation and immune regulation (Turcotte et al., 2015).

The synthesis and degradation of eCBs are tightly regulated by distinct enzymatic pathways that determine the magnitude and duration of ECS signalling. AEA can be synthesized through multiple enzymatic pathways starting from N-acyl-phosphatidylethanolamine (NAPE). The most well-known route involves the direct hydrolysis of NAPE by a NAPE-specific phospholipase D (NAPE-PLD). Alternatively, NAPE can be hydrolysed by a NAPE-selective phospholipase C (NAPE-PLC), producing phospho-anandamide, which is then dephosphorylated to yield AEA. Another pathway involves dual hydrolysis of NAPE acyl chains by the phospholipase B enzyme (ABHD4), followed by the action of glycerophosphodiester phosphodiesterase 1 (GDE1) to release AEA. Lastly, hydrolysis of a single acyl chain can generate lyso-NAPE, from which AEA is liberated by lyso-NAPE-PLD

(Maccarrone et al., 2015; Piomelli, 2003; Rezende et al., 2023; Simon & Cravatt, 2010; Tsuboi et al., 2013). On the other hand, 2-AG is produced through a two-step process. First, phospholipase C (PLC) hydrolyse phosphatidylinositol-bisphosphate (PIP2), generating 1,2-diacylglycerol (DAG). Then, DAG is hydrolysed by diacylglycerol lipase (DAGL), which has two isoforms, namely DAGLα and DAGLβ (Bisogno et al., 2003; Murataeva et al., 2014; Shonesy et al., 2015). Of note, DAGLα seems to be the main isoform responsible for 2-AG production (Tanimura et al., 2010).

Once released, these endocannabinoids are rapidly degraded to terminate their signalling actions. AEA degradation is primarily carried out by fatty acid amino hydrolase (FAAH) (Cravatt et al., 1996), an enzyme responsible for the hydrolysis of numerous fatty acid amides, including ethanolamides. Beyond its involvement on ECS functions, FAAH is an important therapeutical component, as its substrates have in general an extensive range of actions in our organism (Luchicchi et al., 2010). A different pathway to degrade AEA is mediated by cyclooxygenase-2 (COX-2) which oxidizes AEA in order to create prostamides, a class of endogenous molecules with its own physiological and pharmacological function (Rezende et al., 2023; Urquhart et al., 2015; Woodward et al., 2008). Finally, another less investigated pathway for AEA degradation is through N-acylethanolamine-hydrolysing acid amidase (NAAA) that supposedly is engaged when alteration to FAAH activity occurs (Tsuboi et al., 2005; Xie et al., 2022). Finally, 2-AG is primarily degraded through hydrolysis by three key enzymes: monoacylglycerol lipase (MAGL) and the alpha/beta domain-containing hydrolases 6 and 12 (ABHD6 and ABHD12) (Blankman et al., 2007; Rezende et al., 2023). In the mouse brain, MAGL is responsible for approximately 85% of 2-AG hydrolysis and its deletion can lead to up to a tenfold increase in 2-AG levels (Blankman et al., 2007; Schlosburg et al., 2010). ABHD12 and ABHD6 contribute to the remaining hydrolysis, responsible for about 9% and 4%, respectively (Blankman et al., 2007).

3.1.2. Exogenous cannabinoids: Δ^9-THC, CBD & and synthetic cannabinoids

Δ^9-THC is the principal psychotropic compound in cannabis, primarily responsible for its euphoric effects, as well as many of its therapeutic properties, including analgesia, appetite stimulation, and sedation (dos Santos et al., 2021; Stella, 2023). It belongs to the phytocannabinoid class, a diverse group of over 100 terpenophenolic compounds found among the ~400 metabolites produced by *Cannabis sativa* that interact with the ECS (Jurga et al., 2024; Maroon & Bost, 2018). The chemical structure of Δ^9-THC was first elucidated in 1965 by Mechoulam and colleagues, following its isolation from the resin of female Cannabis sativa

inflorescences (Mechoulam & Gaoni, 1965). Like most phytocannabinoids, Δ⁹-THC is biosynthesized in its acidic precursor form, Δ⁹-tetrahydrocannabinolic acid (Δ⁹-THCA), which readily decarboxylates into its active form when exposed to heat or light (Rock & Parker, 2021).

The psychoactive effects of Δ⁹-THC are primarily mediated through its partial agonist activity at CB1Rs in the central nervous system. Compared to the precise, endogenous activation of CB1Rs by eCBs during retrograde synaptic signalling, Δ⁹-THC elicits a broader and less selective response (Blebea et al., 2024; R. G. Pertwee, 2008). Nonetheless, Δ⁹-THC exhibits a range of therapeutic properties - including anticonvulsant, antinociceptive, antiemetic, and appetite-stimulating effects - which support its clinical application in conditions such as multiple sclerosis, epilepsy, neuropathic pain, and cancer (Baker et al., 2003; Blebea et al., 2024; Jurga et al., 2024; Maroon & Bost, 2018; Moore et al., 2021; Pacher et al., 2006; Stella, 2023).

However, the cannabis intoxication occurring with plant varieties high in Δ⁹-THC percentage, is also associated with acute cognitive impairments - including deficits in learning, attention, and working memory - as well as an increased risk of psychiatric conditions such as schizophrenia and psychosis (Crane et al., 2013; Hoch et al., 2025; Joshi & Onaivi, 2021; Ranganathan & D'Souza, 2006; Stella, 2023). Cannabis use disorder (CUD) is a clinically recognized condition linked to chronic cannabis consumption, characterized by a range of cognitive and behavioural impairments, including deficits in memory processing, decision-making, academic and occupational performance, as well as disrupted social functioning (Hoch et al., 2025; Joshi & Onaivi, 2021; Stella, 2023). Whether these effects persist long-term remains still scantly understood (Hoch et al., 2025; Volkow et al., 2016). Importantly, the overall therapeutic or adverse effects of cannabis are thought to depend on the synergistic interactions among its various phytocannabinoids (dos Santos et al., 2021). For instance, high-potency cannabis rich in Δ⁹-THC has been linked to a greater incidence of adverse effects compared to strains with a more balanced cannabinoid profile, particularly those with THC and CBD present in roughly equal proportions (Di Forti et al., 2015; Stella, 2023; Volkow et al., 2016).

The pharmacological actions of Δ⁹-THC are complex and appears to be brain region-dependent, influenced by the cell type-specific of cannabinoid receptor engaged and the G-protein coupling efficiency, which differ between cell subpopulations (Bellocchio et al., 2010). In areas with low CB1R or CB2R density, Δ⁹-THC may even antagonize the effects of endogenous or exogenously administered cannabinoids (Hempel & Xi, 2021a; R. G. Pertwee, 2008).

Pharmacokinetically, Δ⁹-THC is rapidly cleared from plasma but distributes extensively due to its lipophilicity (Caicedo et al., 2025; Chayasirisobhon, 2020). It accumulates in adipose tissue, where peak levels are reached within five days, followed by slow redistribution to other tissues, including the brain (Ashton, 2001; Chayasirisobhon, 2020). In the brain, Δ⁹-THC is unevenly distributed, concentrating in neocortical, limbic, sensory, and motor regions (Eggan & Lewis, 2007; Upadhyay et al., 2023). Its metabolites are primarily excreted via the gastrointestinal tract (~65%) and to a lesser extent via urine (~25%), with enterohepatic recirculation further extending its effects (Agurell et al., 1986; Chayasirisobhon, 2020; Huestis, 2007).

Although the present thesis focuses on CB1Rs and consequently on Δ⁹-THC exposure, certain features of CBD merit mention. As the principal non-psychoactive component of *cannabis*, CBD does not activate CB1R or CB2R receptors, likely explaining its lack of psychotropic effects. Instead, it acts via a myriad of alternative molecular targets: it antagonizes the G protein-coupled receptor 55 (GPR55) and the transient receptor potential of the melastatin type 8 (TRPM8), and serves as an agonist at TRPV1, TRPV2 channels, and the nuclear receptor PPAR-γ (Bisogno et al., 2001; dos Santos et al., 2021). Additionally, CBD functions as a non-competitive CB1R antagonist and an inverse agonist at CB2R (Thomas et al., 2007). Critically, CBD modulates Δ⁹-THC's pharmacological profile, diminishing some of its psychotropic effects while enhancing therapeutic outcomes (Stella, 2023). CBD also exerts anxiolytic, antipsychotic, and neuroprotective effects. Emerging clinical and preclinical evidence support its potential use in treating epilepsy, substance use disorders, schizophrenia, social anxiety, post-traumatic stress disorder, depression, bipolar disorder, sleep disturbances, and Parkinson's disease (Crippa et al., 2018).

The therapeutic relevance of the ECS has driven the development of numerous synthetic cannabinoids. These cannabimimetic compounds aim to create drugs with improved selectivity, efficacy, and pharmacokinetic profiles while minimizing adverse effects. Strategies include the design of selective CB1R or CB2R agonists/antagonists, allosteric modulators, biased agonists, and inhibitors of key metabolic enzymes such as FAAH and MAGL. Additionally, compounds targeting peripheral cannabinoid receptors are being explored to reduce central side effects (Morales & Jagerovic, 2020; Morales & Reggio, 2021). One of the most know and used synthetic cannabinoid is an aminoalkyindole, namely R-(+)-WIN55,212–2, a potent dual CB1R/CB2R receptor agonist (D'mbra et al., 1992).

3.2. Cannabinoid receptors

As previously noted, the ECS comprises two well-characterized cannabinoid receptors: CB1R and CB2R. CB1Rs are among the most abundant GPCRs in the mammalian CNS, with expression levels comparable to those of glutamate and GABA receptors (Chou et al., 2022; R. Pertwee, 2010). In contrast, CB2Rs are primarily found in immune and hematopoietic cells and, within the brain, are mainly localized to microglia and vascular components, though their precise neuronal distribution and functional roles remain subjects of ongoing debate (Atwood & MacKie, 2010; Ferranti & Foster, 2022; Joshi & Onaivi, 2021; Munro et al., 1993; Núñez et al., 2004). Both receptors belong to the GPCR family and share the canonical seven-transmembrane alpha-helical architecture (Iannotti et al., 2016). Beyond CB1R and CB2R, several other receptor classes interact with cannabinoids, including TRP channels - particularly the vanilloid subfamily (TRPVs) - PPARs, and metabotropic receptors such as G protein-coupled receptor 55 (GPR55) interact with various eCBs (Etemad et al., 2022; Lu & MacKie, 2016; Ye et al., 2019) Given the focus of this thesis, the discussion will predominantly centre on brain CB1Rs.

3.2.1. Cellular distribution of CB1R in the brain

CB1R mRNA, transcribed from the CNR1 gene, was identified in brain samples of rodents (Marsicano & Lutz, 1999) and humans (Mailleux & Vanderhaeghen, 1994; Westlake et al., 1994) through in situ hybridization (ISH). Protein-level mapping via immunohistochemistry has revealed a dense and heterogeneous anatomical distribution of CB1Rs around the brain, particularly in regions involved in motor control, cognition, memory, and sensory integration. High CB1R expression is observed in the cerebellum, supporting a role in fine-tuning cerebellar output and motor coordination. The basal ganglia also display prominent CB1R expression, including the substantia nigra pars reticulata (SNr), entopeduncular nucleus, and the dorsolateral caudate-putamen. These areas are key nodes in motor circuitry and suggest that CB1Rs are integral modulators of motor planning and execution (Kano et al., 2009; Moldrich & Wenger, 2000).

The hippocampus and neocortex show substantial CB1R presence, where they are primarily located on specific subsets of GABAergic interneurons. In particular, CB1Rs are highly enriched on cholecystokinin-positive (CCK+) basket cells, which play a critical role in controlling local excitability and network oscillations (Katona et al., 2000; Marsicano et al., 2003). Although CB1R expression on glutamatergic pyramidal neurons is significantly lower,

it is nonetheless functionally important and contributes to activity-dependent modulation of excitatory transmission (Bodor et al., 2005; Katona & Freund, 2012).

Beyond the hippocampus and cortex, CB1Rs are also detected in the olfactory bulb, contributing to sensory processing (Gómez-Sotres et al., 2024; Soria-Gómez et al., 2014), and in limbic structures like the amygdala, involved in emotional regulation (Haghparast et al., 2014; Katona et al., 2001). Lower receptor densities are found in the thalamus and habenula, indicating more specialized or region-specific roles (Dasilva et al., 2012; Soria-Gómez et al., 2015; Zapata & Lupica, 2021).

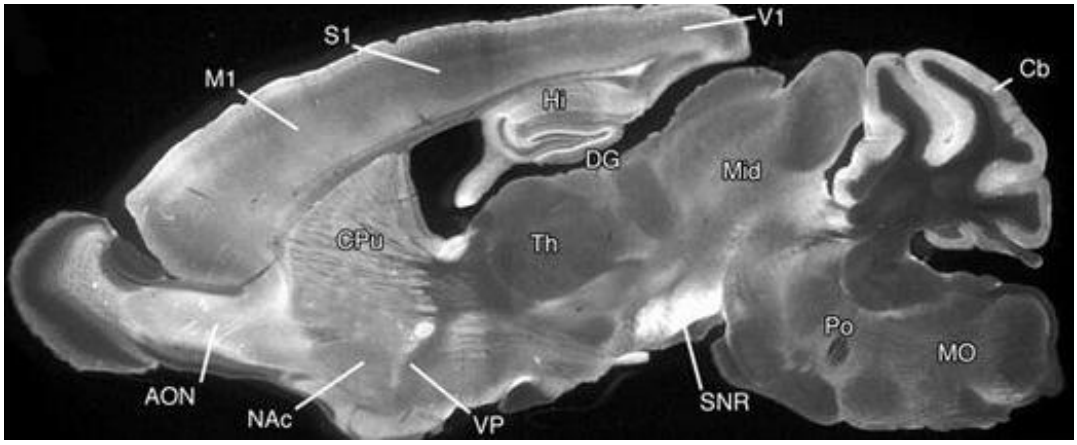

Figure 8. Distribution of CB1 receptors expression in the CNS of adult mice.
The image corresponds to an immunohistochemistry analysis (Kano et al., 2009).

Notably, the density of CB1Rs varies across interneuron subtypes, leading to differential modulation of synaptic transmission (Busquets-Garcia et al., 2017; Fernández-Moncada, Rodrigues, et al., 2024; Katona & Freund, 2012). Although CB1Rs are primarily localized to presynaptic terminals, they are also found post-synaptically. Additionally, CB1Rs have been shown to form heterodimers with other GPCRs, such as dopamine D2, adenosine A2A, and orexin type 1 receptors, suggesting a complex and versatile role in neuromodulation (Katona et al., 1999; Lutz, 2020; Przybyla & Watts, 2010; Xu et al., 2011).

Intriguingly, CB1Rs are not limited to neurons but are also expressed in non-neuronal brain cells, particularly astrocytes. Although astrocytic CB1Rs are present at relatively low levels, their activation has been shown to modulate the energy metabolism, together with triggering the release of gliotransmitters, thereby significantly influencing synaptic transmission (Busquets-Garcia et al., 2017; Eraso-Pichot et al., 2023; Fernández-Moncada & Marsicano, 2023). Despite their modest expression, astroglial CB1Rs play a crucial role in neuron–glia communication and have been implicated in diverse behavioural processes, including memory consolidation and social transmission of stress (Fernández-Moncada, Lavanco, et al., 2024;

Gómez-Sotres et al., 2024; Navarrete & Araque, 2008; Oliveira da Cruz et al., 2016; Robin et al., 2018). This underscores the notion that receptor localization - not merely abundance - is key to understanding CB1R function (Busquets-Garcia et al., 2016, 2017; Fernández-Moncada & Marsicano, 2023; Marsicano & Kuner, 2008). Given the relevance to the central topic of this thesis, a more detailed discussion of astrocytic CB1R mechanisms will follow in the next sections.

3.2.2. Subcellular distribution of CB1R

CB1R is widely expressed on the plasma membrane of neurons, where it primarily functions as a presynaptic modulator of neurotransmitter release. This classical localization enables retrograde endocannabinoid signalling, leading to the suppression of synaptic transmission across a variety of neural circuits (Lu & Mackie, 2021). However, advances in high-resolution imaging and subcellular fractionation techniques have shown that CB1Rs are not only confined to the cell surface. Instead, they are also present in various intracellular compartments, expanding both their anatomical distribution and functional repertoire (Busquets-Garcia et al., 2017; Hebert-Chatelain et al., 2014).

At the subcellular level CB1Rs have been detected within endosomal and lysosomal compartments, where they can initiate G protein-dependent signalling independent of plasma membrane activation (Rozenfeld & Devi, 2008; Thibault et al., 2013).

In 2012, electron microscopy and immunogold labelling combined with controlled functional assays, demonstrated that a small but functionally significant fraction of CB1R in the hippocampus are associated to mitochondrial membranes – referred to as mtCB1R - where they mediate a reduction of O_2 consumption in response to both exogenous and endogenous cannabinoids (Bénard et al., 2012; Hebert-Chatelain et al., 2014). Importantly, mtCB1Rs are not restricted to neurons; they are also expressed in astrocytes, alongside their plasma membrane counterparts, where they play essential roles in modulating diverse cellular processes and influencing behavioural outcomes (Gutiérrez-Rodríguez et al., 2018; Jimenez-Blasco et al., 2020).

Despite significant progress in characterizing the signalling cascades and intracellular dynamics of distinct CB1R subcellular pools, such as those localized at the plasma membrane and mitochondria, the full complexity of this system remains elusive. In particular, the mechanisms governing CB1R trafficking to either mitochondrial or plasma membranes, the turnover rates,

and potential modulation by neuronal activity, metabolic state, or pathological conditions, are still poorly understood (Fernández-Moncada, Rodrigues, et al., 2024).

3.3. CB1R modulation of brain function & behaviour

CB1R activation exert a powerful control of brain functions, influencing a wide array of physiological and behavioural processes, including synaptic transmission, neuroplasticity, emotional regulation, feeding behaviour, pain perception, and energy metabolism. The effects of CB1R activation are highly context-dependent and are mediated through distinct molecular pathways that vary according to the cellular and subcellular localization of the receptor (Busquets-Garcia et al., 2017; Fernández-Moncada, Rodrigues, et al., 2024; Lu & Mackie, 2021).

As elucidated in the previous paragraphs, rather than functioning as a uniform signalling entity, CB1Rs are organized into spatially and functionally distinct pools across various brain cell types - neurons, astrocytes, and other glial populations - as well as within specific subcellular compartments such as the plasma membrane, endosomes, and mitochondria. Each of these pools engages unique intracellular cascades, enabling precise and localized modulation of neuronal activity and intercellular communication. This compartmentalization of CB1R signalling adds a significant layer of complexity to our understanding of endocannabinoid function in the central nervous system.

In the following sections, I will describe the major signalling pathways triggered by CB1R activation and how they differ based on cellular and subcellular localization. Particular attention will be given to how specific CB1R pools contribute to the regulation of brain bioenergetics, synaptic function, and behavioural outcomes. This framework will provide the foundation for understanding the diverse physiological roles of the endocannabinoid system, as well as its possible involvement in neurological and psychiatric disorders.

3.3.1. CB1R-mediated intracellular cascades

One of the central intracellular mechanisms regulating several cell functions, such as cell health, differentiation and proliferation is the AC-cyclic adenosine monophosphate (cAMP) signalling cascade (Aslam & Ladilov, 2023; Sunahara et al., 1996). CB1Rs, primarily coupled to inhibitory Gi/o proteins on their intracellular domains, suppress AC activity upon activation. This leads to reduced cAMP levels and, consequently, diminished activation of protein kinase A (PKA) (Howlett, 2002; Howlett & Abood, 2017; Leo & Abood, 2021). PKA is a Ser/Thr kinase composed of two regulatory and two catalytic subunits. When cAMP binds the

regulatory subunits, the catalytic subunits are released and able to phosphorylate downstream targets. Thus, CB1R activation indirectly suppresses PKA activity via inhibition of the cAMP production (Di Marzo et al., 1998; Fernández-Moncada, Rodrigues, et al., 2024; Leo & Abood, 2021; Piomelli, 2003). This pathway also modulates various ion channels, including voltage-gated K^+ and Ca^{2+} channels, thereby impacting neuronal excitability and synaptic strength (Busquets-Garcia et al., 2017; Y. F. Lin, 2021; Miraucourt et al., 2016; Sánchez et al., 2003). Importantly, retrograde cAMP/PKA signalling is essential for short- and long-term regulation of excitatory and inhibitory synapses, making it a pivotal mechanism in synaptic plasticity (Iannotti et al., 2016; Lu & Mackie, 2021).

Additionally, CB1Rs can directly inhibit voltage-gated Ca^{2+} channels (VGCCs), particularly N- and P/Q-type channels, via Gi/o protein activation. This suppression of Ca^{2+} influx at presynaptic terminals further reduces the probability of synaptic vesicle fusion and neurotransmitter release, thereby reinforcing the CB1R-mediated dampening of synaptic activity (Boczek & Zylinska, 2021). By modulating both excitatory and inhibitory synapses through this pathway, CB1Rs exert a fine-tuned regulatory influence on neuronal excitability. Beyond synaptic transmission, this inhibition of Ca^{2+} entry also has broader implications for neuronal health, as it can protect neurons from Ca^{2+}-induced excitotoxicity, a key contributor to neurodegenerative processes. As such, CB1Rs play a key role in maintaining neuronal homeostasis by regulating both cell viability and synaptic function (Boczek & Zylinska, 2021; Elphick & Egertová, 2001; Kano et al., 2009; Twitchell et al., 1997).

CB1R is not limited to canonical Gi/o-mediated inhibition of AC, but it can also engage a variety of intracellular signalling cascades, depending on the cellular context, receptor density, and receptor compartmentalization. One well-characterized pathway is the activation of the mitogen-activated protein kinase (MAPK) cascade, including ERK1/2, JNK, and p38 MAPKs. This pathway is primarily initiated through βγ subunits released from Gi/o proteins, which can stimulate Ras-related proteins and subsequently trigger a phosphorylation cascade involving Raf, MEK, and ERK. This activation has been implicated in diverse processes such as cell survival, synaptic plasticity, and gene expression (Turu & Hunyady, 2010).

In addition to MAPK signalling, CB1Rs are capable of coupling to alternative G proteins, including Gs and Gq/11. For instance, Gq/11-mediated coupling in astrocytes leads to the activation of phospholipase C-beta (PLCβ), resulting in the hydrolysis of PIP2 into diacylglycerol (DAG) and inositol trisphosphate (IP3). IP3 then promotes the release of Ca^{2+} from intracellular stores via IP3 receptors, while DAG activates protein kinase C (PKC),

influencing downstream targets such as ion channels and transcription factors (Gómez Del Pulgar et al., 2000; Navarrete & Araque, 2010).

Moreover, CB1Rs have been shown to activate the phosphoinositide 3-kinase (PI3K)/Akt signalling pathway through both Gi/o and Gq mechanisms. This pathway is crucial for modulating cell growth, metabolism, and survival, and it plays a role in the neuroprotective and anti-apoptotic effects of CB1R activation in neurons and glia. Importantly, the engagement of these non-canonical cascades may vary across subcellular compartments, adding an additional layer of complexity to CB1R signalling (Blázquez et al., 2015; Haspula & Clark, 2020; Ozaita et al., 2007).

3.3.2. Neuronal CB1R and synaptic plasticity

In neurons, CB1R-mediated signalling governs several forms of synaptic plasticity, including:

- depolarization-induced suppression of excitation and inhibition (DSE and DSI)
- metabotropic-induced suppression of excitation and inhibition (MSE and MSI)
- endocannabinoids-induced long-term depression (eLTD)

(Lu & Mackie, 2021)

DSI and DSE are transient forms of short-term synaptic plasticity triggered by brief postsynaptic depolarization, typically lasting less than 90 seconds. DSI leads to a temporary suppression of GABAergic inhibitory inputs, while DSE affects glutamatergic excitatory transmission (Augustin & Lovinger, 2018; Kreitzer & Regehr, 2001). DSE generally requires longer depolarization for induction and is less prominent in the hippocampus than DSI, likely due to the higher expression of CB1Rs on GABAergic neurons relative to glutamatergic pyramidal cells (Gorzkiewicz & Szemraj, 2018). Interestingly, in the striatum, AEA appears to selectively inhibit excitatory synapses, whereas 2-arachidonoylglycerol 2-AG predominantly modulates inhibitory GABAergic transmission (Maccarrone et al., 2008). Both DSI and DSE are sensitive to CB1R blockade, confirming their mediation by the endocannabinoid system (Martinez Ramirez et al., 2023; Ohno-Shosaku et al., 2001).

MSE and MSI represent more sustained and widespread forms of endocannabinoid-mediated synaptic plasticity. They are initiated through the already described activation of Gq/11-coupled GPCRs, which stimulate PLCβ. This enzyme hydrolyses PIP2 into IP3 and DAG; DAG is subsequently converted to 2-AG, which then retrogradely activates presynaptic CB1Rs to

suppress neurotransmitter release (Augustin & Lovinger, 2018; Lu & Mackie, 2021; Martinez Ramirez et al., 2023). MSE/MSI can be elicited by a range of GPCRs, including muscarinic acetylcholine receptors M1/M3, metabotropic glutamate receptors mGluR1 and mGluR5, and α1-adrenergic receptors (Kano et al., 2009).

Finally, CB1R-mediated eLTD is a widely expressed mechanism of long-lasting synaptic suppression, typically induced by sustained low-frequency stimulation. eLTD is particularly prominent at glutamatergic synapses in both the dorsal and ventral striatum (Chevaleyre & Castillo, 2003; Gerdeman & Lovinger, 2003; Piette et al., 2020; Robbe et al., 2002), and has been implicated in the developmental refinement of cortical circuits (Jiang et al., 2010).

Interestingly, activation of CB1R at distinct subcellular locations within the same neuronal circuit can determine distinct behavioural outcomes. For instance, it has been shown that in the striatonigral pathway, pharmacological stimulation of CB1Rs induces both antinociception and catalepsy in mice. These effects are mediated by different receptor pools within the same neuronal terminals. Specifically, the antinociceptive effect is attributed to plasma membrane CB1Rs (pmCB1Rs), which inhibit cytosolic PKA activity and reduce the release of substance P. In contrast, mtCB1Rs at the same terminals are responsible for cannabinoid-induced catalepsy by suppressing intra-mitochondrial PKA activity, thereby impairing cellular respiration and synaptic transmission (Soria-Gomez et al., 2021). These findings underscore how subcellular-specific CB1R signalling within a single circuit can exert multimodal behavioural control through distinct molecular mechanisms.

3.3.3. Astroglial CB1R and gliotransmission

The discovery of CB1Rs in astrocytes has raised important questions about their role in synaptic regulation. Notably, the signalling mechanisms triggered by astrocytic CB1R activation differ substantially from those mediated by neuronal CB1Rs, adding a further layer of complexity to endocannabinoid signalling (Covelo & Araque, 2016; Navarrete & Araque, 2010). Despite relatively low expression levels, several studies have shown that hippocampal and cortical astrocytes express functional CB1Rs capable of modulating synaptic communication and plasticity (Busquets-Garcia et al., 2017; Eraso-Pichot et al., 2023; Navarrete et al., 2014). Astroglial CB1R, differently from the ones in neurons, have been suggested to be mainly coupled to Gαq/11 proteins. More specifically, both physiological and pharmacological activation of astroglial CB1Rs triggers an increase in intracellular Ca^{2+} levels via a PLC-

dependent signalling cascade, leading to IP3 production and the consequent release of Ca^{2+} from the endoplasmic reticulum (ER) (Covelo & Araque, 2016; Navarrete & Araque, 2008).

These Ca^{2+} transients, in turn, promote the release of various gliotransmitters, which mediate diverse short- and long-term effects on synaptic transmission and plasticity (Covelo et al., 2021). Moreover, this modulation of synaptic activity can occur at distant sites, a phenomenon known as lateral synaptic regulation (Covelo & Araque, 2016). First described in the hippocampal CA1 region, this mechanism involves astrocytic glutamate release that activates presynaptic mGluR1 receptors at distal synapses, enhancing glutamate release and inducing short-term potentiation (Navarrete & Araque, 2010). Thus, eCB signalling creates a spatial profile: synaptic depression near the release site (<60 µm) via presynaptic CB1Rs, and potentiation at more distant synapses (>60 µm) via astroglial CB1Rs. Similar dynamics have been observed in the dorsal striatum, central amygdala, and suprachiasmatic nucleus (SCN) (Covelo et al., 2021).

Notably, the physiological spreading of astrocytic Ca^{2+} events during lateral potentiation requires mtCB1R signalling. Specifically, activation of mtCB1Rs promotes Ca^{2+} transfer from the ER to mitochondria via ER-mitochondria contact sites (MERCs), and the mitochondrial Ca^{2+} uniporter (MCU). Disruption of either mtCB1R or MCU impairs this Ca^{2+} transfer, reducing Ca^{2+} signal propagation and abolishing lateral synaptic potentiation in hippocampal circuits. Thus, mtCB1R is crucial for astrocytic Ca^{2+} dynamics that support eCB-mediated synaptic plasticity (Serrat et al., 2021).

Importantly, astroglial CB1Rs are not only involved in short-term synaptic regulation, but they also mediate different forms of synaptic plasticity (Heifets & Castillo, 2009). In the neocortex, spike timing-dependent long-term depression (tLTD) - a form of synaptic plasticity requiring precise pre- and postsynaptic co-activation - depends on astrocytic CB1R activation, subsequent Ca^{2+} signalling, and SNARE-dependent glutamate release that engages presynaptic NMDA receptors to induce tLTD (Min & Nevian, 2012). Astrocytic CB1Rs also mediate LTD in the hippocampus, where their activation by Δ^9-THC or synthetic agonists elevates glutamate, triggering extra-synaptic NMDA receptor activation and AMPA receptor internalization, impairing spatial working memory (Han et al., 2012). Beyond LTD, endocannabinoids also promote LTP via astrocytic CB1Rs. In hippocampal circuits, astrocytic Ca^{2+} responses to endocannabinoids trigger D-serine release, facilitating NMDA-dependent LTP and memory consolidation (Robin et al., 2018).

3.3.4. CB1R modulation of brain energy metabolism

Recent studies have showed the involvement of the ECS in the regulation of glucose metabolism in brain cells, with CB1R emerging as key modulator of these metabolic processes (Fernández-Moncada, Lavanco, et al., 2024; Fernández-Moncada, Rodrigues, et al., 2024; Jimenez-Blasco et al., 2020). Exposure to Δ^9-THC in rats displays a biphasic effect on brain glucose metabolism, wherein low doses promote glucose consumption, while high doses lead to its reduction (Freedland et al., 2002; Margulies & Hammer, 1991; Miederer et al., 2017). The effects of cannabinoids are well known to be time-dependent (Fernández-Moncada, Rodrigues, et al., 2024). Specifically, Δ^9-THC exposure reduces glucose consumption in certain brain regions after one hour of treatment, but this alteration returns to control levels after six hours in most brain structures (Whitlow et al., 2002). Conversely, administration of a high dose of the synthetic cannabinoid HU210 induces a widespread increase in brain glucose consumption after one hour, which comeback to control levels after 24 hours of exposure (Nguyen et al., 2012). These findings indicate that the time-dependent effects of exogenous cannabinoids on brain glucose metabolism may play a role in the wide range of behavioural changes associated with cannabinoid exposure.

In the brain tissue, CB1R activation at presynaptic terminals suppresses neurotransmitter release, thereby reducing local energy requirements. Following the discovery of mtCB1Rs, it was demonstrated that their activation inhibits mitochondrial complex I activity, reduces OXPHOS, and decreases ATP production, ultimately modulating neuronal excitability and synaptic plasticity (Bénard et al., 2012; Hebert-Chatelain et al., 2014, 2016).

Notably, it has been shown that persistent activation (24 hours) of mtCB1R in astrocytes suppress glycolysis, thereby negatively impacting brain functions and social behaviour (Fig. 9) (Jimenez-Blasco et al., 2020). The long-lasting consequences of astroglial mtCB1R engagement are attributed to the inhibition of soluble adenylyl cyclase (sAC) and PKA signalling, which reduces the phosphorylation of the mitochondrial complex I subunit NDUFS4. Therefore, this leads to a decline in complex I stability and activity, together with diminished ROS production. This impairment of mitochondrial function results in the loss of hypoxia-inducible factor 1 (HIF-1) transcriptional activity, a fundamental regulator of glycolytic enzyme expression (Semenza et al., 1996). Eventually, this mtCB1R-mediated mitochondrial dysfunction leads to decreased astrocytic lactate synthesis, neuronal energetic

stress, and impaired social behaviour following 24 hours of exposure to THC (Fig. 9) (Jimenez-Blasco et al., 2020).

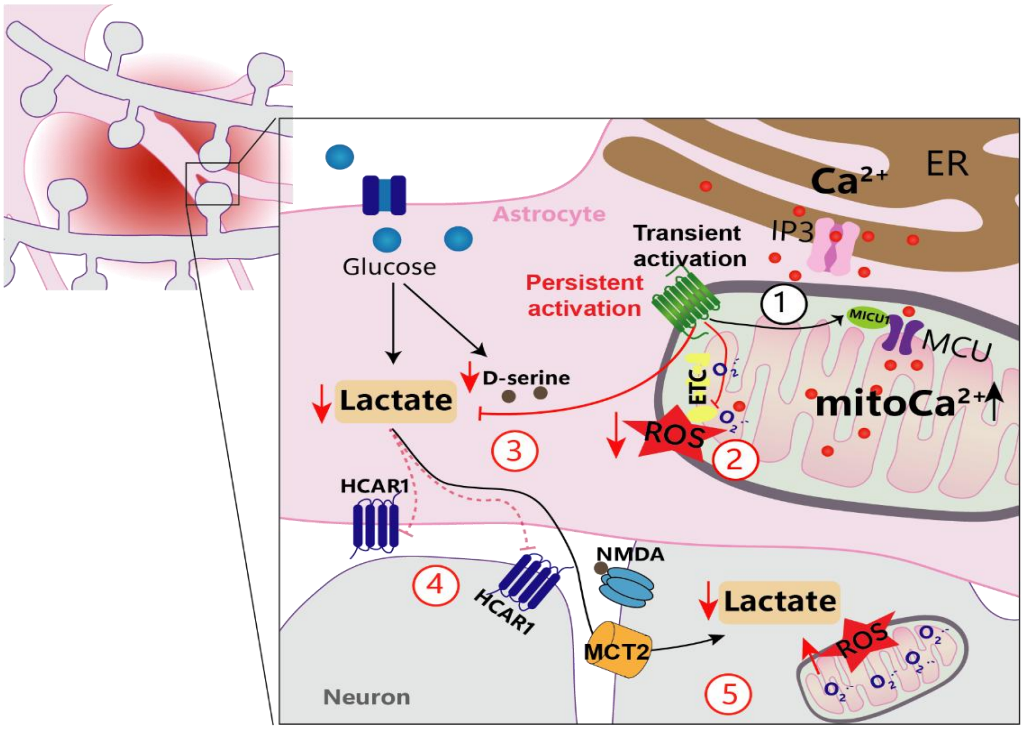

Figure 9: CB1 activation in astrocytes modulates Ca^{2+} dynamics, ROS production and glucose metabolism affecting neuronal functioning.
(1) Transient activation of mtCB1 leads to an ER-dependent increase in mitochondrial Ca^{2+} mediated by the mitochondrial Ca^{2+} uniporter (MCU), MICU1 phosphorylation and increase in lactate. On the other hand, persistent activation of mtCB1 leads to a destabilization of the ETC Complex I and a decrease in ROS, affects glycolytic production of lactate and the production of D-serine (3). Lactate act as a signalling molecule through the HCAR1 receptor, a signalling impaired with mtCB1 persistent activation (4). Lastly, the decrease of lactate transfer from astrocytes to neurons through MCT2 results in neuronal bioenergetic and redox stress (5). Figure adapted from (Jimenez-Blasco et al., 2020 ; Serrat et al., 2021).

Conversely, recent data showed that transient stimulation (5 min) of CB1R in astrocytes leads to an increase in lactate levels in cultured astrocytes in a non-mitochondrial dependent way (Fernández-Moncada, Lavanco, et al., 2024). Following this observation, Fernández-Moncada and collaborators showed that the novel object recognition (NOR) memory impairment of mice lacking CB1R specifically in astrocytes (GFAP-CB1R-KO mice) can be rescued by exogenous lactate administration, in similar way as demonstrated previously with D-serine treatments (Robin et al., 2018). Then, through a pharmacological approach, it was demonstrated that the lactate-mediated rescue effect requires the activation of the lactate cognate receptor hydroxycarboxylic acid receptor 1 (HCAR1), and the activity of the phosphorylated pathway (PP), an astrocyte-specific metabolic cascade that links glycolysis to the synthesis of L-serine, the precursor of D-serine. Finally, and using electrophysiological recordings of synaptic

NDMAR co-agonist binding site, it was demonstrated that lactate enhances synaptic NMDAR activity via an increase in synaptic D-serine availability. Notably, this lactate-mediated NMDAR potentiation was abolished by the inhibition of the PP, indicating that lactate promotes an increase of D-serine availability through the regulation of L-serine synthesis. Of note, the activation of HCAR1 also led to increased synaptic D-serine availability. Overall, these findings suggest that the transient, physiological activation of astrocytic CB1Rs in the hippocampus during the NOR task induces a rise in lactate levels and subsequent activation of HCAR1. This, in turn, modulates the PP and enhances synaptic D-serine availability, ultimately facilitating NMDAR function, which is essential for adequate NOR performance (Fernández-Moncada, Lavanco, et al., 2024).

Interestingly, in the same article described above it was also demonstrated that the CB1R-mediated lactate increase transition into a mtCB1R-depedent lactate decrease after one hour of cannabinoid exposure (Fernández-Moncada, Lavanco, et al., 2024), further emphasizing the central role of temporal dynamics in the regulation of cellular functions by specific subcellular pools of CB1R signalling. This finding, together with behavioural and pharmacological approaches, demonstrated that the impairment in NOR performance induced by exogenous cannabinoid administration is explained by a mtCB1R-dependent reduction in lactate levels, leading to the disruption of the HCAR1-PP-serine-NMDAR signalling cascade (Fernández-Moncada, Lavanco, et al., 2024). Importantly, these results all together suggest that CB1R activation exhibits a biphasic, time-dependent, and subcellular-specific modulation of astrocyte lactate metabolism, further highlighting the time dependent effects of cannabinoids, and the importance of CB1R subcellular localization in modulating brain functions.

OBJECTIVES

Despite representing only 2% of the body weight, the brain consumes up to 20% of the total body energy. Most of the brain energy comes from the full oxidation of glucose (Bélanger et al., 2011; Magistretti & Allaman, 2013), however, a sizeable amount of glucose is partially oxidized and transformed into lactate via a process called aerobic glycolysis (Y. M. Zhang et al., 2023). Current evidence indicates that astrocytes are the primary producers of lactate within the brain, which is subsequently utilized by neurons to meet their energetic demands. Notably, lactate is not only a metabolic substrate but also acts as an important signalling molecule in the brain (Magistretti & Allaman, 2018).

The mechanisms regulating lactate production and release in the brain are poorly understood. CB1R has recently emerged as an important factor playing a complex role in these processes (Fernández-Moncada, Rodrigues, et al., 2024). Whereas persistent (24h) activation of astroglial CB1R leads to a reduction of lactate (Jimenez-Blasco et al., 2020), our recent data show that their transient stimulation (5 min) triggers an increase of lactate levels (Fernández-Moncada, Lavanco, et al., 2024). These data, however, were obtained mainly in cultured astrocytes, and the impact of CB1R activity on lactate levels *in vivo* has never been directly measured.

To address this knowledge gap, the present work was designed to directly measure and characterize CB1R-dependent lactate dynamics *in vivo,* and to explore their behavioural and molecular mechanisms.

Based on this, the work has addressed the following objectives:

1. Develop a reliable protocol for *in vivo* lactate measurements using the genetically encoded biosensor eLACCO2.1 in freely moving mice.
2. Investigate the impact of locomotion on brain lactate levels across different brain regions.
3. Study the role of lactate in the locomotor effects of cannabinoids.
4. Explore the molecular mechanisms underlying CB1R-dependent lactate modulation in cultured astrocytes.

MATERIALS AND METHODS

1. Animals

All animal protocols were conducted in accordance with the Guidelines for the Care and Use of Laboratory Animals and the European Communities Council Directive (2010/63/EU). These protocols were approved by both the French and Italian Ministries, as well as by the Ethical Committee for Animal Welfare of the University of the Catania and the University of Bordeaux.

For the various experiments conducted in this project, we used only males C57BL/6N mice (Janvier, France) and inbred conditional and inducible CB1R mutant mice (provided by the Neurocentre Magendie facility). The CB1R-flox mice carries the CB1R gene flanked by loxP sites (Marsicano et al., 2003). The GFAP-CreERT2-CB1R -inducible knock-out mice (GFAP-CB1-KO) featured an inducible, conditional deletion of the CB1R gene under the control of a tamoxifen-inducible Cre recombinase expressed in GFAP positive cells (Han et al., 2012). For induction of CB1R deletion, 7–9-weeks-old mice were treated daily with 1 mg tamoxifen via intraperitoneally (I.P.) injections (10 mg/mL dissolved in 90% sesame oil, 10% ethanol) for 8 days. After each injection, mice were surveyed and weighted every two days to control their wellbeing. Mice were used 3–5 weeks after the last tamoxifen injection. In addition, DN22-CB1R knock-in mice were used, a transgenic line expressing a mutant version of CB1R lacking the first 22 amino acids and that lacks mitochondrial localization (Bénard et al., 2012). For all experiments, the corresponding wild-type littermates of each line served as controls.

All animals were housed in transparent group cages (6-8 animals per cage) with bedding and nesting material, with ad libitum access to water and food. The animal facility maintained a regulated temperature of 21±2°C on a 12-hour light/dark cycle, with lights on at 7:00 am. Animals were monitored daily by the animal facility staff.

In vitro

2. Primary mixed cortical brain cell cultures

Mixed cortical cultures of neuronal and glial cells were prepared from 1 to 3-day-old neonatal mice. Briefly, mice were euthanized, the brain removed, and cortex dissected in iced cold Hank's balanced salt solution. The tissue was enzymatically digested with trypsin/EDTA for 5 min at 37 °C and the enzymatic digestion was stopped with 10% foetal bovine serum (FBS) in B-27 supplemented neurobasal medium. After this, a gentle dissociation of the tissue was performed by repeatedly passing it through a 1-mL micropipette tip. Obtained cells were left in suspension to allow debris precipitation and removal. Cells were seeded in 18-mm glass coverslips treated with poly-L-lysine and incubated for 90 min to allow cell adhesion. After

this, the medium was replaced with fresh B-27 supplemented neurobasal medium with 10 mM glucose, 0.24 mM pyruvate, 2 mM GlutaMAX™, 100 U/mL penicillin, 100 µg/mL streptomycin and 2.5 µg/mL amphotericin B at 37 °C in a humidified atmosphere of 5% CO_2. At day in vitro (DIV) 13–14, cultures were exposed to 1×10^6 plaque-forming units (pfu) of adenoviral vectors (serotype 5) coding for Laconic, a lactate-sensitive biosensor (San Martín et al., 2013). Measurements were carried out 48–72 h after infection of cells (DIV 16–17). Adenoviral vectors encoding the FRET biosensor were custom-made by Vector Biolabs (PA, USA).

3. HEK293T cultures

HEK293T cells (ATCC, CRL-3216TM, lot 62729596) were cultured in Dulbecco's modified Eagle's medium (DMEM) with 1 g/L glucose, supplemented with 10% FBS, 100 U/mL penicillin, and 100 µg/mL streptomycin, 0.1 mM of Gibco® MEM Non-Essential Amino Acids, and maintained at 37 °C in a humidified atmosphere of 5% CO_2. Cells were transfected 18–24 h before experiments with 1 µg plasmid DNA encoding for the extracellular lactate fluorescent biosensor eLACCO2.1 (Nasu et al., 2023), using polyethylenimine (PEI) as transfection agent.

4. Drug preparation and administration

For in vitro experiments, water-soluble compounds were dissolved directly in the imaging solution (composition detailed below). Drugs prepared as concentrated stocks in DMSO were also diluted into the imaging solution immediately before use. In all cases, control solutions contained equivalent concentrations of solvent to match those used in drug-treated conditions. WIN55,212-2 (Sigma-Aldrich, France) was used at a final concentration of 1 µM, and Go 6983 (Tocris, France) at 5 µM; both were dissolved in DMSO.

5. Fluorescence imaging

Mixed cortical glia-neuron cultures and HEK293T cells were mounted in an open chamber and imaged on wide-field mode with an inverted Leica DMI 6000 microscope (Leica Microsystems, Wetzlar, Germany) equipped with a resolutive HQ2 camera (Photometrics, Tucson, USA). The illumination system used was a Lumencor spectra 7 (Lumencor, Beaverton, USA). The objectives used were an HC PL APO CS 20× dry 0.7 NA and an HCX PL APO CS 40× oil 1.25 NA. Multi-positions were done with a motorized stage Scan IM (Märzhäuser, Wetzlar, Germany). A 37 °C atmosphere was created with an incubator box and an air heating system (Life Imaging Services, Basel, Switzerland). The system was controlled by MetaMorph

software (Molecular Devices, Sunnyvale, USA). Cells were superfused with an imaging solution consisting of (in mM): 10 HEPES, 112 NaCl, 24 NaHCO3, 3 KCl, 1.25 MgCl2, 1.25 CaCl2, 2 glucose, 0.5 sodium lactate and bubbled with air/5% CO2 at 37 °C, at a constant flow of 3 mL/min. Three different focal places were manually selected and astrocytes expressing Laconic were imaged at 40×, and excited at 430 nm for 0.01–0.05 s, emissions were collected at 465–485 nm for mTFP and 542–556 nm for Venus, with image acquisition every 10 s. The ratio between mTFP and Venus was computed and normalized to the baseline.

HEK293 cells expressing eLACCO2.1 were imaged with a 20× objective, excited at 475 nm and 400 nm for 0.05–0.1 s and emission collected at 509–547 nm for GFP, with image acquisition every 10 s. The obtained GFP fluorescence was normalized to the baseline.

In vivo

6. Adeno-associated viruses (AAV)

To monitor lactate dynamics in distinct mouse brain regions, we generated the pAAV-CAG-HA-eLACCO2.1-NGR construct starting from the eLACCO2.1 plasmid (Addgene catalog number #208017). The construct was engineered to enable adeno-associated virus (AAV)–mediated expression of the lactate sensor under the control of the CAG promoter, allowing for broad expression in targeted brain areas. The titration of the virus was between 10^{10} and 10^{11} genomic copies per ml for all batches.

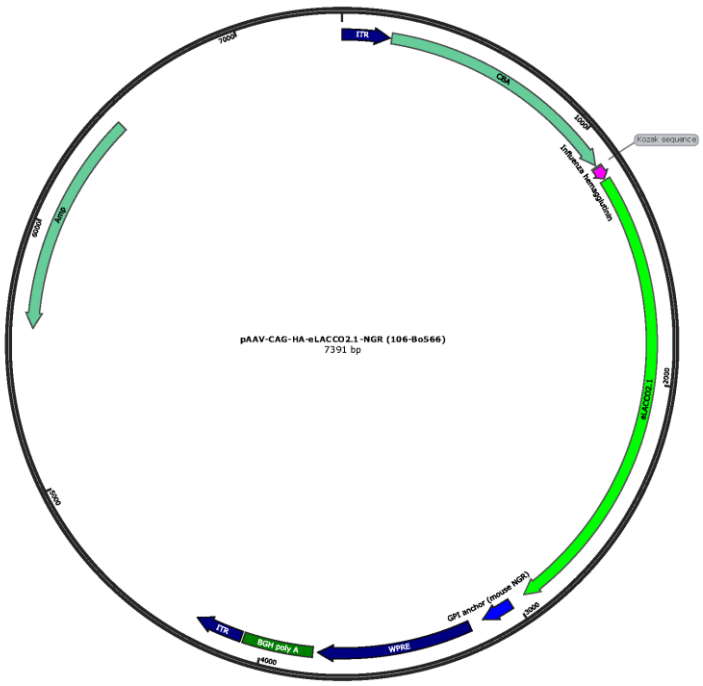

Figure M1. Addgene full sequence map for pAAV-CAG-eLACCO2.1.

7. Surgery for viral injection and optic fiber implantation

Mice were injected intraperitoneally with buprenorphine (0.05 mg/kg, Buprecare), anesthetized with 5% isoflurane, and placed into a stereotaxic apparatus (Model 900, Kopf instruments, CA, USA; with mouse adaptor and lateral ear bars). 2% isoflurane was used for the duration of the surgery. Local analgesia with lidocaine (0.1 ml at 0.5%, Lidor) was used under the skin of the head before incision. For fiber photometry (FP) surgeries, viral injections were delivered unilaterally either in the hippocampus, SNr or dorsal striatum through a glass pipette using a microinjector (NanoInject II, Drummond Scientific). To measure lactate levels in the brain and its correlation with locomotion mice were injected in different brain regions with pAAV-CAG-HA-eLACCO2.1-NGR. For the surgeries in the hippocampus, mice were injected unilaterally with an injection of a total volume of 0.800 µl at a rate of 0.3 µl per min in the following coordinates: anterior-posterior (AP) -2.20; medial-lateral (ML) - 2.00; dorsal-ventral (DV) –1.50. For surgeries in the striatum, mice were injected unilaterally, with 2 injections of 0.750 µl of a total volume of 1.5 µl at a rate of 0.3 µl per min in the following coordinates: first injection AP +0.50, L -2.00, DV –3.50 and second injection AP +0.50, L -2.00, DV –3.00. For the surgeries in the SNr, mice were injected unilaterally with an injection of a total volume of 0.500 µl at a rate of 0.3 µl per min in the following coordinates: AP −3.25, L - 1.35, DV –4.50. Then, for all the different regions, the optical fiber (400 µm diameter, 0.5 NA) was placed 200 µm above the last injection site.

Following surgery, all mice received I.P. injection of 0.2 ml of saline solution and anti-inflammatory drug meloxicam (5 mg/kg, Metacam), that was continued for 2 additional days. Animals continued to be housed in collective cages, and body weight was monitored daily during 4–5 days to assess recovery. FP experiments were carried out 4–5 weeks after surgery.

8. Pharmacological treatment of mice

For the behavioural experiments, sodium lactate (Sigma-Aldrich, France) was prepared at various concentrations by dilution in physiological saline (0.9% NaCl). Δ^9-THC (5 mg/kg or 10 mg/kg), obtained from THC Pharm GmbH (Frankfurt, Germany), was dissolved in a vehicle solution consisting of 0.9% NaCl supplemented with 5% ethanol and 4% Cremophor to ensure solubility and stability of the compound. All solutions were freshly prepared on the day of the experiment to maintain chemical integrity and consistency across trials.

9. Behavioural analyses

Locomotion and fiber photometry recordings

Five to six weeks after surgery, pAAV-CAG-HA-eLACCO2.1-NGR signal was imaged in freely moving miceusing a 470 nm LED to excite the sensor, and 405 nm for the isosbestic control signal. Mice with fiber implants were habituated to the connection for 3 days prior the test, in 10-min sessions in which they were connected and allowed to roam in a novel environment consisting in a single cage with bedding material only. In the case of mice housed in collective cages, all animals were habituated in the same single cage. The fiber photometry set-up recorded the emitted fluorescence with a sCMOS camera (Hamamatsu Orca Flash v3) through an optic fiber (core 400 μm, N.A 0.5) divided in 2 sections: a short fiber implanted in the brain of the mouse and a long fiber (modified patchcord), both connected through a ferrule-ferrule (1.25 mm) connection. To minimize the photobleaching effect of the recording and preserve a high signal to noise ratio, the light intensities in the tip of the patch cord were adjusted to ∼100 μW for the 470 nm channel and ∼50 μW for the 405 nm channel. A custom MATLAB script (Matlabworks) was used to synchronize video recording with fiber photometry, combined with a programmed Arduino board. The sampling rate was settled at either 10 Hz or 20 Hz for both photometry (interleaved) and video recording.

On the test day, mice were connected to the recording apparatus and placed in the novel single cage where they had previously been habituated. Depending on the experimental condition, they received an I.P. injection of either sodium lactate (at varying concentrations), saline (lactate vehicle), Δ^9-THC (5 mg/kg), or cannabinoid drug vehicle (a mix saline, ethanol and Cremophor; See above).

Raw lactate signals were pre-processed by removing the first minute of the recording to decrease the effect of the first exponential photobleaching, and by removing point artifacts. The 470 nm signal was fitted to the isosbestic 405 nm using a polynomial fit of first degree and, for each time point, ΔF/F was calculated as (F470 nm - F405 nm (fitted))/F405 nm (fitted). ΔF/F values were smoothed using a moving average of 0.5 s. Z-score was calculated in the whole recording to take into account the changes in signal intensity during the experiments. The baseline values were used to correct the extracted signal by performing a subtraction of the mean of the baseline to the whole extracted signal.

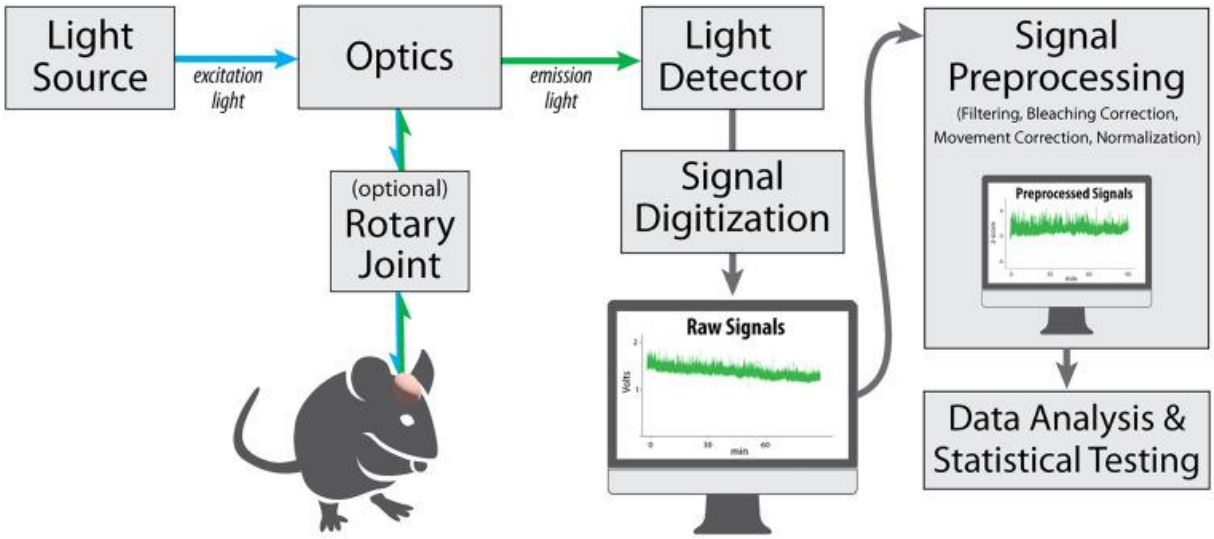

Figure M2. Schematic representation of the setup of a generic rodent in vivo FP experiment.
Figure from (E. H. Simpson et al., 2024).

Δ⁹-THC-induced tetrad assay

Either 5 minutes or 50 minutes after Δ⁹-THC administration (10 mg/kg, I.P.), mice received an injection of sodium lactate (1g/Kg I.P.). 60 min after the Δ⁹-THC injection, animals were sequentially tested for locomotor activity, catalepsy, hypothermia, and antinociception, following established protocols (Metna-Laurent et al., 2017).

For measuring the locomotion, mice were placed in a single actimetry cage (Imetronic, France) equipped by infrared beams, with the number of beam breaks recorded over a 5 minute period (Mariani et al., 2023).

For catalepsy testing, mice were placed in a clean cage without bedding, with a horizontal metal bar (0.7 cm diameter) positioned 4.5 cm above the floor. Animals were gently positioned with their forepaws gripping the bar and hind paws resting on the floor; the duration of immobility in this posture was recorded for 5 trials, with a maximum time of 60 seconds, with a cut-off time applied to avoid fatigue.

Hypothermia is expressed as the difference in the body temperature, measured before and after the injection by rectal probe thermometer (±0.1 °C accuracy); the change in body temperature (Δ °C) was calculated for each animal.

Immediately afterwards, mice were placed in a Hot Plate (BIOSEB) to measure antinociception. The plate was pre-heated at 52°. The escape latency, defined as the time until the mice showed signs of discomfort (paw licking, jumping), was recorded. All equipment was cleaned with ethanol 25% and dried with paper towels between all the trials. All mice used in the experiments

were 8–12 weeks old. Behavioural testing was conducted during the light phase between 9:00 and 15:00 hours to minimize circadian variability

10. Histology

Mice perfusion

Mice were deeply anesthetized with an intraperitoneal injection of pentobarbital (400 mg/kg). Mice were transcardially perfused with 20 mL of phosphate-buffered solution (PBS, 0.1 M, pH 7.4) for 2 min and then with 50 mL of neutral buffered formalin 10% wt/vol (Sigma, HT501128-4L) for 5 min. After perfusion, the brains were isolated and postfixed in neutral buffered formalin 10% wt/vol for 24 h. After this, the brains were transferred to PBS-sucrose 30% wt/vol solution for cryopreservation. Once the brains were completely dehydrated and sunk into the bottom of the tube (on average 3–5 days), brains were frozen in isopentane and cut into coronal sections of 30 µm using a cryostat (Leica Biosystems, CM1950S). Hippocampal slices were stored in an antifreeze solution at −20 °C until further use.

Double immunofluorescence

Free-floating sections were permeabilized in blocking solution (PBS containing 10% donkey serum and 0.3% Triton X-100) for 1 h at room temperature (RT). Sections were then incubated overnight at 4 °C with rabbit anti-GFP primary antibody (1:1000; Invitrogen, A11122) to detect eLACCO2.1 expression. After several washes in PBS, sections were incubated for 2 h at RT with goat anti-rabbit Alexa Fluor 488 secondary antibody (1:500; Invitrogen, A11008). Nuclear staining was performed using 4′,6-diamidino-2-phenylindole (DAPI; 1:20 000; Invitrogen, D3571) diluted in PBS. Finally, sections were washed in PBS and mounted. Immunofluorescence images were acquired using a Leica DM4000 B LED microscope equipped with a Leica DFC365 camera.

11. Statistical analysis

Data are presented as the mean ± standard error of the mean (SEM). All datasets were tested for normal distribution. For comparisons between two independent groups, an unpaired t-test was used for parametric data, and the Mann-Whitney U test was applied for non-parametric data. Group means were compared using one-way analysis of variance (ANOVA) for parametric data, followed by Tukey's post hoc test for pairwise comparisons. In the case of non-parametric data, the Kruskal-Wallis test was used, followed by Dunn's post hoc test. For analyses involving two factors, two-way ANOVA was performed with Sidak's post hoc test for multiple comparisons. Post hoc tests were only conducted if the ANOVA indicated significant

interactions between factors. The specific statistical tests applied to each dataset are detailed in the respective figure legends. Statistical analyses were conducted using GraphPad Prism (version 9 or 10, GraphPad Software), and statistical significance was set at $p < 0.05$.

RESULTS

PART 1 - A lactate-dependent shift of glycolysis mediates synaptic and cognitive processes in male mice

A lactate-dependent shift of glycolysis mediates synaptic and cognitive processes in male mice

Ignacio Fernández-Moncada [1] , Gianluca Lavanco [1,2,16,17], Unai B. Fundazuri [1,17] , Nasrin Bollmohr [1,17], Sarah Mountadem [1,17], Tommaso Dalla Tor [1,2,17], Pauline Hachaguer [1], Francisca Julio-Kalajzic [1], Doriane Gisquet [1], Roman Serrat [1,3], Luigi Bellocchio [1], Astrid Cannich [1], Bérénice Fortunato-Marsol [1], Yusuke Nasu [4,5], Robert E. Campbell [4,6], Filippo Drago [2], Carla Cannizzaro [7], Guillaume Ferreira [3], Anne-Karine Bouzier-Sore [8], Luc Pellerin [9], Juan P. Bolaños [10,11,12], Gilles Bonvento [13], L. Felipe Barros [14,15], Stephane H. R. Oliet [1], Aude Panatier [1,18] & Giovanni Marsicano [1, 18]

[1]Univ. Bordeaux, INSERM, Neurocentre Magendie, U1215, F-33000 Bordeaux, France.

[2]Department of Biomedical and Biotechnological Sciences, Section of Pharmacology, University of Catania, Catania, Italy.

[3]Univ. Bordeaux, INRAE, Bordeaux INP, NutriNeuro, UMR 1286, F-33000 Bordeaux, France.

[4]Department of Chemistry, School of Science, The University of Tokyo, Bunkyo-ku, Tokyo, Japan.

[5]PRESTO, Japan Science and Technology Agency, Chiyoda-ku, Tokyo, Japan.

[6]CERVO Brain Research Center and Department of Biochemistry, Microbiology, and Bioinformatics, Université Laval, Québec City, QC, Canada.

[7]Department of Biomedicine, Neuroscience and Advanced Diagnostics, University of Palermo, Palermo, Italy.

[8]Univ. Bordeaux, CNRS, Centre de Résonance Magnétique des Systèmes Biologiques, UMR 5536, F-33000 Bordeaux, France.

[9]Université de Poitiers et CHU de Poitiers, INSERM, IRMETIST, U1313, Poitiers, France.

[10]Institute of Functional Biology and Genomics (IBFG), Universidad de Salamanca, CSIC, Salamanca, Spain.

[11]Institute of Biomedical Research of Salamanca (IBSAL), Hospital Universitario de Salamanca, Salamanca, Spain.

[12]Centro de Investigación Biomédica en Red de Fragilidad y Envejecimiento Saludable (CIBERFES), Madrid, Spain.

[13]Universite Paris-Saclay, CEA, CNRS, MIRCen, Laboratoire des Maladies Neurodegeneratives, Fontenay-aux-Roses, France.

[14]Centro de Estudios Cientificos, Valdivia, Chile.

[15]Facultad de Medicina y Ciencia, Universidad San Sebastián, Valdivia, Chile.

[16]Present address: Department of Health Promotion, Mother and Child Care, Internal Medicine and Medical Specialties, ‘’G. D’Alessandro”, University of Palermo, Palermo, Italy.
[17]These authors contributed equally: Gianluca Lavanco, Unai B. Fundazuri, Nasrin Bollmohr, Sarah Mountadem, Tommaso Dalla Tor.
[18] These authors jointly supervised this work: Aude Panatier, Giovanni Marsicano. e-mail: ignacio.fernandez-moncada@inserm.fr; giovanni.marsicano@inserm.fr

Abstract

Astrocytes control brain activity via both metabolic processes and gliotransmission, but the physiological links between these functions are scantly known. Here we show that endogenous activation of astrocyte type-1 cannabinoid (CB1) receptors determines a shift of glycolysis towards the lactate-dependent production of d-serine, thereby gating synaptic and cognitive functions in male mice. Mutant mice lacking the CB1 receptor gene in astrocytes (GFAP-CB1-KO) are impaired in novel object recognition (NOR) memory. This phenotype is rescued by the gliotransmitter d-serine, by its precursor l-serine, and also by lactate and 3,5-DHBA, an agonist of the lactate receptor HCAR1. Such lactate-dependent effect is abolished when the astrocyte-specific phosphorylated-pathway (PP), which diverts glycolysis towards l-serine synthesis, is blocked. Consistently, lactate and 3,5-DHBA promoted the co-agonist binding site occupancy of CA1 post-synaptic NMDA receptors in hippocampal slices in a PP-dependent manner. Thus, a tight cross-talk between astrocytic energy metabolism and gliotransmission determines synaptic and cognitive processes.

Introduction

Type-1 cannabinoid (CB1) receptors are G-protein-coupled receptors (GPCRs) prominently expressed across the central nervous system1,2,3. Physiological engagement of CB1 receptors by their endogenous ligands, the endocannabinoids, modulates many behavioral processes, including cognition4. Importantly, CB1 receptors can also be targeted by exogenous cannabinoids, such as Δ9-tetrahydrocannabinol (THC), the main psychoactive component of Cannabis sativa. This exogenous, non-physiological activation can bear therapeutic properties, but it can also alter brain activity, impairing, for instance, cognitive, locomotor and perceptive functions5. Another remarkable feature of CB1 receptor signaling is its subcellular compartmentalization, which deviates from the strict plasma membrane functional localization of most GPCRs. Thus, few but functionally significant brain CB1 receptors are found in

association with mitochondrial membranes (mtCB1 receptors), where they can alter mitochondrial functions and regulate behavior6,7,8,9,10. This uncommon subcellular distribution allows CB1 receptors modulating brain functions via parallel signaling pathways triggered by specific subcellular pools11.

CB1 receptors are highly expressed in neurons, but they are also present at low but functionally very relevant levels in other brain cell types, such as astrocytes12. Notably, astroglial CB1 receptors can govern brain functions and cognitive processes, such as novel object recognition (NOR)13,14. Recently, it has been shown that astrocytes also possess functional mtCB1 receptors8,15,16. In particular, persistent (24 h) activation of mtCB1 receptors in astrocytes results in decreased mitochondrial functions and diminished lactate production. This astroglial metabolic failure brings about neuronal stress and impairment of social behavior as observed 24 h after cannabinoid exposure16.

This work originated from the idea of detailing the specific molecular underpinnings of such negative mtCB1 receptor-dependent control of brain lactate levels. However, early experiments lead to the surprising observation that short-term exposure to cannabinoid agonists can rapidly, reliably, and transiently increase lactate levels in astrocytes. Therefore, we set off to investigate the molecular mechanisms and the relevance of this observation. The results revealed an unexpected molecular link between metabolic and signaling properties of astrocytes, which can regulate physiological cognitive processes.

Results

As previously shown using other methods16, 24-h stimulation of CB1 receptors in cultured astrocytes expressing the reporter Laconic (see ref. 17) led to a reduction of intracellular lactate levels (Supplementary Fig. 1A, B). With the intention to investigate the temporal progression of this effect, we then analyzed the short-term impact of cannabinoid treatment. To our surprise, we observed that acute application of the CB1 agonist WIN55,212-2 (WIN55) was able to rapidly increase lactate levels in cultured astrocytes (Supplementary Fig. 1C, D). Therefore, we decided to investigate the molecular mechanisms and the potential behavioral relevance of this phenomenon from the physiological and pharmacological points of view.

Parallel cultures of astrocytes from wild-type (CB1-WT) and mutant CB1-KO mice expressing the reporter Laconic were shortly exposed to WIN55 (1 μM) and the fluorescent responses were imaged and quantified. We observed that the transient intracellular lactate increase induced by

WIN55 was fully dependent on the presence of the CB1 receptor (Fig. 1a–b). The previously described negative effect of persistent CB1 agonism on lactate levels depends on mtCB1 receptors16. Thus, we tested if this specific subcellular pool was also involved in the short-term lactate increase induced by WIN55. Remarkably, this effect did not require mtCB1 receptors, as the lactate rise was not altered in astrocytes derived from DN22-CB1-KI mice, a knock-in line in which the DN22-CB1 protein (a mutant version of CB1 lacking mitochondrial localization7) replaces the wild-type protein7,18 (Fig. 1a–c). Of note, the basal levels of lactate or capacity to produce lactate were not altered by the genotype of the astrocytes (Supplementary Fig. 2A–C). Moreover, blockade of mitochondrial oxidative phosphorylation (OXPHOS) with sodium azide triggered lactate increases with similar amplitude and kinetics in CB1-WT, CB1-KO, and DN22-CB1-KI astrocytes (Supplementary Fig. 2D–I). These data indicate that the differential acute effects of WIN55 on these cells could not be ascribed to differences in their basal levels of lactate or to their general ability to produce or accumulate this metabolite.

Intracellular increases of lactate can be due to enhanced production, but also to decreased release. To dissect these components in the acute effects of cannabinoid on lactate dynamics, we measured astrocyte lactate production via a transport-stop technique17,19. The effect of the broad monocarboxylate transporter (MCT) inhibitor Diclofenac20,21 on lactate accumulation is fully reversible (Supplementary Fig. 3A, B). This allows devising a paired assessment of lactate production by measuring the rate of accumulation upon MCT block, before and during WIN55 application (Supplementary Fig. 3C). Stimulation of CB1 receptors in WT astrocytes resulted in a significant increase in the rate of intracellular lactate accumulation, indicating augmented lactate production (Supplementary Fig. 3C, D). To exert its physiological functions, lactate is generally extruded from astrocytes into the extracellular space22,23. Thus, we next asked whether the WIN55-induced lactate production was accompanied by increased release of the metabolite. To explore this possibility, we adapted a “sniffer cells” strategy24,25, in which HEK cells expressing an extracellular lactate fluorescent biosensor26 are able to detect the amount of ambient lactate levels in an extracellular medium (Fig. 1d), in the presence of a constant buffer superfusion. Whereas WIN55 did not alter the extracellular lactate levels in a pure culture of sniffer cells, its application to a co-culture of sniffer cells with CB1-WT astrocytes led to an extracellular lactate accumulation (Fig. 1e, f). Importantly, extracellular lactate remained unchanged upon WIN55 exposure when sniffers cells were mixed with CB1-KO astrocytes (Fig. 1e, f).

Next, we asked what molecular mechanisms might participate in the astrocyte CB1 receptor-mediated lactate increase. The protein kinase C (PKC) has been shown to be transiently activated by CB1 receptor activation and to mediate short-term amnesic effects of cannabinoids27. After verifying that the magnitudes of sequential WIN55-induced lactate increases are similar (Supplementary Fig. 4A, B), we quantified the effect of WIN55 on lactate levels before and during exposure to Go 6983, a broad pharmacological blocker of PKC activity28,29 (Fig. 1g, h and Supplementary Fig. 4C). Interestingly, the inhibitor completely abolished the lactate increase induced by WIN55 (Fig. 1h, i and Supplementary Fig. 4C).

Thus, opposite to the persistent negative effects involving mitochondrial CB1 receptor signaling16, short-term activation of non-mitochondrial associated astroglial CB1 receptors results into the PKC-dependent transient stimulation of lactate production and release.

To determine if the quick stimulation of lactate metabolism mediated by astroglial CB1 receptors is relevant for brain functions, we took advantage of the known role of endocannabinoid signaling in the long-term memory version of the novel object recognition (NOR) task14. Mice lacking CB1 receptors in cells expressing the astrocyte marker glial fibrillary acidic protein (GFAP-CB1-KO mice)30 are impaired in long-term NOR performance14. This phenotype has been explained by impairment of hippocampal synaptic d-serine availability and consequent impairment of synaptic N-Methyl-D-Aspartate Receptors (NMDAR) functions during the consolidation phase of this task14. Noteworthy, it is not known if this physiological control of NOR performance depends on the mitochondrial pool of astroglial CB1 receptors. To address this point, we used a specific double-viral rescue approach to delete astroglial CB1 receptors and re-express either the CB1-WT or the DN22-CB1 proteins in the hippocampus of CB1-floxed mice8,11,14,31, thereby generating Control, HPC-GFAP-CB1-KO, HPC-GFAP-CB1-RS, and HPC-GFAP-DN22-CB1-RS mice, respectively (see "Methods" section, Supplementary Table 1 and Fig. 2a). As expected14, the deletion of CB1 receptors from hippocampal astrocytes resulted in impaired NOR performance (Fig. 2b). Remarkably, this impairment of HPC-GFAP-CB1-KO mice was rescued by re-expression of both wild-type CB1 and mutant DN22-CB1 in HPC-GFAP-CB1-RS and HPC-GFAP-DN22-CB1-RS, respectively (Fig. 2b and Supplementary Fig. 5). This indicates that mtCB1 receptor signaling is not necessary for physiological endocannabinoid-dependent control of NOR performance.

The data collected so far show that non-mitochondrial astroglial CB1 receptors can both increase lactate accumulation and mediate physiological NOR performance. Considering that

efficient lactate metabolism is required for several behavioral processes22,32, we asked whether this metabolic function of astroglial CB1 receptors might contribute to determining the synaptic activity required for NOR memory consolidation. A post-training intraperitoneal (I.P.) injection of lactate at a concentration known to reach the brain parenchyma (1 g/kg)33, was able to fully rescue the NOR impairment of GFAP-CB1-KO mice (Fig. 3a and Supplementary Fig. 6A). Next, we asked whether this rescuing effect was due to the energetic or signaling properties of lactate in the brain22,34. To disentangle this point, we tested if the hydroxycarboxylic acid receptor 1 (HCAR1)35,36 is involved in this effect of lactate. An I.P. injection of the HCAR1 agonist 3,5-dihydroxybenzoic acid (3,5-DHBA; 240 mg/kg)37 had no effect on wild-type animals, but it fully rescued the NOR impairment of GFAP-CB1-KO littermates (Fig. 3a and Supplementary Fig. 6A), indicating that the effect of lactate is likely due to activation of its cognate receptor. As both lactate and 3,5-DHBA rescuing effects were very similar to the one obtained with d-serine14, we hypothesized that astroglial CB1 receptor control of lactate signaling might participate in the regulation of synaptic d-serine levels to provide physiological NOR performance. d-serine is an amino acid derived from l-serine38,39,40,41, which, in the adult brain, is mainly produced by astrocytes via the consumption of the glycolytic intermediate 3-phosphoglycerate (3PG) in the phosphorylated pathway38 (Fig. 3b). To test whether astroglial CB1 receptor-dependent increase of lactate might impact l-serine activity in the brain, we first assessed the potential impact of l-serine on astroglial CB1 receptor-dependent NOR performance. An I.P. injection of l-serine (0.5 g/kg) was also able to rescue the memory deficit of GFAP-CB1-KO mice (Fig. 3a and Supplementary Fig. 6A), suggesting that the impaired d-serine availability in these mutants14 might be ascribed to a decreased astroglial l-serine production. To address this idea and identify the potential relationship between lactate and serine signaling, we adopted a pharmacological approach to inhibit phosphoglycerate dehydrogenase (PHGDH), the enzyme providing the first step of l-serine production in the phosphorylated pathway38 (Fig. 3b). The administration of high doses of the PHGDH blocker NCT-503 (Fig. 3c)42 alone impaired long-term NOR memory consolidation, possibly due to direct inhibition of l- and d-serine availability (Supplementary Fig. 6B, C). Thus, we performed a full dose-response study to identify a sub-effective dose of NCT-503 that does not alter long-term memory formation per se (Supplementary Fig. 6B, C). Then, we tested the ability of lactate or 3,5-DHBA to rescue the memory impairment of GFAP-CB1-KO mice under vehicle or in the presence of 6 mg/kg NCT-503. This treatment did not alter the NOR performance of GFAP-CB1-WT mice ($P = 0.8037$, compare Fig. 3a and d; Supplementary Table 2) or the impaired memory of their GFAP-CB1-KO littermates (Fig. 3d

and Supplementary Fig. 6D). Conversely, the drug fully abolished both the lactate- and 3,5-DHBA-induced rescue of NOR performance of GFAP-CB1-KO mice (Fig. 3d and Supplementary Fig. 6D). Importantly, the delivery of l-serine was still able to rescue the long-term memory impairment in the presence of the same dose of NCT-503 (Fig. 3d and Supplementary Fig. 6D), indicating that the activation of HCAR1 promotes l-serine via PHGDH-dependent stimulation of the phosphorylated pathway.

To explore how HCA1R signaling might impact astrocyte glucose metabolism to promote the PP-dependent production of l-serine, we quantified the effect of 3,5-DHBA on both the entry and exit points of glycolysis in cultured astrocytes. In order to measure glucose consumption, we used a glucose-sensitive fluorescent biosensor43 and we measured glucose levels under conditions of glucose transport blockade44 (Supplementary Fig 7A). Interestingly, 3,5-DHBA (1 mM) approximately doubled glucose consumption (Fig. 3e and Supplementary Fig. 7B). In parallel, we observed that 3,5-DHBA exposure caused a lactate increase (Fig. 3f and Supplementary Fig. 7C, D). Therefore, HCAR1 activation by lactate might generally increase glycolysis, thereby promoting all downstream metabolites, including lactate derived from pyruvate and l-serine from 3PG. However, are these pathways equally potentiated by HCAR1 activation? To explore this question, we analyzed our data with a mathematical model to extract further information on the metabolic fluxes20,45. We modeled the fate of glucose consumption toward pyruvate/lactate or branched pathways using a parameter that we called "efficiency of glucose-to-pyruvate/lactate conversion" (E – Fig. 3g, see "Methods" section for details). Using this model, we observed that at $E = 0.7$ the lactate increase induced by 3,5-DHBA was much smaller than predicted by a 2-fold increase in glucose consumption (Fig. 3h, purple line). Interestingly, by simulating a decrease in E during the glycolytic stimulation (E*), the simulated lactate concentration reached the observed lactate increase induced by 3,5-DHBA (Fig. 3h – blue line). Importantly, similar results were observed for lower (0.5) or higher (0.9) basal E values (Supplementary Fig. 7E–G), indicating that the results are independent of the starting "efficiency" of glucose-to-pyruvate/lactate conversion. Thus, our mathematical analysis indicated that, despite the increase of glycolysis, the "efficiency" of glucose-to-lactate conversion is reduced by 3,5-DHBA (Fig. 3g, h and Supplementary Fig. 7E–G). In other words, these data suggest that HCAR1 activation promotes biased glucose metabolism, resulting in higher efficiency of alternative branched pathways, like the PP.

Overall, these results indicate that the physiological activation of astroglial CB1 receptors enables cognitive performance via stimulation of lactate supply, activation of HCAR1

signaling, and further potentiation of biased glucose metabolism, which ultimately increases l- and d-serine availability via the phosphorylated pathway.

These results suggest that lactate might control synaptic d-serine availability, eventually resulting in the adequate signaling of NMDARs. However, it is still possible that the mechanisms underlying the rescue effect of lactate in the NOR performance of GFAP-CB1-KO mice are explained by compensatory mechanisms developed under the specific conditions of the mutant mice. In other words, the deletion of the CB1 gene in astrocytes might induce alterations that provide lactate with functions that it does not have under physiological conditions. To address this point and to clarify the role of lactate levels on the dynamics of synaptic d-serine availability, we explored if the link between these metabolites as observed in the GFAP-CB1-KO mice is also present in WT animals. To analyze the synaptic d-serine availability, we performed electrophysiological extracellular field recordings (fEPSPs) of synaptic NMDARs in the stratum radiatum of CA1 area in wild-type hippocampal slices14,41,46 (NMDAR-fEPSPs, Supplementary Fig. 8A). In control conditions, the co-agonist binding site occupancy of synaptic NMDARs are not fully saturated, thus exogenous bath application of d-serine (50 μM) results in the increase of synaptic NMDAR activity and therefore an increase of NMDAR-fEPSPs slope14,41,46 (Fig. 4a). Intriguingly, bath application of exogenous lactate (2 mM) was able to potentiate NMDAR activity with a magnitude similar to the one induced by exogenous d-serine (Fig. 4a). However, this lactate-induced potentiation was slower than the one triggered by d-serine (Fig. 4b). To test whether this lactate effect was downstream the increase in d-serine availability, the co-agonist binding sites of synaptic NMDARs were first saturated with exogenous d-serine (50 μM) and then lactate was bath applied. Notably, lactate application had no impact on the slope of NMDAR-fEPSPs and therefore on synaptic NMDAR activity in these conditions (Fig. 4c), suggesting that the potentiating effect of the metabolite might be due to a downstream increase in d-serine availability. However, it is still possible that the application of d-serine might cause a “ceiling effect”, impeding a serine-independent effect of lactate to be observed. Therefore, we directly tested whether the activity of the phosphorylated pathway was necessary for the potentiation of synaptic NMDAR activity by lactate. Notably, this effect was blunted in slices preincubated with NCT-503 (Fig. 4d and Supplementary Fig. 8B), showing that PHGDH activity is a required step of the process. Of note, the potentiation induced by d-serine was not altered by NCT-503 (Supplementary Fig. 8C), further suggesting that lactate plays an upstream role in the astrocyte cascade leading to increased d-serine availability at synaptic NMDARs. Finally, we tested

whether HCAR1 signaling was involved in the lactate-mediated control of synaptic d-serine availability. Bath application of 3,5-DHBA (1 mM) resulted in the increase of synaptic NMDARs activity (Fig. 4e). However, and importantly, prior application of 3,5-DHBA (1 mM) resulted in a complete occlusion of the exogenous d-serine effect on NMDAR activity (Fig. 4f), indicating that the activation of HCAR1 promotes an increase in synaptic d-serine availability. These results confirm that lactate can modulate the phosphorylated pathway via activation of HCAR1 signaling to control synaptic d-serine availability independently of CB1 receptor genetic deletion, supporting a physiological role for this phenomenon.

The data described so far are compatible with a scenario, in which acute activation of hippocampal astroglial CB1 receptors leads to increased lactate production and release. This lactate would in turn promote l- and d-serine signaling at NMDARs via activation of HCAR1, eventually mediating consolidation of NOR memory. This physiological scenario seems at odds with the previously described pharmacological effects of CB1 receptor activation7,16,47. Indeed, in vivo activation of CB1 receptors by drugs does not only reduce lactate levels16, but it also impairs long-term NOR memory7,47. Therefore, we wondered what could be the mechanistic explanation of these opposite effects of endogenous and pharmacological activation of CB1 receptors. The major differences between endogenous and exogenous CB1 receptor agonists rely on their spatiotemporal features. Specifically, whereas the physiological production of endocannabinoids is generally spatially restricted and is followed by rapid degradation1,48,49, exogenous cannabinoids are likely to unselectively spread throughout the body and their action is temporally limited only by their pharmacokinetic properties1. In other words, the effects of physiologically produced endocannabinoids are generally very local and short-lasting, whereas the effects of exogenously administered CB1 receptor agonists are global and long-lasting. Based on this reasoning, we asked what is the time course and the mechanisms possibly mediating the switch between the CB1 receptor-dependent increase (present data) and decrease of lactate (see ref. 16) in cultured astrocytes. A 70-min-long application of WIN55 to astrocyte cultures expressing the Laconic lactate sensor resulted in a temporal biphasic effect, with the acute increase of lactate occurring during the first 5–10 min and a later shift towards a decrease, which became significant at 60–70 min after application (Fig. 5a and Supplementary Fig. 9A). We previously showed that the decrease of lactate observed after 24-h cannabinoid incubation requires mtCB1 receptors16. Consistently, 70 min treatment of astrocytes derived from DN22-CB1-KI mice with WIN55 resulted in an increase of lactate, which never shifted to a decrease (Fig. 5b and Supplementary Fig. 9B). Altogether, these data indicate that the

respective mtCB1 receptor-independent increase and mtCB1 receptor-dependent decrease of lactate levels in astrocytes are a function of time.

We next asked whether this increase/decrease switch effect of cannabinoids might bear behavioral relevance. Using the same strategy as described in Fig. 2, we found that the NOR-impairing effect of the plant-derived CB1 receptor agonist THC is absent in mice lacking mtCB1 receptors (HPC-GFAP-DN22-CB1-RS; Supplementary Table 1; Fig. 5c and Supplementary Fig. 9C). This indicates a first mechanistic difference between physiological control of NOR performance by the endocannabinoid signaling (mtCB1 receptor-independent, Fig. 2b) and the disrupting effect of exogenous cannabinoids on the same process (mtCB1 receptor-dependent, Fig. 5c and Supplementary Fig. 9C). Thus, we next wondered if this effect of THC might be linked to a mtCB1 receptor-dependent decrease of lactate. To address this issue, we tested whether lactate could rescue the effect of THC, similarly as it does in mice lacking CB1 receptors from astrocytes. The simultaneous administration of lactate and THC immediately after the acquisition of NOR did not alter the effect of the cannabinoid drug (Fig. 5d and Supplementary Fig. 9D). Intriguingly, however, the administration of lactate 1 h after THC completely reverted the impairment of long-term NOR performance (Fig. 5e and Supplementary Fig. 9E). Importantly, this effect of lactate was mimicked by 3,5-DHBA (Fig. 5e and Supplementary Fig. 9E), strongly suggesting that the effects of THC on NOR are due to a mtCB1 receptor-dependent decrease of lactate signaling through the HCAR1 receptor. This suggests that the rescuing effect of lactate on the THC effect might involve the PP cascade, similarly to physiological NOR memory consolidation. To address this possibility, we administered the PP inhibitor NCT-503 together with lactate 1 h after THC treatment. Notably, this treatment abolished the rescuing effect of lactate (Fig. 5e and Supplementary Fig. 9E). Altogether, these data clearly indicate that lactate signaling is required to consolidate NOR memory. This signaling is disrupted by the insufficient production of lactate occurring both in absence of physiological CB1 receptor activity and during pharmacological stimulation of mtCB1 receptors in astrocytes.

Discussion

This study reveals an astrocyte-dependent metabolic interaction between lactate signaling, the phosphorylated pathway, synaptic d-serine availability, and cognitive performance in mice. Our data are compatible with a scheme whereupon endogenous activation of astroglial CB1 receptors leads to a temporary increase of lactate, which in turn activates HCAR1 signaling,

switching glycolysis towards serine production, and ultimately providing the NMDAR activity necessary for physiological novel object recognition (Supplementary Fig. 10). Interestingly, the prolonged exposure of astrocytes to exogenous cannabinoids results in impaired cognitive performance through a specular mechanism that involves activation of astroglial mtCB1 receptors and inhibition of the same lactate signaling (Supplementary Fig. 10). Thus, these data provide a mechanistic link between astroglial energy metabolism and gliotransmission, and they explain the differential effects of physiological versus the pharmacological impact of CB1 receptor activation on cognitive processes.

Astroglial CB1 receptors have been shown to control synaptic plasticity in different brain regions and to determine cognitive processes12,14,50,51,52. The regulation of astrocyte Ca^{2+} signaling is generally indicated as the cellular mechanism underlying these functions46,53,54. Only recently, cannabinoid signaling was linked to specific metabolic control of behavior, showing that persistent activation of astroglial mtCB1 receptors can reduce lactate production by astrocytes and induce a bioenergetic crisis in neurons, eventually resulting in impairment of social interactions16. Here, using lactate-sensitive fluorescent biosensors, we confirmed that long-term application of cannabinoids reduces lactate levels in astrocytes16, but we found also that short-term activation of astroglial CB1 receptors stimulates lactate production and release. Consistent with this observation, the exogenous administration of lactate is sufficient to rescue the NOR impairment of GFAP-CB1-KO mice. Lactate levels increase in the brain parenchyma during neural workload34, a phenomenon explained by a shift from complete to partial glucose oxidation and known as aerobic glycolysis55. Several signals have been proposed to initiate this metabolic shift, such as glutamate56,57, extracellular K+ rises58,59, and others24,60,61. The present data indicate that astroglial CB1 receptor signaling participates in these processes, suggesting that it can trigger aerobic glycolysis and concomitant increase in extracellular lactate levels. When compared to other brain signals, the effect of CB1 receptor activation on lactate metabolism shares a similar time scale to the effects of extracellular K+ rises, which activate astrocyte glycolysis within seconds62,63 and promote a phenomenon of metabolic recruitment of neighboring astrocytes59. However, endocannabinoid signaling is thought to be highly local1,48,49, a characteristic similar to glutamate which does not diffuse far from its release sites64. This suggests that CB1 receptors may provide fast and local signaling to trigger astrocyte lactate metabolism, working in parallel or synergistically with other brain signals that control astrocyte metabolic functions.

Our data show that PKC activity is required for this phenomenon. PKC signaling is very complex and formed by several isozymes exerting different control of cellular activity65,66,67. Astrocytes express different types of PKC isozymes68, but their role in astrocyte metabolic function is almost unexplored69,70. However, in other cell types, PKC signaling modulates glucose uptake71,72,73,74,75,76, glycolytic flux77,78,79,80, and lactate dehydrogenase activity81. Thus, it will be very interesting to address the detailed characterization of the intracellular machinery linking CB1 receptors, PKC, and lactate metabolism. In this context, the present data demonstrate that deletion of (mt)CB1 receptors does not alter basal lactate metabolism, and amplitude and kinetics of lactate accumulation induced by OXPHOS inhibition. However, astroglial lactate metabolism is regulated by diverse stimuli, including neuronal signals22,59, cellular stress, or alterations in mitochondrial respiration17,82. These stimuli can trigger a plethora of intracellular cascades, which could each interact with (mt)CB1 receptors. Thus, we cannot presently exclude that potential alterations in different mechanisms regulating lactate production might exist in cells lacking (mt)CB1 receptors. Further studies will deal with this potential issue by exploring how CB1 receptors might interact with other stimuli that modulate astroglial lactate metabolism.

Noteworthy, our present and previous16 data altogether indicate that activation of CB1 receptors results in a biphasic time-dependent modulation of astrocyte lactate metabolism. We previously showed that persistent pharmacological activation (24 h) of astroglial mtCB1 receptors decreases lactate production, thereby causing neuronal bioenergetic stress and impairing social interactions in mice16. Conversely, in the present study, we report that a short-term activation (<10 min) of non-mitochondrial astrocyte CB1 receptors results in a transient increase of intracellular lactate. Here we found that this switch between the increase and decrease of lactate levels by cannabinoids occurs within one hour, indicating that time plays a fundamental role in determining the modalities (e.g., functional engagement of mitochondrial or non-mitochondrial CB1 receptors) and the outcome of cannabinoid signaling. This bimodal and subcellular-specific action on lactate levels resembles the recently described differential involvement of neuronal plasma membrane and mitochondrial CB1 receptors in cannabinoid-induced antinociception and catalepsy, respectively11. However, those subcellular-specific effects of cannabinoids occur simultaneously, whereas the differential impact on lactate levels involve an important temporal component. In this context, it is interesting to note that the physiological control of NOR performance and its pharmacological impairment by cannabinoid agonists intersect at the same molecular pathway, which is promoted or inhibited in a time-

dependent manner. Indeed, the physiological activation of non-mitochondrial CB1 receptors seems to transiently increase lactate levels and successive signaling, whereas persistent presence of CB1 agonists engages mtCB1 receptors to decrease the metabolite levels. Our data show that this temporal dichotomy bears important functional and behavioral consequences. Indeed, they are consistent with a scenario whereupon physiological and pharmacological activation of CB1 receptors trigger opposite effects mediated by different subcellular populations of the receptor (Supplementary Fig. 9). Thus, endocannabinoids mobilized during physiological consolidation of NOR memory activate non-mitochondrial CB1 receptors to increase lactate levels, HCAR1 signaling, PP activity, serine availability and NMDAR synaptic functions (Supplementary Fig. 9). Conversely, pharmacological administration of exogenous cannabinoid agonists reaches astroglial mtCB1 receptors, triggering the exact opposite cascade, ultimately impairing NOR memory consolidation (Supplementary Fig. 9).

Lactate has traversed a long way from being initially viewed as little more than mere cellular waste, to become a relevant metabolite for brain physiology22,34. Astrocyte-derived lactate has been shown to modulate neuronal functions via multiple mechanisms83,84,85,86,87,88,89,90,91,92,93. Most of these proposed mechanisms, however, are linked to the consumption of lactate as an energy substrate for neuronal activity, which likely fuels mitochondrial energy production, but also increases the cytosolic NADH levels, which potentiate NMDAR activity and promote expression of plasticity genes87. Indeed, the potentiation of NMDAR activity by lactate in our electrophysiological experiments is significantly blunted by the blockade of the phosphorylated pathway by NCT-503. However, a nonsignificant “residual” level of potentiation was consistently observed in these experiments, suggesting that multiple mechanisms likely link lactate to synaptic functions. This said, the present data reveal a receptor-dependent impact of lactate on cognitive processes: the control of d-serine synthesis and its synaptic availability. This process requires the HCAR1 signaling-dependent modulation of the phosphorylated pathway in astrocytes38,41. This signaling process likely works in parallel with the other described effects of lactate in the brain that have been shown to be essential to sustain learning and memory processes (including monocarboxylate transporter-dependent uptake and metabolism)87,92,93,94,95. It is reasonable to speculate that these multiple mechanisms might allow astrocytes to minimize the resources required to cooperate with neurons to fulfill different behavioral tasks.

Important to note, that the activation of HCAR1 has been suggested to reduce neuronal functions90,91,96, which might contradict our results. However, careful dose-dependent

experiments using the 3,5-DHBA agonist in hippocampal slices showed that HCAR1 activation exerts a biphasic effect on CA1 pyramidal neurons, with low doses decreasing and high dose increasing their excitability88. The concentration of 3,5-DHBA (1 mM) used here corresponds to a high dose that increases CA1 pyramidal cells excitability88. Thus, our results are in line with the literature and support a more complex view of HCAR1 signaling in the brain. Our data show that HCAR1 activation induces a sort of biased increase in glucose metabolism, which determines an increased availability of glycolytic intermediates and favors their diversion towards branched pathways, like the PP. This idea implies that activation of HCAR1 exerts multiple effects on the glycolytic flux of astrocytes. The molecular link(s) between HCAR1 signaling and the phosphorylated pathway are largely unknown, and future studies will address the details of this signaling cascade, investigating the anatomical localization of HCAR197,98,99, the molecular components involved in the stimulation of glucose consumption, and the exact mechanisms that allow the diversion of glucose-derived intermediates towards the PP. HCAR1 is generally considered to couple with Gi proteins35,36, which would not intuitively fit with a stimulatory effect on cellular processes. However, whereas they inhibit cAMP/PKA activity, Gi proteins can activate several cellular pathways, such as extracellular regulated kinases (ERK)100,101. Moreover, GPCRs are now known to couple promiscuously with different types of G proteins in different cells or even subcellular compartments102,103,104. Future work will define the details of the HACR1 signaling involved in the regulation of serine production. Indeed, although virtually nothing is known about the molecular regulation of the enzymes of the phosphorylated pathway, it is possible that G protein-triggered signaling might impact the activity of at least some of them (e.g., via specific kinase- and/or Ca^{2+} -dependent processes).

The spatiotemporal pattern of lactate-stimulated l-serine activity might also play a potentially important mechanistic role in the link between CB1 receptors and NMDAR activity. It is possible that the CB1-dependent increase of lactate and the production of l-serine coexist in a single astrocyte, but they are separated in time. In other words, upon CB1 receptor activation, astrocytes may first accumulate lactate, and then trigger HCAR1 signaling to promote l-serine. Alternatively, CB1 receptor-stimulated astrocytes might act as net lactate providers, whereas another astrocyte population expressing HCAR1 may possibly be responsible for the l-serine production upon stimulation by lactate. This possibility might be similar to the specific gating of striatal circuits by distinctive astrocyte subpopulations105, and the recently proposed secondary metabolic recruitment induced by the diffusion of lactate away from its release

site59. Further focused studies will be necessary to fully unveil the mechanisms explaining the interaction between lactate, HCAR1 signaling, and l-serine. However, the discovery of the existence of such interaction reveals key connections between metabolic processes (lactate) and synaptic signaling (d-serine), which are required for cognitive processes.

D-serine is a gliotransmitter and co-agonist of synaptic NMDARs14,41,106,107,108. Despite that both neurons and astrocytes can likely release this amino acid39,52, astrocytes are the main producers of its precursor l-serine40, thereby representing the main controllers of the total amount of d-serine in the brain. By showing that astrocyte-borne lactate promotes d-serine signaling via HCAR1-dependent stimulation of the phosphorylated pathway, our results underscore another way by which astrocytes modulate brain functions. Thus, this study contributes to a unifying concept of astrocyte metabolic functions and gliotransmission. These two processes are often considered as independent entities. For instance, researchers either study just astrocytes metabolic processes or the impact of astrocytes functions on synaptic activity109,110,111,112, with little interactions between these points of view. This is particularly true when the roles of astrocytes are investigated in the frame of cognition and high mental processes. In this study, we merged the observation that type-1 cannabinoid CB1 receptors can rapidly and transiently promote lactate metabolism and the regulation of d-serine synaptic functions by endocannabinoid signaling in astrocytes. Moreover, we identified the same metabolic/signaling cascade as the target of prolonged pharmacological impairment of cognition by cannabinoid drugs. Therefore, these data show the tight functional link existing between metabolic and signaling processes. This unified notion will have to be taken into account in future studies aimed at understanding the role of astrocytes in promoting and controlling brain functions and behavior, and in investigating neurological and psychiatric disorders characterized by cognitive impairment.

Methods

Animals

All experiments were conducted in strict compliance with the European Union recommendations (2010/63/EU) and were approved by the French Ministry of Agriculture and Fisheries (authorization number 3306369) and the local ethical committee (authorization APAFIS#18111). Animals used in the study were divided into two categories. The first group consisted of female and male CB1-KO, CB1-DN22, or CB1-WT mice, used as breeders to obtain newborn mice for primary cultures. The second category corresponds to animals used

for behavior or electrophysiology studies, consisting of male C57BL/6N (JANVIER, France), male CB1f/f, male GFAP-CB1-KO mutant and GFAP-CB1-WT littermate mice (two to three-months-old). Animals were housed in groups under standard conditions, with free access to food and water, in a day/night cycle of 12/12 h (light on at 7 am), at 22 ± 2 °C, and 50% humidity. Specific deletion of CB1 on GFAP-positive cells in adult mice was obtained via the loxP/Cre system, with a tamoxifen-inducible CreERT2 recombinase113 encoded under the GFAP promoter30. Female mice carrying the "floxed" CB1 gene (CB1f/f)114 were crossed with CB1f/f;GFAP-CreERT2, to obtain CB1f/f;GFAP-CreERT2 and CB1f/f littermates, named throughout the text GFAP-CB1-KO and GFAP-CB1-WT, respectively. For induction of CB1 deletion, 7–9-weeks-old mice were treated daily with 1 mg tamoxifen via intraperitoneally (I.P.) injections (10 mg/mL dissolved in 90% sesame oil, 10% ethanol) for 8 days. After each injection, mice were surveilled and weighted every two days to control their wellbeing. Mice were used 3–5 weeks after the last tamoxifen injection14,30.

Surgery and viral stereotaxic injection

Male CB1f/f (CB1-flox) mice were anesthetized in a box containing 5% Isoflurane (Virbac, France) before being placed in a stereotaxic frame (Model 900, Kopf Instruments, CA, USA) in which 1.5%–2.0% of Isoflurane was continuously supplied via an anesthetic mask during the whole duration of the experiment. For viral intra-hippocampal AAV delivery, mice were submitted to stereotaxic surgery, and AAV vectors were injected with the help of a microsyringe (0.25 mL Hamilton syringe with a 30-gauge beveled needle) attached to a pump (UMP3-1, World Precision Instruments, FL, USA). Where specified, CB1-flox mice were injected directly into the hippocampus (HPC) (0.5 µL per injection site at a rate of 0.5 µL per min), with the following coordinates: HPC, AP −1.8; ML ± 1; DV −2.0 and −1.5. Following virus delivery, the syringe was left in place for 1 min before being slowly withdrawn from the brain. To induce the deletion of hippocampal astroglial CB1 receptors and the rescue (RS) of CB1 receptor expression either with WT or mutant DN22 sequences, mice were injected in the hippocampus with the following combination of viral particles: (i) AAV-CAG-DIO-empty + AAV-GFAP-GFP (Control mice), (ii) AAV-GFAP-CRE-mCherry + AAV-CAG-DIO-empty (HPC-GFAP-CB1-KO mice), (iii) AAV-GFAP-CRE-mCherry + AAV-CAG-DIO-CB1-GFP (HPC-GFAP-CB1-RS mice), and (iv) AAV-GFAP-CRE-mCherry + AAV-CAG-DIO-DN22-CB1-GFP (HPC-GFAP-DN22-CB1-RS mice). Animals were used around 4–5 weeks after local AAV infusions. Mice were weighed daily and individuals who failed to regain the pre-surgery body weight were excluded from the behavioral experiments.

Mixed cortical brain cell cultures

Mixed cortical cultures of neuronal and glial cells were prepared from 1 to 3-day-old neonatal mice44. Briefly, mice were euthanized, the brain removed, and cortex dissected in iced cold Hank's balanced salt solution. The tissue was enzymatically digested with trypsin/EDTA for 5 min at 37 °C and the enzymatic digestion was stopped with 10% FBS in B-27 supplemented neurobasal medium. After this, a gentle dissociation of the tissue was performed by repeatedly passing it through a 1-mL micropipette tip. Obtained cells were left in suspension to allow debris precipitation and removal. Cells were seeded in 18-mm glass coverslips treated with poly-L-lysine and incubated for 90 min to allow cell adhesion. After this, the medium was replaced with fresh B-27 supplemented neurobasal medium with 10 mM glucose, 0.24 mM pyruvate, 2 mM GlutaMAXTM, 100 U/mL penicillin, 100 µg/mL streptomycin and 2.5 µg/mL amphotericin B at 37 °C in a humidified atmosphere of 5% CO2. At day in vitro (DIV) 13–14, cultures were exposed to 1 × 106 plaque-forming units (pfu) of adenoviral vectors (serotype 5) coding either for Laconic (the lactate-sensitive biosensor)17 or FLII12Pglu700µΔ6 (glucose-sensitive biosensor)43. Measurements were carried out 48–72 h after infection of cells (DIV 16-17). Adenoviral vectors encoding the FRET biosensor were custom-made by Vector Biolabs (PA, USA).

Cell lines

HEK293T cells (ATCC, CRL-3216TM, lot 62729596) were cultured in Dulbecco's modified Eagle's medium (DMEM) with 1 g/L glucose, supplemented with 10% fetal bovine serum (FBS), 100 U/mL penicillin, and 100 µg/mL streptomycin, 0.1 mM of Gibco® MEM Non-Essential Amino Acids, and maintained at 37 °C in a humidified atmosphere of 5% CO2. For "sniffers cells" experiments, cells were transfected 18–24 h before experiments with 1 µg plasmid DNA encoding for the extracellular lactate fluorescent biosensor eLACCO2.1 (Ref. 26), using polyethylenimine (PEI) as transfection agent. On the day of the experiment, the DMEM media was replaced with B-27 supplemented neurobasal (used for the mixed glia-neuron culture) and cells were detached gently with a micropipette. Immediately after, the cell suspension was seeded on mixed glia-neuron and incubated for 4–5 h before imaging.

Drug preparation and administration

For in vitro experiments, water-soluble drugs were dissolved directly in the imaging solution (see below for its composition). Drugs or their concentrated stocks prepared in DMSO were diluted directly in the imaging solution. The imaging solution contained the same amount of solvent respectively to the drug(s). For behavioral experiments, sodium lactate, 3,5-Dihydroxybenzoic (3,5-DHBA), and L-serine were prepared in saline (0.9% NaCl). Δ9-tetrahydrocannabinol (THC) and NCT-503 were prepared in a mixture of saline with 2.5% cremophor and 2.5% DMSO to obtain a solution of 0.6 mg/ml. All drugs were injected I.P. with a 26G needle, either immediately after the acquisition phase of the NOR task or after 1-h post-acquisition phase. For the injection of two drugs, a 5 min pause between injections was performed. Vehicles contained the same amounts of solvents respectively to the drug. All drugs were prepared fresh before the experiments.

Histology

Mice perfusion

Mice were deeply anesthetized with an intraperitoneal injection of pentobarbital (400 mg/kg). Mice were transcardially perfused with 20 mL of phosphate-buffered solution (PBS, 0.1 M, pH 7.4) for 2 min and then with 50 mL of neutral buffered formalin 10% wt/vol (Sigma, HT501128-4L;) for 5 min. After perfusion, the brains were isolated and postfixed in neutral buffered formalin 10% wt/vol for 24 h. After this, the brains were transferred to PBS-sucrose 30% wt/vol solution for cryopreservation. Once the brains were completely dehydrated and sunk into the bottom of the tube (on average 3–5 days), brains were frozen in isopentane and cut into coronal sections of 30 μm using a cryostat (Leica Biosystems, CM1950S). Hippocampal slices were stored in an antifreeze solution at −20 °C until further use.

Double immunofluorescence

Free-floating sections were permeabilized in a blocking solution (PBS + 10% donkey serum + 0.3% Triton X-100) for 1 h at room temperature (RT). Then, sections were incubated overnight at 4 °C with a mix of primary antibodies: chicken anti-GFAP (1:500, Abcam ab4674) and rabbit anti-GFP (1:1000, Invitrogen A11122). After several washes with PBS, slices were incubated for 2 h at RT with a mix of secondary antibodies: goat anti-chicken Alexa Fluor 647 (1:500, Invitrogen A32933) and goat anti-rabbit Alexa Fluor 488 (1:500, Invitrogen A11008). Then, sections were incubated with 4’,6-diamidino-2-phenylindole (DAPI,1:20000, Invitrogen D3571) diluted in PBS to visualize cell nuclei. Finally, sections were washed in PBS and

mounted. Immunofluorescence images were taken with a Microscope Leica DM 4000 BLED equipped with a Camera Leica DFC 365.

Fluorescence imaging

Mixed cortical glia-neuron cultures, HEK293T cells, or a co-culture of mixed glia-neuron culture with HEK293 cells (sniffers), were mounted in an open chamber and imaged on wide-field mode with an inverted Leica DMI 6000 microscope (Leica Microsystems, Wetzlar, Germany) equipped with a resolutive HQ2 camera (Photometrics, Tucson, USA). The illumination system used was a Lumencor spectra 7 (Lumencor, Beaverton, USA). The objectives used were an HC PL APO CS 20× dry 0.7 NA and an HCX PL APO CS 40× oil 1.25 NA. Multi-positions were done with a motorized stage Scan IM (Märzhäuser, Wetzlar, Germany). A 37 °C atmosphere was created with an incubator box and an air heating system (Life Imaging Services, Basel, Switzerland). The system was controlled by MetaMorph software (Molecular Devices, Sunnyvale, USA). Cells were superfused with an imaging solution consisting of (in mM): 10 HEPES, 112 NaCl, 24 NaHCO3, 3 KCl, 1.25 MgCl2, 1.25 CaCl2, 2 glucose, 0.5 sodium lactate and bubbled with air/5% CO2 at 37 °C, at a constant flow of 3 mL/min. Astrocytes expressing Laconic were imaged at 40×, and excited at 430 nm for 0.01–0.05 s, emissions collected at 465–485 nm for mTFP and 542–556 nm for Venus, with image acquisition every 10 s. The ratio between mTFP and Venus was computed and normalized to the baseline. To quantify the basal lactate level (Supplementary Figs. 1A, B and 2A, B), the biosensor occupancy was computed as a proxy of intracellular lactate level with the following equation: $\text{Occupancy} = (R0 - Rmin)/(Rmax - Rmin)$, in which R0: basal mTFP/Venus ratio (before any drug treatment), Rmin: steady-state mTFP/Venus ratio induced by sodium oxamate (6 mM) or pyruvate (10 mM), Rmax: steady-state mTFP/Venus ratio obtained after MCTs block (1 μM AR-C155858) or 10 mM lactate. Lactate production rates (Fig. 1e, f) were computed by fitting a linear rate to the first minutes of lactate accumulation during MCTs block with 0.5 mM diclofenac. Glucose consumption rates (Fig. 3e, f) were computed by fitting a linear rate to the glucose decrease induced by cytochalasin B (20 μM) as described previously44. HEK293 cells expressing eLACCO2.1 (either alone or in co-culture) were imaged with a 20× objective, excited at 475 nm for 0.05–0.1 s and emission collected at 509–547 nm for GFP, with image acquisition every 10 s. The obtained GFP fluorescence was normalized to the baseline.

Novel object recognition memory task

The novel object recognition (NOR) test took place in an L-shaped maze as previously described14,115. The behavior task was carried out in a room adjacent to mice housing with a light intensity of 50 ± 3 lux. An overhung video camera over the maze was used to record mice behavior and scoring was performed offline. The task consisted of 3 sequential daily trials of 9 min each. On day 1, the habituation phase, mice were placed in the center of the maze and allowed to freely explore the arms in the absence of any objects. On day 2, the acquisition phase, mice were placed in the center of the maze with the presence of two identical objects positioned at the extremities of each arm and left to freely explore the maze and the objects. On day 3, the long-term memory test phase (24 h after acquisition session), similarly to day 2, mice were placed in the center of the maze with two objects but one of the familiar objects was replaced by a novel object of a different shape, color, and texture, and mice were left to explore both objects. The position of the novel object and the associations of novel and familiar were randomized. All objects were previously tested to avoid biased preference. The apparatus as well as objects were cleaned before experimental use and between each animal testing with water and at the end of the experimental session with ethanol 70%. Some animals were used in two consecutive experiments: (i) First NOR task, with an injection of the vehicle immediately after the acquisition phase, and (ii) one week after the first NOR task, a second NOR task (with different objects) was performed, and an injection of drugs (NCT-503, THC, 3,5-DHBA, etc.) was done immediately after the acquisition phase. Cognitive performance was assessed by the discrimination index (DI), computed as the difference between the time spent exploring the novel (TN) and the familiar object (TF) divided by the total exploration time (TN + TF): DI = [TN-TF]/[TN + TF]. Object exploration was defined as the nose-poking of the objects. Mice with a total exploration time <15 s were not included in the data analysis. Memory performance was also evaluated by directly comparing the exploration time of novel and familiar objects, respectively. Experienced investigators evaluating the exploration were blind to the treatment and/or genotype of the animals. Normally, mice carried out the task without issues, however, some mice performed behaviors incompatible with the test (i.e., not exploring both objects, either by chance or due to peeing in a maze arm and refusing to cross over the urine.) These mice were returned to the home cage and retested one hour after. If mice failed again to perform the behavioral task, they were excluded from the experiment.

Electrophysiology

Slice preparation

After being anesthetized with 5% isoflurane for two minutes, C57BL/6N mice (12–16 weeks old) were decapitated, and the brain quickly extracted in ice-cold artificial cerebrospinal fluid (aCSF) containing (in mM): 125 NaCl, 2.5 KCl, 1 NaH2PO4, 1.2 MgCl2, 0.6 CaCl2, 26 NaHCO3 and 11 Glucose (pH 7.3, 305 mosmol/kg). Coronal hippocampal slices (350 µm) were prepared using a vibratome (Leica VT1200 S) and hemisected. Next, Slices were incubated in aCSF containing 2 mM MgCl2 and 1 mM CaCl2 for 30 min at 33 °C. Finally, slices were allowed to rest for 1 h at room temperature before starting recordings.

NMDAR field excitatory postsynaptic potentials recordings

Slices were transferred into a recording chamber, maintained at 32 °C, and perfused continuously with aCSF (3 mL/min) containing this time 1.3 mM MgCl2 and 2.5 mM CaCl2. Extracellular field excitatory postsynaptic potentials (fEPSPs) were recorded with a Multiclamp 700B amplifier (Axon Instruments, Inc.) using pipettes (2–4 MΩ) filled with aCSF and placed in the stratum radiatum of the hippocampal CA1 area. The stimulation of the Schaffer collaterals (0.05 Hz, 100 µs duration) with a concentric bipolar tungsten electrode was used to induce synaptic responses. Recorded signals were filtered at 2 kHz and digitized at 10 kHz via a DigiData 1440 (Axon Instruments, Inc.). Data were collected and analyzed offline using pClamp 10.7 software (Axon Instruments Inc.). For each experiment, a stable baseline was recorded for at least 15 min before starting the Input/Output measurement. The stimulation amplitude that evokes 50% of the maximal response was used for recordings. NMDA-fEPSPs were then isolated with low Mg2+ aCSF (0.2 mM) in the presence of 2,3-dihydroxy-6-nitro-7-sulfamoyl-benzo[f]quinoxaline-2,3-dione (NBQX, 10 µM) to block AMPA/kainate receptors, respectively. To study the co-agonist binding site occupancy of synaptic NMDARs, after obtaining a 20-min stable response, d-serine (50 µM) was bath applied for 30 min. The same protocol was applied with lactate (2 mM). For occlusion experiments, the first drug was bath applied 20 min before the recording and then during the whole experiment. Drugs used were d-serine (50 µM), lactate (2 mM), the PHGDH inhibitor NCT-503 (10–20 µM) and the HCAR1 agonist 3,5-DHBA (1 mM). d-AP5 (50 µM) was applied at the end of 3,5-DHBA occlusion experiments to confirm that NMDA-fEPSPs were mediated by NMDA receptors (Supplementary Fig. 7A, B). NMDAR-fEPSPs slopes were measured as a linear fit of the rising phase, between time points set in the baseline period and corresponding to 20% and 60% of the peak amplitude. The change in slope was normalized to the baseline slope taken during the 15 min immediately before drug applications. Representative NMDAR-fEPSPs traces are the

average of successive sweeps that correspond to the last 10 min of baseline versus the last 10 min of drug applications.

Mathematical modeling

The dynamics of pyruvate and lactate were simulated with a model published previously20 but with modifications (explained below). The set of ordinary differential equations used were the following:

(1) $dT_{out}/dt = (K_{off}\_H \times TH_{out}) + (f_1 \times T_{in}) - (K_{on} \times T_{out} \times H_{out}) - (f_1 \times T_{out})$

(2) $dT_{in}/dt = (K_{off}\_H \times TH_{in}) + (f_1 \times T_{out}) - (K_{on} \times T_{in} \times H_{in}) - (f_1 \times T_{in})$

(3) $dTH_{out}/dt = (K_{on} \times T_{out} \times H_{out}) + (K_{off}\_L \times THL_{out}) + (K_{off}\_P \times THP_{out}) -$

$(K_{off}\_H \times TH_{out}) - (K_{on} \times TH_{out} \times L_{out}) - (K_{on} \times TH_{out} \times P_{out})$

(4) $dTH_{in}/dt = (K_{on} \times T_{in} \times H_{in}) + (K_{off}\_L \times THL_{in}) + (K_{off}\_P \times THP_{in}) - (K_{off}\_H \times TH_{in}) -$

$(K_{on} \times TH_{in} \times L_{in}) - (K_{on} \times TH_{in} \times P_{in})$

(5) $dTHL_{out}/dt = (K_{on} \times TH_{out} \times L_{out}) + (f_2 \times THL_{in}) - (K_{off}\_L \times THL_{out}) - (f_2 \times THL_{out})$

(6) $dTHL_{in}/dt = (K_{on} \times TH_{in} \times L_{in}) + (f_2 \times THL_{out}) - (K_{off}\_L \times THL_{in}) - (f_2 \times THL_{in})$

(7) $dTHP_{out}/dt = (K_{on} \times TH_{out} \times P_{out}) + (f_2 \times THP_{in}) - (K_{off}\_P \times THP_{out}) - (f_2 \times THP_{out})$

(8) $dTHP_{in}/dt = (K_{on} \times TH_{in} \times P_{in}) + (f_2 \times THP_{out}) - (K_{off}\_P \times THP_{in}) - (f_2 * THP_{in})$

(9) $dL_{in}/dt = (LDH_{fw} \times P_{in}) + (K_{off}\_L \times THL_{in}) - (LDH_{rv} \times L_{in}) - (K_{on} \times TH_{in} \times L_{in})$

(10) $dP_{in}/dt = Glycolysis*E + (LDH_{rv} \times L_{in}) + (K_{off}\_P \times THP_{in}) - (K_{on} \times TH_{in} \times Pin) -$

$(LDH_{fw} \times P_{in}) - (Mito \times P_{in})$

Equations 1–8 represent the eight possible conformations of the MCT carrier: outward- and inward-facing, either empty (Tout and Tin), loaded with a proton (THout and THin), loaded with both proton and lactate (THLout and THLin), and loaded with both proton and pyruvate (THPout and THPin). Equations 9 and 10 represent cytosolic lactate and pyruvate. The association constant Kon for protons, lactate, and pyruvate was set at 108 m^{-1} s^{-1} (diffusion-limited); the dissociation constants Koff_H, Koff_L, and Koff_P were 20 s^{-1}, 7.6 × 107 s^{-1}, and 7.6 × 106 s^{-1} (for MCT1). Carrier translocation rates f1 (empty) and f2 (loaded) were set at 200 and 3000 s^{-1}. Rate constants were 0.139 s^{-1} (Mito, mitochondrial pyruvate import),

0.5 s−1 (LDHforward, pyruvate to lactate), and 0.025 s−1 (LDHreverse, lactate to pyruvate). The cytosolic and extracellular pH was set to 7.2 (63 nM) and 7.4 (40 nM), respectively. The extracellular value of lactate was set to 0.5 mM. To explore if the activation of glucose consumption by HCAR1 signaling (Fig. 3e) might result in the diversion of carbons toward branched pathways, first, the data shown in Fig. 3g (and Supplementary Fig. 7C) was transformed to lactate concentration using a two-point calibration with $\Delta R = 0.38$ as described previously17. Using this data, it was quantified (i) the average lactate production (40 μM/s), (ii) the basal lactate concentration (1.49 mM), and the lactate increase induced by 3,5-DHBA ($\Delta Lac = 0.6$ mM). To simulate a diversion of carbons toward branched pathways, the parameter "Glycolysis" on Eq. 10, was multiplied by a number between 1 and 0.1 to simulate a change in the "efficiency" of glucose-to-lactate conversion (E; see Supplementary Fig. 7E for a graphical representation). Simulations were carried out either with $E = 0.5$ (Fig. 3h), 0.7 or 0.9 (Supplementary Fig. 7) in basal conditions (i.e., before glycolysis stimulation), and a decrease in E during glycolysis stimulation (E*) was simulated. The "Glycolysis" value was adjusted to obtain a lactate production of 40 μM/s for all E values tested. The amount of total carrier was slightly adjusted to achieve identical basal lactate levels for all E values tested.

Quantification and statistical analysis

All graphs, linear regressions, and statistical analyses were performed using GraphPad software (version 8 or 10). Data is presented as time course (average of imaged cells ± SEM, from a representative experiment), scatter plots of individual cells, and bars + symbols. In some experimental data, the SEM is small enough to be contained inside symbols. Otherwise, time courses without error bars correspond to a representative cell from an independent experiment and are indicated in the relevant figure legend. All data was analyzed for outliers using the ROUT method (false discovery rate of 1%), and for normality with the Shapiro–Wilk test. To perform the statistical analysis, the electrophysiology data was averaged every 5 min. Differences between groups were assessed using the average of each independent experiment using either by paired t-test, unpaired t-test, one-way ANOVA followed by Tukey's multiple comparison test, Kruskal–Wallis followed by Dunn's multiple comparison test, Mixed-effects model followed by Dunnett's multiple comparison test or two-way ANOVA followed by Tukey's multiple comparison test. $P < 0.05$ was considered significant and is annotated in each figure and available in Supplementary Tables 2 and 3. Otherwise, nonsignificant data is indicated as NS.

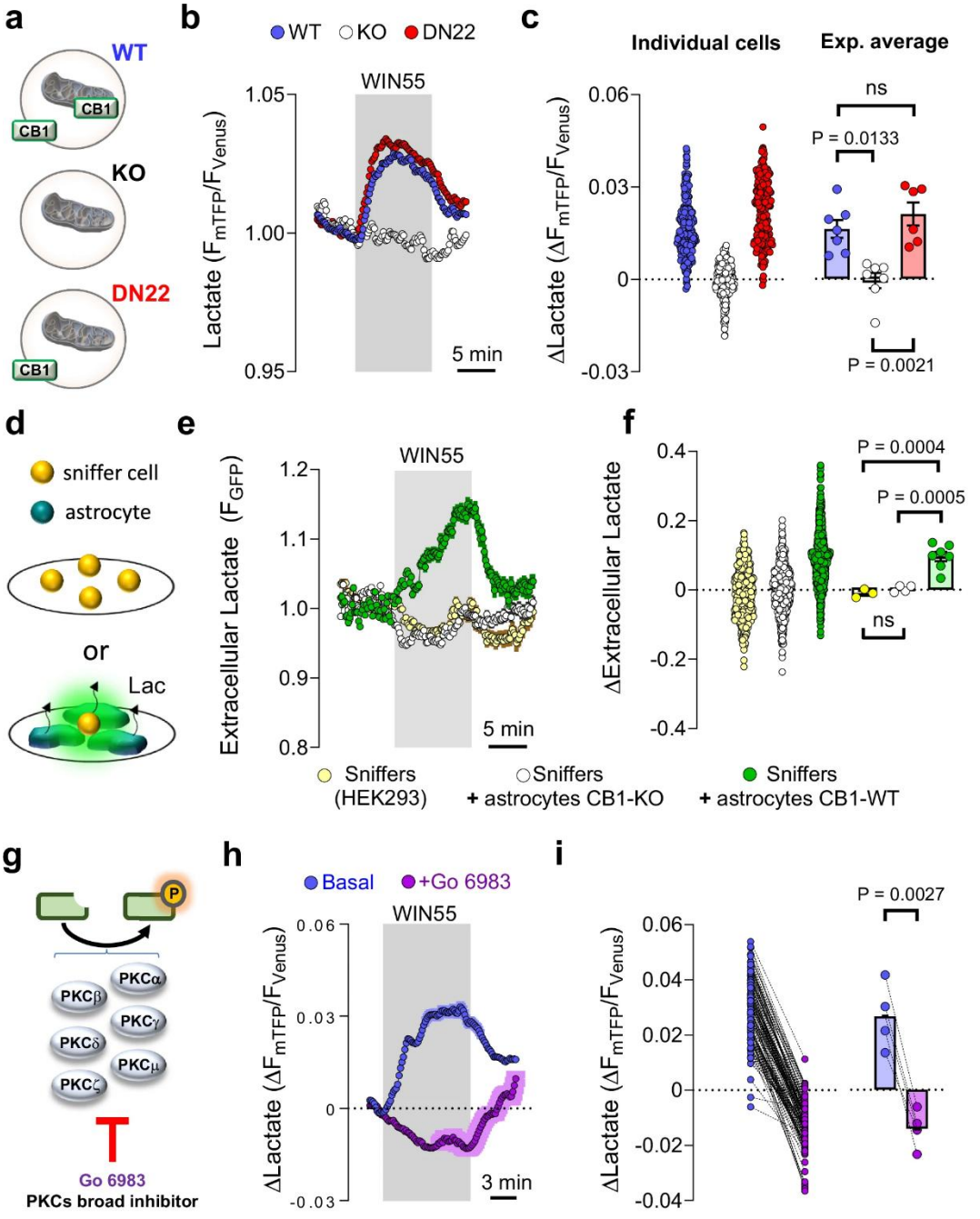

Fig. 1: Acute stimulation of astrocytes lactate metabolism by CB1 receptors. a *Subcellular localization of CB1 receptors in the primary astrocytes culture models.* ***b*** *Intracellular lactate measurement during exposure to WIN55 (1 μM), in CB1-WT (blue circles, average of 42 cells), CB1-KO (white circles, average of 29 cells), and DN22-CB1-KI (red circles, average of 42 cells) astrocytes.* ***c*** *Quantification of lactate changes after 5 min exposure to WIN55. CB1-WT: n = 7247 cells. CB1-KO: n = 7252 cells. DN22-CB1-KI: n = 6235 cells.* ***d*** *Sniffer cell strategy for the determination of extracellular lactate levels. HEK cells expressing an extracellular lactate fluorescent biosensor (sniffers cells) were cultured alone or in co-culture with astrocytes.* ***e*** *Extracellular lactate measurements during exposure to WIN55*

(1 μM), in a pure culture of sniffers cells (yellow circles, average of 81 cells), a co-culture of sniffers cells, and CB1-WT astrocytes (green circles, average of 76 cells) and a co-culture of sniffers cells and CB1-KO astrocytes (white circles, average of 102 cells). ***f*** *Quantification of the extracellular lactate levels after 10 min exposure to WIN55. Sniffer culture: n = 3406 cells. Sniffer + CB1-WT astrocytes co-culture: n = 7997 cells. Sniffer + CB1-KO astrocytes co-culture: n = 4469 cells.* ***g*** *Scheme depicting the PKC isozymes inhibited by Go 6983.* ***h*** *Intracellular lactate measurement during exposure to WIN55 (1 μM), in CB1-WT astrocytes, before (blue) and during exposure to the broad PKC inhibitor Go 6983 (purple). N = 4124 cells.* ***i*** *Quantification of lactate changes after 5 min exposure to WIN55, before (blue) and during exposure to Go 6983 (purple), n = 4124 cells analyzed. Data corresponds to the average (mean ± SEM) of representative of a single (**b**, **e**) or all experiments (**g**). Circles in scatter or before-after plots correspond to individual cells (**c**, **f**, **i**). Bars correspond to experiments average (mean ± SEM), with circles representing individual experiment average (**c**, **f**, **i**). Statistical analysis was performed using a Kruskal–Wallis test followed by Dunn's multiple comparison test (**c**), One-way ANOVA followed by Tukey's multiple comparison test (**f**) and two-tailed paired t-test (**i**). See Supplementary Table **2** for more details on statistical analyses. Source data are provided as a Source Data file.*

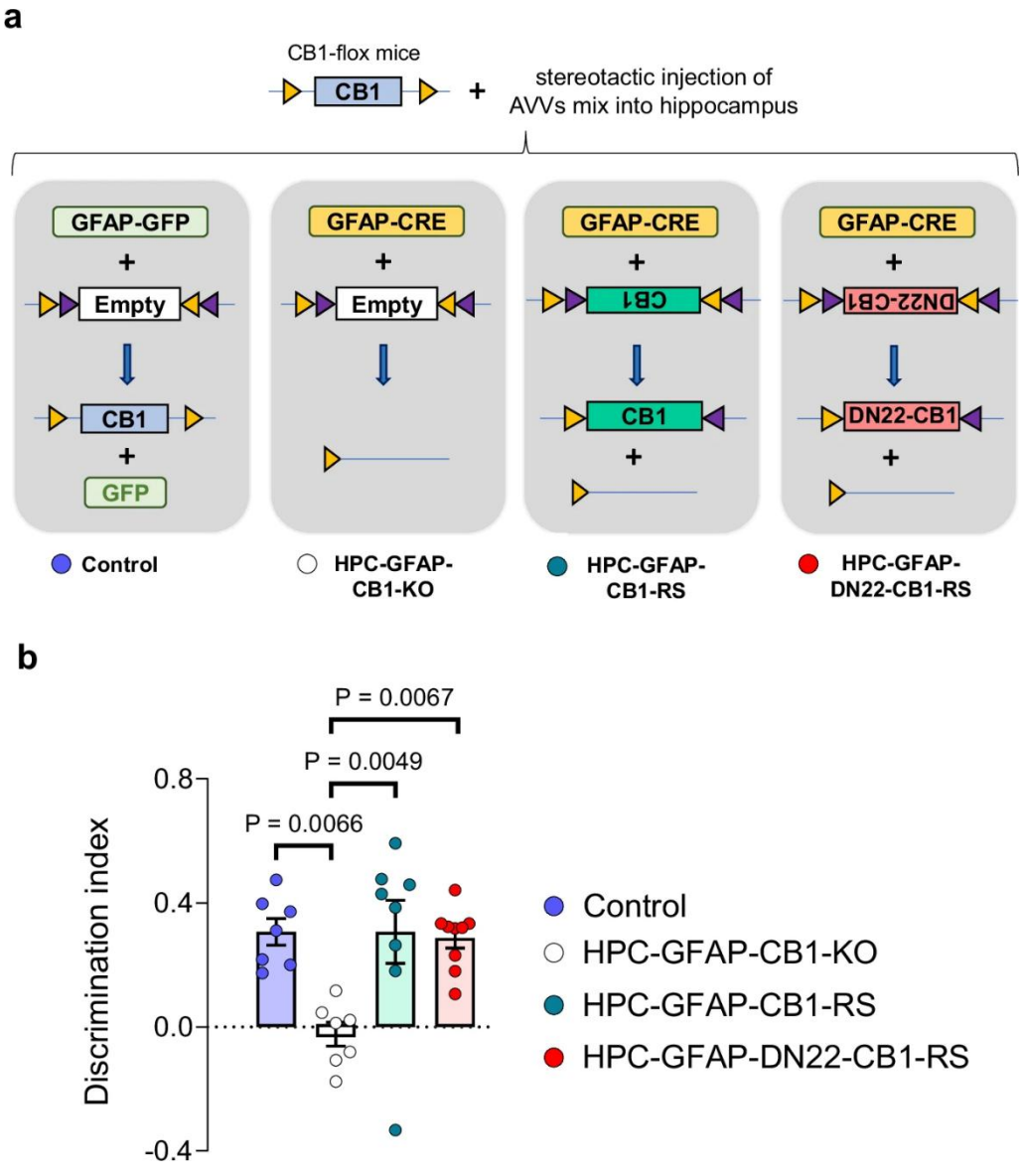

Fig. 2: The astroglial mtCB1 receptor is not necessary for physiological NOR performance. ***a*** *Schematic of the viral approach used for deletion of hippocampal astroglial CB1 receptors and expression rescue with either wild-type or DN22-CB1 sequences. Four groups of animals; Control, HPC-GFAP-CB1-KO, HPC-GFAP-CB1-RS, and HPC-GFAP-DN22-CB1-RS mice; were obtained by stereotactic injection of a mix of specific AAV constructs (see Methods section for details).* ***b*** *Summary of NOR performance in Control (blue), HPC-GFAP-CB1-KO (white), HPC-GFAP-CB1-RS (teal), and HPC-GFAP-DN22-CB1-RS (red) mice, n = 7–9 mice per condition. Bars correspond to experiment average (mean ± SEM) and circles represent individual animals (**b**). Statistical analysis was performed using a One-way ANOVA followed by Tukey's multiple comparison test (**b**). See Supplementary Table **2** for more details on statistical analyses. Source data are provided as a Source Data file.*

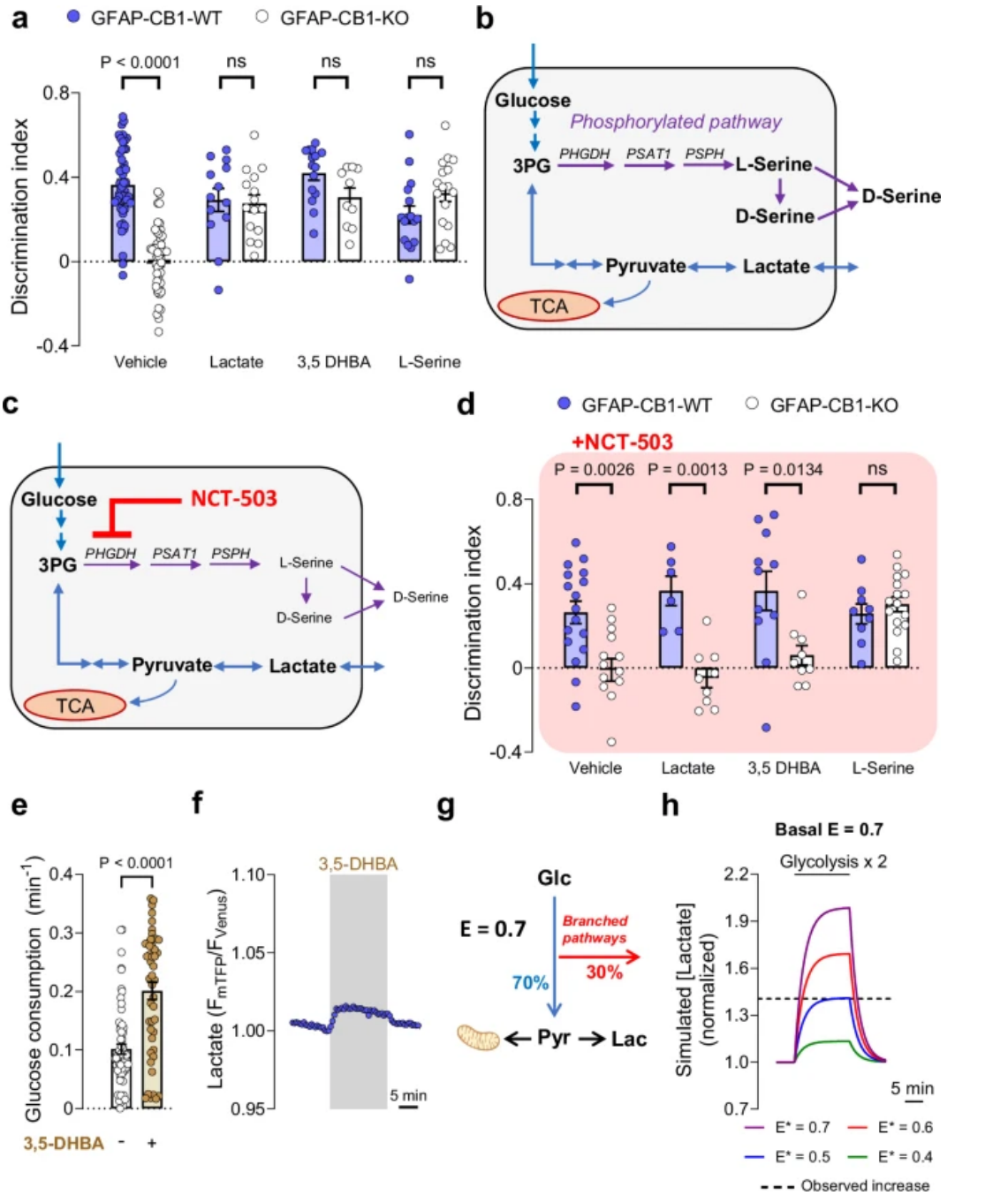

Fig. 3: Lactate promotes NOR performance via receptor-dependent stimulation of the phosphorylated pathway. ***a*** *NOR performance of GFAP-CB1-WT (blue circles) and GFAP-CB1-KO (white circles) mice. Animals were treated with an I.P. injection of either vehicle, lactate (1 g/kg), 3,5-DHBA (240 mg/kg), or l-serine (0.5 g/kg), immediately after the acquisition phase. N = 18–53 mice per condition.* ***b*** *Scheme depicting the lactate production and phosphorylated pathway, and their interaction at the level of 3-phosphoglycerate (3PG).* ***c*** *Scheme depicting the effect of a sub-effective dose of NCT-503 on the l-serine synthesis.* ***d*** *NOR performance of GFAP-CB1-WT (blue circles) and GFAP-CB1-KO (white circles) mice. Animals were treated with an I.P. injection of either vehicle + NCT-503 (6 mg/kg), lactate (1 g/kg) + NCT-503, 3,5-DHBA (240 mg/kg) + NCT-503 or l-serine (0.5 g/kg) + NCT-503,*

immediately after the acquisition phase. N = 6–20 mice per condition. ***e*** *Glucose consumption in control (n = 4, 63 cells) and 3,5-DHBA treated (n = 4, 48 cells) astrocytes.* ***f*** *Intracellular lactate measurement during exposure to 3,5-DHBA (1 mM). An average of 54 cells from a single experiment.* ***g*** *Schematic representation of the mathematical model used to analyze the data. The glucose-to-pyruvate/lactate conversion "efficiency" (E) controls how much glucose is directed into pyruvate/lactate synthesis or into branched pathways (e.g., phosphorylated pathway). At E = 0.7, 70% of consumed glucose goes into pyruvate and 30% into branched pathways. Pyruvate can be consumed by mitochondria or transformed into lactate at a fixed rate.* ***h*** *Numerical simulation of intracellular lactate concentration (normalized to baseline) with basal E = 0.7, during a two-fold increase in glycolysis. During this stimulation, a decrease in glucose-to-pyruvate/lactate conversion (E*) was simulated. The observed increase in intracellular lactate induced by 3,5-DHBA is indicated by a discontinuous line. Bars correspond to experiments average (mean ± SEM) and circles represent individual animals (****a****,* ***d****) or single cells (****f****). Data corresponds to the average (mean ± SEM) of representative of experiment (****g****). Solid line corresponds to a single numerical simulation (****h****). Statistical analysis was performed using a two-way ANOVA followed by Tukey's multiple comparison test (****a****,* ***d****) or two-tailed Mann–Whitney test (****e****). See Supplementary Table* ***2*** *for more details on statistical analyses. Source data are provided as a Source Data file.*

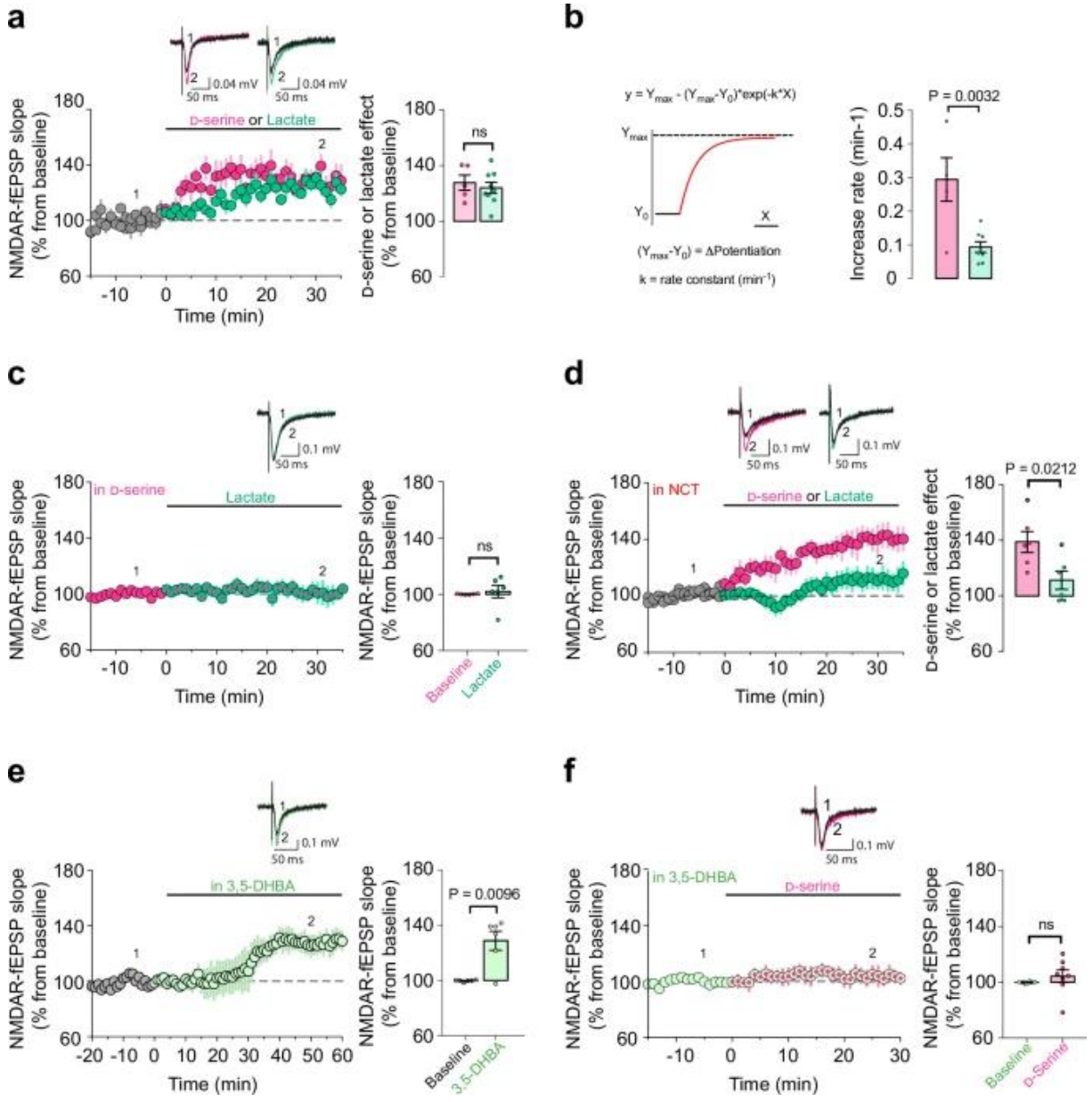

Fig. 4: Synaptic d-serine availability is modulated by lactate. ***a*** *Representative averaged NMDAR-fEPSPs traces from 30 consecutive sweeps evoked (1) 10 min before and (2) during (25–35 min) bath application of d-serine (magenta) or lactate (green). The summary plots show the effect of d-serine (50 μM – magenta circles, n = 5 slices, 4 mice) or lactate (2 mM – green circles, n = 9 slices, 8 mice) on NMDAR-mediated fEPSPs slopes in WT hippocampal slices.* ***b*** *Increase rate of NMDAR-mediated fEPSPs potentiation induced by lactate (n = 8) or d-serine (n = 5) shown in* ***(a)****. Data obtained by fitting a non-linear model.* ***c*** *Representative averaged NMDAR-fEPSPs traces evoked (1) 10 min before and (2) during (25–35 min) bath application of lactate (green) in the presence of d-serine. The summary plots show the NMDAR-fEPSPs slopes before (magenta) and during lactate exposure (2 mM – magenta/green, n = 6 slices, 6 mice) in slices preincubated with d-serine (50 μM).* ***d*** *Representative*

averaged NMDAR-fEPSPs traces evoked (1) 10 min before and (2) during (25–35 min) bath application of d-serine (in magenta) or lactate (in green) in the presence of NCT-503. The summary plots show the effect of exogenous d-serine (50 μM – magenta, n = 6 slices, 6 mice) or lactate (2 mM – green, n = 6 slices, 6 mice) on NMDAR-mediated fEPSPs slopes in slices preincubated with NCT-503 (10–20 μM). ***e*** *Representatives NMDAR-fEPSPs traces evoked (1) 10 min before and (2) during bath application (25–35 min) of 3,5-DHBA (light green). Summary plots showing the effect of 3,5-DHBA (1 mM – light green circles, n = 6 slices, 4 mice) on NMDAR-mediated fEPSPs slopes.* ***f*** *Representatives NMDAR-fEPSPs traces evoked (1) before and (2) during bath application of exogenous d-serine in the presence of 3,5-DHBA. The summary plots show the NMDAR-fEPSPs slopes before (light green) and during exogenous d-serine exposure (50 μM – light green/magenta circles, n = 8 slices, 5 mice) in slices preincubated with 3,5-DHBA (1 mM). Data are presented as mean ± SEM (**a**, **c**–**f**). Bars correspond to the experiment average (mean ± SEM) and circles represent single measurement (**a**–**f**). Statistical analysis was performed using a two-tailed unpaired t-test (**a**–**f**). See Supplementary Table **2** for more details on statistical analyses. Source data are provided as a Source Data file.*

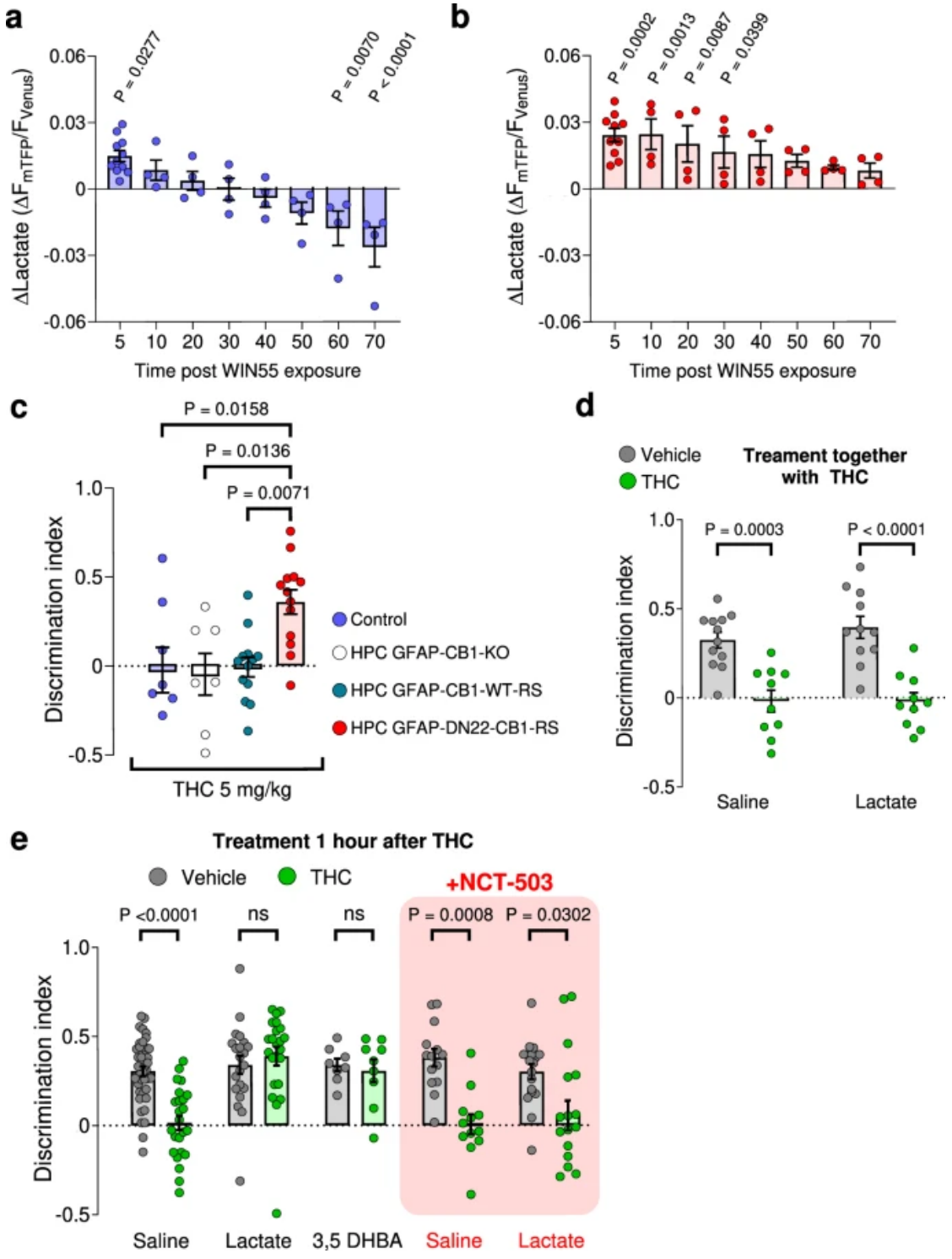

Fig. 5: THC impairs NOR performance via mtCB1 receptor-dependent inhibition of the phosphorylated pathway. a *Intracellular lactate changes measured at different time points during a 70 min WIN55 exposure in CB1-WT astrocytes. N = 4164 cells analyzed. Data from Fig.* ***1c*** *(5 min quantification) is included in the graph.* ***b*** *Intracellular lactate changes measured at different time points*

during a 70 min WIN55 exposure in DN22-CB1-KI astrocytes. N = 4192 cells analyzed. Data from Fig. ***1c*** *(5 min quantification) is included in the graph.* ***c*** *Summary of NOR performance in Control (blue), HPC-GFAP-CB1-KO (white), HPC-GFAP-CB1-RS (teal), and HPC-GFAP-DN22-CB1-RS (red) mice, treated with an I.P. injection of THC (5 mg/kg) immediately after acquisition phase. N = 7–13 mice per condition.* ***d*** *NOR performance of mice treated either with an I.P. injection of either vehicle (gray) + saline, THC (5 mg/kg, green) + saline, vehicle + lactate (1 g/kg) or THC (5 mg/kg) + lactate (1 g/kg), immediately after the acquisition phase. N = 10–12 mice per condition.* ***e*** *NOR performance of mice treated either with an I.P. injection of vehicle (gray) or THC (5 mg/kg, green) immediately after the acquisition phase. After 1-h post-THC or vehicle treatment, mice were treated with an I.P. injection of either saline, lactate (1 g/kg), 3,5-DHBA (240 mg/kg), NCT-503 (6 mg/kg) + saline or NCT-503 + lactate. N = 8–49 mice per condition. Bars correspond to the experiment average (mean ± SEM) and circles represent an experiment average (****a****,* ***b****) or represent individual animals (****c****,* ***d****,* ***e****). Statistical analysis was performed using a Mixed-effects model (REML) followed by Dunnett's multiple comparison test (****a****,* ***b****) and a two-way ANOVA test by Tukey's multiple comparison test (****c****,* ***d****,* ***e****). See Supplementary Table* ***2*** *for more details on statistical analyses. Source data are provided as a Source Data file.*

References

1. Busquets-Garcia, A., Bains, J. & Marsicano, G. CB1 receptor sig- naling in the brain: extracting specificity from ubiquity. Neu- ropsychopharmacol 43, 4–20 (2018).

2. Zou, S. & Kumar, U. Cannabinoid receptors and the endocanna- binoid system: signaling and function in the central nervous sys- tem. Int. J. Mol. Sci. 19, 833 (2018).

3. Martinez Ramirez, C. E. et al. Endocannabinoid signaling in the central nervous system. Glia 71, 5–35 (2023).

4. Busquets-Garcia, A. et al. Dissecting the cannabinergic control of behavior: the where matters. BioEssays 37, 1215–1225 (2015).

5.Stella, N. THC and CBD: similarities and differences between sib- lings. Neuron 111, 302–327 (2023).

6. Benard, G. et al. Mitochondrial CB(1) receptors regulate neuronal energy metabolism. Nat. Neurosci. 15, 558–564 (2012).

7. Hebert-Chatelain, E. et al. A cannabinoid link between mitochon- dria and memory. Nature 539, 555–559 (2016).

8. Serrat, R. et al. Astroglial ER-mitochondria calcium transfer med- iates endocannabinoid-dependent synaptic integration. Cell Rep. 37, 110133 (2021).

9. Robledo-Menendez, A., Vella, M., Grandes, P.& Soria-Gomez, E. Cannabinoid control of hippocampal functions: the where mat- ters. FEBS J. 289, 2162–2175 (2022).

10. Jong, Y.-J. I., Harmon, S. K. & O'Malley, K. L. Intracellular GPCRs play key roles in synaptic plasticity. ACS Chem. Neurosci. 9, 2162–2172 (2018).

11. Soria-Gomez, E. et al. Subcellular specificity of cannabinoid effects in striatonigral circuits. Neuron 109, 1513–1526.e11 (2021).

12. Covelo, A., Eraso-Pichot, A., Fernández-Moncada, I., Serrat, R. & Marsicano, G. CB1R-dependent regulation of astrocyte physiology and astrocyte-neuron interactions. Neuropharmacology 195, 108678 (2021).

13. Ramon-Duaso, C., Conde-Moro, A. R. & Busquets-Garcia, A. Astroglial cannabinoid signaling and behavior. Glia https://doi. org/10.1002/glia.24171 (2022).

14. Robin, L. M. et al. Astroglial CB1 receptors determine synaptic D-serine availability to enable recognition memory. Neuron 98, 935–944.e5 (2018).

15. Gutiérrez-Rodríguez, A. et al. Localization of the cannabinoid type- 1 receptor in subcellular astrocyte compartments of mutant mouse hippocampus. Glia 66, 1417–1431 (2018).

16. Jimenez-Blasco, D. et al. Glucose metabolism links astroglial mitochondria to cannabinoid effects. Nature 583, 603–608 (2020).

17. San Martín, A. et al. A genetically encoded FRET lactate sensor and its use to detect the Warburg effect in single cancer cells. PLoS ONE 8, e57712 (2013).

18. Soria-Gomez, E. et al. Habenular CB1 receptors control the expression of aversive memories. Neuron 88, 306–313 (2015).

19. Barros, L. F. et al. Small is fast: astrocytic glucose and lactate metabolism at cellular resolution. Front. Cell. Neurosci. 7, 27 (2013).

20. Contreras-Baeza, Y. et al. Monocarboxylate transporter 4 (MCT4) is a high affinity transporter capable of exporting lactate in high- lactate microenvironments. J. Biol. Chem. 294, 20135–20147 (2019).

21. Sasaki, S. et al. Effect of diclofenac on SLC16A3/MCT4 by the Caco-2 cell line. Drug Metab. Pharmacokinet. 31, 218–223 (2016).

22. Magistretti, P. J. & Allaman, I. Lactate in the brain: from metabolic end-product to signalling molecule. Nat. Rev. Neurosci. 19, 235–249 (2018).

23. Zuend, M. et al. Arousal-induced cortical activity triggers lactate release from astrocytes. Nat. Metab. 2, 179–191 (2020).

24. Lerchundi, R. et al. NH4(+) triggers the release of astrocytic lactate via mitochondrial pyruvate shunting. Proc. Natl Acad. Sci. USA 112, 11090–11095 (2015).

25. Sotelo-Hitschfeld, T. et al. Channel-mediated lactate release by K^+-stimulated astrocytes. J. Neurosci. 35, 4168–4178 (2015).

26. Nasu, Y. et al. Lactate biosensors for spectrally and spatially multiplexed fluorescence imaging. Nat. Commun. 14, 6598 (2023).

27. Busquets-Garcia, A. et al. Hippocampal protein kinase C signaling mediates the short-term memory impairment induced by delta9- tetrahydrocannabinol. Neuropsychopharmacology https://doi. org/10.1038/npp.2017.175 (2017).

28. Gschwendt, M., Kittstein, W. & Johannes, F. J. Differential effects of suramin on protein kinase C isoenzymes. A novel tool for dis- criminating protein kinase C activities. FEBS Lett. 421, 165–168 (1998).

29. Gschwendt, M. et al. Inhibition of protein kinase C mu by various inhibitors. Differentiation from protein kinase c isoenzymes. FEBS Lett. 392, 77–80 (1996).

30. Han, J. et al. Acute cannabinoids impair working memory through astroglial CB1 receptor modulation of hippocampal LTD. Cell 148, 1039–1050 (2012).

31. Oliveira da Cruz, J. F. et al. Specific hippocampal interneurons shape consolidation of recognition memory. Cell Rep. 32, 108046 (2020).

32. Veloz Castillo, M. F., Magistretti, P. J. & Calì, C. l-Lactate: food for thoughts, memory and behavior. Metabolites 11, 548 (2021).

33. Carrard, A. et al. Peripheral administration of lactate produces antidepressant-like effects. Mol. Psychiatry 23, 488 (2018).

34. Barros, L. F. Metabolic signaling by lactate in the brain. Trends Neurosci. 36, 396–404 (2013).

35. Morland, C. et al. The lactate receptor, G-protein-coupled recep- tor 81/hydroxycarboxylic acid receptor 1: expression and action in brain. J. Neurosci. Res. 93, 1045–1055 (2015).

36. Hu, J. et al. The roles of GRP81 as a metabolic sensor and inflam- matory mediator. J. Cell Physiol. 235, 8938–8950 (2020).

37. Lev-Vachnish, Y. et al. L-Lactate promotes adult hippocampal neurogenesis. Front. Neurosci. 13, 403 (2019).

38. Maugard, M., Vigneron, P.-A., Bolaños, J. P. & Bonvento, G. l-Serine links metabolism with neurotransmission. Prog. Neurobiol. 197, 101896 (2021).

39. Coyle, J. T., Balu, D. & Wolosker, H. D-serine, the shape-shifting NMDA receptor co-agonist. Neurochem. Res. 45,1344–1353 (2020).

40. Neame, S. et al. The NMDA receptor activation by d-serine and glycine is controlled by an astrocytic Phgdh-dependent serine shuttle. Proc. Natl Acad. Sci. USA 116, 20736–20742 (2019).

41. Le Douce, J. et al. Impairment of glycolysis-derived l-serine pro- duction in astrocytes contributes to cognitive deficits in Alzhei- mer's Disease. Cell Metab. 31, 503–517.e8 (2020).

42. Pacold, M. E. et al. A PHGDH inhibitor reveals coordination of serine synthesis and one-carbon unit fate. Nat. Chem. Biol. 12, 452–458 (2016).

43. Takanaga, H., Chaudhuri, B. & Frommer, W. B. GLUT1 and GLUT9 as major contributors to glucose influx in HepG2 cells identified by a high sensitivity intramolecular FRET glucose sensor. Biochim. Biophys. Acta 1778, 1091–1099 (2008).

44. Bittner, C. X. et al. High resolution measurement of the glycolyticrate. Front. Neuroenergetics 2, 26 (2010).

45. Fernández-Moncada, I. et al. Bidirectional astrocytic GLUT1 acti- vation by elevated extracellular K. Glia 69, 1012–1021 (2021).

46. Papouin, T., Dunphy, J., Tolman, M., Foley, J. C. & Haydon, P. G. Astrocytic control of synaptic function. Philos. Trans. R. Soc. Lond. B Biol. Sci. 372, 20160154 (2017).

47. Puighermanal, E. et al. Cannabinoid modulation of hippocampal long-term memory is mediated by mTOR signaling. Nat. Neurosci. 12, 1152–1158 (2009).

48. Piomelli, D. The molecular logic of endocannabinoid signalling. Nat. Rev. Neurosci. 4, 873–884 (2003).

49. Dudok, B. & Soltesz, I. Imaging the endocannabinoid signaling system. J. Neurosci. Methods 367, 109451 (2022).

50. Araque, A., Castillo, P. E., Manzoni, O. J. & Tonini, R. Synaptic functions of endocannabinoid signaling in health and disease. Neuropharmacology 124, 13–24 (2017).

51. Oliveira, J. F. & Araque, A. Astrocyte regulation of neural circuit activity and network states. Glia 70, 1455–1466 (2022).

52. Sherwood, M. W., Oliet, S. H. R. & Panatier, A. NMDARs, coin- cidence detectors of astrocytic and neuronal activities. Int. J. Mol. Sci. 22, 7258 (2021).

53. Savtchouk, I. & Volterra, A. Gliotransmission: beyond black-and- white. J. Neurosci. 38, 14–25 (2018).

54. Durkee, C. A. & Araque, A. Diversity and specificity of astrocyte- neuron communication. Neuroscience 396, 73–78 (2019).

55. Barros, L. F. et al. Aerobic Glycolysis in the Brain: Warburg and Crabtree Contra Pasteur. Neurochem. Res. https://doi.org/10. 1007/s11064-020-02964-w (2020).

56. Pellerin, L. & Magistretti, P. J. Glutamate uptake into astrocytes stimulates aerobic glycolysis: a mechanism coupling neuronal activity to glucose utilization. Proc. Natl Acad. Sci. USA 91, 10625–10629 (1994).

57. Zimmer, E. R. et al. [18F]FDG PET signal is driven by astroglial glutamate transport. Nat. Neurosci. 20, 393–395 (2017).

58. Fernández-Moncada, I. et al. Neuronal control of astrocytic respiration through a variant of the Crabtree effect. Proc. Natl Acad. Sci. USA 115, 1623–1628 (2018).

59. Barros, L. F., Ruminot, I., Sotelo-Hitschfeld, T., Lerchundi, R. & Fernández-Moncada, I. Metabolic recruitment in brain tissue. Annu. Rev. Physiol. 85, 115–135 (2023).

60. San Martín, A., Arce-Molina, R., Galaz, A., Pérez-Guerra, G. & Bar- ros, L. F. Nanomolar nitric oxide concentrations quickly and reversibly modulate astrocytic energy metabolism. J. Biol. Chem. 292, 9432–9438 (2017).

61. Mazucanti, C. H., Kawamoto, E. M., Mattson, M. P., Scavone, C. & Camandola, S. Activity-dependent neuronal Klotho enhances astrocytic aerobic glycolysis. J. Cereb. Blood Flow. Metab. 39, 1544–1556 (2019).

62. Bittner, C. X. et al. Fast and reversible stimulation of astrocytic glycolysis by K+ and a delayed and persistent effect of glutamate. J. Neurosci. 31, 4709–4713 (2011).

63. Ruminot, I. et al. NBCe1 mediates the acute stimulation of astro- cytic glycolysis by extracellular K. J. Neurosci. 31, 14264–14271 (2011).

64. Jensen, T. P. et al. Multiplex imaging relates quantal glutamate release to presynaptic Ca^{2+} homeostasis at multiple synapses in situ. Nat. Commun. 10, 1414 (2019).

65. Callender, J. A. & Newton, A. C. Conventional protein kinase C in the brain: 40 years later. Neuronal Signal 1, NS20160005 (2017).

66. Battaini, F. Protein kinase C isoforms as therapeutic targets in nervous system disease states. Pharm. Res. 44, 353–361 (2001).

67. Newton, A. C. Protein kinase C: perfectly balanced. Crit. Rev. Biochem. Mol. Biol. 53, 208–230 (2018).

68. Slepko, N., Patrizio, M. & Levi, G. Expression and translocation of protein kinase C isoforms in rat microglial and astroglial cultures. J. Neurosci. Res. 57, 33–38 (1999).

69. Pearce, B., Morrow, C. & Murphy, S. A role for protein kinase C in astrocyte glycogen metabolism. Neurosci. Lett. 90, 191–196 (1988).

70. Clarke, D. et al. Phorbol esters stimulate 2-deoxyglucose uptake in

glia, but not neurons. Brain Res. 421, 358–362 (1987).

71. Lee, E. E. et al. A protein kinase C phosphorylation motif in GLUT1 affects glucose transport and is mutated in GLUT1 deficiency syndrome. Mol. Cell 58, 845–853 (2015).

72. Deziel, M. R., Lippes, H. A., Rampal, A. L. & Jung, C. Y. Phosphor- ylation of the human erythrocyte glucose transporter by protein kinase C: localization of the site of in vivo and in vitro phosphor- ylation. Int J. Biochem. 21, 807–814 (1989).

73. Witters, L. A., Vater, C. A. & Lienhard, G. E. Phosphorylation of the glucose transporter in vitro and in vivo by protein kinase C. Nature 315, 777–778 (1985).

74. Tsuru, M. et al. Role of PKC isoforms in glucose transport in 3T3-L1 adipocytes: insignificance of atypical PKC. Am. J. Physiol. Endo- crinol. Metab. 283, E338–E345 (2002).

75. Khayat, Z. A. et al. Rapid stimulation of glucose transport by mitochondrial uncoupling depends in part on cytosolic Ca2+ and cPKC. Am. J. Physiol. 275, C1487–C1497 (1998).

76. Hutchinson, D. S. & Bengtsson, T. alpha1A-adrenoceptors activate glucose uptake in L6 muscle cells through a phospholipase C-, phosphatidylinositol-3 kinase-, and atypical protein kinase C-dependent pathway. Endocrinology 146, 901–912 (2005).

77. Blair, D., Dufort, F. J. & Chiles, T. C. Protein kinase Cβ is critical for the metabolic switch to glycolysis following B-cell antigen receptor engagement. Biochem. J. 448, 165–169 (2012).

78. Liu, L. et al. Protein kinase C-iota-mediated glycolysis promotes non-small-cell lung cancer progression. Onco Targets Ther. 12, 5835–5848 (2019).

79. Otake, S. et al. Regulation of the expression and activity of glucose and lactic acid metabolism-related genes by protein kinase C in skeletal muscle cells. Biol. Pharm. Bull. 36, 1435–1439 (2013).

80. Xu, W. et al. Crosstalk of protein kinase C ε with Smad2/3 promotes tumor cell proliferation in prostate cancer cells by enhancing aerobic glycolysis. Cell Mol. Life Sci. 75, 4583–4598 (2018).

81. Hong, S.-S., Gibney, G. T., Esquilin, M., Yu, J. & Xia, Y. Effect of protein kinases on lactate dehydrogenase activity in cortical neurons during hypoxia. Brain Res. 1009, 195–202 (2004).

82. Fernández-Moncada, I. & Barros, L. F. Non-preferential fuelling of the Na(+)/K(+)-ATPase pump. Biochem. J. 460, 353–361 (2014).

83. Bouzier-Sore, A.-K., Voisin, P., Canioni, P., Magistretti, P. J. & Pel- lerin, L. Lactate is a preferential oxidative energy substrate over glucose for neurons in culture. J. Cereb. Blood Flow. Metab. 23, 1298–1306 (2003).

84. Bouzier-Sore, A.-K. et al. Competition between glucose and lactate as oxidative energy substrates in both neurons and astrocytes: a comparative NMR study. Eur. J. Neurosci. 24, 1687–1694 (2006).

85. Wyss, M. T., Jolivet, R., Buck, A., Magistretti, P. J. & Weber, B. In vivo evidence for lactate as a neuronal energy source. J. Neurosci. 31, 7477–7485 (2011).

86. Hung, Y. P., Albeck, J. G., Tantama, M. & Yellen, G. Imaging cyto- solic NADH-NAD(+) redox state with a genetically encoded fluor- escent biosensor. Cell Metab. 14, 545–554 (2011).

87. Yang, J. et al. Lactate promotes plasticity gene expression by potentiating NMDA signaling in neurons. Proc. Natl Acad. Sci. USA 111, 12228–12233 (2014).

88. Herrera-López, G.& Galván, E. J. Modulation of hippocampal excitability via the hydroxycarboxylic acid receptor 1. Hippo- campus 28, 557–567 (2018).

89. Jorwal, P. & Sikdar, S. K. Lactate reduces epileptiform activity through HCA1 and GIRK channel activation in rat subicular neu- rons in an in vitro model. Epilepsia 60, 2370–2385 (2019).

90. Briquet, M. et al. Activation of lactate receptor HCAR1 down- modulates neuronal activity in rodent and human brain tissue. J. Cereb. Blood Flow. Metab. 42, 1650–1665 (2022).

91. Bozzo, L., Puyal, J. & Chatton, J.-Y. Lactate modulates the activity of primary cortical neurons through a receptor-mediated path- way. PLoS ONE 8, e71721 (2013).

92. Roumes, H. et al. Lactate transporters in the rat barrel cortex sustain whisker-dependent BOLD fMRI signal and behavioral per- formance. Proc. Natl Acad. Sci. USA 118, e2112466118 (2021).

93. Netzahualcoyotzi, C. & Pellerin, L. Neuronal and astroglial mono- carboxylate transporters play key but distinct roles in hippocampus-dependent learning and memory formation. Prog. Neurobiol. 194, 101888 (2020).

94. Suzuki, A. et al. Astrocyte-neuron lactate transport is required for long-term memory formation. Cell 144, 810–823 (2011).

95. Newman, L. A., Korol, D. L. & Gold, P. E. Lactate produced by glycogenolysis in astrocytes regulates memory processing. PLoS ONE 6, e28427 (2011).

96. Abrantes, H. et al. The lactate receptor HCAR1 modulates neuronal network activity through the activation of Gα and Gβγ subunits. J. Neurosci. 39, 4422–4433 (2019).

97. Lauritzen, K. H. et al. Lactate receptor sites link neurotransmission, neurovascular coupling, and brain energy metabolism. Cereb. Cortex 24, 2784–2795 (2014).

98. Roy, S. C., Napit, P. R., Pasula, M., Bheemanapally, K. & Briski, K. P. G protein-coupled lactate receptor GPR81 control of ventrolateral ventromedial hypothalamic nucleus glucoregulatory neuro- transmitter and 5′-AMP-activated protein kinase expression. Am. J. Physiol. Regul. Integr. Comp. Physiol. 324, R20–R34 (2023).

99. Murakami, R. et al. Immunoreactivity of receptor and transporters for lactate located in astrocytes and epithelial cells of choroid plexus of human brain. Neurosci. Lett. 741, 135479 (2021).

100. Smith, J. S. & Rajagopal, S. The β-arrestins: multifunctional reg- ulators of G protein-coupled receptors. J. Biol. Chem. 291, 8969–8977 (2016).

101. Belcheva, M. M. & Coscia, C. J. Diversity of G protein-coupled receptor signaling pathways to ERK/MAP kinase. Neurosignals 11, 34–44 (2002).

102. Fasciani, I. et al. GPCRs in intracellular compartments: new targets for drug discovery. Biomolecules 12, 1343 (2022).

103. Gusach, A., García-Nafría, J. & Tate, C. G. New insights into GPCR coupling and dimerisation from cryo-EM structures. Curr. Opin. Struct. Biol. 80, 102574 (2023).

104. Inoue, A. et al. Illuminating G-protein-coupling selectivity of GPCRs. Cell 177, 1933–1947.e25 (2019).

105. Martín, R., Bajo-Grañeras, R., Moratalla, R., Perea, G. & Araque, A. Circuit-specific signaling in astrocyte-neuron networks in basal ganglia pathways. Science 349, 730–734 (2015).

106. Panatier, A. et al. Glia-derived D-serine controls NMDA receptor activity and synaptic memory. Cell 125, 775–784 (2006).

107. Papouin, T. et al. Synaptic and extrasynaptic NMDA receptors are gated by different endogenous coagonists. Cell 150, 633–646 (2012).

108. Sherwood, M. W., Arizono, M., Panatier, A., Mikoshiba, K. & Oliet, S. H. R. Astrocytic IP3Rs: beyond IP3R2. Front. Cell. Neurosci. 15, 695817 (2021).

109. Akther, S. & Hirase, H. Assessment of astrocytes as a mediator of memory and learning in rodents. Glia 70, 1484–1505 (2022).

110. Hirrlinger, J. & Nimmerjahn, A. A perspective on astrocyte reg- ulation of neural circuit function and animal behavior. Glia 70, 1554–1580 (2022).

111. Lyon, K. A. & Allen, N. J. From synapses to circuits, astrocytes regulate behavior. Front. Neural Circuits 15, 786293 (2021).

112. Fernández-Moncada, I. & Marsicano, G. Astroglial CB1 receptors, energy metabolism, and gliotransmission: an integrated signaling system? Essays Biochem. 67, 49–61 (2023).

113. Hirrlinger, P. G., Scheller, A., Braun, C., Hirrlinger, J. & Kirchhoff, F. Temporal control of gene recombination in astrocytes by trans- genic expression of the tamoxifen-inducible DNA recombinase variant CreERT2. Glia 54, 11–20 (2006).

114. Marsicano, G. et al. CB1 cannabinoid receptors and on-demand defense against excitotoxicity. Science 302, 84–88 (2003).

115. Da Cruz, J. F. O. et al. An alternative maze to assess novel object recognition in mice. Bio Protoc. 10, e3651 (2020).

ACKNOWLEDGEMENTS

We would like to thank Delphine Gonzales, Nathalie Aubailly, Ruby Racunica, Jean-Baptiste Bernard and all the personnel of the Animal Facilities of the NeuroCentre Magendie for mouse care. We also thank the genotyping platform of the Neurocentre Magendie for the help in the experiments. The microscopy was done in the Bordeaux Imaging Center a service unit of the CNRS-INSERM and Bordeaux University, member of the national infrastructure France BioImaging supported by the French National Research Agency (ANR-10-INBS-04). We thank all past and present members of Marsicano's lab for useful discussions and for their invaluable support. This study was funded by Inserm (to G.M., A.P. and S.H.R.O.); CNRS (to A.P. and S.H.R.O.); the European Research Council (Micabra, ERC-2017-AdG-786467, to G.M.); Fondation pour la Recherche Medicale (DRM20101220445, to G.M); EMBO Long-term Fellowship ALTF87-2018 (to I.F-M.); the Human Frontiers Science Program (to G.M.); Region Aquitaine (CanBrain, AAP2022A-2021-16763610 and -17219710 to A.-K.B.-S., L.P., A.P. and G.M.); French State/Agence Nationale de la Recherche (ERA-Net Neuron CanShank, ANR-21-NEU2-0001-04, to G.M), (CaMeLS, ANR-23-CE16-0022-01 to G.M., A.P. and G.B.), (Hippobese, ANR-23-CE14-0004-03, to G.F. and G.M.), (BrainFuel, ANR-21-CE44-0023-01 to A.-K.B.-S., L.P and AP.), (Excigly, ANR-20-CE16-0009-03 to S.H.R.O.), (Astrocom ANR-19-CE16-0015 to A.P.), (ANR-19-CE14-0039 to L.B.); the French government in the framework of the University of Bordeaux's IdEx "Investments for the Future" program / GPR BRAIN_2030 / RRI IMPACT, the Japan Society for the Promotion of Science (21K14738, to Y.N. and 19H05633, to R.E.C.) and the Japan Science and Technology Agency (JPMJPR22E9, to Y.N.), Fondation Alzheimer (to G.B.), the NextGenerationEU/PRTR and Agencia Estatal de Investigación (10.13039/501100011033; PID2019-105699RB-I00; PID2022-138813OB-I00 and PDC2021-121013-I00 to J.P.B); European Comission action HORIZON-TMA-MSCA-DN (ETERNITY, 101072759, to J.P.B), La Caixa Research Health grant LCF/PR/HR23/52430016 (to J.P.B. and G.M.) and Fondecyt 1230145 & BMBF-ANID 180045 (to L.F.B.).

AUTHORS CONTRIBUTION

IFM conceived the study, wrote the manuscript and performed most experiments; GL, UBF, NB and SM performed behavioral and electrophysiological experiments; TDT performed imaging experiments; PH, RS, LB, AC and BFM helped with experiments; FJK and DG performed the histology analyses; YN and REC generated and provided sensor constructs, provided expertise and support for the experiments; FD, CC, GF, AKBS, LP, JPB, GB, LFB and SHRO provided theoretical support and ideas; AP conceived the study; GM conceived the study and wrote the manuscript; all authors edited and approved the manuscript.

COMPETING INTERESTS

Authors declare no conflict of interest.

Supplemental Material for

A lactate-dependent shift of glycolysis mediates synaptic and cognitive processes in male mice

Ignacio Fernández-Moncada [1] , Gianluca Lavanco [1,2,16,17], Unai B. Fundazuri [1,17] , Nasrin Bollmohr [1,17], Sarah Mountadem [1,17], Tommaso Dalla Tor [1,2,17], Pauline Hachaguer [1], Francisca Julio-Kalajzic [1], Doriane Gisquet [1], Roman Serrat [1,3], Luigi Bellocchio [1], Astrid Cannich [1], Bérénice Fortunato-Marsol [1], Yusuke Nasu [4,5], Robert E. Campbell [4,6], Filippo Drago [2], Carla Cannizzaro [7], Guillaume Ferreira [3], Anne-Karine Bouzier-Sore [8], Luc Pellerin [9], Juan P. Bolaños [10,11,12], Gilles Bonvento [13], L. Felipe Barros [14,15], Stephane H. R. Oliet [1], Aude Panatier [1,18] & Giovanni Marsicano [1, 18]

[1]Univ. Bordeaux, INSERM, Neurocentre Magendie, U1215, F-33000 Bordeaux, France.

[2]Department of Biomedical and Biotechnological Sciences, Section of Pharmacology, University of Catania, Catania, Italy.

[3]Univ. Bordeaux, INRAE, Bordeaux INP, NutriNeuro, UMR 1286, F-33000 Bordeaux, France.

[4]Department of Chemistry, School of Science, The University of Tokyo, Bunkyo-ku, Tokyo, Japan.

[5]PRESTO, Japan Science and Technology Agency, Chiyoda-ku, Tokyo, Japan.

[6]CERVO Brain Research Center and Department of Biochemistry, Microbiology, and Bioinformatics, Université Laval, Québec City, QC, Canada.

[7]Department of Biomedicine, Neuroscience and Advanced Diagnostics, University of Palermo, Palermo, Italy.

[8]Univ. Bordeaux, CNRS, Centre de Résonance Magnétique des Systèmes Biologiques, UMR 5536, F-33000 Bordeaux, France.

[9]Université de Poitiers et CHU de Poitiers, INSERM, IRMETIST, U1313, Poitiers, France.

[10]Institute of Functional Biology and Genomics (IBFG), Universidad de Salamanca, CSIC, Salamanca, Spain.

[11]Institute of Biomedical Research of Salamanca (IBSAL), Hospital Universitario de Salamanca, Salamanca, Spain.

[12]Centro de Investigación Biomédica en Red de Fragilidad y Envejecimiento Saludable (CIBERFES), Madrid, Spain.

[13]Universite Paris-Saclay, CEA, CNRS, MIRCen, Laboratoire des Maladies Neurodegeneratives, Fontenay-aux-Roses, France.
[14]Centro de Estudios Cientificos, Valdivia, Chile.
[15]Facultad de Medicina y Ciencia, Universidad San Sebastián, Valdivia, Chile.
[16]Present address: Department of Health Promotion, Mother and Child Care, Internal Medicine and Medical Specialties, ''G. D'Alessandro", University of Palermo, Palermo, Italy. [17]These authors contributed equally: Gianluca Lavanco, Unai B. Fundazuri, Nasrin Bollmohr, Sarah Mountadem, Tommaso Dalla Tor.
[18] These authors jointly supervised this work: Aude Panatier, Giovanni Marsicano. e-mail: ignacio.fernandez-moncada@inserm.fr; giovanni.marsicano@inserm.fr

Inventory of Supporting Information

Supplementary Fig. 1 Differential effect of cannabinoids on astrocyte lactate level.

Supplementary Fig. 2 The basal lactate level and accumulation upon mitochondria inhibition is not altered by CB1 receptor subcellular localization.

Supplementary Fig. 3 Activation of astroglial CB1 receptors increases lactate production.

Supplementary Fig. 4 The PKC signaling controls the CB1 receptor-mediated intracellular lactate increase.

Supplementary Fig. 5 The mitochondrial localization of CB1 receptors is not necessary for physiological novel object exploration.

Supplementary Fig. 6 Inhibition of the phosphorylated pathway impairs long-term NOR memory in WT mice and in lactate-treated GFAP-CB1-KO mice.

Supplementary Fig. 7 Activation of HCA1R promotes a biased glucose metabolism.

Supplementary Fig. 8 Lactate requires the phosphorylated pathway to potentiate NMDAR function.

Supplementary Fig. 9 Lactate rescues the THC-mediated impairment in novel object exploration via HCAR1 signaling and L-serine production.

Supplementary Fig. 10 A lactate-dependent shift of glycolysis mediates synaptic and cognitive processes.

Supplementary Table 1 Details of the double-viral rescue approach to study mtCB1 receptor involvement in NOR performance

Supplementary Table 2 Statistics details of Main Figures.

Supplementary Table 3 Statistics details of Supplementary Figures.

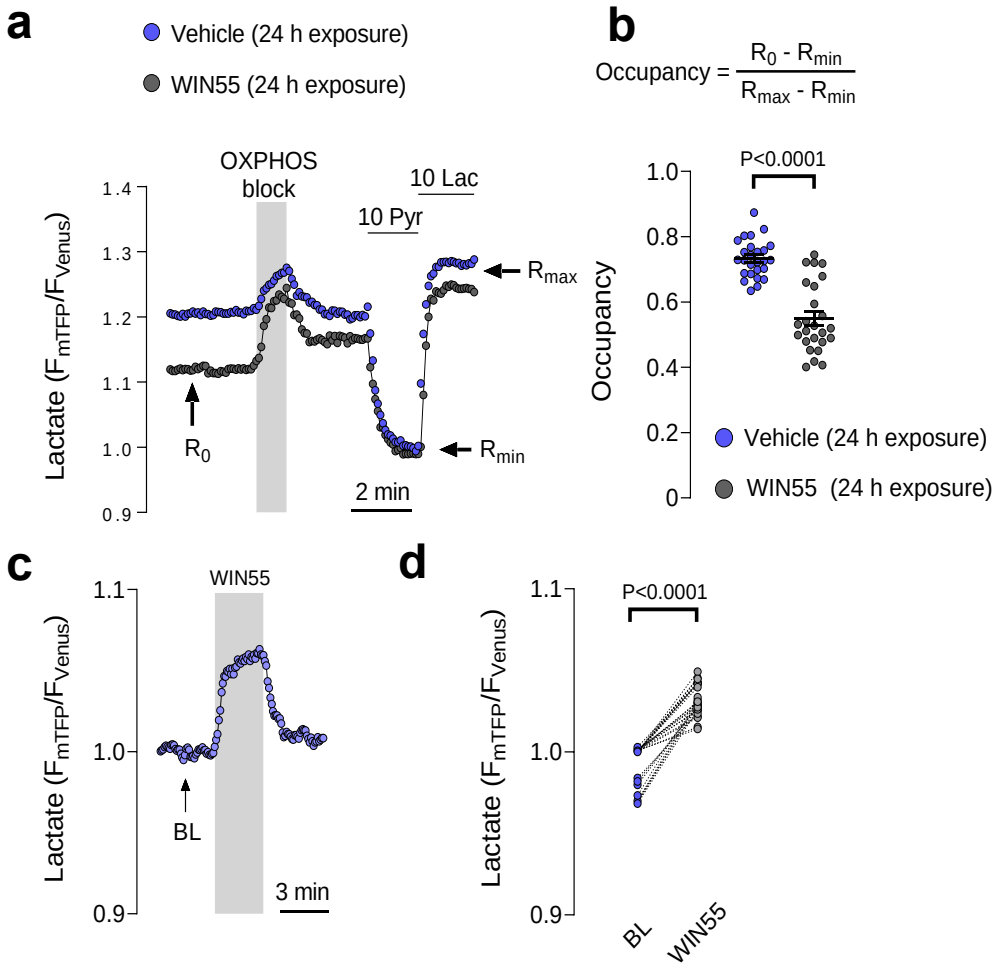

Supplementary Figure 1 – Differential effect of cannabinoids on astrocyte lactate level. ***a****, Intracellular lactate imaging in astrocytes previously incubated with WIN55 (2 μM) or vehicle (DMSO) for 24 hours. After treatment, and to determine the basal lactate level (occupancy), cells were imaged and exposed sequentially to an OXPHOS blocker (5 mM sodium azide), pyruvate (10 mM) and lactate (10 mM).* R_0*, basal ratio.* R_{min}*, minimum ratio.* R_{max}*, maximum ratio. Data was normalized to* R_{min} *to emphasize the difference in* R_0*.* ***b****, Basal lactate level (occupancy) after 24 hours treatment with WIN55 (2 μM) or vehicle (DMSO). Data was computed as occupancy =* $(R_0\text{-}R_{min})/(R_{max}\text{-}R_{min})$*, using* R_0*,* R_{min} *and* R_{max} *from experiments similar to panel A. Vehicle, n=3, 26 cells. WIN55, n=3, 25 cells.* ***c****, Intracellular lactate imaging in astrocytes acutely exposed to WIN55 (2 μM). BL = baseline.* ***d****, Summary of intracellular lactate level at baseline (BL) and after 3 min exposure to WIN55 (2 μM), in experiments similar to Supplementary Fig. 1C, n=3, 26 cells. Data correspond to representative cells (****a****,****c****). Circles*

*in scatter and before-after plots correspond to single cells (**b**,**d**). Statistical analysis was performed using a two-tailed unpaired t-test (**b**) and two-tailed paired t-test (**d**). See Supplementary Table 3 for more details.*

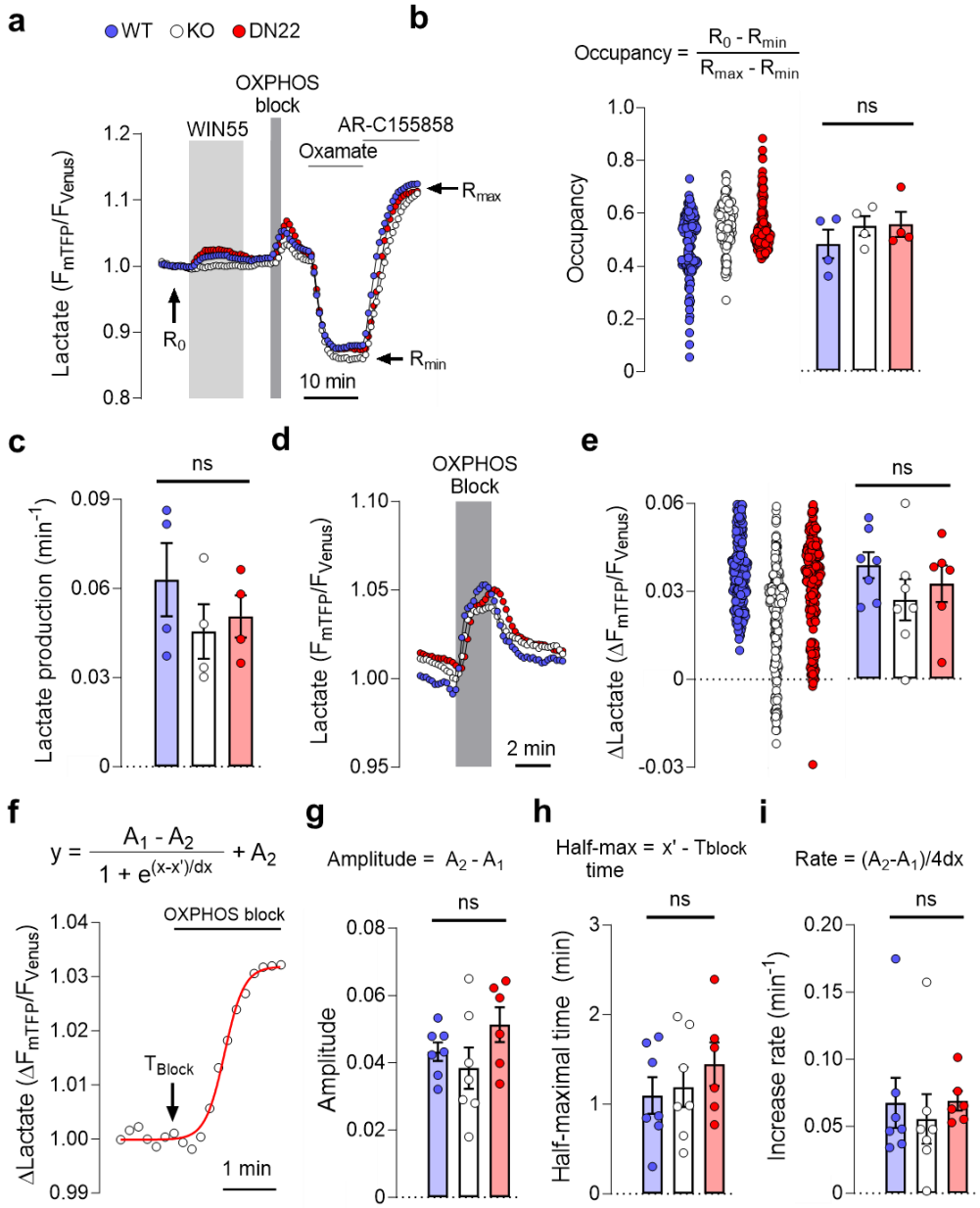

***Supplementary Figure 2 – The basal lactate level and accumulation upon mitochondria inhibition is not altered by CB1 receptor subcellular localization. a**, Intracellular lactate imaging in astrocytes. To determine the basal lactate level (occupancy), cells exposed sequentially to WIN55 (1 μM), OXPHOS block (5 mM azide), Oxamate (6 mM) and AR-C155858 (1 μM). R_0, basal ratio. R_{min}, minimum ratio. R_{max}, maximum ratio. Average of 4 independent experiments. Cells: WT=158, KO=145, DN22=154. **b**, Basal lactate level (occupancy) in CB1-WT, CB1-KO and DN22-CB1-KI astrocytes. Data was computed as occupancy = $(R_0-R_{min})/(R_{max}-R_{min})$, using R_0, R_{min} and R_{max} obtained from experiments similar to panel A. N = 4, cells analyzed: CB1-WT=158, CB1-KO=145, DN22-CB1-KI =154. **c**, Basal lactate*

production rates in WT, KO and DN22 astrocytes. N=4 ***d****, Intracellular lactate accumulation induced by OXPHOS block (5 mM sodium azide). Average of several cells in a representative experiment (CB1-WT=32, CB1-KO=48, DN22-CB1-KI =36 cells).* ***e****, Summary of intracellular lactate levels after 2 min of OXPHOS block (5 mM sodium azide), in experiments similar to those shown in panel C. CB1-WT: n=7, 247 cells. CB1-KO: n=7, 227 cells. DN22-CB1-KI: n=6, 205 cells.* ***f****, Representative non-linear fitting of a sigmoidal model (Boltzmann equation, on top) to the lactate increase induced by OXPHOS blocking. The fitted parameters* A_1, A_2, *x' and dx were used to compute the amplitude, half-maximal time and increase rate presented in panel G-I.* T_{block}*, time of exposure to OXPHOS blocker sodium azide.* ***g****, Amplitude of lactate changes induced by OXPHOS block obtained from a non-linear fitting data. CB1-WT: n=7; CB1-KO: n=7; DN22-CB1-KI: n=6.* ***h****, Half-maximal time of lactate changes induced by OXPHOS block obtained from a non-linear fitting data. CB1-WT: n=7; CB1-KO: n=7; DN22-CB1-KI: n=6.* ***I****, Half-maximal time of lactate changes induced by OXPHOS block obtained from a non-linear fitting data. CB1-WT: n=7; CB1-KO: n=7; DN22-CB1-KI: n=6. Data corresponds to the experiments average and represented as mean±SEM (****a****,****d****). Circles in scatter plots correspond to single cells (****b****,****e****). Bars correspond to experiments average (mean±SEM) and circles represent individual experiment average (****b****,****c****,****e****,****g****,****h****,****i****). Statistical analysis was performed using Kruskal-Wallis test followed by Dunn's multiple comparison test (****b****), One-way ANOVA followed by Tukey's multiple comparison test (****c****,****e****,****g****,****h****,****i****). See Supplementary Table 3 for more details.*

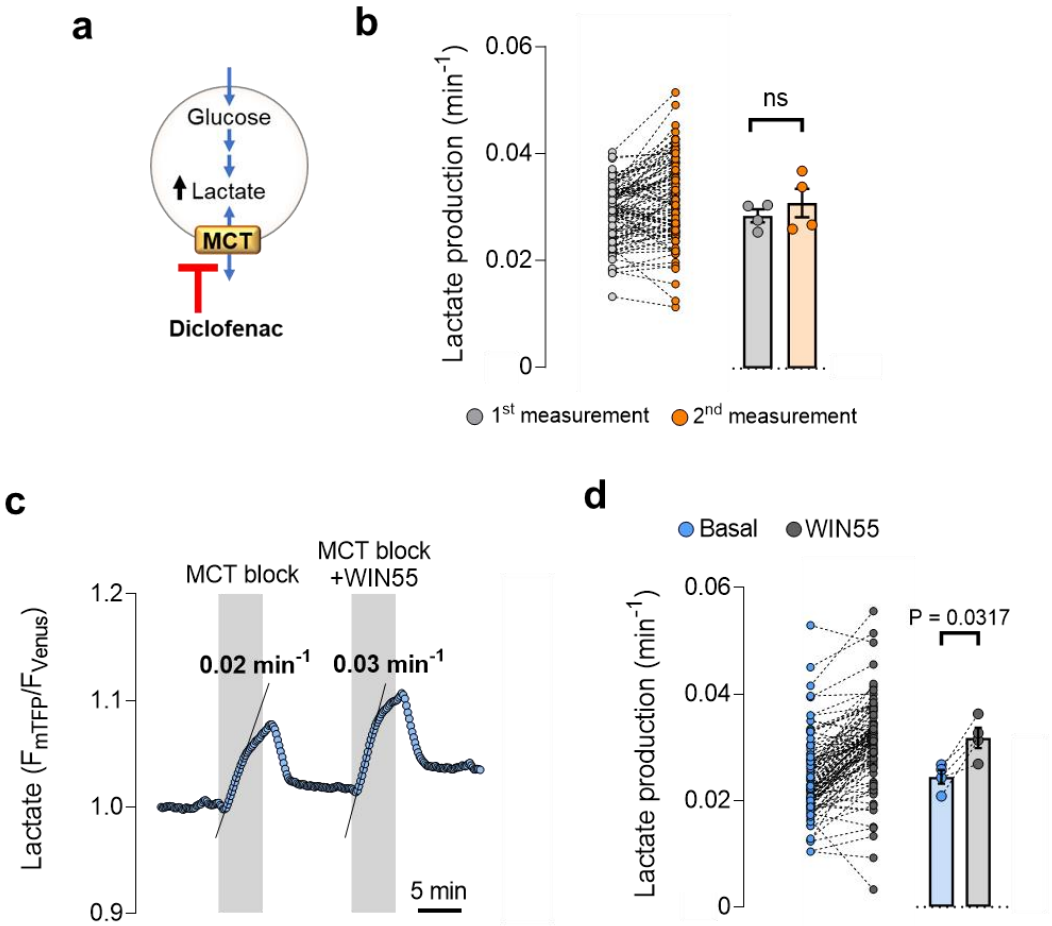

***Supplementary Figure 3 – Activation of astroglial CB1 receptors increases lactate production. a**, Transport stop protocol for measurement of lactate production. Diclofenac is a broad inhibitor of monocarboxylate transporter (MCT) activity. The blockade of MCT causes an intracellular lactate accumulation that is proportional to its rate of production. **b**, Summary of two sequential measurements of basal lactate production with diclofenac. N=4, 95 cells analyzed. **c**, Measurement of lactate production before and during exposure to WIN55 (1 μM). The production rate is indicated with a solid line above the corresponding lactate accumulation. **D**, Summary of the lactate production rates before (pale blue circles) and during exposure to WIN55 (grey circles), computed from experiments similar to panel E. N=4, 102 cells. Data corresponds to representative cell I. Circles in before – after plots correspond to single cells (**b**,**d**). Bars correspond to experiments average (mean±SEM) and circles represent individual experiment average (**b**,**d**). Statistical analysis was performed using a paired two-tailed paired t-test (**b,d**). See Supplementary Table 3 for more details.*

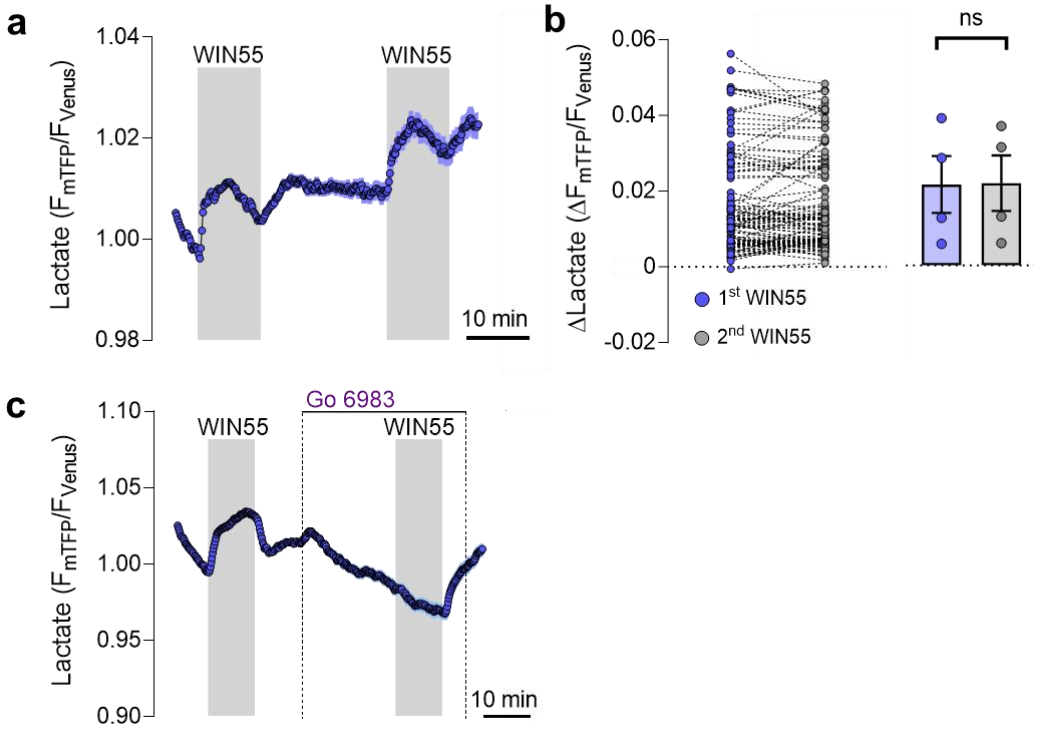

Supplementary Figure 4 – The PKC signaling controls the CB1 receptor-mediated intracellular lactate increase. a, *Intracellular lactate measurement during exposure two sequential exposure to WIN55 (1 µM). N=1, 42 cells.* ***b****, Quantification of lactate change induced by the first (blue) and second (grey) WIN55 exposure. N=4, 114 cells analyzed.* ***c****, Intracellular lactate measurement during the sequential exposure to WIN55 (1 µM), Go 6983 (5 µM) and WIN55 + Go 6983. N=1, 40 cells. Data corresponds to the average of a single experiment (****a****,****d****). Circles in before – after plots correspond to single cells (****b****). Bars correspond to experiments average (mean±SEM) and circles represent individual experiment average (****b****). Statistical analysis was performed using a paired two-tailed paired t-test (****b****). See Supplementary Table 3 for more details.*

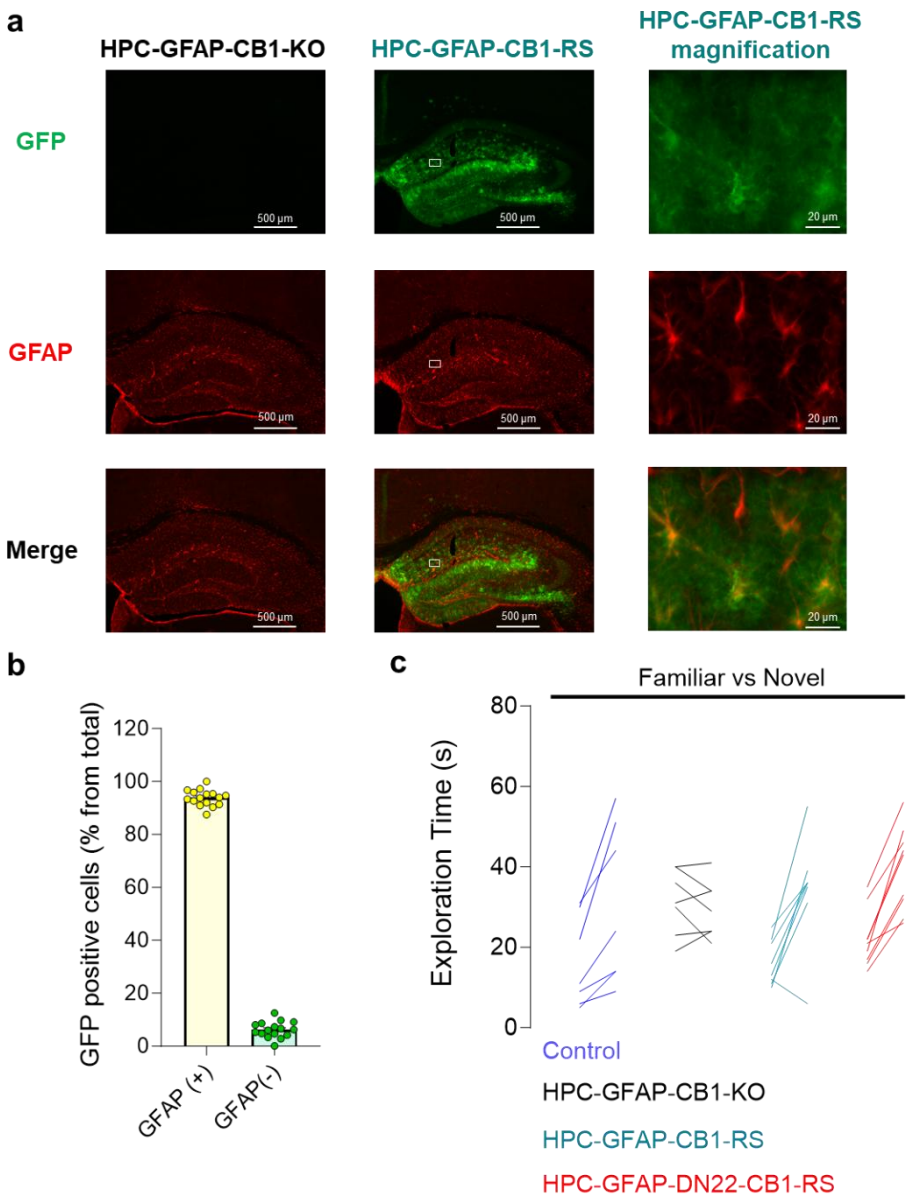

Supplementary Figure 5 – The mitochondrial localization of CB1 receptors is not necessary for physiological novel object exploration. a, *Histological analysis of the expression of CB1-GFP and the astrocyte marker GFAP, in hippocampus sections obtained from HPC-GFAP-CB1-KO and HPC-GFAP-CB1-WT-RS. The white boxes inside the HPC-GFAP-CB1-WT-RS images correspond to the magnification site shown in the third column of images.* ***b****, Quantification of GFP-positive cells in the CA1 region of the hippocampus of HPC-GFAP-CB1-WT-RS mice. N = 4 mice, 30 – 91 cells analyzed in 4 sections per mice.* ***c****, Exploration times of familiar versus novel objects in the NOR task, from Control (blue lines), HPC-GFAP-CB1-KO (black lines), HPC-GFAP-CB1-WT-RS (teal lines) and HPC-GFAP- DN22-CB1-RS (red lines) animals, n = 7-9 mice per condition. A single line corresponds to an individual animal. See Supplementary Table 3 for more details.*

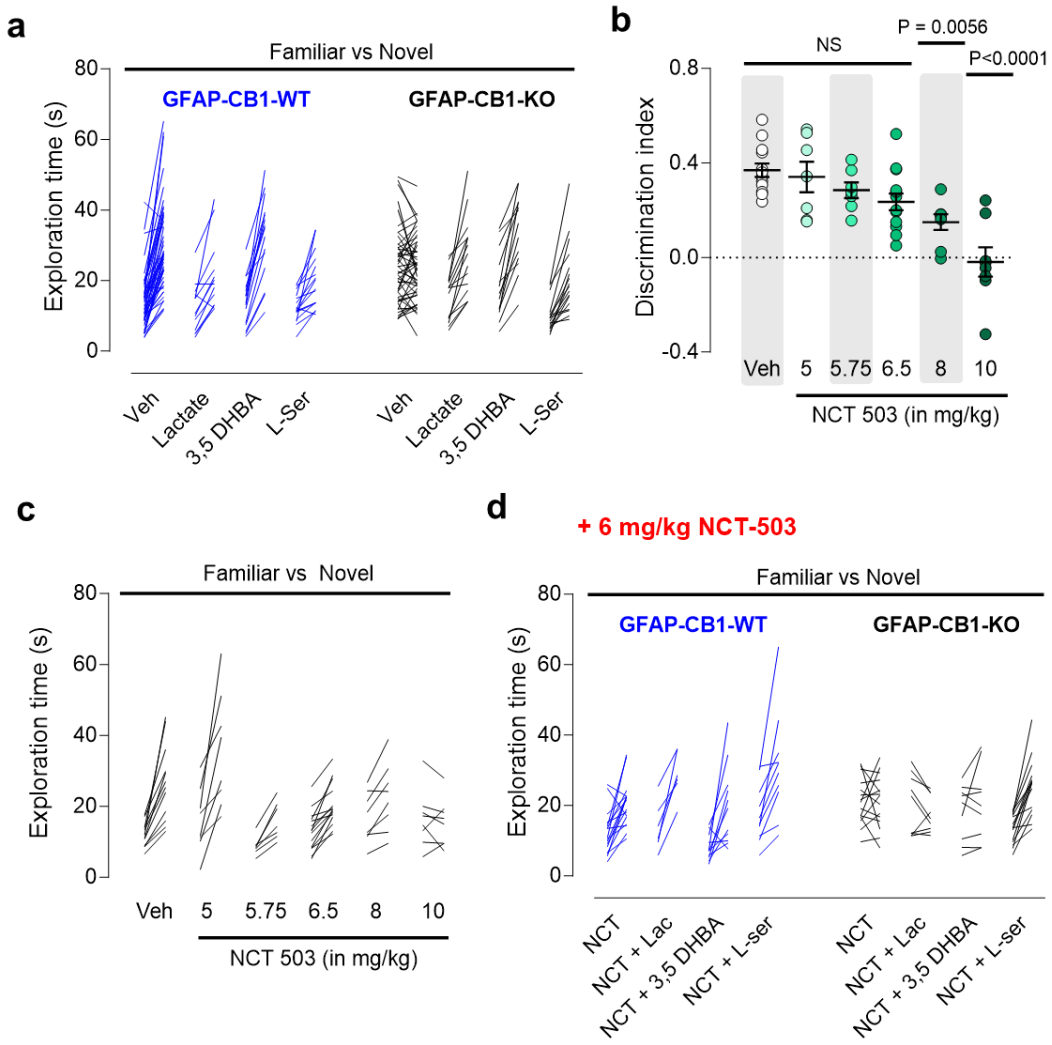

Supplementary Figure 6 – Inhibition of the phosphorylated pathway impairs long-term NOR memory in WT mice and in lactate-treated GFAP-CB1-KO mice. a*, Exploration time of familiar versus novel objects in the NOR task of GFAP-CB1-WT (blue lines) and GFAP-CB1-KO mice (black lines) mice, treated either with vehicle (veh), 1 g/kg lactate (Lac) or 0.5 g/kg L-serine (L-Ser), immediately after the acquisition phase. GFAP-CB1-WT, n=13-18 animals. GFAP-CB1-KO, n= 15-23 animals.* ***b****, NOR performance in wild-type mice treated either with vehicle or incremental doses of NCT-503. N=7-15 mice per condition.* ***c****, Exploration time of familiar versus novel object in the NOR task of wild-type mice treated either with vehicle or incremental doses of NCT-503. N= 7-15 mice per condition.* ***d****, Exploration time of familiar versus novel object in the NOR task, of mice treated either with vehicle + 6 mg/kg NCT-503 (NCT), 1 g/kg lactate + 6 mg/kg NCT-503 (NCT + Lac) or 0.5 g/kg L-serine + 6 mg/kg NCT-503 (NCT + L-Ser), immediately after the acquisition phase. GFAP-CB1-WT mice (blue lines), n=6-12 animals. GFAP-CB1-KO mice (black lines), n= 9-16 animals. A single line corresponds to an individual animal (****a****,* ***c****,* ***d****). Data is presented as scatter plot with the line and whisker corresponding to the mean±SEM and circles to individual animals (****b****). Statistical analysis was performed with a One-way ANOVA followed by Tukey's multiple comparison test (****b****). See Supplementary Table 3 for more details.*

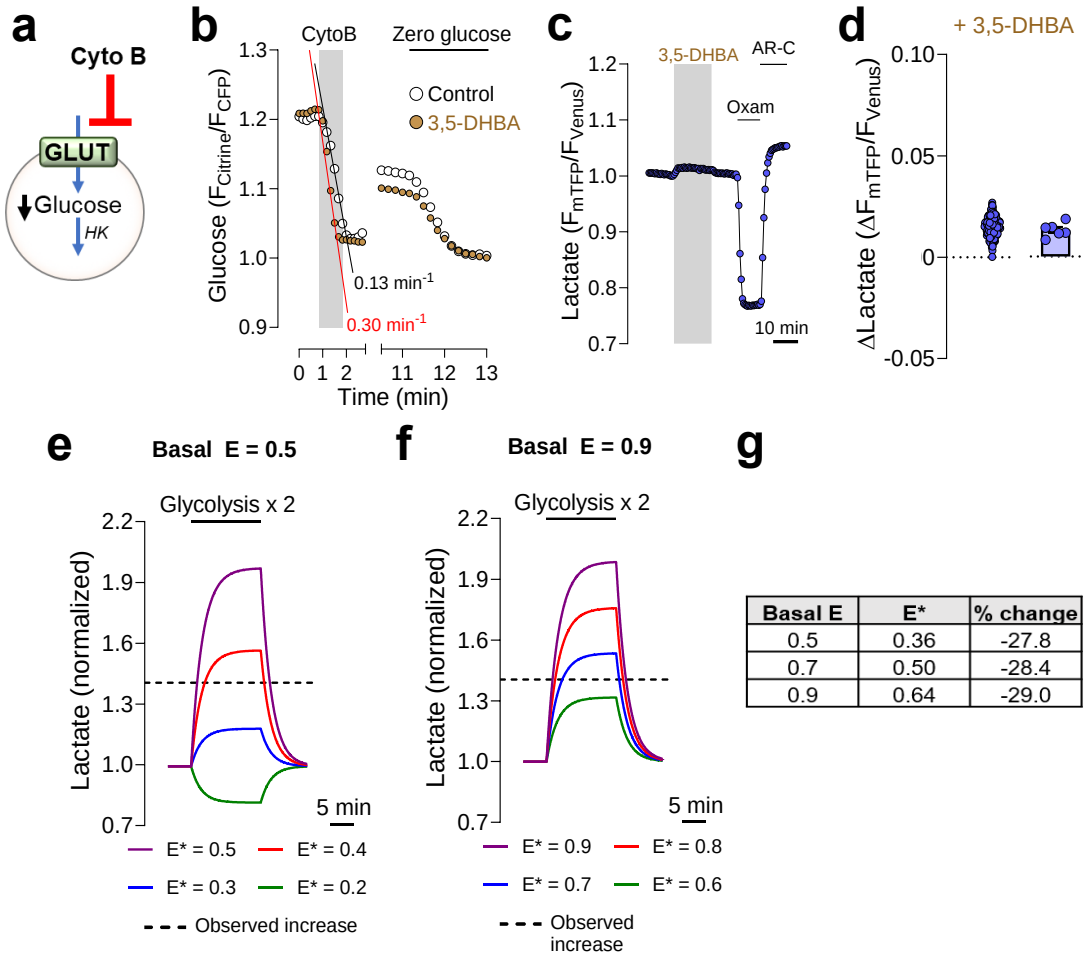

Basal E	E*	% change
0.5	0.36	-27.8
0.7	0.50	-28.4
0.9	0.64	-29.0

Supplementary Figure 7 – Activation of HCA1R promotes a biased glucose metabolism. a*, Transport stop protocol for measurement of glucose consumption. Cytochalasin B is an inhibitor of glucose transporter (GLUT) activity. The blockade of GLUT causes an intracellular glucose decrease that is proportional to its rate of consumption by hexokinase (HK), the first enzyme of glycolysis.* ***b****, Intracellular glucose measurement during exposure to cytochalasin B (CytoB, 20 µM). Astrocytes were treated with 3,5-DHBA (1 mM) for 15 min before exposure to CytoB.* ***c****, Complete trace of the Fig. 3G intracellular lactate measurement during exposure to 3,5-DHBA, showing the two-point calibration used for transforming the fluorescent ratio to concentration.* ***d****, Quantification of lactate changes induced by 3,5 DHBA obtained from similar experiments as shown in Fig 3G. N = 6, 222 cells.* ***e****, Numerical simulation of intracellular lactate concentration (normalized to baseline) with basal E = 0.5, during a two-fold increase in glycolysis. During this stimulation, a decrease in glucose-to-pyruvate/lactate conversion (E*) was simulated. The recorded increase in intracellular lactate concentration induced by 3,5-DHBA (see methods) is marked by a discontinuous line.* ***f****, Numerical simulation of intracellular lactate concentration (normalized to baseline) with basal E = 0.9, during a two-fold increase in glycolysis. During this stimulation, a decrease in glucose-to-pyruvate/lactate conversion (E*) was simulated. The recorded increase in intracellular lactate concentration induced by 3,5-DHBA (see methods) is marked by a discontinuous line.* ***g****, Summary of the E* values required to*

*obtain the observed intracellular lactate concentration induced by 3,5-DHBA for each basal E simulated. Data corresponds to representative cells (**b**). Data corresponds to the average (mean±SEM) of representative of experiment (**c**). Circles in scatter plot correspond to individual cells (**d**). Bars correspond to experiments average (mean±SEM) and circles represent experiment average (**d**). Solid line corresponds to a single numerical simulation (**e**,**f**).*

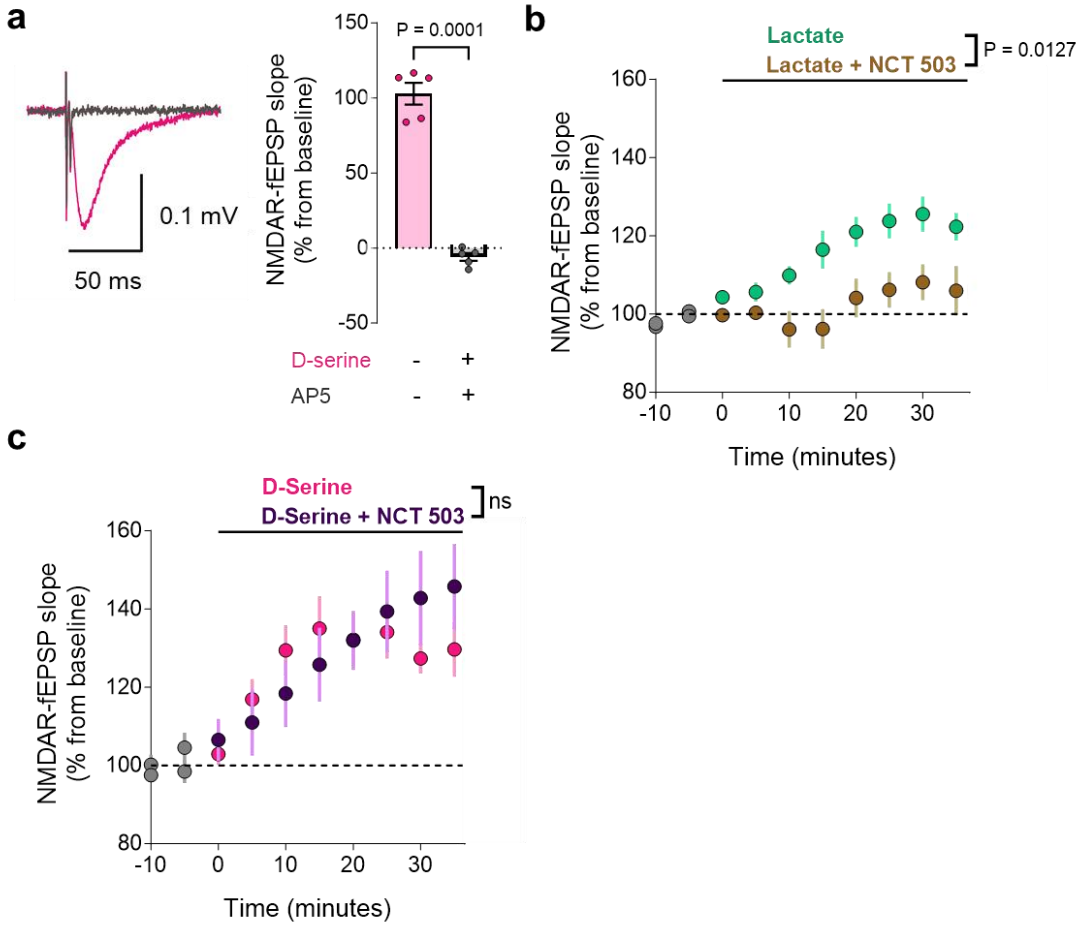

***Supplementary Figure 8 – Lactate requires the phosphorylated pathway to potentiate NMDAR function. a**, Representative averaged traces from 20 consecutives sweeps evoked in the presence of, before (in magenta) and after bath application of d -AP5 (50 µM) + d -serine (50 µM). Quantification of the NMDAR-fEPSP slopes in presence of d-serine (50 µM), before and after application d-AP5 (50 µM) are shown in the bar plot, n=5. **b**, NMDAR-mediated fEPSP slopes in the presence of lactate (data from Fig. 4A, n=9) and lactate + NCT-503 (data from Fig. 4D, n=6). **c**, NMDAR- fEPSP slopes induced by d-serine (same as Fig. 4A, n=6) and d-serine after NCT-503 preincubation (data from Fig. 4D, n=6). Bars correspond to experiments average (mean±SEM) and circles represent individual experiment average (**a**). Data corresponds to the experiments average and represented as mean±SEM. Data points were averaged every 5 mins (**b**,**c**). Statistical analysis was performed using a two-tailed paired t-test (**a**) and two-way ANOVA (**b**,**c**). See Supplementary Table 3 for more details.*

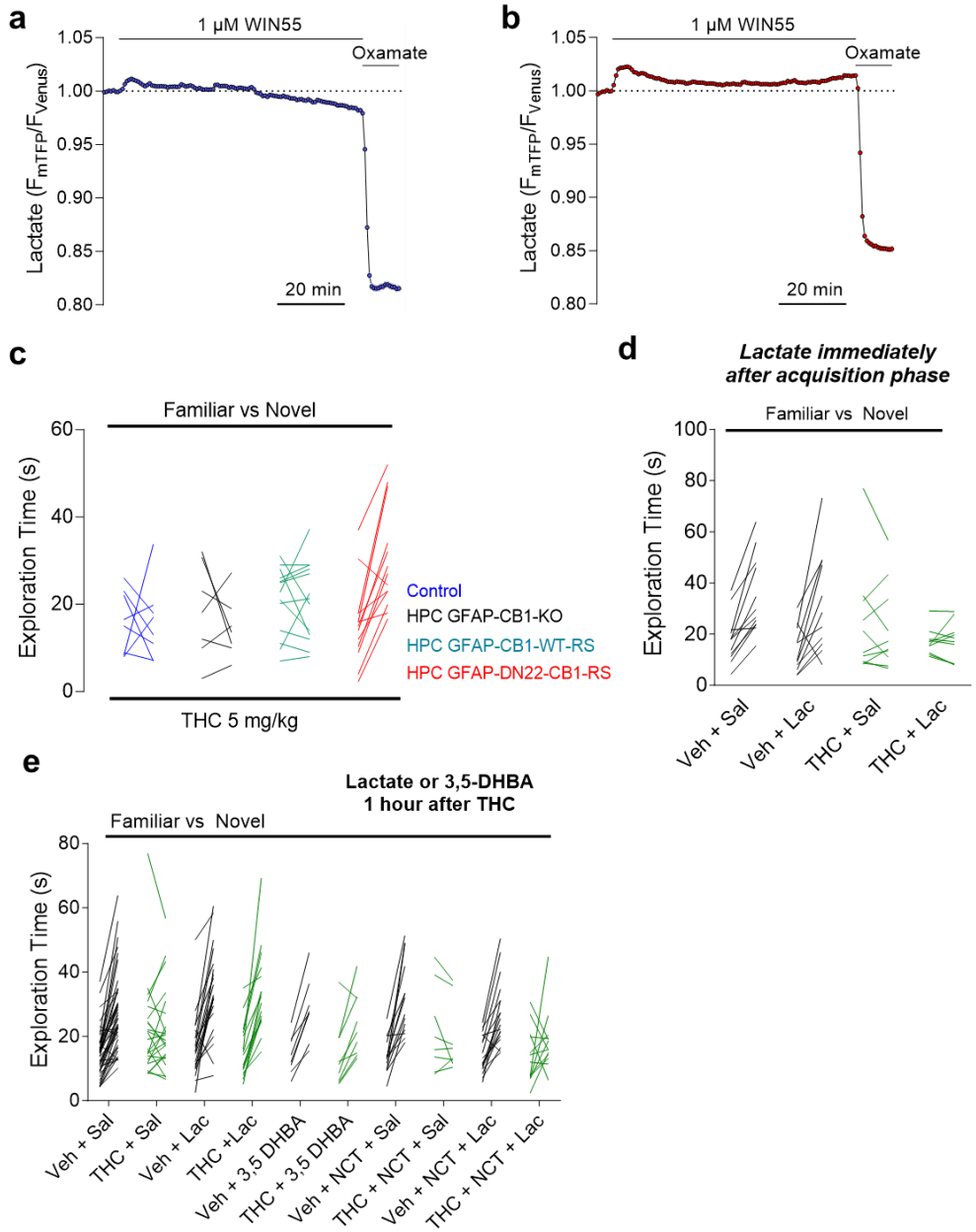

Supplementary Figure 9 – Lactate rescues the THC-mediated impairment in novel object exploration via HCAR1 signaling and L-serine production. a*, Intracellular lactate imaging in CB1-WT astrocytes exposed to WIN55 (1 µM) during 70 min. After this, cells were exposed to oxamate to deplete lactate levels for biosensor calibration.* ***b****, Intracellular lactate imaging in DN22-CB1-KI astrocytes exposed to WIN55 (1 µM) during 70 min. After this, cells were exposed to oxamate to deplete lactate levels for biosensor calibration.* ***c****, Exploration times of familiar versus novel objects in the NOR task, from Control (blue lines), GFAP-CB1-KO (black lines), GFAP-CB1-WT-RS (teal lines) and GFAP- DN22-CB1-RS (red lines) animals treated with THC (5 mg/kg immediately after the acquisition phase. N = 7 – 13 mice per condition.* ***d****, Exploration time of familiar versus novel objects in the NOR task of mice treated with an IP injection of either vehicle (veh) + saline (sal), vehicle + lactate (lac, 1 g/kg), THC (5 mg/kg) + saline or THC (5 mg/kg) + lactate (1 g/kg), immediately after the acquisition phase. N= 10 –*

12 mice per condition. ***e****, Exploration time of familiar versus novel objects in the NOR task of mice treated with an IP injection of either vehicle (veh) or THC (5 mg/kg), immediately after the acquisition phase. After 1-hour post-THC treatment, mice were treated with an IP injection of either saline (sal), lactate (lac, 1g/kg), 3,5-DHBA (240 mg/kg), NCT-503 (NCT, 6 mg/kg) + saline or NCT-503 + lactate. N = 8 – 49 mice per condition. Experiments correspond to a representative cell (****a****, ****b****). A single line corresponds to an individual animal (****c****, ****d****, ****e****). See Supplementary Table 3 for more details.*

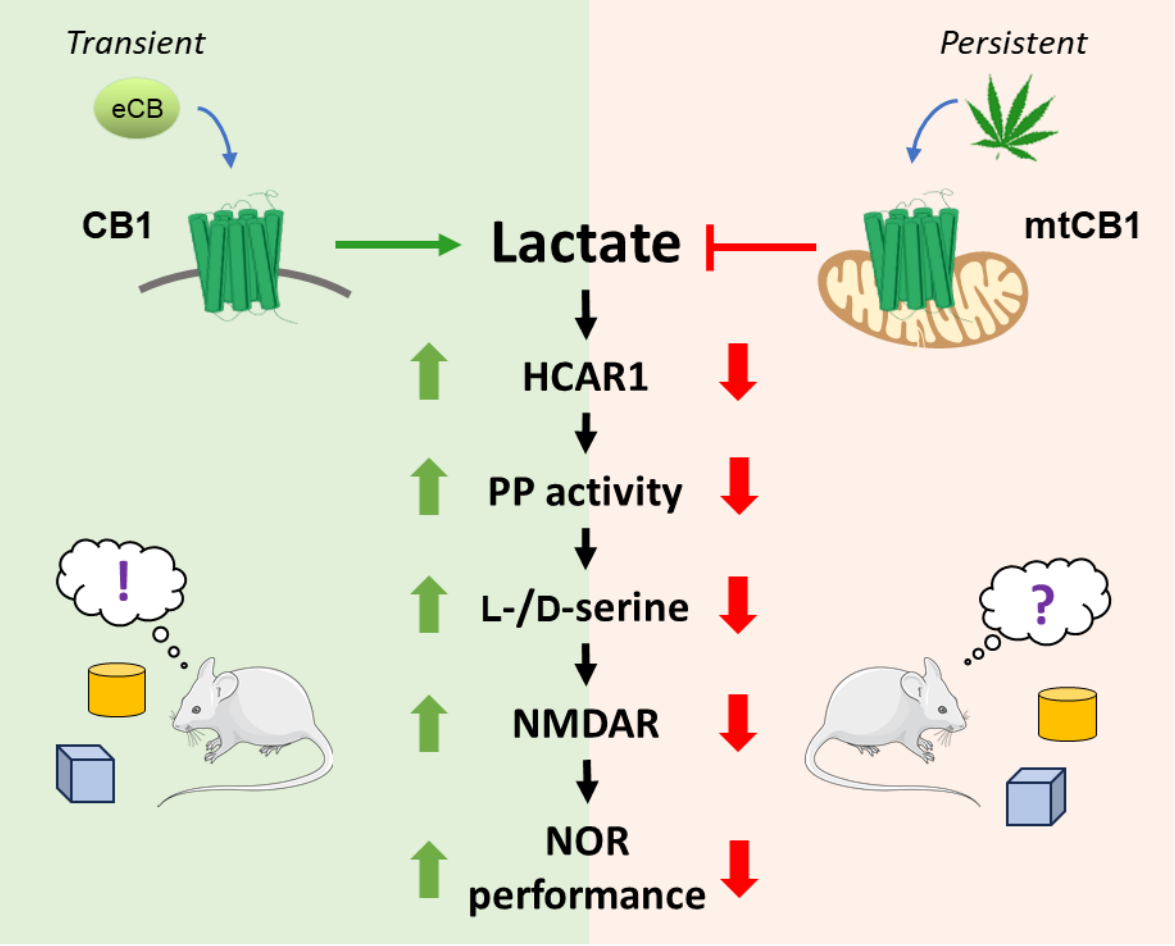

Supplementary Figure 10 – A lactate-dependent shift of glycolysis mediates synaptic and cognitive processes. *Lactate promotes cognitive performance via a cascade involving HCAR1 and phosphorylated pathway (PP) activity, thereby increasing L-/D-serine levels and NMDAR activity to allow an adequate NOR memory consolidation. Importantly, whereas transient activation of non-mitochondrial CB1 receptors promote this novel lactate signaling to promote cognitive performance, the persistent activation of mitochondrial CB1 receptors impairs the lactate signaling and disrupt the consolidation of NOR memory via a specular mechanism.*

Supplementary table 1.

Details of the double viral rescue approach to study mtCB1 receptor involvement in NOR performance

Mice	AAV-1*	AAV-2*	Outcome	Mitochondrial Localization of CB1?	Name of used mutant mice
CB1-flox	GFAP-GFP	CAG-DIO-Empty	CB1-WT	yes	Control
CB1-flox	GFAP-Cre	CAG-DIO-Empty	CB1-KO in GFAP positive cells	no	HPC-GFAP-CB1-KO
CB1-flox	GFAP-Cre	CAG-DIO-CB1-GFP	Re-expression of CB1-WT in GFAP positive cells (CB1 in all subcellular locations)	yes	HPC-GFAP-CB1-RS
CB1-flox	GFAP-Cre	CAG-DIO-DN22-CB1-GFP	Re-expression of DN22-CB1 in GFAP positive cells (CB1 excluded from mitochondria)	no	HPC-GFAP-DN22-CB1-RS

Supplementary Table 2 - Main figures statistics details

Group sizes, statistical tests and P-values (page 1/2)

Figure	Group	N	Mean	SEM	Statistical test	P value	Multiple comparisons (reported in figure)	P value
Fig. 1C	CB1-WT	7	0.0162	0.0029	Kruskal Wallis test	<0.0001	CB1-WT vs. CB1-KO	0.0133
	CB1-KO	7	-0.0005	0.0025			CB1-WT vs. DN22-CB1	>0.9999
	DN22-CB1	6	0.0211	0.0038			CB1-KO vs. DN22-CB1	0.0021
Fig 1F	Sniffers	3	-0.0105	0.0059	One way ANOVA	0.0001	Sniffers vs Sniffers + Astro CB1-WT	0.0004
	Sniffers + Astro CB1-WT	7	0.0959	0.0134			Sniffers vs Sniffers + Astro CB1-KO	0.8163
	Sniffers + Astro CB1-KO	4	0.0022	0.0049			Sniffers + Astro CB1-WT vs Sniffers + Astro CB1-KO	0.0005
Fig. 1I	Basal	4	0.0341	0.005184	Two tailed paired T-test	<0.0001		
	Go 6983	4	-0.01105	0.004554				
Fig. 2B	Control	7	0.306	0.043	One way ANOVA	0.002	Control vs. HPC-GFAP-CB1-KO	0.0065
	HPC-GFAP-CB1-KO	7	-0.024	0.038			Control vs. HPC-GFAP-CB1-RS	>0.9999
	HPC-GFAP-CB1 RS	8	0.306	0.102			Control vs. HPC-GFAP-DN22-CB1-RS	0.9962
	HPC-GFAP-DN22-CB1-RS	9	0.287	0.033			HPC-GFAP-CB1-KO vs. HPC-GFAP-CB1-RS	0.0049
							HPC-GFAP-CB1-KO vs. HPC-GFAP-DN22-CB1-RS	0.0067
							HPC-GFAP-CB1-KO vs. HPC-GFAP-DN22-CB1-RS	0.9957
Fig. 3 B,D	Vehicle : GFAP-CB1-WT	50	0.3637	0.0246	Two way ANOVA		Vehicle:GFAP-CB1-WT vs. Vehicle:GFAP-CB1-KO	<0.0001
	Vehicle : GFAP-CB1-KO	49	0.0005	0.0239	Interaction	<0.0001	Vehicle:GFAP-CB1-WT vs. Lactate:GFAP-CB1-WT	0.9958
	Lactate : GFAP-CB1-WT	13	0.2927	0.0547	Treatment	<0.0001	Vehicle:GFAP-CB1-WT vs. L-Serine:GFAP-CB1-WT	0.2718
	Lactate : GFAP-CB1-KO	15	0.2760	0.0407	Genotype	<0.0001	Vehicle:GFAP-CB1-WT vs. 3,5 DHBA:GFAP-CB1-WT	0.9995
	3,5-DHBA : GFAP-CB1-WT	15	0.4190	0.0331			Vehicle:GFAP-CB1-WT vs. NCT:GFAP-CB1-WT	0.8037
	3,5-DHBA : GFAP-CB1-KO	10	0.3046	0.0440			Vehicle:GFAP-CB1-WT vs. NCT + Lac:GFAP-CB1-WT	>0.9999
	L-serine : GFAP-CB1-WT	16	0.2216	0.0419			Vehicle:GFAP-CB1-WT vs. NCT + L-Serine:GFAP-CB1-WT	0.9503
	L-serine : GFAP-CB1-KO	17	0.3246	0.0403			Vehicle:GFAP-CB1-WT vs. NCT + 3,5-DHBA:GFAP-CB1-WT	>0.9999
	Vehicle : GFAP-CB1-WT : NCT-503	17	0.2631	0.0532			Vehicle:GFAP-CB1-KO vs. Lactate:GFAP-CB1-KO	<0.0001
	Vehicle : GFAP-CB1-KO : NCT-503	14	-0.0097	0.0533			Vehicle:GFAP-CB1-KO vs. L-Serine:GFAP-CB1-KO	<0.0001
	Lactate : GFAP-CB1-WT : NCT-503	6	0.3656	0.0701			Vehicle:GFAP-CB1-KO vs. 3,5 DHBA:GFAP-CB1-KO	0.0001
	Lactate : GFAP-CB1-KO : NCT-503	9	-0.0186	0.0467			Vehicle:GFAP-CB1-KO vs. NCT:GFAP-CB1-KO	>0.9999
	3,5-DHBA : GFAP-CB1-WT : NCT-503	9	0.2565	0.0480			Lactate:GFAP-CB1-WT vs. Lactate:GFAP-CB1-KO	>0.9999
	3,5-DHBA : GFAP-CB1-KO : NCT-503	9	0.0599	0.0460			Lactate:GFAP-CB1-WT vs. L-Serine:GFAP-CB1-WT	0.9995
	L-serine : GFAP-CB1-WT : NCT-503	11	0.3655	0.0926			Lactate:GFAP-CB1-WT vs. 3,5 DHBA:GFAP-CB1-WT	0.8778
	L-serine : GFAP-CB1-KO : NCT-503	16	0.3019	0.0954			Lactate:GFAP-CB1-WT vs. NCT + Lac:GFAP-CB1-WT	>0.9999
							L-Serine:GFAP-CB1-WT vs. L-Serine:GFAP-CB1-KO	0.951
							L-Serine:GFAP-CB1-KO vs. 3,5 DHBA:GFAP-CB1-KO	>0.9999
							3,5 DHBA:GFAP-CB1-WT vs. 3,5 DHBA:GFAP-CB1-KO	0.9689
							3,5 DHBA:GFAP-CB1-WT vs. NCT:GFAP-CB1-WT	0.4767
							3,5 DHBA:GFAP-CB1-WT vs. NCT + 3,5-DHBA:GFAP-CB1-WT	>0.9999
							NCT:GFAP-CB1-WT vs. NCT:GFAP-CB1-KO	0.0026
							NCT + Lac:GFAP-CB1-WT vs. NCT + Lac:GFAP-CB1-KO	0.0013
							NCT + L-Serine:GFAP-CB1-WT vs. NCT + L-Serine:GFAP-CB1-KO	>0.9999
							NCT + 3,5-DHBA:GFAP-CB1-WT vs. NCT + 3,5-DHBA:GFAP-CB1-KO	0.0134
Fig 3E	Control	63 cells	0.1014	0.0086	Mann-Whitney	<0.0001		
	3,5-DHBA	48 cells	0.2011	0.0148				
Fig. 4A	Lactate	8	124	11.86	Two-tailed unpaired T-test	0.5027		
	D-serine	5	127.7	12.25				
Fig. 4B	Lactate	8	0.09335	0.01583	Two-tailed unpaired T-test	0.0032		
	D-Serine	5	0.294	0.06443				
Fig. 4C	baseline	6	100.1	0.1091	Two-tailed paired T-test	0.6782		
	Lactate	6	102.1	4.389				
Fig. 4D	Lactate + NCT-503	6	111.4	6.615	Two-tailed unpaired T-test	0.0212		
	D-Serine + NCT-503	6	138.8	7.576				
	baseline (NCT-503)	6	99.92	0.1241	Two-tailed paired T-test	0.143		
	Lactate + NCT-503	6	111.4	6.615				
Fig. 4F	Baseline	6	101	0.747	Two-tailed paired T-test	0.0096		
	3,5-DHBA	6	128.8	6.888				
	Baseline	8	100.6	0.8498	Two-tailed paired T-test	0.4576		
	D-serine	8	104.2	4.463				

Supplementary Table 2 – Main figures statistics details

Group sizes, statistical tests and P-values (page ½)

Fig. 5A	5 min post WIN55	11	0.0149	0.0024	Mixed-effects model	<0.0001	baseline vs. 5 min	0.0277
	10 min post WIN55	4	0.0085	0.0045			baseline vs. 10 min	0.3801
	20 min post WIN55	4	0.0037	0.0042			baseline vs. 20 min	0.9626
	30 min post WIN55	4	-0.0001	0.0049			baseline vs. 30 min	>0.9999
	40 min post WIN55	4	-0.0042	0.0040			baseline vs. 40 min	0.9315
	50 min post WIN55	4	-0.0110	0.0049			baseline vs. 50 min	0.1578
	60 min post WIN55	4	-0.0179	0.0078			baseline vs. 60 min	0.007
	70 min post WIN55	4	-0.0264	0.0090			baseline vs. 70 min	<0.0001
Fig. 5B	5 min post WIN55	10	0.0242	0.0030	Mixed-effects model	0.001	baseline vs. 5 min	0.0002
	10 min post WIN55	4	0.0245	0.0069			baseline vs. 10 min	0.0013
	20 min post WIN55	4	0.0202	0.0082			baseline vs. 20 min	0.0087
	30 min post WIN55	4	0.0165	0.0072			baseline vs. 30 min	0.0399
	40 min post WIN55	4	0.0155	0.0060			baseline vs. 40 min	0.0573
	50 min post WIN55	4	0.0125	0.0029			baseline vs. 50 min	0.1711
	60 min post WIN55	4	0.0095	0.0011			baseline vs. 60 min	0.4141
	70 min post WIN55	4	0.0081	0.0034			baseline vs. 70 min	0.5788
Fig. 5C	Control	8	-0.0226	0.1276	One way ANOVA	0.002	Control vs. HPC-GFAP-CB1-KO	0.9981
	HPC-GFAP-CB1-KO	7	-0.0466	0.1176			Control vs. HPC-GFAP-CB1-RS	0.9991
	HPC-GFAP-CB1-RS	13	-0.0062	0.0545			Control vs. HPC-GFAP-DN22-CB1-RS	0.0158
	HPC-GFAP-DN22-CB1-RS	13	0.3594	0.0679			HPC-GFAP-CB1-KO vs. HPC-GFAP-CB1-RS	0.9884
							HPC-GFAP-CB1-KO vs. HPC-GFAP-DN22-CB1-RS	0.0136
							HPC-GFAP-CB1-KO vs. HPC-GFAP-DN22-CB1-RS	0.0071
Fig 5D	Vehicle : Saline	12	0.3246	0.0444	Two way ANOVA		Saline:Vehicle vs. Saline:THC	0.0003
	THC : Saline	11	-0.0178	0.0610	Interaction	0.505	Saline:Vehicle vs. Lactate:Vehicle	0.7752
	Vehicle : Lactate	10	0.3953	0.0620	Lactate	0.5317	Saline:Vehicle vs. Lactate:THC	0.0003
	THC : Lactate	10	-0.0200	0.0484	THC	<0.0001	Saline:THC vs. Lactate:Vehicle	<0.0001
							Saline:THC vs. Lactate:THC	>0.9999
							Lactate:Vehicle vs. Lactate:THC	<0.0001
Fig. 5E	Vehicle : Saline	42	0.305362	0.027283	Two way ANOVA		Saline + Vehicle vs. Saline + THC	<0.0001
	THC : Saline	24	0.015965	0.04061	Interaction	0.0001	Saline + Vehicle vs. Lactate 1h after + Vehicle	0.9999
	Vehicle : Lactate	21	0.339832	0.051617	Treatment 2	<0.0001	Saline + Vehicle vs. Lactate 1h after + THC	0.9011
	THC : Lactate	23	0.387984	0.051963	THC	<0.0001	Saline + Vehicle vs. 3,5 DHBA 1h after + Vehicle	>0.9999
	Vehicle : 3,5-DHBA	8	0.339324	0.03525			Saline + Vehicle vs. 3,5 DHBA 1h after + THC	>0.9999
	THC : 3,5-DHBA	9	0.306085	0.062923			Saline + Vehicle vs. NCT + Vehicle	0.982
	Vehicle : Saline : NCT-503	14	0.380169	0.049533			Saline + Vehicle vs. NCT + THC	0.0016
	THC : Saline : NCT-503	12	0.006681	0.055404			Saline + THC vs. Lactate 1h after + THC	<0.0001
	Vehicle : Lactate : NCT-503	18	0.300849	0.042664			Saline + THC vs. 3,5 DHBA 1h after + Vehicle	0.0119
	THC : Lactate : NCT-503	17	0.054124	0.083171			Saline + THC vs. 3,5 DHBA 1h after + THC	0.0252
							Saline + THC vs. NCT + Vehicle	<0.0001
							Saline + THC vs. NCT + THC	>0.9999
							Saline + THC vs. Lactate + NCT + THC	>0.9999
							Lactate 1h after + Vehicle vs. Lactate 1h after + THC	0.9992
							Lactate 1h after + Vehicle vs. Lactate + NCT + THC	0.003
							3,5 DHBA 1h after + Vehicle vs. 3,5 DHBA 1h after + THC	>0.9999
							Lactate + NCT + Vehicle vs. Lactate + NCT + THC	0.0302

Supplementary Table 3 – Main figures statistics details

Group sizes, statistical tests and P-values

Figure	Group	N	Mean	SEM	Statistical test	P value	Multiple comparisons (reported in figure)	P value
Ext. data Fig 1B	Vehicle	3	0.7325	0.01123	Two-tailed unpaired T-test	<0.0001		
	WIN55	3	0.5498	0.02122				
Ext. data Fig 1D	Baseline (BL)	3	0.9929	0.002431	Two-tailed paired T-test	<0.0001		
	WIN55	3	1.032	0.001816				
Ext. data Fig 2B	CB1-WT	4	0.4798	0.05392	Kruskal-Wallis test	0.6298	CB1-WT vs. CB1-KO	0.9804
	CB1-KO	4	0.5483	0.03634			CB1-WT vs. DN22-CB1	>0.9999
	DN22-WT	4	0.5541	0.0473			CB1-KO vs. DN22-CB1	>0.9999
Ext. data Fig 2C	CB1-WT	4	0.06298	0.01233	One way ANOVA	0.4612	CB1-WT vs. CB1-KO	0.449
	CB1-KO	4	0.04552	0.009156			CB1-WT vs. DN22-CB1	0.6554
	DN22-WT	4	0.05058	0.007127			CB1-KO vs. DN22-CB1	0.9295
Ext. data Fig 2D	CB1-WT	7	0.0385	0.004412	One way ANOVA	0.3815	CB1-WT vs. CB1-KO	0.3496
	CB1-KO	7	0.02675	0.006981			CB1-WT vs. DN22-CB1	0.7466
	DN22-WT	6	0.0322	0.00623			CB1-KO vs. DN22-CB1	0.8022
Ext. data Fig 3B	First measurement	4	0.02854	0.001203	Two-tailed paired T-test	0.2564		
	Second measurement	4	0.03095	0.002664				
Ext. data Fig 3D	Basal	4	0.02441	0.0013	Two-tailed paired T-test	0.0317		
	WIN55	4	0.03174	0.001944				
Ext. data Fig 4B	First measurement	4	0.02143	0.007549	Two-tailed paired T-test	0.391		
	Second measurement	4	0.02148	0.007517				
Ext. data Fig 5B	GFP (+) - GFAP (+)	4	93.81	0.762				
	GFP (+) - GFAP (-)	4	6.195	0.762				
Ext. data Fig 6B	Vehicle	13	0.3688	0.02855	One way ANOVA	<0.0001	Vehicle vs. 5 mg/kg	0.9973
	5 mg/kg NCT-503	7	0.3407	0.06452			Vehicle vs. 5.75 mg/kg	0.7351
	5.75 mg/kg NCT-503	7	0.2842	0.03302			Vehicle vs. 6.5 mg/kg	0.0911
	6.5mg/kg NCT-503	15	0.2353	0.03493			Vehicle vs. 8 mg/kg	0.0056
	8 mg/kg NCT-503	8	0.1494	0.03349			Vehicle vs. 10 mg/kg	<0.0001
	10 mg/kg NCT-503	8	-0.01882	0.06185			5 mg/kg vs. 5.75 mg/kg	0.964
							5 mg/kg vs. 6.5 mg/kg	0.4935
							5 mg/kg vs. 8 mg/kg	0.0667
							5 mg/kg vs. 10 mg/kg	<0.0001
							5.75 mg/kg vs. 6.5 mg/kg	0.9622
							5.75 mg/kg vs. 8 mg/kg	0.3556
							5.75 mg/kg vs. 10 mg/kg	0.0005
							6.5 mg/kg vs. 8 mg/kg	0.6613
							6.5 mg/kg vs. 10 mg/kg	0.0006
							8 mg/kg vs. 10 mg/kg	0.1195
Ext. data Fig 7D	3,5-DHBA	4	0.01303	0.001426				
Ext. data Fig 8A	D-serine	5	102.7	7.238	Two-tailed paired T-test	0.0001		
	D-serine + D-APS	5	-5.945	2.604				
Ext. data Fig 8B		N			Two way ANOVA			
	Lactate	9			Time x Treatment	0.0007		
	Lactate + NCT-503	5			Time	<0.0001		
					Treatment	0.0127		
Ext. data Fig 8C		N			Two way ANOVA	P value		
	D-serine	6			Time x Treatment	0.0604		
	D-serine + NCT-503	4			Time	<0.0001		
					Treatment	0.6915		

PART 2 – Unpublished data: Cannabinoid type-1 receptor signalling and its role in regulating brain lactate dynamics in freely moving mice

In this doctoral thesis, we investigated the impact of CB1R activity on brain lactate levels both *in vivo* and *in vitro*, with particular emphasis on how locomotion influences brain extracellular lactate dynamics. Following the presentation of the published article, the thesis continues with unpublished data. For clarity and coherence, the results are organized into four chapters, aligned with the main objectives. Chapter I describes the development of a reliable protocol to measure *in vivo* lactate fluctuations in freely moving mice. Chapter II examines the effects of locomotion on brain lactate levels across different brain regions, while Chapter III addresses the contribution of lactate to the locomotor effects of cannabinoids. Finally, Chapter IV explores the molecular mechanisms underlying CB1R-dependent modulation of lactate in cultured astrocytes.

Chapter I. Development of a reliable protocol for *in vivo* lactate measurement using eLacco2.1 in freely moving mice.

As already extensively described in this thesis, CB1R has emerged as a key element in regulating brain metabolism and lactate production (Fernández-Moncada, Rodrigues, et al., 2024). Persistent activation of astroglial mtCB1R for 24 hours has been shown to decrease lactate production and release (Jimenez-Blasco et al., 2020), whereas our recent findings indicate that transient stimulation (5 minutes) produces the opposite effect, leading to an elevation in lactate levels (Fernández-Moncada, Lavanco, et al., 2024). These observations, however, were obtained primarily from cultured astrocytes, and the consequences of CB1R activation on lactate dynamics *in vivo* remain unknown. This paucity of knowledge can now be tackled thanks to the development of a novel extracellular lactate fluorescent biosensor, eLACCO2.1 (Nasu et al., 2023), which as shown in this thesis, allow the direct monitoring of brain lactate levels in freely moving mice. Until then, high resolution analysis of lactate dynamics had been investigated *in vivo* in a few studies, but these were conducted mainly in head-fixed mice using the FRET-based sensor Laconic combined with two-photon microscopy (Mächler et al., 2016; Zuend et al., 2020), an approach that provides high spatial resolution but restricts animals from freely moving and requires demanding technical conditions. By contrast, FP, despite offering lower spatial resolution, allows reliable real-time monitoring of fluorescent biosensors signal in freely behaving mice, making it more suitable for addressing the behavioural questions of this work.

Since the recording of lactate dynamics in freely moving mice had not yet been established at the start of this thesis, a substantial part of the initial work was devoted to developing reliable experimental protocols. As a first step, we determined the isosbestic point of the biosensor *in*

vitro, a prerequisite for its use in fiber photometry. The isosbestic point corresponds to the excitation wavelength at which the fluorescence of the biosensor remains unchanged regardless of whether lactate is bound, and is therefore critical for generating a reference signal that controls for movement artifacts, fluctuations in biosensor expression, or changes in illumination. For determining the eLACCO2.1 isosbestic wavelength, we expressed the biosensor in HEK293T cells and exposed them to sequential increases of extracellular lactate changes (**Fig R1A**). Then, I tested whether a 400 nm excitation, an isosbestic wavelength found in some GFP-based biosensors, was a suitable isosbestic point for eLACCO2.1 biosensor. While the fluorescence resulting from 470 nm excitation increased during stepwise rise of extracellular lactate, the fluorescence resulting from 400 nm did not (**Fig R1B**). Thus, the data indicated that an excitation at 400 nm correspond to the eLACCO2.1 isosbestic point, in agreement with the original characterization of the sensor (Nasu et al., 2023), which provided a less accurate value. This result provided a necessary reference channel for subsequent *in vivo* experiments, ensuring the accuracy and reliability of lactate measurements in freely moving mice (**Fig. R1A-B**)

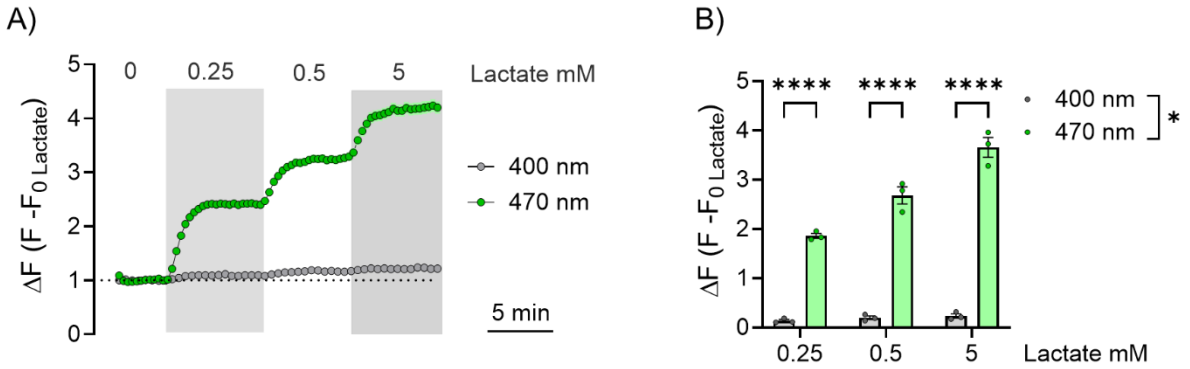

Figure R1. In vitro Determination of eLACCO2.1 isosbestic point.
*A) Representative trace of extracellular lactate recording in HEK293 cells. Cells have been excited at two different wavelengths, 470 nm for the lactate sensitive signal (in green) and 400 nm for the hypothetical isosbestic point (in grey) under increasing lactate concentrations, in order to determine the isosbestic point of the biosensor. Data have been normalized to 0 lactate. B) Quantification of dose response of lactate levels. n= 180 cells/3 experiments. Two-way ANOVA: **** P<0.0001.*

Once the isosbestic point was determined, we proceeded to optimize the conditions for *in vivo* FP recordings of eLACCO2.1 biosensor. FP has traditionally been developed and optimized for monitoring Ca^{2+} dynamics, which posed challenges in configuring the setup to reliably detect lactate signals. Unlike Ca^{2+}, lactate fluctuations occur on a slower timescale and follow distinct kinetics, requiring specific adjustments in acquisition parameters. In addition, because eLACCO2.1 had only recently been developed, achieving robust expression *in vivo* proved difficult. We tested several promoters, including GFAP (specific for astrocytes), Synapsin (specific for neurons), and CAG (general promoter), but only the ubiquitous CAG promoter

yielded sufficient expression, likely due to its ability to drive strong and broad expression across multiple cell types. Finally, given the original aim of the project - to investigate the relationship between brain lactate dynamics, CB1R activity, and memory - we initially targeted the hippocampus for biosensor expression. This choice was motivated not only by the region's accessibility for viral injections and recordings, but also by its central role in memory processing and its high density of CB1Rs, making it a biologically relevant site for our study. After these validations, we proceeded to perform FP recordings in freely moving mice expressing eLACCO2.1 in the hippocampus. To test the responsiveness of the sensor *in vivo*, animals received intraperitoneal (I.P.) injections of either lactate or vehicle (veh). Lactate injections produced a clear increase in fluorescence signal compared to veh-treated controls (**Fig. R2A**). This effect followed a dose-dependent pattern (**Fig. R2B**), demonstrating not only that eLACCO2.1 can reliably detect changes in extracellular lactate levels *in vivo*, but also that the sensor exhibits sufficient sensitivity and dynamic range to capture physiologically relevant fluctuations. These results provided a critical validation of our FP approach, allowing us to move forward to experiments addressing lactate dynamics during behaviour. However, it should be noted that recordings from lactate-injected mice exhibited a pronounced fluorescence drift (**Fig. 2RA**), which likely influenced the magnitude of the observed increase. For this reason, this experiment should be repeated to strengthen the robustness of this validation.

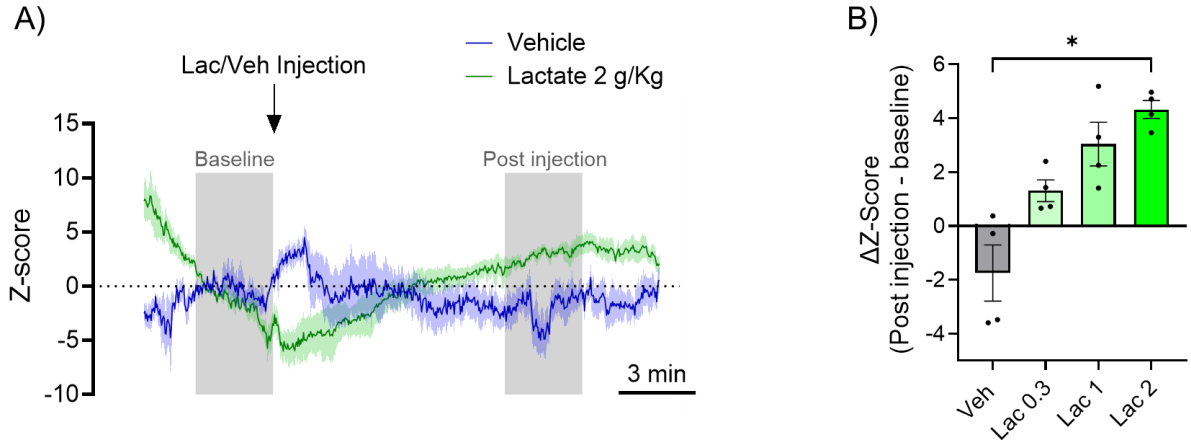

Figure R2. FP recording of eLACCO2.1 signal in freely moving mice.
*A) Averaged FP traces of eLACCO2.1 recordings in mice treated with an IP injection of either veh or 2 g/kg lactate. Injection at 6 min of recording. Baseline: 3 – 6 min of recording. Post injection: 15 – 18 min of recording. B) Quantification of lactate changes induced by increasing doses of exogenously administered lactate. Baseline Z-Score (0) is the averaged signal for the last 3 minutes before injections. Recordings lasted 21 minutes, with IP injection after 6 minutes. n=4 mice. One-way ANOVA: * P<0.05*

To complement these functional experiments, we next examined the expression of eLACCO2.1 in the hippocampus. Immunofluorescence analyses confirmed a strong and widespread expression of the biosensor in transduced cells within the injection site, thereby validating the effectiveness of our viral strategy (**Fig. R3**).

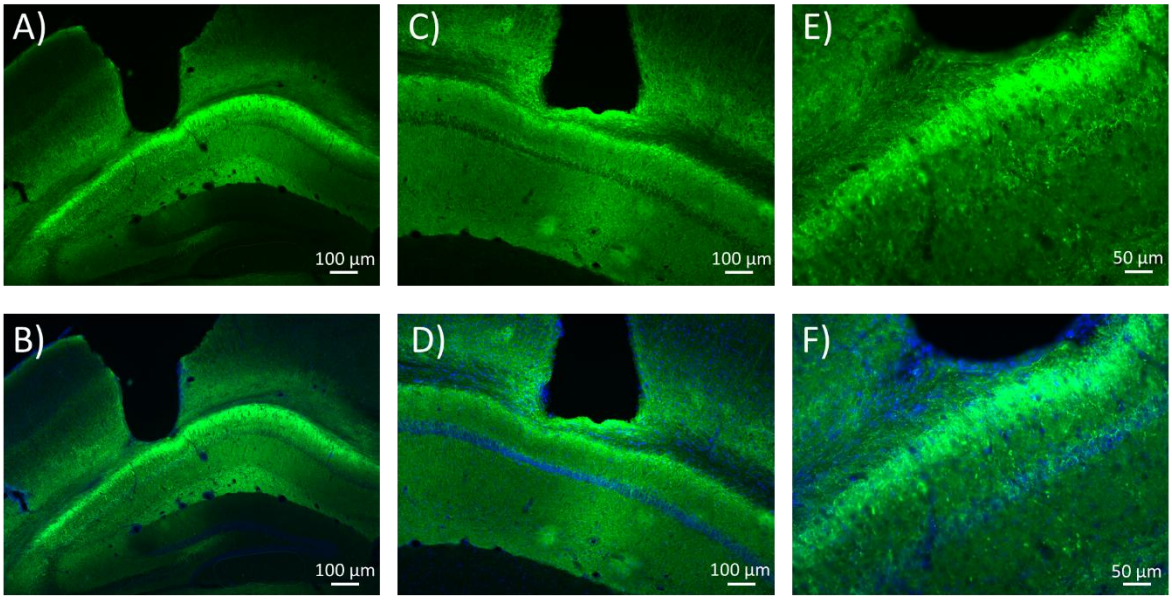

Figure R3. CAG promoter-mediated expression of eLACCO2.1 in the hippocampus.
Representative fluorescence images of hippocampal sections showing robust expression of eLACCO2.1 (green). Panels B, D, and F include DAPI staining (blue) for nuclear visualization. Images are shown at both low (A–D, 100 µm scale bars) and higher (E–F, 50 µm scale bars) magnification, confirming strong and widespread sensor expression within the targeted region. The track of the implanted optical fiber can also be observed, confirming correct placement of fiber optic.

Chapter II. Investigation of the impact of locomotion on brain lactate levels across different brain regions.

Once we established that it is indeed possible to monitor lactate dynamics in freely moving mice, we sought to determine whether these changes could be linked to behavioural processes. Lactate plays a critical role in memory formation and consolidation (Alberini et al., 2017; Newman et al., 2011; Suzuki et al., 2011), and astrocytic CB1Rs are also known to be essential for memory regulation (Robin et al., 2018). In line with this, our recent work demonstrated that GFAP-CB1-KO mice, which lack CB1Rs in astrocytes, can recover their associated memory impairments through lactate treatments, indicating that astroglial CB1Rs are fundamental for brain lactate production and that lactate itself is a key mediator of memory processes (Fernández-Moncada, Lavanco, et al., 2024). Based on this background, our initial aim was to investigate the relationship between lactate dynamics in freely moving mice, astrocytic CB1R activity, and memory. However, despite considerable effort, technical limitations (possibly low sensor efficiency and/or the complexity of the required protocols) resulted in data difficult to

interpret due the lack of proper tools to carry out correlation analysis of behaviour - lactate signal during our first trials. Therefore, we decided to focus on a more controlled experiment based on pharmacological treatments, by considering that another aim of this work was attempting to record *in vivo* the impact of CB1R activation on brain lactate levels. As previously described, *in vitro* data showed that persistent stimulation of mtCB1Rs for 24 hours led to a reduction in lactate production and release (Jimenez-Blasco et al., 2020), whereas transient activation of astroglial CB1Rs for 5 minutes resulted in increased lactate levels (Fernández-Moncada, Lavanco, et al., 2024). Thus, we tested whether pharmacological activation of CB1R can alter extracellular brain levels in a similar fashion as observed *in vitro*. Surprisingly, we did not detect a direct effect of Δ⁹-THC exposure on extracellular lactate levels in freely moving mice. However, this approach revealed a consistent pattern whereby lactate levels were lower upon periods of inactivity, suggesting that locomotion strongly influences brain lactate levels (**Fig. R4**).

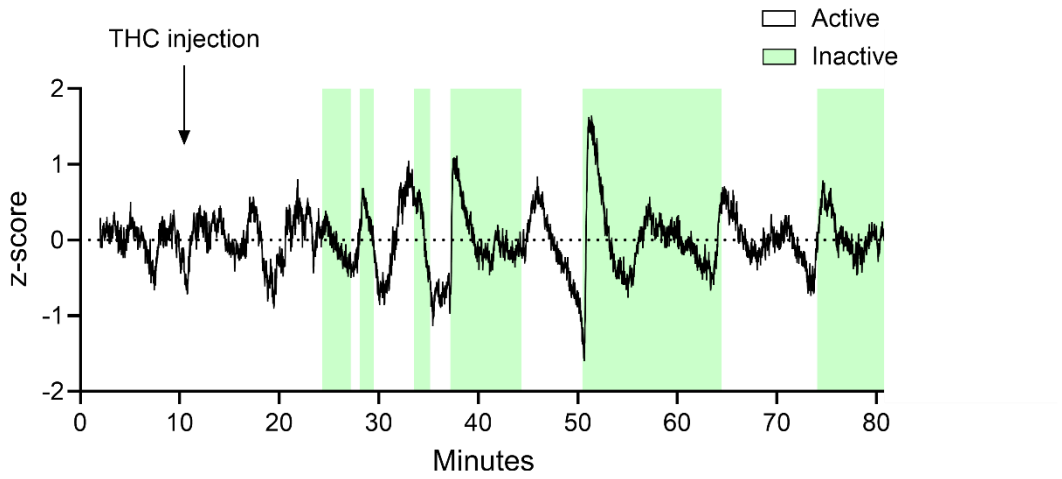

Figure R4. Representative trace of FP recordings of eLACCO2.1 signal in a freely moving mouse. *Arrow indicates the IP injection of 5 mg/Kg Δ⁹-THC. Green areas indicate inactive behavioural phases. Recordings lasted 81 minutes, with injection after 11 minutes.*

Once we identified a consistent pattern whereby brain lactate levels fluctuated with locomotor activity, we next asked whether this effect was influenced by Δ⁹-THC and whether it occurred similarly across different brain regions. Recordings were performed under the same conditions as before: 81 minutes in total, with an I.P. injection of either Δ⁹-THC or veh at minute 11, in a paired design manner where each mouse received both treatments in separate sessions. Accordingly, our initial recordings were performed in the hippocampus, as this was the region in which we had already optimized the technique and collected preliminary data. To analyse the effect of immobility, we developed a Python-based pipeline that identified all immobility events lasting at least 180 seconds and separated by a minimum interval of 15 seconds (**Fig.**

R5A). For each event, we compared lactate levels immediately preceding and during immobility. Specifically, we quantified changes in biosensor signal at three specific time points: (i) 15 s before immobility (called T1, corresponding to 0-15 s of extracted event), (ii) 15 s during the early phase of immobility (called T2, corresponding to 45 – 60 s of extracted event), and (iii) 15 s during the late phase of immobility (called T3, corresponding to 150 – 165 s of extracted event), to assess both changes before onset and maintenance of inactivity (**Fig. R5A**).

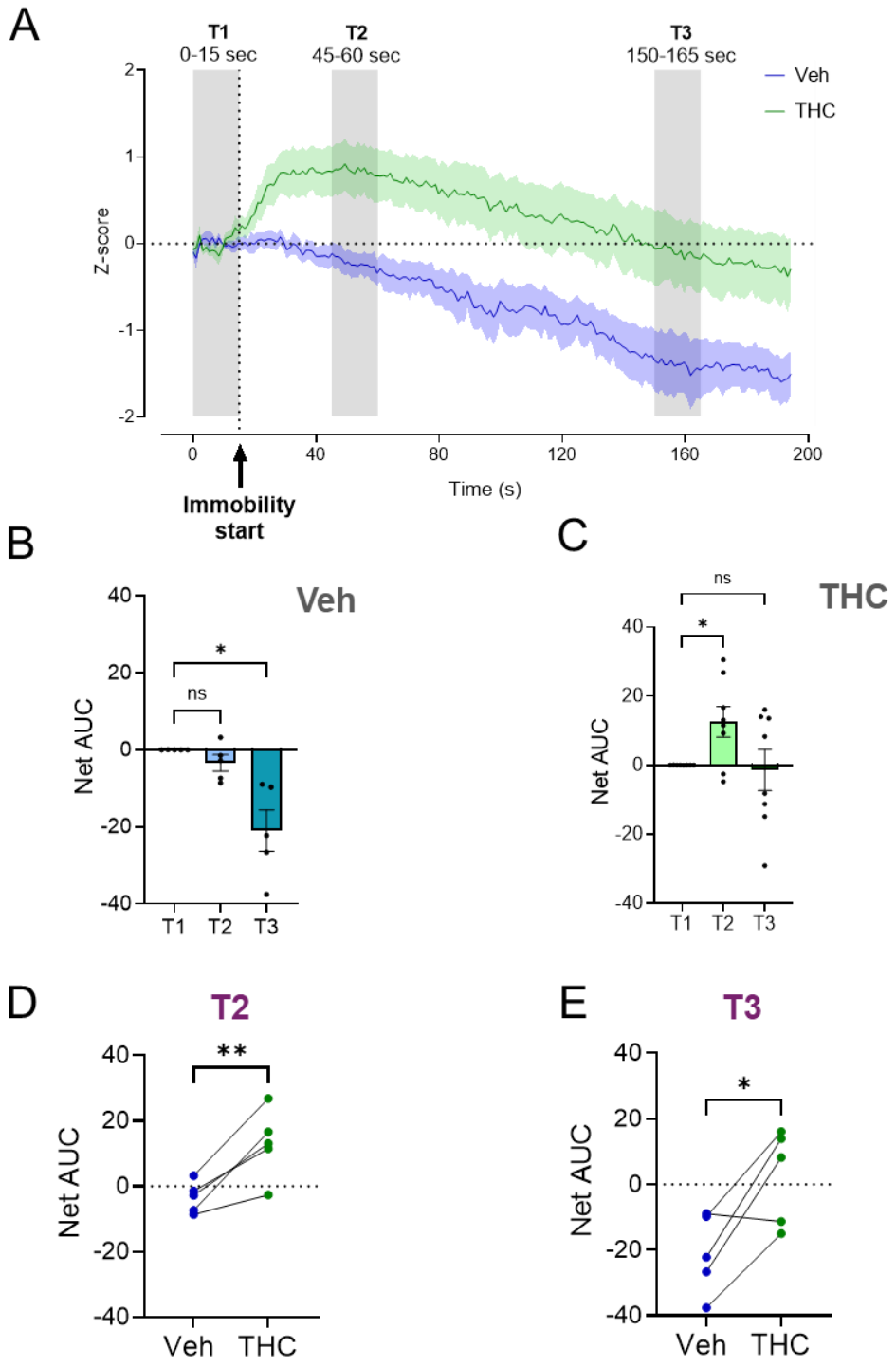

Figure R5. Hippocampal lactate levels before and during immobility in veh or Δ⁹-THC treated mice. *A) Averaged FP traces of eLACCO2.1 signal, with time periods T1, T2 and T3 highlighted (see main text for details). Δ⁹-THC, n = 8; veh, n =5. B, C) Quantification of lactate levels in mice injected IP with either veh (B) or Δ⁹-THC (C) at three time points: T1, T2, and T3. One-way ANOVA: *p < 0.05, p>0.05 (not significant, ns). D) Quantification of the difference in net AUC at T2 for veh- and Δ⁹-THC-treated mice. N=5 mice. Paired t-test: **p<0.001. E) Quantification of the difference in net AUC at T3 for veh- and Δ⁹-THC-treated mice. N=5 mice. Paired t-test: *p<0.05.*

Under veh treatment, lactate levels did not differ between the pre-immobility period and the early phase of immobility but showed a significant decrease during the late phase (**Fig. R5A-B**). In contrast, Δ⁹-THC administration produced the opposite effect: lactate levels increased during the early phase of immobility, while no further difference between the pre-immobility period and the late phase was observed (**Fig. R5A** and **Fig.R5C**). These results indicate that the early and late phases of immobility follow distinct patterns depending on whether animals received veh or Δ⁹-THC, with significant differences between the two treatments observed in both T2 and T3 time periods (**Fig R5D-E**). Together, these findings suggest that Δ⁹-THC shifts the timing of lactate regulation during immobility in the hippocampus. Prompted by this observation we investigated whether similar effects occur in other brain regions.

Next, we investigated whether similar patterns were present in the striatum, a region strongly involved in motor regulation, using a similar approach as described for the hippocampus. Interestingly, the results suggested that lactate dynamics during locomotion differ between brain regions. Under veh treatment, as in the hippocampus, lactate levels did not differ between the pre-immobility and early immobility phases but showed a significant decrease during the late phase (**Fig. R6A-B**). However, in contrast to the hippocampus, Δ⁹-THC administration did not produce any significant changes in lactate levels between the pre-immobility period and either the early or late phases of immobility (**Fig. R6A** and **Fig. R6C**). Contrary to the hippocampus, there is a slight tendency of decrease in the early phase after Δ⁹-THC administration (**Fig. R6C**). These findings indicate that in the striatum, lactate regulation across immobility phases depends on treatment condition, but the dynamics differ from those observed in the hippocampus. Importantly, in this case, no significant differences were found between veh- and Δ⁹-THC-treated mice in either T2 or T3 time periods (**Fig R6D-E**). Together, these results highlight that the impact of Δ⁹-THC on lactate dynamics is likely brain region-specific, suggesting that hippocampal and striatal circuits may rely on distinct metabolic regulation during behavioural states.

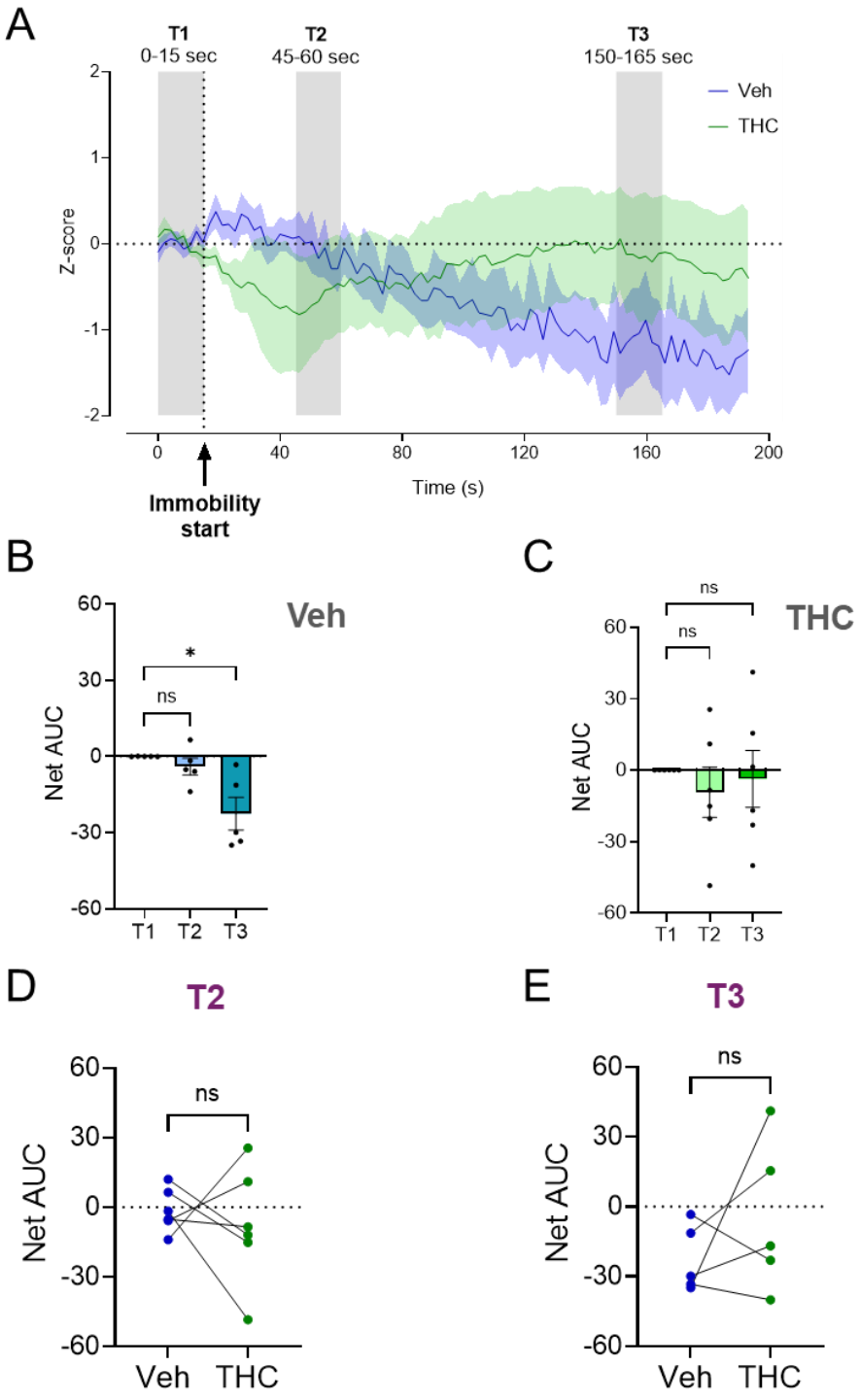

Figure R6. Striatal lactate levels before and during immobility in veh or Δ⁹-THC treated mice.
*A) Averaged FP traces of eLACCO2.1 recordings, with T1, T2 and T3 periods highlighted. N= 7 Δ⁹-THC, 6 veh. B, C) Quantification of lactate levels in mice injected IP with either veh (B) or Δ⁹-THC (C) at three time points: T1, T2, and T3. One-way ANOVA: *p < 0.05, p>0.05 (not significant, ns). D) Quantification of the difference in net AUC at T2 for veh- and Δ⁹-THC-treated mice. N=5 mice. Paired t-test p>0.05 (not significant, ns). E) Quantification of the difference in net AUC at T3 for veh- and Δ⁹-THC-treated mice. N=5 mice. Paired t-test: p>0.05 (not significant, ns).*

To further explore whether this regional specificity extended beyond the hippocampus and striatum, we finally examined lactate dynamics in the substantia nigra pars reticulata (SNr), a basal ganglia output nucleus critically involved in the motor control. The SNr also represents a particularly relevant region in the context of this work, as it has been shown that the behavioural effects of cannabinoids in the SNr depend on the precise subcellular localization of CB1Rs within striatonigral terminals (Soria-Gomez et al., 2021), making it an ideal site to disentangle spatial aspects of CB1R-mediated neuromodulation. Interestingly, the results again pointed to region-specific differences in lactate dynamics. Using a similar quantification strategy as before, we observed that under veh treatment lactate levels showed no significant decrease during the late phase of immobility which differed from both the hippocampus and striatum data, although a tendency toward reduction could be observed (**Fig. R7A-B**). Moreover, Δ⁹-THC administration did not produce any significant changes in lactate levels between the pre-immobility period and either the early or late phases of immobility (**Fig. R7A** and **Fig. R7C**). Consistently, no significant differences were detected between veh- and Δ⁹-THC-treated mice in either T2 or T3 time points (**Fig. R7D-E**). There is however a tendency of increase with Δ⁹-THC treatment in both immobility phases (**Fig. R7D-E**). Together, these findings indicate that lactate dynamics in the SNr follow yet another distinct profile, reinforcing the idea that Δ⁹-THC differentially modulates metabolic regulation across brain regions.

Taken together, our results reveal that the regulation of brain lactate dynamics during immobility differ from each brain region recorded. In the hippocampus, veh-treated mice possessed a late-phase decrease in lactate **(Fig. R5B)**, whereas Δ⁹-THC treatment induced an early-phase lactate increase and abolished the late-phase drop in lactate (**Fig. R5C)**. Consistent with this, treatment groups differed significantly in both T2 and T3 phases (**Fig. R5D-E**). In the striatum, veh treated mice also had a late-phase lactate decrease (**Fig. R6B**), but Δ⁹-THC treatments produced no detectable change across phases (**Fig. R6C)**, and no significant differences were observed between-treatments during T2 and T3 phase (**Fig. R6D-E**). By contrast, lactate levels in the SNr remained largely stable across immobility phases in veh-treated mice, with only a tendency toward reduction during the late phase (**Fig. R7B)**, whereas no significant effect of Δ⁹-THC treatments were detected (**Fig. R7C**). Accordingly, no differences between treatments were found at T2 and T3 time points (**Fig. R7D-E**). These findings highlight that the impact of locomotor state and cannabinoid signalling on lactate availability is not uniform across the brain but instead likely reflects distinct region-dependent

patterns of metabolic regulation. Nevertheless, additional batches of mice will be required to confirm the robustness of these observations.

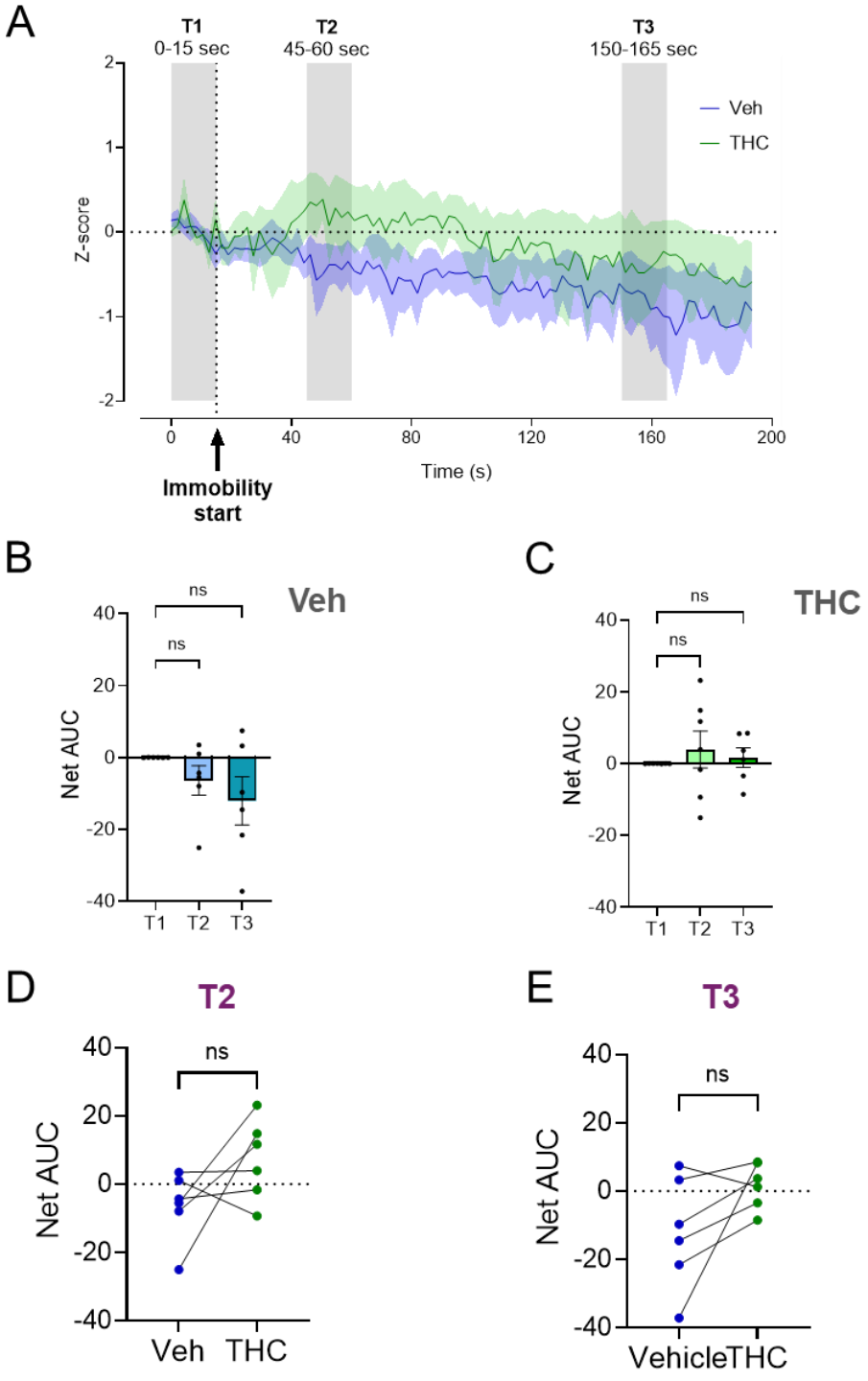

Figure R7. SNr lactate levels before and during immobility in veh or Δ⁹-THC treated mice.
A) Averaged FP traces of eLACCO2.1 recordings, with T1, T2 and T3 periods highlighted. N= 7 Δ⁹-THC, 6 veh. B, C) Quantification of lactate levels in mice injected IP with either veh (B) or Δ⁹-THC (C) at three time points: T1, T2 and T3. One-way ANOVA: p>0.05 (not significant, ns). D) Quantification of the difference in net AUC at T2 for veh- and Δ⁹-THC-treated mice. N=6 mice. Paired t-test p>0.05 (not significant, ns). E) Quantification of the difference in net AUC at T3 for veh- and Δ⁹-THC-treated mice. N=6 mice. Paired t-test: p>0.05 (not significant, ns).

Chapter III. Contribution of lactate to the locomotor effects of cannabinoids.

One of the main effects of high doses of cannabinoids in mice is a pronounced reduction of locomotion, accompanied by other well-characterized responses such as antinociception, hypothermia, and catalepsy (Stella, 2023). These effects are mediated primarily through CB1R activation and are commonly assessed using the tetrad behavioural paradigm, which provides a robust measure of cannabinoid activity *in vivo* (Metna-Laurent et al., 2017). Building on the growing evidence that lactate functions not only as an energy substrate but also as a signalling molecule influencing neuronal and behavioural processes (Magistretti & Allaman, 2018), together with our findings that lactate dynamics in the brain vary according to activity state, we asked whether lactate could rescue the canonical hypo-locomotive effects of cannabinoids. To test this, we evaluated the impact of lactate treatments on the THC-induced tetrad, a behavioural battery that includes assessments of locomotor activity, nociception, catalepsy, and body temperature. To carry out experiments, mice received an I.P. injection of Δ⁹-THC (10 mg/kg), followed five minutes later by an I.P. injection of lactate (1 g/kg), and their behaviours were subsequently evaluated after one hour of Δ⁹-THC exposure. As expected, Δ⁹-THC administration produced the characteristic tetrad responses, including marked hypolocomotion, hypothermia, antinociception, and catalepsy. However, subsequent lactate administration failed to rescue any of these behavioural effects (**Fig. R8A-D**). Particularly, no differences were observed in locomotor activity between mice treated with Δ⁹-THC alone and those treated with Δ⁹-THC followed by a lactate injection, indicating that lactate did not counteract the hypolocomotive effect of cannabinoids (**Fig. R8A**). Similarly, lactate injection did not alter Δ⁹-THC-induced changes in body temperature, nociceptive thresholds, or cataleptic behaviour (**Fig. R8B-D**). These results demonstrate that systemic lactate administration does not reverse the known hypo-locomotive effects of cannabinoids.

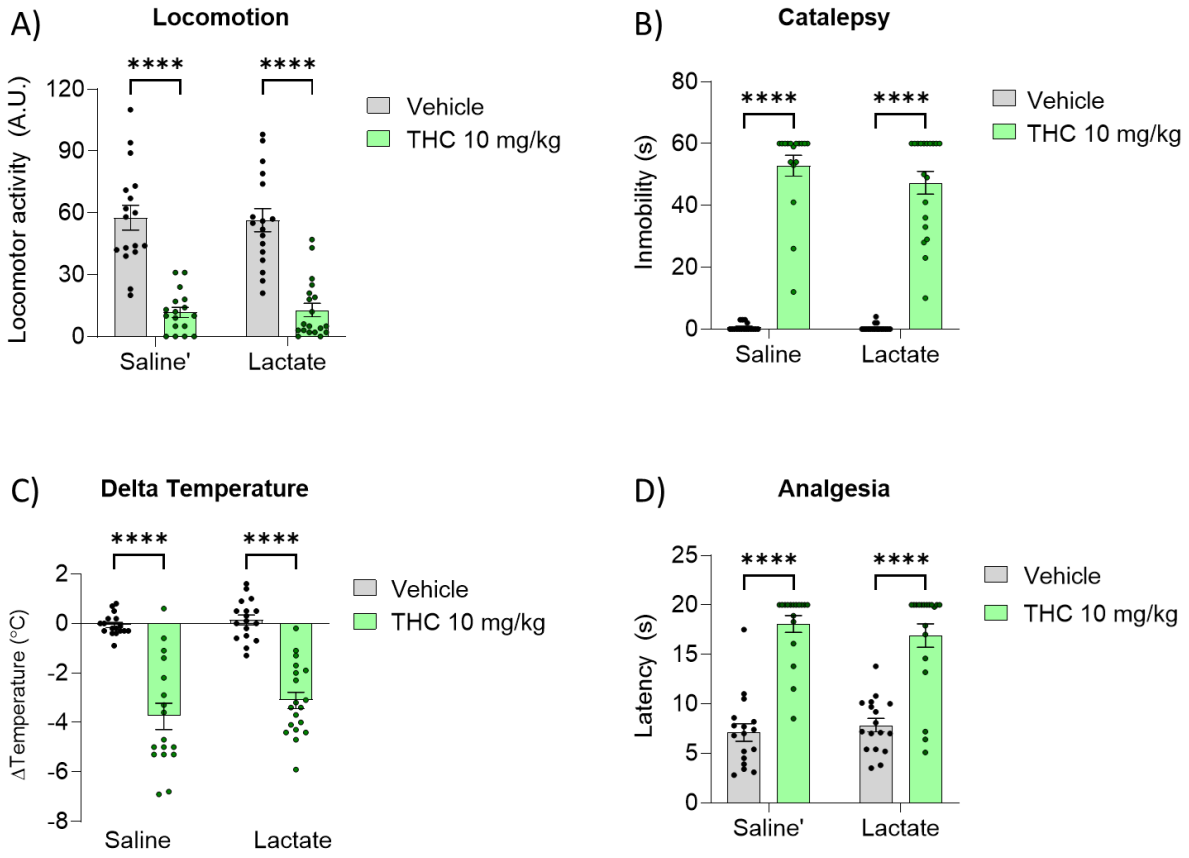

Figure R8. Lactate treatments did not rescue the hypo-locomotive effect of Δ⁹-THC.
*A) Quantification of locomotor activity using activity cages (see methods). B) Quantification of catalepsy using the bar test. C) Quantification of body temperature changes induced by THC treatment. D) Quantification of thermal antinociception using the hot plate assay. Mice were treated with veh or Δ⁹-THC (10 mg/kg, IP), followed 5 minutes later by saline or lactate (1 g/kg, IP). N=70 mice, 3 independent experiments. Data analysed by two-way ANOVA. No interaction was observed (p>0.05). A main effect of THC was detected (**** P<0.0001), indicating that lactate treatment did not alter Δ⁹-THC–induced hypolocomotion, catalepsy, hypothermia, or antinociception.*

Chapter IV. Exploration of the molecular mechanisms underlying CB1R-dependent lactate modulation in cultured astrocytes.

In parallel with the *in vivo* experiments, we also performed studies on cultured astrocytes to investigate in greater detail the molecular mechanisms underlying the switch we previously described between the transient (5 min) and persistent (24 h) effects of CB1R activation on lactate levels. In the same study included in Part 1 of the Results, we also demonstrated that the persistent effect of WIN55 on lactate levels in cultured astrocytes occurs earlier than previously reported. While it had been previously shown to occurs after 24 hours of treatment (Jimenez-Blasco et al., 2020), our recent findings revealed that this effect is already detectable after just 1 hour (Fernández-Moncada, Lavanco, et al., 2024). Moreover, in the same study we investigated the molecular mechanisms underlying the CB1R-mediated increase in astrocytic lactate levels. PKC is known to be transiently activated downstream of CB1R stimulation and to mediate the short-term amnesic effects of cannabinoids (Busquets-Garcia et al., 2018). To test whether PKC contributes to lactate regulation, we quantified the effect of WIN55 on lactate levels in the presence of Go 6983, a broad pharmacological inhibitor of PKC activity. Strikingly, PKC blockade completely abolished the transient lactate increase normally induced by WIN55 (Fernández-Moncada, Lavanco, et al., 2024). Based on these results, we next asked how PKC activity might influence the persistent effect of cannabinoids on lactate levels in cultured astrocytes. Importantly, as expected, we confirmed that the persistent effect of WIN55 mediated by mtCB1Rs emerged after 1 hour, and that Go 6983 blocked the transient lactate increase. Moreover, broad PKC inhibition abolished the persistent decrease and also led to a progressive rise in lactate levels over time (**Fig. R8A-B**).

Finally, to exclude the possibility that the observed increase reflected cell stress or damage during prolonged co-exposure to Go 6983 and WIN55, we performed parallel control experiments with Go 6983 alone. Although technical issues again prevented us from obtaining a complete dataset, preliminary data suggest that a long exposure to Go 6983 alone does not affect basal lactate levels in cultured astrocytes (**Fig. R8C**). In addition, in the averaged traces from this experiment, small peaks can be observed (**Fig. R8C**); these do not reflect biological events but are artifacts caused by instability of the microscope, in particular problems with autofocus, which increasingly affected our recordings at this stage.

Together, these findings support the idea that PKC activity is required not only for the transient but also for the persistent regulation of lactate by CB1Rs in astrocytes, although technical limitations prevented us from fully consolidating this conclusion.

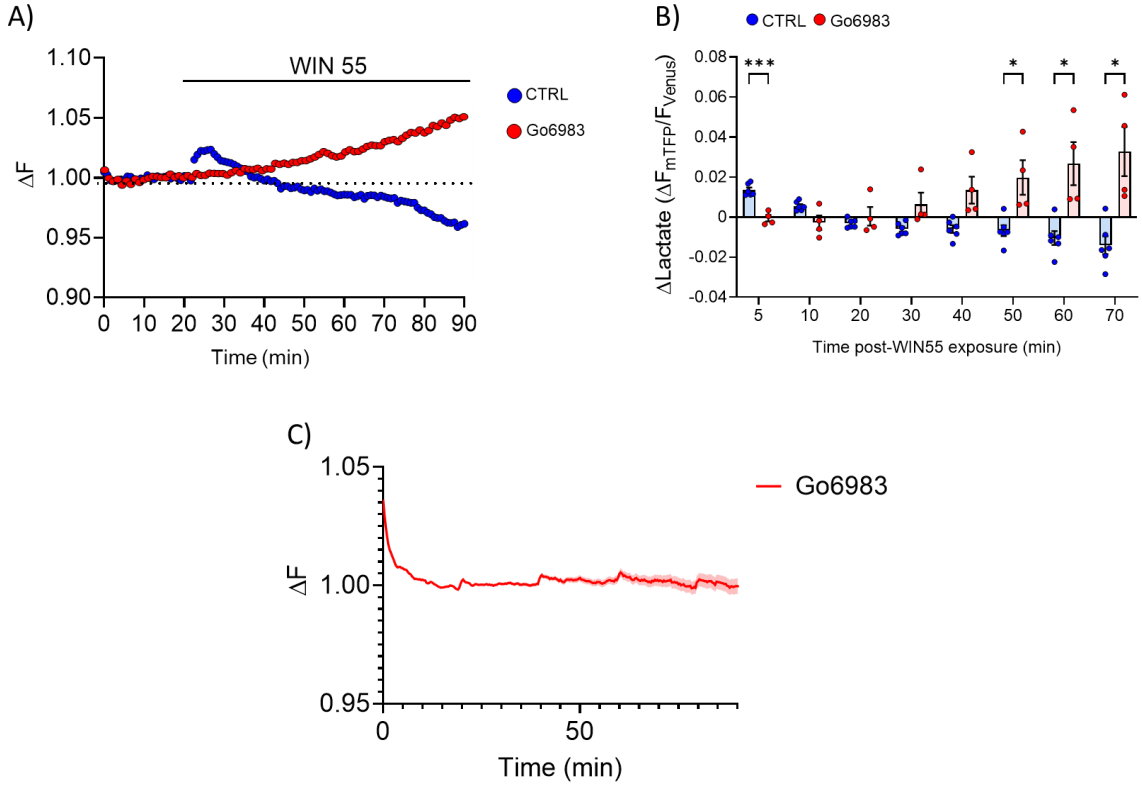

Figure R9. PKC inhibition abolishes both transient and persistent effects of CB1R activation on astrocytic lactate levels.

*A) Representative traces of intracellular lactate recordings in CB1R-WT astrocytes before and during exposure to WIN55 (1 μM), either under control conditions (blue) or in the presence of the broad PKC inhibitor Go 6983 (red). B) Quantification of lactate changes during 70 minutes of WIN55 exposure, with in absence (blue) or presence of Go 6983 (red). n = 4 replicates obtained from2 independent cultures. Two-way ANOVA: p < 0.05. Two-way ANOVA: * P<0.05. C) Averaged traces of intracellular lactate recordings during 90 minutes of exposure to Go 6983 alone.*

DISCUSSION

In this thesis, we investigated how CB1R activity shapes lactate dynamics in the brain, both *in vivo* and *in vitro*, and whether lactate contributes to cannabinoid-induced behavioural effects. Using the extracellular lactate biosensor eLACCO2.1 (Nasu et al., 2023), we developed, for the first time, protocols for real-time monitoring of lactate dynamics in freely moving mice using FP, and demonstrated that lactate levels fluctuate with locomotor activity in a brain region-specific manner. We further showed that cannabinoids alter the temporal profile of lactate dynamics during immobility in the hippocampus, but not in a clear and significant way in the striatum or SNr, suggesting that CB1R-dependent modulation of metabolic function is heterogeneous across brain regions. Finally, we examined the role of lactate in well-known cannabinoid-mediated behaviours, and the molecular mechanisms underlying the regulation of lactate in astrocytes, identifying PKC as a key mediator of both transient and persistent effects of CB1R on astrocytic lactate levels *in vitro*.

This discussion is structured into four sections, corresponding to the results chapters, followed by a concluding summary of the main findings and their broader implications.

Chapter I. Development of a reliable protocol for *in vivo* lactate measurements using eLacco2.1 in freely moving mice.

Prior to this work, real-time monitoring of brain lactate dynamics was largely limited to head-fixed experiments using two-photon microscopy and FRET-based biosensors like Laconic (Mächler et al., 2016; Zuend et al., 2020). While these methods offer high spatial resolution, they are technically demanding and incompatible with the study of freely moving animals and specific behaviours outputs without the use of expensive and complex hardware. With the recent development of the GFP-based biosensor eLACCO2.1 (Nasu et al., 2023), we aimed to establish a method for monitoring brain lactate dynamics *in vivo* using FP. Although FP has lower spatial resolution, it enables robust, real-time measurement of metabolite fluctuations in freely behaving mice (at the fraction of the cost of state-of-the-art two-photon microscope), making it well suited for addressing neurobiological questions in more naturalistic and/or etiological-relevant conditions.

A critical step in this work was determining the biosensor's isosbestic point, which can be used for artifact correction in dual-wavelength recordings with FP. By validating 400 nm as a suitable isosbestic wavelength in HEK293T cells, we established a reliable reference signal, confirming and refining the eLACCO2.1 initial characterization.

This technical foundation enabled the implementation of FP-based lactate imaging in freely moving mice - marking, to our knowledge, the first such application - and allowed us to explore behaviourally relevant metabolic fluctuations across brain regions. Since FP has been widely used to monitor Ca^{2+} dynamics, adapting this technique to study lactate posed significant challenges. Lactate and Ca^{2+} are fundamentally different: they operate on distinct time scales, follow different signalling kinetics, and involve different cellular pathways. As a result, protocols optimized for Ca^{2+} sensors were not directly transferable to lactate imaging.

Developing a reliable protocol for detecting lactate fluctuations required extensive optimization of acquisition parameters and sensor expression. One key technical hurdle was achieving sufficient *in vivo* expression of the eLACCO2.1 biosensor. We tested several promoters - GFAP, Synapsin, and CAG - but only the ubiquitous CAG promoter produced reliable expression levels suitable for detection. This likely reflects several factors. First, FP relies on bulk fluorescence detection, which requires strong and widespread expression; cell-type-specific promoters like GFAP and Synapsin drive more restricted and often weaker expression, reducing overall signal. Second, eLACCO2.1 may not yet be sensitive enough to detect physiologically relevant lactate fluctuations when expressed at low levels or in sparse populations. More importantly, lactate is dynamically exchanged between astrocytes and neurons, being primarily produced by astrocytes and then shuttled to neurons as an energy source (Brooks, 2018; Magistretti & Allaman, 2018). Therefore, expressing the biosensor in only one of these cell types may limit its ability to reliably detect extracellular lactate fluctuations. Ubiquitous expression via the CAG promoter likely provides better coverage across cell types and compartments, improving the chance of detecting physiologically relevant lactate dynamics. Future versions of the biosensor with improved signal-to-noise ratio or enhanced fluorescence may overcome this limitation and enable cell-type-specific applications. Despite these obstacles, we successfully established high -quality recordings of extracellular brain lactate levels in freely moving mice, a first in the field. This opened new opportunities for exploring the dynamic metabolic interactions between astrocytes and neurons under physiological conditions.

Chapter II. Investigation of the impact of locomotion on brain lactate levels across different brain regions.

Having established that extracellular lactate dynamics can be reliably monitored in freely moving mice using eLACCO2.1, we next sought to explore whether these fluctuations are linked to behavioural processes. Although previous work has shown that astrocytic CB1Rs are

crucial for memory and lactate regulation (Fernández-Moncada, Lavanco, et al., 2024; Robin et al., 2018), our initial attempts to link lactate signals with memory-related behaviours in freely moving mice were limited by technical constraints. This may reflect the limited sensitivity of the sensor and the complexity of the experimental setup, which made early data difficult to interpret, particularly in the absence of tools for precise correlation between behaviour and lactate signals. However, with improved analysis pipelines and more refined experimental approaches polished during the course of this thesis, these preliminary datasets will be revisited in due time, and they could likely provide valuable insight into how lactate fluctuates during exploration, learning and memory-related processes.

We therefore shifted our attention to a pharmacological approach to test whether CB1R activation modulates lactate levels *in vivo*, as previously shown *in vitro* (Fernández-Moncada, Lavanco, et al., 2024; Jimenez-Blasco et al., 2020). Based on these findings, we expected to observe either a transient increase in lactate shortly after Δ⁹-THC injection, or a persistent decrease developing over time. Unexpectedly, we did not observe a clear effect of Δ⁹-THC on lactate levels in freely moving mice.

This unexpected result led us to examine the data from a different perspective. A consistent pattern emerged across conditions: lactate levels decreased during immobility, suggesting that locomotor state itself exerts a strong influence on brain lactate dynamics. We began by investigating whether Δ⁹-THC affects brain lactate levels during transitions into immobility, and whether such changes vary across brain regions. Our initial focus was the hippocampus, not due to its specific role in locomotion, but because our experimental protocol was already optimized for this region and preliminary data were available. While the hippocampus is not classically associated with motor control, it serves as a useful model for detecting generalized effects of cannabinoids on brain metabolism, especially given its high density of CB1Rs and well-characterized astrocyte-neuron metabolic interactions (De Oliveira Alvares et al., 2008; Theparambil et al., 2024). We looked at how lactate levels changed right before the onset of immobility, and during two phases afterward: an early and a late stage of immobility. Our goal was to see whether Δ⁹-THC altered the pattern of lactate changes during these periods, and if this could change across different brain regions.

In the hippocampus veh-treated mice exhibited a delayed decrease in extracellular lactate following the onset of immobility, consistent with a reduction in metabolic demand during rest (Aalling et al., 2018; Caporale et al., 2021). This aligns with what would be expected as the brain shifts into a lower-activity state. In contrast, Δ⁹-THC-treated animals showed a different

pattern: instead of a gradual decline, they exhibited an early increase in lactate levels, which then returned to baseline during the later phase of immobility. This shift suggests that activation of CB1R by Δ⁹-THC alters lactate dynamics in the hippocampus during periods of reduced activity. Rather than allowing lactate levels to fall in line with reduced activity, Δ⁹-THC appears to transiently boost lactate availability. This finding indicates that CB1R activation by Δ⁹-THC may disrupt the normal link between locomotor activity and lactate regulation. Specifically, it suggests that lactate production and release can become uncoupled from immediate neuronal energy demand. One possible mechanism is a direct effect on astrocytic glycolysis: Δ⁹-THC may stimulate lactate production via CB1R on astrocytes, independently of neuronal activity levels.

In the striatum, a region critical for motor control and heavily involved in basal ganglia circuits (Rocha et al., 2023), we observed a lactate profile that partially mirrored the hippocampal pattern under veh treatment. Specifically, lactate levels remained stable in the early phase of immobility but showed a significant decrease during the late phase. This is consistent with the idea that reductions in neuronal activity during prolonged immobility leads to lower metabolic demand and a corresponding drop in brain lactate levels. However, unlike the hippocampus, Δ⁹-THC did not produce a shift in the timing or amplitude of lactate changes in the striatum. Although there was a slight tendency toward a decrease in the early phase (the exact opposite of what we observed in the hippocampus), this did not reach statistical significance, and no major differences were observed between vehicle- and Δ⁹-THC-treated conditions at any time point. This suggests that cannabinoid-induced modulation of lactate dynamics is either weaker in the striatum or governed by different mechanisms compared to the hippocampus. One possible explanation is that difference in neural circuitry and CB1R distribution within the striatum may not favour the same type of astrocyte-neuron metabolic coupling observed in the hippocampus. Alternatively, this may also suggest that cannabinoid modulation of lactate metabolism is weaker or operates differently in the striatum, possibly due to regional differences in CB1R distribution, astrocyte-neuron metabolic coupling, or distinct circuit functions (Mathur & Lovinger, 2012; Soria-Gomez et al., 2021). In this context, striatal astrocytes may contribute differently to local lactate dynamics or respond to CB1R activation with less pronounced metabolic output.

Finally, we extended our analysis to the SNr, a major output nucleus of the basal ganglia and a critical regulator of motor control (Partanen & Achim, 2022a). Moreover, the SNr is also particularly relevant to this study as the behavioural effects of cannabinoids in this region have

been shown to depend on the precise subcellular localization of CB1Rs at striatonigral terminals (Soria-Gomez et al., 2021). This makes the SNr an ideal site to explore spatial aspects of CB1R-mediated neuromodulation and its potential influence on metabolic regulation. Under veh treatment, lactate levels remained relatively stable throughout immobility, with only a slight, non-significant decrease observed in the late phase. Despite the lack of statistical significance, this trend mirrored the patterns seen in the hippocampus and striatum, supporting the idea that prolonged immobility is associated with reduced neuronal activity and a corresponding decline in metabolic demand, and thus extracellular lactate levels. Similarly, Δ^9-THC administration did not produce significant alterations in lactate levels, although a modest tendency toward increased lactate was observed in both early and late phases.

This relative stability may reflect unique features of SNr circuitry and metabolism. Unlike the hippocampus and striatum, the SNr is composed primarily of GABAergic projection neurons with high tonic firing rates and receives dense inhibitory input from striatal afferents (Partanen & Achim, 2022b; F. M. Zhou & Lee, 2011). CB1Rs in this region are known to exert precise, subcellular-specific effects, particularly at striatonigral terminals (Soria-Gomez et al., 2021), and may not broadly influence astrocytic metabolism in the same way as in other brain regions. Additionally, given the role of SNr as a downstream integrator of basal ganglia output (Lai et al., 2020; Rocha et al., 2023), its metabolic demands may be more constant, and less directly coupled to behavioural state transitions like immobility.

The absence of significant lactate modulation by Δ^9-THC in the SNr reinforces the idea that the impact of CB1R activation on brain metabolism is not homogeneous. Instead, it appears to be shaped by the specific cellular architecture, functional role, and CB1R distribution of each region. While hippocampal lactate dynamics are clearly sensitive to both locomotor state and cannabinoid signalling, the striatum shows a more behaviourally driven pattern, and the SNr appears largely resistant to both. These brain region-specific outcomes highlight the importance of investigating neurometabolic regulation within the context of local circuit function. They also suggest that cannabinoids may affect brain energy metabolism in a highly selective manner, with distinct consequences depending on the target region and behavioural context. However, these findings should be interpreted with caution, as they require replication in additional experimental cohorts to confirm their robustness. Additionally, it would be valuable to explore alternative analysis approaches. In the current study, our analysis focused on the first 180 seconds of immobility, compared to the 15 seconds immediately preceding it. However, it would be interesting to examine how the results change when comparing the final phase of

immobility to the period immediately after, when mice resume movement. This could provide further insight into how lactate dynamics evolve not only during transitions into inactivity but also during the return to an active state.

Chapter III. Contribution of lactate to the locomotor effects of cannabinoids.

One of the best-established effects of cannabinoids in rodents is the induction of a behavioural profile characterized by hypolocomotion, hypothermia, catalepsy, and antinociception, commonly referred to as the "tetrad" assay (Metna-Laurent et al., 2017; Stella, 2023). These effects are primarily mediated by CB1Rs and have long served as a reliable readout of cannabinoid activity *in vivo*. In this context, and by considering the emerging role of astrocyte-derived lactate as a neuromodulatory signal involved in various brain functions (Magistretti & Allaman, 2018), along with our findings showing that lactate dynamics vary with activity state, we asked whether systemic lactate administration could modulate this cannabinoid-induced behavioural profile, particularly its effects on locomotion.

To test this, we evaluated whether a systemic lactate injection could rescue the behavioural deficits induced by Δ^9-THC in the tetrad assay. Mice received an injection of Δ^9-THC (10 mg/kg, I.P.), followed five minutes later an injection of either saline or lactate (1 g/kg, I.P.), and their behaviour responses were tested one hour later. As expected, Δ^9-THC plus saline treatments robustly induced all four behavioural features of the tetrad. However, lactate treatment had no detectable impact on locomotor suppression, catalepsy, hypothermia, and antinociception. These results indicate that, at least under these specific experimental conditions, exogenous lactate does not reverse or modulate these acute behavioural effects of cannabinoids.

This finding suggests that the influence of lactate on behavioural outputs may be only related to cognitive processes. While lactate may serve as a crucial metabolic signal in circuits involved in cognitive function, particularly in the hippocampus, it may not be directly linked to other brain functions like nociception or motor control, and its exogenous delivery is therefore not sufficient to counteract the widespread neurophysiological effects of a high-dose CB1R activation. The behaviours assessed in the tetrad are primarily driven by alterations in neurotransmission across different circuits, including cortical, striatal, and brainstem areas (Hempel & Xi, 2021b; Metna-Laurent et al., 2017). CB1Rs at these sites acutely suppress synaptic activity and network excitability, and this effect may simply overpower any modulatory input from lactate under these systemic conditions.

It is also worth considering that the mode and timing of lactate delivery may play a critical role. Future experiments should explore different time points for lactate injection to determine whether more precise temporal alignment alters behavioural outcomes of Δ^9-THC exposure. In addition, systemic administration likely results in widespread, non-targeted elevation of lactate, lacking the spatial or temporal specificity of endogenous astrocyte-derived signalling. Alternatively, the neuromodulatory effects of lactate may depend on being locally produced and tightly coupled to neuronal activity patterns, conditions that are not replicated by a systemic I.P. injection.

In future experiments, it may be interesting to deliver lactate locally into specific brain regions, given the brain region-dependent differences in lactate dynamics observed in Chapter II. Although an initial attempt using intracerebroventricular injection was unsuccessful, follow-up experiments using implanted cannulas for region-specific lactate delivery, such as into the SNr or striatum, could provide clearer insights into the potential spatial specificity of lactate treatments and their impact on cannabinoid-induced behaviours.

Chapter IV. Exploration of the molecular mechanisms underlying CB1R-dependent lactate modulation in cultured astrocytes.

In this final part of the study, we investigated the intracellular signalling pathways underlying CB1R-mediated regulation of lactate production in astrocytes. This work builds on earlier findings from our group, which demonstrated that mtCB1Rs reduces lactate production and release with prolonged activation (Jimenez-Blasco et al., 2020), while transient stimulation of astroglial CB1Rs increases lactate production and release (Fernández-Moncada, Lavanco, et al., 2024). The goal of this chapter was to further clarify the temporal dynamics of these opposing effects and to explore the molecular mechanisms driving this switch.

We first replicated the observation that persistent CB1R activation suppress the lactate metabolism, however and surprisingly, this effect emerged much earlier than previously reported. While earlier studies described this effect at 24 hours post-stimulation (Jimenez-Blasco et al., 2020), our more recent data show that a significant reduction in lactate levels can already be observed within the first hour of exposure to the CB1R agonist WIN55 (Fernández-Moncada, Lavanco, et al., 2024). This suggests that the metabolic shift induced by CB1R activation occurs rapidly and may play a more immediate role in reshaping astrocytic support of neuronal energy demands.

In parallel, we examined the role of PKC, a key downstream effector in several CB1R signalling pathways and implicated in the short-term synaptic effects of cannabinoids (Busquets-Garcia et al., 2018). Using the broad PKC inhibitor Go 6983, we found that blocking PKC activity abolished both the transient lactate increase and the later persistent decrease induced by WIN55. These findings identify PKC as a crucial mediator of CB1R-dependent lactate regulation in astrocytes and suggest that PKC may be involved in coordinating the signalling switch between early and late metabolic responses. Interestingly, PKC inhibition not only blocked the WIN55-induced decrease in lactate levels observed after ~ 1 hour but also appeared to induce a progressive increase in lactate over time. This was an unexpected result and raised the possibility that disrupting PKC signalling during CB1R activation may unmask an alternative or compensatory pathway leading to lactate accumulation. We also considered that the combined pharmacological stress of WIN55 and PKC inhibition induces a state of cellular distress, which could itself contribute to altered lactate dynamics. To determine whether PKC inhibition alone could explain this effect, we conducted control experiments applying Go 6983 in the absence of WIN55. Preliminary data from these experiments suggest that PKC inhibition by itself does not alter baseline lactate levels. However, due to technical problems with the microscope during this stage, we were unable to collect sufficient data for proper quantification and statistical analysis. Thus, while the available traces show no clear change, we cannot yet draw firm conclusions about the effects of PKC inhibition alone.

Taken together, these findings support a model in which CB1R activation dynamically regulates astrocytic lactate production through a PKC-dependent mechanism. PKC appears to act as a key switch: it is necessary for the transient increase in lactate following brief CB1R activation, and also for the later suppression of lactate associated with sustained stimulation. Since the transient lactate increase is independent of mtCB1Rs, while the persistent decrease relies on this subcellular pool, this suggests that distinct PKC isoforms (Battaini, 2001; Newton, 2018), and/or PKC activity in different subcellular compartments, may mediate these opposing effects. Future studies using isoform-specific or compartment-targeted PKC inhibitors could help disentangle the roles of individual PKC variants in regulating lactate dynamics downstream of CB1R activation.

These *in vitro* results also offer potential insight into our *in vivo* findings. The lack of a robust lactate response to Δ^9-THC in freely moving mice may reflect a complex integration of cell-type-specific, time-dependent, and pathway-specific effects that are difficult to resolve using bulk measurement techniques like FP. The temporal sensitivity of CB1R-PKC signalling may

also contribute to the regional and behavioural specificity of lactate dynamics observed in earlier chapters.

Future studies should aim to clarify the mechanistic role of PKC in this process, potentially through isoform-specific inhibition or genetic knockdown, and explore how PKC interacts with key metabolic components such as glycolytic enzymes, lactate transporters, or mitochondrial regulators.

Overall, our study establishes, for the first time, a robust framework for monitoring brain lactate dynamics in freely moving mice. Beyond the technical advance, it sheds light on how CB1Rs modulate lactate metabolism and locomotor behaviour in a dynamic, brain region-specific, and time-dependent manner. In the hippocampus, Δ^9-THC disrupts the typical link between behavioural state and lactate levels, triggering a transient increase in lactate even during inactivity. In contrast, the striatum and SNr show minimal or no response, underscoring regional differences in how brain metabolism responds to cannabinoids. Importantly, systemic delivery of lactate does not appear to modulate acute behavioural triggered by Δ^9-THC exposure, suggesting its role may be more circuit-specific and dependent on precise timing and localization.

At the molecular level, we identified PKC as a central mediator of CB1R-dependent lactate regulation in astrocytes, controlling both the transient rise and persistent suppression of lactate production and release. This mechanism may underlie some of the temporal complexity seen *in vivo*, and future work should clarify how it operates across brain regions and behavioural states.

This thesis provides a new insight into how cannabinoid signalling intersects with brain energy metabolism. It highlights lactate not only as a metabolic substrate but also as a dynamically regulated signal - one that may bridge astrocytic function, neuronal activity, and behaviour in a region - and context-specific manner.

REFERENCES

Aalling, N. N., Nedergaard, M., & DiNuzzo, M. (2018). Cerebral metabolic changes during sleep. *Current Neurology and Neuroscience Reports*, *18*(9), 57. https://doi.org/10.1007/S11910-018-0868-9

Abbott, N. J. (2013). Blood-brain barrier structure and function and the challenges for CNS drug delivery. *Journal of Inherited Metabolic Disease*, *36*(3), 437–449. https://doi.org/10.1007/S10545-013-9608-0

Abbott, N. J., Patabendige, A. A. K., Dolman, D. E. M., Yusof, S. R., & Begley, D. J. (2010). Structure and function of the blood-brain barrier. *Neurobiology of Disease*, *37*(1), 13–25. https://doi.org/10.1016/J.NBD.2009.07.030

Adel, Y., & Alexander, S. P. H. (2021). Neuromolecular Mechanisms of Cannabis Action. In *Advances in Experimental Medicine and Biology* (Vol. 1264, pp. 15–28). Springer. https://doi.org/10.1007/978-3-030-57369-0_2

Afridi, R., Rahman, M. H., & Suk, K. (2022). Implications of glial metabolic dysregulation in the pathophysiology of neurodegenerative diseases. *Neurobiology of Disease*, *174*. https://doi.org/10.1016/J.NBD.2022.105874

Agurell, S., Halldin, M., Lindgren, J. E., Ohlsson, A., Widman, M., Gillespie, H., & Hollister, L. (1986). Pharmacokinetics and metabolism of delta 1-tetrahydrocannabinol and other cannabinoids with emphasis on man. *Pharmacological Reviews*, *38*(1).

Akther, S., & Hirase, H. (2022). Assessment of astrocytes as a mediator of memory and learning in rodents. *Glia*, *70*(8), 1484–1505. https://doi.org/10.1002/GLIA.24099

Alahmari, A. (2021). Blood-Brain Barrier Overview: Structural and Functional Correlation. *Neural Plasticity*, *2021*, 6564585. https://doi.org/10.1155/2021/6564585

Albaik, M., Sheikh Saleh, D., Kauther, D., Mohammed, H., Alfarra, S., Alghamdi, A., Ghaboura, N., & Sindi, I. A. (2024). Bridging the gap: glucose transporters, Alzheimer's, and future therapeutic prospects. *Frontiers in Cell and Developmental Biology*, *12*, 1344039. https://doi.org/10.3389/FCELL.2024.1344039/XML/NLM

Alberini, C. M., Cruz, E., Descalzi, G., Bessières, B., & Gao, V. (2017). Astrocyte glycogen and lactate: new insights into learning and memory mechanisms. *Glia*, *66*(6), 1244. https://doi.org/10.1002/GLIA.23250

Allen, M., Huang, B. S., Notaras, M. J., Lodhi, A., Barrio-Alonso, E., Lituma, P. J., Wolujewicz, P., Witztum, J., Longo, F., Chen, M., Greening, D. W., Klann, E., Ross, M. E., Liston, C., & Colak, D. (2022). Astrocytes derived from ASD individuals alter behavior and destabilize neuronal activity through aberrant Ca2+ signaling. *Molecular Psychiatry 2022 27:5*, *27*(5), 2470–2484. https://doi.org/10.1038/s41380-022-01486-x

Almeida, A., Moncada, S., & Bolaños, J. P. (2004). Nitric oxide switches on glycolysis through the AMP protein kinase and 6-phosphofructo-2-kinase pathway. *Nature Cell Biology*, *6*(1), 45–51. https://doi.org/10.1038/NCB1080

Andersen, J. V. (2025). The Glutamate/GABA-Glutamine Cycle: Insights, Updates, and Advances. *Journal of Neurochemistry*, *169*(3), e70029. https://doi.org/10.1111/JNC.70029

Andersen, J. V., Schousboe, A., & Wellendorph, P. (2023). Astrocytes regulate inhibitory neurotransmission through GABA uptake, metabolism, and recycling. *Essays in Biochemistry*, *67*(1), 77–91. https://doi.org/10.1042/EBC20220208

Ando, Y., Okada, H., Takemura, G., Suzuki, K., Takada, C., Tomita, H., Zaikokuji, R., Hotta, Y., Miyazaki, N., Yano, H., Muraki, I., Kuroda, A., Fukuda, H., Kawasaki, Y., Okamoto, H., Kawaguchi, T., Watanabe, T., Doi, T., Yoshida, T., … Ogura, S. (2018). Brain-Specific Ultrastructure of Capillary Endothelial Glycocalyx and Its Possible Contribution for Blood Brain Barrier. *Scientific Reports*, *8*(1). https://doi.org/10.1038/S41598-018-35976-2

Araque, A., Carmignoto, G., Haydon, P. G., Oliet, S. H. R., Robitaille, R., & Volterra, A. (2014). Gliotransmitters travel in time and space. *Neuron*, *81*(4), 728–739. https://doi.org/10.1016/J.NEURON.2014.02.007

Araque, A., Parpura, V., Sanzgiri, R. P., & Haydon, P. G. (1999). Tripartite synapses: glia, the unacknowledged partner. *Trends in Neurosciences*, *22*(5), 208–215. https://doi.org/10.1016/S0166-2236(98)01349-6

Arnold, P. K., & Finley, L. W. S. (2023). Regulation and function of the mammalian tricarboxylic acid cycle. *Journal of Biological Chemistry*, *299*(2), 102838. https://doi.org/10.1016/J.JBC.2022.102838

Ashton, C. H. (2001). Pharmacology and effects of cannabis: A brief review. In *British Journal of Psychiatry* (Vol. 178, Issue FEB., pp. 101–106). Br J Psychiatry. https://doi.org/10.1192/bjp.178.2.101

Aslam, M., & Ladilov, Y. (2023). Editorial: Advances in cAMP signaling research: basic and translational aspects. *Frontiers in Physiology*, *14*, 1266718. https://doi.org/10.3389/FPHYS.2023.1266718

Attwell, D., Buchan, A. M., Charpak, S., Lauritzen, M., MacVicar, B. A., & Newman, E. A. (2010). Glial and neuronal control of brain blood flow. *Nature*, *468*(7321), 232–243. https://doi.org/10.1038/NATURE09613

Atwood, B. K., & MacKie, K. (2010). CB 2: A cannabinoid receptor with an identity crisis. In *British Journal of Pharmacology*. https://doi.org/10.1111/j.1476-5381.2010.00729.x

Augustin, S. M., & Lovinger, D. M. (2018). Functional Relevance of Endocannabinoid-Dependent Synaptic Plasticity in the Central Nervous System. *ACS Chemical Neuroscience*, *9*(9), 2146. https://doi.org/10.1021/ACSCHEMNEURO.7B00508

Bacci, A., Huguenard, J. R., & Prince, D. A. (2004). Long-lasting self-inhibition of neocortical interneurons mediated by endocannabinoids. *Nature*, *431*(7006), 312–316. https://doi.org/10.1038/nature02913

Bai, W., & Zhou, Y. G. (2017). Homeostasis of the Intraparenchymal-Blood Glutamate Concentration Gradient: Maintenance, Imbalance, and Regulation. *Frontiers in Molecular Neuroscience*, *10*. https://doi.org/10.3389/FNMOL.2017.00400

Bak, L. K., Schousboe, A., & Waagepetersen, H. S. (2006). The glutamate/GABA-glutamine cycle: aspects of transport, neurotransmitter homeostasis and ammonia transfer. *Journal of Neurochemistry*, *98*(3), 641–653. https://doi.org/10.1111/J.1471-4159.2006.03913.X

Baker, D., Pryce, G., Giovannoni, G., & Thompson, A. J. (2003). The therapeutic potential of cannabis. In *Lancet Neurology* (Vol. 2, Issue 5, pp. 291–298). Lancet Neurol. https://doi.org/10.1016/S1474-4422(03)00381-8

Barros, L. F. (2022). How expensive is the astrocyte? *Journal of Cerebral Blood Flow & Metabolism*, *42*(5), 738. https://doi.org/10.1177/0271678X221077343

Barros, L. F., Bittner, C. X., Loaiza, A., & Porras, O. H. (2007). A quantitative overview of glucose dynamics in the gliovascular unit. *Glia*, *55*(12), 1222–1237. https://doi.org/10.1002/GLIA.20375

Barros, L. F., & Deitmer, J. W. (2010). Glucose and lactate supply to the synapse. *Brain Research Reviews*, *63*(1–2), 149–159. https://doi.org/10.1016/J.BRAINRESREV.2009.10.002

Barros, L. F., Ruminot, I., San Martín, A., Lerchundi, R., Fernández-Moncada, I., & Baeza-Lehnert, F. (2021). Aerobic Glycolysis in the Brain: Warburg and Crabtree Contra Pasteur. *Neurochemical Research*, *46*(1), 15–22. https://doi.org/10.1007/S11064-020-02964-W

Barros, L. F., San Martín, A., Ruminot, I., Sandoval, P. Y., Fernández-Moncada, I., Baeza-Lehnert, F., Arce-Molina, R., Contreras-Baeza, Y., Cortés-Molina, F., Galaz, A., & Alegría, K. (2017). Near-critical GLUT1 and Neurodegeneration. *Journal of Neuroscience Research*, *95*(11), 2267–2274. https://doi.org/10.1002/JNR.23998

Barros, L. F., & Weber, B. (2018). CrossTalk proposal: an important astrocyte-to-neuron lactate shuttle couples neuronal activity to glucose utilisation in the brain. *The Journal of Physiology*, *596*(3), 347–350. https://doi.org/10.1113/JP274944

Battaini, F. (2001). Protein kinase C isoforms as therapeutic targets in nervous system disease states. *Pharmacological Research*, *44*(5), 353–361. https://doi.org/10.1006/PHRS.2001.0893

Battista, N., Tommaso, M. Di, Bari, M., & Maccarrone, M. (2012). The endocannabinoid system: An overview. *Frontiers in Behavioral Neuroscience*, *6*(FEBRUARY 2012). https://doi.org/10.3389/fnbeh.2012.00009

Bélanger, M., Allaman, I., & Magistretti, P. J. (2011). Brain energy metabolism: focus on astrocyte-neuron metabolic cooperation. *Cell Metabolism*, *14*(6), 724–738. https://doi.org/10.1016/J.CMET.2011.08.016

Bellocchio, L., Lafentre, P., Cannich, A., Cota, D., Puente, N., Grandes, P., Chaouloff, F., Piazza, P. V., & Marsicano, G. (2010). Bimodal control of stimulated food intake by the endocannabinoid system. *Nature Neuroscience 2010 13:3*, *13*(3), 281–283. https://doi.org/10.1038/NN.2494

Bellot-Saez, A., Kékesi, O., Morley, J. W., & Buskila, Y. (2017). Astrocytic modulation of neuronal excitability through K+ spatial buffering. *Neuroscience and Biobehavioral Reviews*, *77*, 87–97. https://doi.org/10.1016/J.NEUBIOREV.2017.03.002

Bénard, G., Massa, F., Puente, N., Lourenço, J., Bellocchio, L., Soria-Gómez, E., Matias, I., Delamarre, A., Metna-Laurent, M., Cannich, A., Hebert-Chatelain, E., Mulle, C., Ortega-Gutiérrez, S., Martín-Fontecha, M., Klugmann, M., Guggenhuber, S., Lutz, B., Gertsch, J., Chaouloff, F., … Marsicano, G. (2012). Mitochondrial CB1 receptors regulate neuronal energy metabolism. *Nature Neuroscience 2012 15:4*, *15*(4), 558–564. https://doi.org/10.1038/nn.3053

Benarroch, E. E. (2014). Brain glucose transporters: implications for neurologic disease. *Neurology*, *82*(15), 1374–1379. https://doi.org/10.1212/WNL.0000000000000328

Bergersen, L. H. (2014). Lactate transport and signaling in the brain: potential therapeutic targets and roles in body–brain interaction. *Journal of Cerebral Blood Flow & Metabolism*, *35*(2), 176. https://doi.org/10.1038/JCBFM.2014.206

Bisogno, T., Berrendero, F., Ambrosino, G., Cebeira, M., Ramos, J. A., Fernandez-Ruiz, J. J., & Di Marzo, V. (1999). Brain Regional Distribution of Endocannabinoids: Implications for Their Biosynthesis and Biological Function. *Biochemical and Biophysical Research Communications*, *256*(2), 377–380. https://doi.org/10.1006/BBRC.1999.0254

Bisogno, T., Hanuš, L., De Petrocellis, L., Tchilibon, S., Ponde, D. E., Brandi, I., Moriello, A. S., Davis, J. B., Mechoulam, R., & Di Marzo, V. (2001). Molecular targets for cannabidiol and its synthetic analogues: effect on vanilloid VR1 receptors and on the cellular uptake and enzymatic hydrolysis of anandamide. *British Journal of Pharmacology*, *134*(4), 845–852. https://doi.org/10.1038/SJ.BJP.0704327

Bisogno, T., Howell, F., Williams, G., Minassi, A., Cascio, M. G., Ligresti, A., Matias, I., Schiano-Moriello, A., Paul, P., Williams, E. J., Gangadbaran, U., Hobbs, C., Di Marzo, V., & Doherty, P. (2003). Cloning of the first sn1-DAG lipases points to the spatial and temporal regulation of endocannabinoid signaling in the brain. *Journal of Cell Biology*, *163*(3), 463–468. https://doi.org/10.1083/jcb.200305129

Bisogno, T., Melck, D., Bobrov, M. Y., Gretskaya, N. M., Bezuglov, V. V., De Petrocellis, L., & Di Marzo, V. (2000). N-acyl-dopamines: novel synthetic CB(1) cannabinoid-receptor ligands and inhibitors of anandamide inactivation with cannabimimetic activity in vitro

and in vivo. *Biochemical Journal*, *351*(Pt 3), 817. https://doi.org/10.1042/0264-6021:3510817

Blankman, J. L., Simon, G. M., & Cravatt, B. F. (2007). A Comprehensive Profile of Brain Enzymes that Hydrolyze the Endocannabinoid 2-Arachidonoylglycerol. *Chemistry and Biology*, *14*(12), 1347–1356. https://doi.org/10.1016/j.chembiol.2007.11.006

Blázquez, C., Chiarlone, A., Bellocchio, L., Resel, E., Pruunsild, P., García-Rincón, D., Sendtner, M., Timmusk, T., Lutz, B., Galve-Roperh, I., & Guzmán, M. (2015). The CB_1 cannabinoid receptor signals striatal neuroprotection via a PI3K/Akt/mTORC1/BDNF pathway. *Cell Death and Differentiation*, *22*(10), 1618–1629. https://doi.org/10.1038/CDD.2015.11

Blebea, N. M., Pricopie, A. I., Vlad, R. A., & Hancu, G. (2024). Phytocannabinoids: Exploring Pharmacological Profiles and Their Impact on Therapeutical Use. *International Journal of Molecular Sciences*, *25*(8), 4204. https://doi.org/10.3390/IJMS25084204

Boado, R. J., Wu, D., & Windisch, M. (1999). In vivo upregulation of the blood–brain barrier GLUT1 glucose transporter by brain-derived peptides. *Neuroscience Research*, *34*(4), 217–224. https://doi.org/10.1016/S0168-0102(99)00056-5

Boczek, T., & Zylinska, L. (2021). Receptor-Dependent and Independent Regulation of Voltage-Gated Ca2+ Channels and Ca2+-Permeable Channels by Endocannabinoids in the Brain. *International Journal of Molecular Sciences*, *22*(15), 8168. https://doi.org/10.3390/IJMS22158168

Bodor, Á. L., Katona, I., Nyíri, G., Mackie, K., Ledent, C., Hájos, N., & Freund, T. F. (2005). Endocannabinoid signaling in rat somatosensory cortex: Laminar differences and involvement of specific interneuron types. *Journal of Neuroscience*, *25*(29), 6845–6856. https://doi.org/10.1523/JNEUROSCI.0442-05.2005

Bolaños, J. P., Almeida, A., & Moncada, S. (2010). Glycolysis: a bioenergetic or a survival pathway? *Trends in Biochemical Sciences*, *35*(3), 145–149. https://doi.org/10.1016/J.TIBS.2009.10.006

Bonvento, G., & Bolaños, J. P. (2021). Astrocyte-neuron metabolic cooperation shapes brain activity. *Cell Metabolism*, *33*(8), 1546–1564. https://doi.org/10.1016/J.CMET.2021.07.006

Bouzier-Sore, A. K., Voisin, P., Bouchaud, V., Bezancon, E., Franconi, J. M., & Pellerin, L. (2006). Competition between glucose and lactate as oxidative energy substrates in both neurons and astrocytes: a comparative NMR study. *The European Journal of Neuroscience*, *24*(6), 1687–1694. https://doi.org/10.1111/J.1460-9568.2006.05056.X

Brazhe, A., Verisokin, A., Verveyko, D., & Postnov, D. (2023). Astrocytes: new evidence, new models, new roles. *Biophysical Reviews*, *15*(5), 1303. https://doi.org/10.1007/S12551-023-01145-7

Brooks, G. A. (2009). Cell–cell and intracellular lactate shuttles. *The Journal of Physiology*, *587*(Pt 23), 5591. https://doi.org/10.1113/JPHYSIOL.2009.178350

Brooks, G. A. (2018). The Science and Translation of Lactate Shuttle Theory. *Cell Metabolism*, *27*(4), 757–785. https://doi.org/10.1016/J.CMET.2018.03.008

Brownlee, N. N. M., Wilson, F. C., Curran, D. B., Lyttle, N., & McCann, J. P. (2020). Neurocognitive outcomes in adults following cerebral hypoxia: A systematic literature review. *NeuroRehabilitation*, *47*(2), 83–97. https://doi.org/10.3233/NRE-203135

Bugiani, M., Plug, B. C., Man, J. H. K., Breur, M., & van der Knaap, M. S. (2021). Heterogeneity of white matter astrocytes in the human brain. *Acta Neuropathologica 2021 143:2*, *143*(2), 159–177. https://doi.org/10.1007/S00401-021-02391-3

Bullmore, E., & Sporns, O. (2012). The economy of brain network organization. *Nature Reviews. Neuroscience*, *13*(5), 336–349. https://doi.org/10.1038/NRN3214

Busquets-Garcia, A., Bains, J., & Marsicano, G. (2017). CB1 Receptor Signaling in the Brain: Extracting Specificity from Ubiquity. *Neuropsychopharmacology 2018 43:1*, *43*(1), 4–20. https://doi.org/10.1038/npp.2017.206

Busquets-García, A., Bolaños, J. P., & Marsicano, G. (2022). Metabolic Messengers: endocannabinoids. *Nature Metabolism 2022 4:7*, *4*(7), 848–855. https://doi.org/10.1038/S42255-022-00600-1

Busquets-Garcia, A., Gomis-González, M., Salgado-Mendialduá, V., Galera-López, L., Puighermanal, E., Martín-Garcia, E., Maldonado, R., & Ozaita, A. (2018). Hippocampal Protein Kinase C Signaling Mediates the Short-Term Memory Impairment Induced by Delta9-Tetrahydrocannabinol. *Neuropsychopharmacology : Official Publication of the*

American College of Neuropsychopharmacology, *43*(5), 1021–1031. https://doi.org/10.1038/NPP.2017.175

Busquets-Garcia, A., Gomis-González, M., Srivastava, R. K., Cutando, L., Ortega-Alvaro, A., Ruehle, S., Remmers, F., Bindila, L., Bellocchio, L., Marsicano, G., Lutz, B., Maldonado, R., & Ozaita, A. (2016). Peripheral and central CB1 cannabinoid receptors control stress-induced impairment of memory consolidation. *Proceedings of the National Academy of Sciences of the United States of America*, *113*(35), 9904–9909. https://doi.org/10.1073/pnas.1525066113

Caicedo, D. A., Pérez-Mañá, C., Farré, M., & Papaseit, E. (2025). An Overview of the Potential for Pharmacokinetic Interactions Between Drugs and Cannabis Products in Humans. *Pharmaceutics 2025, Vol. 17, Page 319*, *17*(3), 319. https://doi.org/10.3390/PHARMACEUTICS17030319

Campolongo, P., & Trezza, V. (2012). The endocannabinoid system: a key modulator of emotions and cognition. *Frontiers in Behavioral Neuroscience*, *6*(OCTOBER 2012), 73. https://doi.org/10.3389/FNBEH.2012.00073

Caporale, A., Lee, H., Lei, H., Rao, H., Langham, M. C., Detre, J. A., Wu, P. H., & Wehrli, F. W. (2021). Cerebral metabolic rate of oxygen during transition from wakefulness to sleep measured with high temporal resolution OxFlow MRI with concurrent EEG. *Journal of Cerebral Blood Flow and Metabolism*, *41*(4), 780–792. https://doi.org/10.1177/0271678X20919287/SUPPL_FILE/SJ-PDF-1-JCB-10.1177_0271678X20919287.PDF

Chandel, N. S. (2021). Amino Acid Metabolism. *Cold Spring Harbor Perspectives in Biology*, *13*(4), a040584. https://doi.org/10.1101/CSHPERSPECT.A040584

Chatton, J. Y., Magistretti, P. J., & Barros, L. F. (2016). Sodium signaling and astrocyte energy metabolism. *Glia*, *64*(10), 1667–1676. https://doi.org/10.1002/GLIA.22971

Chayasirisobhon, S. (2020). Mechanisms of Action and Pharmacokinetics of Cannabis. *The Permanente Journal*, *25*(1), 19.200. https://doi.org/10.7812/TPP/19.200

Cheong, E., & Lee, C. J. (2025). Gliotransmission in physiologic and pathologic conditions. *Handbook of Clinical Neurology*, *209*, 93–116. https://doi.org/10.1016/B978-0-443-19104-6.00003-6

Chevaleyre, V., & Castillo, P. E. (2003). Heterosynaptic LTD of hippocampal GABAergic synapses: A novel role of endocannabinoids in regulating excitability. *Neuron*, *38*(3), 461–472. https://doi.org/10.1016/S0896-6273(03)00235-6

Chuquet, J., Quilichini, P., Nimchinsky, E. A., & Buzsáki, G. (2010). Predominant enhancement of glucose uptake in astrocytes versus neurons during activation of the somatosensory cortex. *The Journal of Neuroscience : The Official Journal of the Society for Neuroscience*, *30*(45), 15298–15303. https://doi.org/10.1523/JNEUROSCI.0762-10.2010

Clarke, D. D., & Sokoloff, L. (1999). *Substrates of Cerebral Metabolism*. https://www.ncbi.nlm.nih.gov/books/NBK28048/

Cohen-Salmon, M., Guille, N., & Boulay, A. C. (2025). Development of perivascular astrocyte processes. *Frontiers in Neuroscience*, *19*, 1585340. https://doi.org/10.3389/FNINS.2025.1585340

Covelo, A., & Araque, A. (2016). Lateral regulation of synaptic transmission by astrocytes. *Neuroscience*, *323*, 62–66. https://doi.org/10.1016/j.neuroscience.2015.02.036

Covelo, A., & Araque, A. (2018). Neuronal activity determines distinct gliotransmitter release from a single astrocyte. *ELife*, *7*. https://doi.org/10.7554/ELIFE.32237

Covelo, A., Eraso-Pichot, A., Fernández-Moncada, I., Serrat, R., & Marsicano, G. (2021). CB1R-dependent regulation of astrocyte physiology and astrocyte-neuron interactions. *Neuropharmacology*, *195*, 108678. https://doi.org/10.1016/J.NEUROPHARM.2021.108678

Crane, N. A., Schuster, R. M., Fusar-Poli, P., & Gonzalez, R. (2013). Effects of cannabis on neurocognitive functioning: Recent advances, neurodevelopmental influences, and sex differences. In *Neuropsychology Review* (Vol. 23, Issue 2, pp. 117–137). Neuropsychol Rev. https://doi.org/10.1007/s11065-012-9222-1

Cravatt, B. F., Giang, D. K., Mayfield, S. P., Boger, D. L., Lerner, R. A., & Gilula, N. B. (1996). Molecular characterization of an enzyme that degrades neuromodulatory fatty-acid amides. *Nature*, *384*(6604), 83–87. https://doi.org/10.1038/384083a0

Crippa, J. A., Guimarães, F. S., Campos, A. C., & Zuardi, A. W. (2018). Translational Investigation of the Therapeutic Potential of Cannabidiol (CBD): Toward a New Age. *Frontiers in Immunology*, *9*(SEP). https://doi.org/10.3389/FIMMU.2018.02009

Cryer, P. E. (2007). Hypoglycemia, functional brain failure, and brain death. *The Journal of Clinical Investigation*, *117*(4), 868–870. https://doi.org/10.1172/JCI31669

Daneman, R., & Prat, A. (2015). The blood-brain barrier. *Cold Spring Harbor Perspectives in Biology*, *7*(1). https://doi.org/10.1101/CSHPERSPECT.A020412

Dasilva, M. A., Grieve, K. L., Cudeiro, J., & Rivadulla, C. (2012). Endocannabinoid CB1 receptors modulate visual output from the thalamus. *Psychopharmacology*, *219*(3), 835–845. https://doi.org/10.1007/S00213-011-2412-3

de Ceglia, R., Ledonne, A., Litvin, D. G., Lind, B. L., Carriero, G., Latagliata, E. C., Bindocci, E., Di Castro, M. A., Savtchouk, I., Vitali, I., Ranjak, A., Congiu, M., Canonica, T., Wisden, W., Harris, K., Mameli, M., Mercuri, N., Telley, L., & Volterra, A. (2023). Specialized astrocytes mediate glutamatergic gliotransmission in the CNS. *Nature 2023 622:7981*, *622*(7981), 120–129. https://doi.org/10.1038/s41586-023-06502-w

De Oliveira Alvares, L., Genro, B. P., Diehl, F., & Quillfeldt, J. A. (2008). Differential role of the hippocampal endocannabinoid system in the memory consolidation and retrieval mechanisms. *Neurobiology of Learning and Memory*, *90*(1), 1–9. https://doi.org/10.1016/J.NLM.2008.01.009

De Vivo, D. C., Trifiletti, R. R., Jacobson, R. I., Ronen, G. M., Behmand, R. A., & Harik, S. I. (1991). Defective glucose transport across the blood-brain barrier as a cause of persistent hypoglycorrhachia, seizures, and developmental delay. *The New England Journal of Medicine*, *325*(10), 703–709. https://doi.org/10.1056/NEJM199109053251006

Descalzi, G., Gao, V., Steinman, M. Q., Suzuki, A., & Alberini, C. M. (2019). Lactate from astrocytes fuels learning-induced mRNA translation in excitatory and inhibitory neurons. *Communications Biology*, *2*(1). https://doi.org/10.1038/S42003-019-0495-2

Devane, W. A., Hanuš, L., Breuer, A., Pertwee, R. G., Stevenson, L. A., Griffin, G., Gibson, D., Mandelbaum, A., Etinger, A., & Mechoulam, R. (1992). Isolation and structure of a brain constituent that binds to the cannabinoid receptor. *Science (New York, N.Y.)*, *258*(5090), 1946–1949. https://doi.org/10.1126/SCIENCE.1470919

Devraj, K., Klinger, M. E., Myers, R. L., Mokashi, A., Hawkins, R. A., & Simpson, I. A. (2011). GLUT-1 GLUCOSE TRANSPORTERS IN THE BLOOD-BRAIN BARRIER: DIFFERENTIAL PHOSPHORYLATION. *Journal of Neuroscience Research*, *89*(12), 10.1002/jnr.22738. https://doi.org/10.1002/JNR.22738

Di Forti, M., Marconi, A., Carra, E., Fraietta, S., Trotta, A., Bonomo, M., Bianconi, F., Gardner-Sood, P., O'Connor, J., Russo, M., Stilo, S. A., Marques, T. R., Mondelli, V., Dazzan, P., Pariante, C., David, A. S., Gaughran, F., Atakan, Z., Iyegbe, C., … Murray, R. M. (2015). Proportion of patients in south London with first-episode psychosis attributable to use of high potency cannabis: A case-control study. *The Lancet Psychiatry*, *2*(3), 233–238. https://doi.org/10.1016/S2215-0366(14)00117-5

Di Marzo, V., Melck, D., Bisogno, T., & De Petrocellis, L. (1998). Endocannabinoids: Endogenous cannabinoid receptor ligands with neuromodulatory action. In *Trends in Neurosciences* (Vol. 21, Issue 12, pp. 521–528). Elsevier Ltd. https://doi.org/10.1016/S0166-2236(98)01283-1

Díaz-García, C. M., Mongeon, R., Lahmann, C., Koveal, D., Zucker, H., & Yellen, G. (2017). Neuronal Stimulation Triggers Neuronal Glycolysis and Not Lactate Uptake. *Cell Metabolism*, *26*(2), 361-374.e4. https://doi.org/10.1016/J.CMET.2017.06.021

Dienel, G. A. (2017). Lack of appropriate stoichiometry: Strong evidence against an energetically important astrocyte-neuron lactate shuttle in brain. *Journal of Neuroscience Research*, *95*(11), 2103–2125. https://doi.org/10.1002/JNR.24015

D'mbra, T. E., Estep, K. G., Bell, M. R., Eissenstat, M. A., Josef, K. A., Ward, S. J., Haycock, D. A., Baizman, E. R., Casiano, F. M., Beglin, N. C., Chippari, S. M., Grego, J. D., Kullnig, R. K., & Daley, G. T. (1992). Conformationally Restrained Analogues of Pravadoline: Nanomolar Potent, Enantioselective, (Aminoalkyl)indole Agonists of the Cannabinoid Receptor. *Journal of Medicinal Chemistry*, *35*(1), 124–135. https://doi.org/10.1021/jm00079a016

dos Santos, R. G., Hallak, J. E. C., & Crippa, J. A. S. (2021). Neuropharmacological Effects of the Main Phytocannabinoids: A Narrative Review. *Advances in Experimental Medicine and Biology*, *1264*, 29–45. https://doi.org/10.1007/978-3-030-57369-0_3

Doyle, J. P., Dougherty, J. D., Heiman, M., Schmidt, E. F., Stevens, T. R., Ma, G., Bupp, S., Shrestha, P., Shah, R. D., Doughty, M. L., Gong, S., Greengard, P., & Heintz, N. (2008).

Application of a translational profiling approach for the comparative analysis of CNS cell types. *Cell*, *135*(4), 749–762. https://doi.org/10.1016/J.CELL.2008.10.029

Duran, J., Saez, I., Gruart, A., Guinovart, J. J., & Delgado-García, J. M. (2013). Impairment in long-term memory formation and learning-dependent synaptic plasticity in mice lacking glycogen synthase in the brain. *Journal of Cerebral Blood Flow and Metabolism : Official Journal of the International Society of Cerebral Blood Flow and Metabolism*, *33*(4), 550–556. https://doi.org/10.1038/JCBFM.2012.200

Ebert, D., Haller, R. G., & Walton, M. E. (2003). Energy contribution of octanoate to intact rat brain metabolism measured by 13C nuclear magnetic resonance spectroscopy. *The Journal of Neuroscience : The Official Journal of the Society for Neuroscience*, *23*(13), 5928–5935. https://doi.org/10.1523/JNEUROSCI.23-13-05928.2003

Eggan, S. M., & Lewis, D. A. (2007). Immunocytochemical Distribution of the Cannabinoid CB1 Receptor in the Primate Neocortex: A Regional and Laminar Analysis. *Cerebral Cortex*, *17*(1), 175–191. https://doi.org/10.1093/CERCOR/BHJ136

Eid, T., Lee, T. S. W., Patrylo, P., & Zaveri, H. P. (2018). Astrocytes and Glutamine Synthetase in Epileptogenesis. *Journal of Neuroscience Research*, *97*(11), 1345. https://doi.org/10.1002/JNR.24267

Elphick, M. R., & Egertová, M. (2001). The neurobiology and evolution of cannabinoid signalling. In *Philosophical Transactions of the Royal Society B: Biological Sciences* (Vol. 356, Issue 1407, pp. 381–408). Royal Society. https://doi.org/10.1098/rstb.2000.0787

Eraso-Pichot, A., Brasó-Vives, M., Golbano, A., Menacho, C., Claro, E., Galea, E., & Masgrau, R. (2018). GSEA of mouse and human mitochondriomes reveals fatty acid oxidation in astrocytes. *Glia*, *66*(8), 1724–1735. https://doi.org/10.1002/GLIA.23330

Eraso-Pichot, A., Pouvreau, S., Olivera-Pinto, A., Gomez-Sotres, P., Skupio, U., & Marsicano, G. (2023). Endocannabinoid signaling in astrocytes. *Glia*, *71*(1), 44–59. https://doi.org/10.1002/GLIA.24246

Escalada, P., Ezkurdia, A., Ramírez, M. J., & Solas, M. (2024). Essential Role of Astrocytes in Learning and Memory. *International Journal of Molecular Sciences*, *25*(3), 1899. https://doi.org/10.3390/IJMS25031899

Fernández-Moncada, I., Lavanco, G., Fundazuri, U. B., Bollmohr, N., Mountadem, S., Dalla Tor, T., Hachaguer, P., Julio-Kalajzic, F., Gisquet, D., Serrat, R., Bellocchio, L., Cannich, A., Fortunato-Marsol, B., Nasu, Y., Campbell, R. E., Drago, F., Cannizzaro, C., Ferreira, G., Bouzier-Sore, A. K., … Marsicano, G. (2024). A lactate-dependent shift of glycolysis mediates synaptic and cognitive processes in male mice. *Nature Communications*, *15*(1). https://doi.org/10.1038/S41467-024-51008-2

Fernández-Moncada, I., & Marsicano, G. (2023). Astroglial CB1 receptors, energy metabolism, and gliotransmission: an integrated signaling system? *Essays in Biochemistry*, *67*(1), 49–61. https://doi.org/10.1042/EBC20220089

Fernández-Moncada, I., Rodrigues, R. S., Fundazuri, U. B., Bellocchio, L., & Marsicano, G. (2024). Type-1 cannabinoid receptors and their ever-expanding roles in brain energy processes. *Journal of Neurochemistry*, *168*(5), 693–703. https://doi.org/10.1111/JNC.15922

Fernie, A. R., Carrari, F., & Sweetlove, L. J. (2004). Respiratory metabolism: glycolysis, the TCA cycle and mitochondrial electron transport. *Current Opinion in Plant Biology*, *7*(3), 254–261. https://doi.org/10.1016/J.PBI.2004.03.007

Freedland, C. S., Whitlow, C. T., Miller, M. D., & Porrino, L. J. (2002). Dose-dependent effects of Delta9-tetrahydrocannabinol on rates of local cerebral glucose utilization in rat. *Synapse (New York, N.Y.)*, *45*(2), 134–142. https://doi.org/10.1002/SYN.10089

Furuya, S. (2008). An essential role for de novo biosynthesis of L-serine in CNS development. *Asia Pac J Clin Nutr*, *17*(S1), 312–315.

García-Rodríguez, D., & Giménez-Cassina, A. (2021). Ketone Bodies in the Brain Beyond Fuel Metabolism: From Excitability to Gene Expression and Cell Signaling. *Frontiers in Molecular Neuroscience*, *14*. https://doi.org/10.3389/FNMOL.2021.732120

Gerdeman, G. L., & Lovinger, D. M. (2003). Emerging roles for endocannabinoids in long-term synaptic plasticity. In *British Journal of Pharmacology* (Vol. 140, Issue 5, pp. 781–789). https://doi.org/10.1038/sj.bjp.0705466

Giaume, C., Naus, C. C., Sáez, J. C., & Leybaert, L. (2021). Glial Connexins and Pannexins in the Healthy and Diseased Brain. *Physiological Reviews*, *101*(1), 93–145. https://doi.org/10.1152/PHYSREV.00043.2018

Gibbs, M. E. (2016). Role of Glycogenolysis in Memory and Learning: Regulation by Noradrenaline, Serotonin and ATP. *Frontiers in Integrative Neuroscience*, *9*(JAN2016). https://doi.org/10.3389/FNINT.2015.00070

Gómez Del Pulgar, T., Velasco, G., & Guzmán, M. (2000). The CB1 cannabinoid receptor is coupled to the activation of protein kinase B/Akt. *Biochemical Journal*, *347*(2), 369–373. https://doi.org/10.1042/0264-6021:3470369

Gómez-Sotres, P., Skupio, U., Dalla Tor, T., Julio-Kalajzic, F., Cannich, A., Gisquet, D., Bonilla-Del Rio, I., Drago, F., Puente, N., Grandes, P., Bellocchio, L., Busquets-Garcia, A., Bains, J. S., & Marsicano, G. (2024). Olfactory bulb astrocytes link social transmission of stress to cognitive adaptation in male mice. *Nature Communications*, *15*(1). https://doi.org/10.1038/S41467-024-51416-4

Gorzkiewicz, A., & Szemraj, J. (2018). Brain endocannabinoid signaling exhibits remarkable complexity. *Brain Research Bulletin*, *142*, 33–46. https://doi.org/10.1016/J.BRAINRESBULL.2018.06.012

Gradisnik, L., & Velnar, T. (2023). Astrocytes in the central nervous system and their functions in health and disease: A review. *World Journal of Clinical Cases*, *11*(15), 3385. https://doi.org/10.12998/WJCC.V11.I15.3385

Guerra-Gomes, S., Sousa, N., Pinto, L., & Oliveira, J. F. (2018). Functional Roles of Astrocyte Calcium Elevations: From Synapses to Behavior. *Frontiers in Cellular Neuroscience*, *11*. https://doi.org/10.3389/FNCEL.2017.00427

Gutiérrez-Rodríguez, A., Bonilla-Del Río, I., Puente, N., Gómez-Urquijo, S. M., Fontaine, C. J., Egaña-Huguet, J., Elezgarai, I., Ruehle, S., Lutz, B., Robin, L. M., Soria-Gómez, E., Bellocchio, L., Padwal, J. D., van der Stelt, M., Mendizabal-Zubiaga, J., Reguero, L., Ramos, A., Gerrikagoitia, I., Marsicano, G., & Grandes, P. (2018). Localization of the cannabinoid type-1 receptor in subcellular astrocyte compartments of mutant mouse hippocampus. *Glia*, *66*(7), 1417–1431. https://doi.org/10.1002/GLIA.23314

Haber, R. S., Weinstein, S. P., O'Boyle, E., & Morgello, S. (1993). Tissue distribution of the human GLUT3 glucose transporter. *Endocrinology*, *132*(6), 2538–2543. https://doi.org/10.1210/ENDO.132.6.8504756

Haghparast, A., Shamsizadeh, A., Samandari, R., Omranifard, A., Vaziri, A., & Razavi, Y. (2014). Cannabinoid receptors in the basolateral amygdala are involved in the potentiation

of morphine rewarding properties in the acquisition, but not expression of conditioned place preference in rats. *Brain Research*, *1565*, 28–36. https://doi.org/10.1016/J.BRAINRES.2014.04.003

Halestrap, A. P., & Price, N. T. (1999). The proton-linked monocarboxylate transporter (MCT) family: structure, function and regulation. *Biochemical Journal*, *343*(Pt 2), 281. https://doi.org/10.1042/0264-6021:3430281

Han, J., Kesner, P., Metna-Laurent, M., Duan, T., Xu, L., Georges, F., Koehl, M., Abrous, D. N., Mendizabal-Zubiaga, J., Grandes, P., Liu, Q., Bai, G., Wang, W., Xiong, L., Ren, W., Marsicano, G., & Zhang, X. (2012). Acute cannabinoids impair working memory through astroglial CB1 receptor modulation of hippocampal LTD. *Cell*, *148*(5), 1039–1050. https://doi.org/10.1016/J.CELL.2012.01.037

Hanus, L., Abu-Lafi, S., Fride, E., Breuer, A., Vogel, Z., Shalev, D. E., Kustanovich, I., & Mechoulam, R. (2001). 2-arachidonyl glyceryl ether, an endogenous agonist of the cannabinoid CB1 receptor. *Proceedings of the National Academy of Sciences of the United States of America*, *98*(7), 3662–3665. https://doi.org/10.1073/PNAS.061029898

Harada, K., Kamiya, T., & Tsuboi, T. (2016). Gliotransmitter Release from Astrocytes: Functional, Developmental, and Pathological Implications in the Brain. *Frontiers in Neuroscience*, *9*(JAN), 499. https://doi.org/10.3389/FNINS.2015.00499

Harris, J. J., Jolivet, R., & Attwell, D. (2012). Synaptic energy use and supply. *Neuron*, *75*(5), 762–777. https://doi.org/10.1016/J.NEURON.2012.08.019

Haspula, D., & Clark, M. A. (2020). Cannabinoid Receptors: An Update on Cell Signaling, Pathophysiological Roles and Therapeutic Opportunities in Neurological, Cardiovascular, and Inflammatory Diseases. *International Journal of Molecular Sciences*, *21*(20), 7693. https://doi.org/10.3390/IJMS21207693

Haydon, P. G., & Carmignoto, G. (2006). Astrocyte control of synaptic transmission and neurovascular coupling. *Physiological Reviews*, *86*(3), 1009–1031. https://doi.org/10.1152/PHYSREV.00049.2005

Hebert-Chatelain, E., Desprez, T., Serrat, R., Bellocchio, L., Soria-Gomez, E., Busquets-Garcia, A., Pagano Zottola, A. C., Delamarre, A., Cannich, A., Vincent, P., Varilh, M., Robin, L. M., Terral, G., García-Fernández, M. D., Colavita, M., Mazier, W., Drago, F., Puente, N., Reguero, L., … Marsicano, G. (2016). A cannabinoid link between

mitochondria and memory. *Nature 2016 539:7630*, *539*(7630), 555–559. https://doi.org/10.1038/nature20127

Hebert-Chatelain, E., Reguero, L., Puente, N., Lutz, B., Chaouloff, F., Rossignol, R., Piazza, P. V., Benard, G., Grandes, P., & Marsicano, G. (2014). Cannabinoid control of brain bioenergetics: Exploring the subcellular localization of the CB1 receptor. *Molecular Metabolism*, *3*(4), 495–504. https://doi.org/10.1016/J.MOLMET.2014.03.007

Heifets, B. D., & Castillo, P. E. (2009). Endocannabinoid signaling and long-term synaptic plasticity. In *Annual Review of Physiology* (Vol. 71, pp. 283–306). Annu Rev Physiol. https://doi.org/10.1146/annurev.physiol.010908.163149

Hempel, B., & Xi, Z. X. (2021a). Receptor mechanisms underlying the CNS effects of cannabinoids: CB1 receptor and beyond. *Advances in Pharmacology (San Diego, Calif.)*, *93*, 275. https://doi.org/10.1016/BS.APHA.2021.10.006

Hempel, B., & Xi, Z. X. (2021b). Receptor mechanisms underlying the CNS effects of cannabinoids: CB1 receptor and beyond. *Advances in Pharmacology (San Diego, Calif.)*, *93*, 275. https://doi.org/10.1016/BS.APHA.2021.10.006

Herculano-Houzel, S. (2014). The glia/neuron ratio: how it varies uniformly across brain structures and species and what that means for brain physiology and evolution. *Glia*, *62*(9), 1377–1391. https://doi.org/10.1002/GLIA.22683

Herkenham, M., Lynn, A. B., Little, M. D., Johnson, M. R., Melvin, L. S., De Costa, B. R., & Rice, K. C. (1990). Cannabinoid receptor localization in brain. *Proceedings of the National Academy of Sciences of the United States of America*. https://doi.org/10.1073/pnas.87.5.1932

Herrero-Mendez, A., Almeida, A., Fernández, E., Maestre, C., Moncada, S., & Bolaños, J. P. (2009). The bioenergetic and antioxidant status of neurons is controlled by continuous degradation of a key glycolytic enzyme by APC/C–Cdh1. *Nature Cell Biology 2009 11:6*, *11*(6), 747–752. https://doi.org/10.1038/NCB1881

Hoch, E., Volkow, N. D., Friemel, C. M., Lorenzetti, V., Freeman, T. P., & Hall, W. (2025). Cannabis, cannabinoids and health: a review of evidence on risks and medical benefits. *European Archives of Psychiatry and Clinical Neuroscience*, *275*(2), 281–292. https://doi.org/10.1007/S00406-024-01880-2

Holt, M. G. (2023). Astrocyte heterogeneity and interactions with local neural circuits. *Essays in Biochemistry*, *67*(1), 93–106. https://doi.org/10.1042/EBC20220136

Houten, S. M., Violante, S., Ventura, F. V., & Wanders, R. J. A. (2016). The Biochemistry and Physiology of Mitochondrial Fatty Acid β-Oxidation and Its Genetic Disorders. *Annual Review of Physiology*, *78*, 23–44. https://doi.org/10.1146/ANNUREV-PHYSIOL-021115-105045

Howlett, A. C. (2002). The cannabinoid receptors. *Prostaglandins & Other Lipid Mediators*, *68–69*, 619–631. https://doi.org/10.1016/S0090-6980(02)00060-6

Howlett, A. C., & Abood, M. E. (2017). CB1 and CB2 Receptor Pharmacology. *Advances in Pharmacology (San Diego, Calif.)*, *80*, 169–206. https://doi.org/10.1016/BS.APHA.2017.03.007

Huestis, M. A. (2007). Human Cannabinoid Pharmacokinetics. *Chemistry & Biodiversity*, *4*(8), 1770. https://doi.org/10.1002/CBDV.200790152

Iannotti, F. A., Di Marzo, V., & Petrosino, S. (2016). Endocannabinoids and endocannabinoid-related mediators: Targets, metabolism and role in neurological disorders. *Progress in Lipid Research*, *62*, 107–128. https://doi.org/10.1016/J.PLIPRES.2016.02.002

Jha, M. K., & Morrison, B. M. (2020). Lactate Transporters Mediate Glia-Neuron Metabolic Crosstalk in Homeostasis and Disease. *Frontiers in Cellular Neuroscience*, *14*, 589582. https://doi.org/10.3389/FNCEL.2020.589582

Jiang, B., Huang, S., de Pasquale, R., Millman, D., Song, L., Lee, H. K., Tsumoto Tadaharu, T., & Kirkwood Alfredo, A. (2010). The maturation of GABAergic transmission in visual cortex requires endocannabinoid-mediated LTD of inhibitory inputs during a critical period. *Neuron*, *66*(2), 248–259. https://doi.org/10.1016/j.neuron.2010.03.021

Jimenez-Blasco, D., Agulla, J., Lapresa, R., Garcia-Macia, M., Bobo-Jimenez, V., Garcia-Rodriguez, D., Manjarres-Raza, I., Fernandez, E., Jeanson, Y., Khoury, S., Portais, J. C., Padro, D., Ramos-Cabrer, P., Carmeliet, P., Almeida, A., & Bolaños, J. P. (2024). Weak neuronal glycolysis sustains cognition and organismal fitness. *Nature Metabolism 2024 6:7*, *6*(7), 1253–1267. https://doi.org/10.1038/s42255-024-01049-0

Jimenez-Blasco, D., Busquets-Garcia, A., Hebert-Chatelain, E., Serrat, R., Vicente-Gutierrez, C., Ioannidou, C., Gómez-Sotres, P., Lopez-Fabuel, I., Resch-Beusher, M., Resel, E.,

Arnouil, D., Saraswat, D., Varilh, M., Cannich, A., Julio-Kalajzic, F., Bonilla-Del Río, I., Almeida, A., Puente, N., Achicallende, S., … Marsicano, G. (2020). Glucose metabolism links astroglial mitochondria to cannabinoid effects. *Nature*, *583*(7817), 603–608. https://doi.org/10.1038/S41586-020-2470-Y

Jolivet, R., Magistretti, P. J., & Weber, B. (2009). Deciphering neuron-glia compartmentalization in cortical energy metabolism. *Frontiers in Neuroenergetics*, *1*(1), 498. https://doi.org/10.3389/NEURO.14.004.2009

Joshi, N., & Onaivi, E. S. (2021). Psychiatric Disorders and Cannabinoid Receptors. *Advances in Experimental Medicine and Biology*, *1264*, 131–153. https://doi.org/10.1007/978-3-030-57369-0_9

Jourdain, P., Allaman, I., Rothenfusser, K., Fiumelli, H., Marquet, P., & Magistretti, P. J. (2016). L-Lactate protects neurons against excitotoxicity: implication of an ATP-mediated signaling cascade. *Scientific Reports*, *6*, 21250. https://doi.org/10.1038/SREP21250

Jurga, M., Jurga, A., Jurga, K., Kaźmierczak, B., Kuśmierczyk, K., & Chabowski, M. (2024). Cannabis-Based Phytocannabinoids: Overview, Mechanism of Action, Therapeutic Application, Production, and Affecting Environmental Factors. *International Journal of Molecular Sciences*, *25*(20), 11258. https://doi.org/10.3390/IJMS252011258

Kano, M., Ohno-Shosaku, T., Hashimotodani, Y., Uchigashima, M., & Watanabe, M. (2009). Endocannabinoid-mediated control of synaptic transmission. In *Physiological Reviews* (Vol. 89, Issue 1, pp. 309–380). American Physiological Society. https://doi.org/10.1152/physrev.00019.2008

Katona, I., & Freund, T. F. (2008). Endocannabinoid signaling as a synaptic circuit breaker in neurological disease. In *Nature Medicine* (Vol. 14, Issue 9, pp. 923–930). Nature Publishing Group. https://doi.org/10.1038/nm.f.1869

Katona, I., & Freund, T. F. (2012). Multiple Functions of Endocannabinoid Signaling in the Brain. *Annual Review of Neuroscience*, *35*, 529. https://doi.org/10.1146/ANNUREV-NEURO-062111-150420

Katona, I., Rancz, E. A., Acsády, L., Ledent, C., Mackie, K., Hájos, N., & Freund, T. F. (2001). Distribution of CB1 Cannabinoid Receptors in the Amygdala and their Role in the Control of GABAergic Transmission. *The Journal of Neuroscience*, *21*(23), 9506. https://doi.org/10.1523/JNEUROSCI.21-23-09506.2001

Katona, I., Sperlágh, B., Maglóczky, Z., Sántha, E., Köfalvi, A., Czirják, S., Mackie, K., Vizi, E. S., & Freund, T. F. (2000). GABAergic interneurons are the targets of cannabinoid actions in the human hippocampus. *Neuroscience*, *100*(4), 797–804. https://doi.org/10.1016/S0306-4522(00)00286-4

Katona, I., Sperlágh, B., Sík, A., Käfalvi, A., Vizi, E. S., Mackie, K., & Freund, T. F. (1999). Presynaptically located CB1 cannabinoid receptors regulate GABA release from axon terminals of specific hippocampal interneurons. *Journal of Neuroscience*, *19*(11), 4544–4558. https://doi.org/10.1523/jneurosci.19-11-04544.1999

Kayanos, T., Fukumotoo, H., Eddyl, R. L., Fan7, Y.-S., Byersl, M. G., Showsl, T. B., & Bell, G. I. (1988). Evidence for a family of human glucose transporter-like proteins. Sequence and gene localization of a protein expressed in fetal skeletal muscle and other tissues. *THE JOURNAL OF BIOLOGICAL CHEMISTRY*, *263*(30), 15245–15248. https://doi.org/10.1016/S0021-9258(19)37577-5

Khakh, B. S., & Deneen, B. (2019). The Emerging Nature of Astrocyte Diversity. *Annual Review of Neuroscience*, *42*, 187–207. https://doi.org/10.1146/ANNUREV-NEURO-070918-050443

Kierans, S. J., & Taylor, C. T. (2024). Glycolysis: A multifaceted metabolic pathway and signaling hub. *The Journal of Biological Chemistry*, *300*(11). https://doi.org/10.1016/J.JBC.2024.107906

Knott, A. B., Perkins, G., Schwarzenbacher, R., & Bossy-Wetzel, E. (2008). Mitochondrial fragmentation in neurodegeneration. *Nature Reviews. Neuroscience*, *9*(7), 505–518. https://doi.org/10.1038/NRN2417

Koehler, R. C., Roman, R. J., & Harder, D. R. (2009). Astrocytes and the regulation of cerebral blood flow. In *Trends in Neurosciences*. https://doi.org/10.1016/j.tins.2008.11.005

Koepsell, H. (2020). Glucose transporters in brain in health and disease. *Pflugers Archiv*, *472*(9), 1299. https://doi.org/10.1007/S00424-020-02441-X

Kofuji, P., & Araque, A. (2021). Astrocytes and Behavior. *Annual Review of Neuroscience*, *44*, 49. https://doi.org/10.1146/ANNUREV-NEURO-101920-112225

Kölker, S., Steiner, R., & Kölker StefanKoelker, S. (2018). Metabolism of amino acid neurotransmitters: the synaptic disorder underlying inherited metabolic diseases. *Journal*

of Inherited Metabolic Disease, *41*(6), 1055–1063. https://doi.org/10.1007/S10545-018-0201-4

Kreitzer, A. C., & Regehr, W. G. (2001). Retrograde inhibition of presynaptic calcium influx by endogenous cannabinoids at excitatory synapses onto Purkinje cells. *Neuron*, *29*(3), 717–727. https://doi.org/10.1016/S0896-6273(01)00246-X

Kumar Jha, M., Jeon, S., & Suk, K. (2012). Pyruvate Dehydrogenase Kinases in the Nervous System: Their Principal Functions in Neuronal-glial Metabolic Interaction and Neuro-metabolic Disorders. *Current Neuropharmacology*, *10*(4), 393–403. https://doi.org/10.2174/157015912804143586

Lai, Y. Y., Kodama, T., Hsieh, K. C., Nguyen, D., & Siegel, J. M. (2020). Substantia nigra pars reticulata-mediated sleep and motor activity regulation. *Sleep*, *44*(1), zsaa151. https://doi.org/10.1093/SLEEP/ZSAA151

Lamanna, J. C., Salem, N., Puchowicz, M., Erokwu, B., Koppaka, S., Flask, C., & Lee, Z. (2009). Ketones suppress brain glucose consumption. *Advances in Experimental Medicine and Biology*, *645*, 301–306. https://doi.org/10.1007/978-0-387-85998-9_45

Lauritzen, K. H., Morland, C., Puchades, M., Holm-Hansen, S., Hagelin, E. M., Lauritzen, F., Attramadal, H., Storm-Mathisen, J., Gjedde, A., & Bergersen, L. H. (2014). Lactate receptor sites link neurotransmission, neurovascular coupling, and brain energy metabolism. *Cerebral Cortex (New York, N.Y. : 1991)*, *24*(10), 2784–2795. https://doi.org/10.1093/CERCOR/BHT136

Lecrux, C., Bourourou, M., & Hamel, E. (2019). How reliable is cerebral blood flow to map changes in neuronal activity? *Autonomic Neuroscience : Basic & Clinical*, *217*, 71–79. https://doi.org/10.1016/J.AUTNEU.2019.01.005

Lei, L., Wang, Y. F., Chen, C. Y., Wang, Y. T., & Zhang, Y. (2024). Novel insight into astrocyte-mediated gliotransmission modulates the synaptic plasticity in major depressive disorder. *Life Sciences*, *355*, 122988. https://doi.org/10.1016/J.LFS.2024.122988

Leibowitz, A., Boyko, M., Shapira, Y., & Zlotnik, A. (2012). Blood Glutamate Scavenging: Insight into Neuroprotection. *International Journal of Molecular Sciences 2012, Vol. 13, Pages 10041-10066*, *13*(8), 10041–10066. https://doi.org/10.3390/IJMS130810041

Lemtiri-Chlieh, F., & Levine, E. S. (2022). 2-AG and anandamide enhance hippocampal long-term potentiation via suppression of inhibition. *Frontiers in Cellular Neuroscience*, *16*, 1023541. https://doi.org/10.3389/FNCEL.2022.1023541/BIBTEX

Lenaz, G., Tioli, G., Falasca, A. I., & Genova, M. L. (2016). Complex I function in mitochondrial supercomplexes. *Biochimica et Biophysica Acta*, *1857*(7), 991–1000. https://doi.org/10.1016/J.BBABIO.2016.01.013

Leo, L. M., & Abood, M. E. (2021). CB1 Cannabinoid Receptor Signaling and Biased Signaling. *Molecules*, *26*(17), 5413. https://doi.org/10.3390/MOLECULES26175413

Lerchundi, R., Fernández-Moncada, I., Contreras-Baeza, Y., Sotelo-Hitschfeld, T., Mächler, P., Wyss, M. T., Stobart, J., Baeza-Lehnert, F., Alegría, K., Weber, B., & Barros, L. F. (2015). NH4(+) triggers the release of astrocytic lactate via mitochondrial pyruvate shunting. *Proceedings of the National Academy of Sciences of the United States of America*, *112*(35), 11090–11095. https://doi.org/10.1073/PNAS.1508259112

Lia, A., Di Spiezio, A., Speggiorin, M., & Zonta, M. (2023). Two decades of astrocytes in neurovascular coupling. *Frontiers in Network Physiology*, *3*, 1162757. https://doi.org/10.3389/FNETP.2023.1162757

Liang, H., Bourdon, A. K., Chen, L. Y., Phelix, C. F., & Perry, G. (2018). Gibbs Free-Energy Gradient along the Path of Glucose Transport through Human Glucose Transporter 3. *ACS Chemical Neuroscience*, *9*(11), 2815–2823. https://doi.org/10.1021/ACSCHEMNEURO.8B00223/SUPPL_FILE/CN8B00223_SI_004.AVI

Lin, M. T., & Beal, M. F. (2006). Mitochondrial dysfunction and oxidative stress in neurodegenerative diseases. *Nature*, *443*(7113), 787–795. https://doi.org/10.1038/NATURE05292

Lin, Y. F. (2021). Potassium channels as molecular targets of endocannabinoids. *Channels*, *15*(1), 408. https://doi.org/10.1080/19336950.2021.1910461

Liu, C. Y., Yang, Y., Ju, W. N., Wang, X., & Zhang, H. L. (2018). Emerging Roles of Astrocytes in Neuro-Vascular Unit and the Tripartite Synapse With Emphasis on Reactive Gliosis in the Context of Alzheimer's Disease. *Frontiers in Cellular Neuroscience*, *12*. https://doi.org/10.3389/FNCEL.2018.00193

Liu, H., Wang, S., Wang, J., Guo, X., Song, Y., Fu, K., Gao, Z., Liu, D., He, W., & Yang, L. L. (2025). Energy metabolism in health and diseases. *Signal Transduction and Targeted Therapy 2025 10:1*, *10*(1), 1–71. https://doi.org/10.1038/s41392-025-02141-x

Lopez-Fabuel, I., Le Douce, J., Logan, A., James, A. M., Bonvento, G., Murphy, M. P., Almeida, A., & Bolaños, J. P. (2016). Complex I assembly into supercomplexes determines differential mitochondrial ROS production in neurons and astrocytes. *Proceedings of the National Academy of Sciences of the United States of America*, *113*(46), 13063–13068. https://doi.org/10.1073/PNAS.1613701113

Lowe, H., Toyang, N., Steele, B., Bryant, J., & Ngwa, W. (2021). The Endocannabinoid System: A Potential Target for the Treatment of Various Diseases. *International Journal of Molecular Sciences*, *22*(17). https://doi.org/10.3390/IJMS22179472

Lu, H. C., & Mackie, K. (2021). Review of the Endocannabinoid System. *Biological Psychiatry: Cognitive Neuroscience and Neuroimaging*, *6*(6), 607–615. https://doi.org/10.1016/J.BPSC.2020.07.016

Luchicchi, A., Lecca, S., Carta, S., Pillolla, G., Muntoni, A. L., Yasar, S., Goldberg, S. R., & Pistis, M. (2010). Effects of fatty acid amide hydrolase inhibition on neuronal responses to nicotine, cocaine and morphine in the nucleus accumbens shell and ventral tegmental area: Involvement of PPAR-α nuclear receptors. *Addiction Biology*, *15*(3), 277–288. https://doi.org/10.1111/j.1369-1600.2010.00222.x

Lutz, B. (2020). Neurobiology of cannabinoid receptor signaling. *Dialogues in Clinical Neuroscience*, *22*(3), 207. https://doi.org/10.31887/DCNS.2020.22.3/BLUTZ

MacAulay, N. (2020). Molecular mechanisms of K+ clearance and extracellular space shrinkage—Glia cells as the stars. *Glia*, *68*(11), 2192–2211. https://doi.org/10.1002/GLIA.23824

Maccarrone, M., Bab, I., Bíró, T., Cabral, G. A., Dey, S. K., Di Marzo, V., Konje, J. C., Kunos, G., Mechoulam, R., Pacher, P., Sharkey, K. A., & Zimmer, A. (2015). Endocannabinoid signaling at the periphery: 50 years after THC. *Trends in Pharmacological Sciences*, *36*(5), 277. https://doi.org/10.1016/J.TIPS.2015.02.008

Maccarrone, M., Rossi, S., Bari, M., De Chiara, V., Fezza, F., Musella, A., Gasperi, V., Prosperetti, C., Bernardi, G., Finazzi-Agrò, A., Cravatt, B. F., & Centonze, D. (2008).

Anandamide inhibits metabolism and physiological actions of 2-arachidonoylglycerol in the striatum. *Nature Neuroscience*, *11*(2), 152–159. https://doi.org/10.1038/nn2042

Mächler, P., Wyss, M. T., Elsayed, M., Stobart, J., Gutierrez, R., Von Faber-Castell, A., Kaelin, V., Zuend, M., San Martín, A., Romero-Gómez, I., Baeza-Lehnert, F., Lengacher, S., Schneider, B. L., Aebischer, P., Magistretti, P. J., Barros, L. F., & Weber, B. (2016). In Vivo Evidence for a Lactate Gradient from Astrocytes to Neurons. *Cell Metabolism*, *23*(1), 94–102. https://doi.org/10.1016/J.CMET.2015.10.010

Macvicar, B. A., & Newman, E. A. (2015). Astrocyte Regulation of Blood Flow in the Brain. *Cold Spring Harbor Perspectives in Biology*, *7*(5), a020388. https://doi.org/10.1101/CSHPERSPECT.A020388

Madrer, N., Perera, N. D., Uccelli, N. A., Abbondanza, A., Andersen, J. V., Carsana, E. V., Demmings, M. D., Fernandez, R. F., de Fragas, M. G., Gbadamosi, I., Kulshrestha, D., Lima-Filho, R. A. S., Marian, O. C., Markussen, K. H., McGovern, A. J., Neal, E. S., Sarkar, S., Šimončičová, E., Soto-Verdugo, J., … Fernández-Moncada, I. (2025). Neural Metabolic Networks: Key Elements of Healthy Brain Function. *Journal of Neurochemistry*, *169*(6), e70084. https://doi.org/10.1111/JNC.70084

Magistretti, P. J., & Allaman, I. (2013). Brain Energy Metabolism. *Neuroscience in the 21st Century: From Basic to Clinical*, 1591–1620. https://doi.org/10.1007/978-1-4614-1997-6_56

Magistretti, P. J., & Allaman, I. (2018). Lactate in the brain: from metabolic end-product to signalling molecule. *Nature Reviews Neuroscience 2018 19:4*, *19*(4), 235–249. https://doi.org/10.1038/NRN.2018.19

Magistretti, P. J., & Pellerin, L. (1999). Astrocytes couple synaptic activity to glucose utilization in the brain. *News in Physiological Sciences*. https://doi.org/10.1152/physiologyonline.1999.14.5.177

Mailleux, P., & Vanderhaeghen, J. J. (1994). Glutamatergic regulation of cannabinoid receptor gene expression in the caudate-putamen. *European Journal of Pharmacology: Molecular Pharmacology*, *266*(2), 193–196. https://doi.org/10.1016/0922-4106(94)90110-4

Mallick, K., Paul, S., Banerjee, S., & Banerjee, S. (2024). Lipid Droplets and Neurodegeneration. *Neuroscience*, *549*, 13–23. https://doi.org/10.1016/J.NEUROSCIENCE.2024.04.014

Margineanu, M. B., Mahmood, H., Fiumelli, H., & Magistretti, P. J. (2018). L-Lactate Regulates the Expression of Synaptic Plasticity and Neuroprotection Genes in Cortical Neurons: A Transcriptome Analysis. *Frontiers in Molecular Neuroscience*, *11*, 411617. https://doi.org/10.3389/FNMOL.2018.00375/XML

Margulies, J. E., & Hammer, R. P. (1991). Δ9-Tetrahydrocannabinol alters cerebral metabolism in a biphasic, dose-dependent mannier in rat brain. *European Journal of Pharmacology*, *202*(3), 373–378. https://doi.org/10.1016/0014-2999(91)90281-T

Mariani, Y., Covelo, A., Rodrigues, R. S., Julio-Kalajzić, F., Pagano Zottola, A. C., Lavanco, G., Fabrizio, M., Gisquet, D., Drago, F., Cannich, A., Baufreton, J., Marsicano, G., & Bellocchio, L. (2023). Striatopallidal cannabinoid type-1 receptors mediate amphetamine-induced sensitization. *Current Biology : CB*, *33*(22), 5011-5022.e6. https://doi.org/10.1016/J.CUB.2023.09.075

Mariani, Y., Dalla-Tor, T., Garavaldi, T., Julio-Kalajzić, F., Gisquet, D., Gomez-Sotres, P., Cannich, A., Gambino, G., Drago, F., Serrat, R., Hurel, I., Chaouloff, F., Pouvreau, S., Bellocchio, L., Marsicano, G., & Covelo, A. (2025). Astroglial CB1 Reveal Sex-Specific Synaptic Effects of Amphetamine. *Glia*, *73*(8), 1673. https://doi.org/10.1002/GLIA.70026

Marina, N., Christie, I. N., Korsak, A., Doronin, M., Brazhe, A., Hosford, P. S., Wells, J. A., Sheikhbahaei, S., Humoud, I., Paton, J. F. R., Lythgoe, M. F., Semyanov, A., Kasparov, S., & Gourine, A. V. (2020). Astrocytes monitor cerebral perfusion and control systemic circulation to maintain brain blood flow. *Nature Communications 2020 11:1*, *11*(1), 1–9. https://doi.org/10.1038/s41467-019-13956-y

Maroon, J., & Bost, J. (2018). Review of the neurological benefits of phytocannabinoids. *Surgical Neurology International*, *9*(1), 91. https://doi.org/10.4103/SNI.SNI_45_18

Marsicano, G., Goodenough, S., Monory, K., Hermann, H., Eder, M., Cannich, A., Azad, S. C., Cascio, M. G., Ortega-Gutiérrez, S., Van der Stelt, M., López-Rodríguez, M. L., Casanova, E., Schütz, G., Zieglgänsberger, W., Di Marzo, V., Behl, C., & Lutz, B. (2003). CB1 cannabinoid receptors and on-demand defense against excitotoxicity. *Science*, *302*(5642), 84–88. https://doi.org/10.1126/science.1088208

Marsicano, G., & Kuner, R. (2008). Anatomical distribution of receptors, ligands and enzymes in the brain and in the spinal cord: Circuitries and neurochemistry. In *Cannabinoids and*

the Brain (Vol. 9780387743493, pp. 161–201). Springer US. https://doi.org/10.1007/978-0-387-74349-3_10

Marsicano, G., & Lafenêtre, P. (2009). Roles of the endocannabinoid system in learning and memory. *Current Topics in Behavioral Neurosciences*, *1*, 201–230. https://doi.org/10.1007/978-3-540-88955-7_8

Marsicano, G., & Lutz, B. (1999). Expression of the cannabinoid receptor CB1 in distinct neuronal subpopulations in the adult mouse forebrain. *European Journal of Neuroscience*, *11*(12), 4213–4225. https://doi.org/10.1046/j.1460-9568.1999.00847.x

Martinez Ramirez, C. E., Ruiz-Pérez, G., Stollenwerk, T. M., Behlke, C., Doherty, A., & Hillard, C. J. (2023). Endocannabinoid signaling in the central nervous system. *Glia*, *71*(1), 5–35. https://doi.org/10.1002/GLIA.24280

Massa, M. L., Gagliardino, J. J., & Francini, F. (2011). Liver glucokinase: An overview on the regulatorymechanisms of its activity. *IUBMB Life*, *63*(1), 1–6. https://doi.org/10.1002/IUB.411

Mathur, B. N., & Lovinger, D. M. (2012). Endocannabinoid–Dopamine Interactions in Striatal Synaptic Plasticity. *Frontiers in Pharmacology*, *3*, 66. https://doi.org/10.3389/FPHAR.2012.00066

Matsuda, L. A., Lolait, S. J., Brownstein, M. J., Young, A. C., & Bonner, T. I. (1990). Structure of a cannabinoid receptor and functional expression of the cloned cDNA. *Nature*, *346*(6284), 561–564. https://doi.org/10.1038/346561A0

McNay, E. C., & Pearson-Leary, J. (2019). GluT4: a central player in hippocampal memory and brain insulin resistance. *Experimental Neurology*, *323*, 113076. https://doi.org/10.1016/J.EXPNEUROL.2019.113076

Meccariello, R., Santoro, A., D'Angelo, S., Morrone, R., Fasano, S., Viggiano, A., & Pierantoni, R. (2020). The Epigenetics of the Endocannabinoid System. *International Journal of Molecular Sciences*, *21*(3), 1113. https://doi.org/10.3390/IJMS21031113

Mechoulam, R., Ben-Shabat, S., Hanus, L., Ligumsky, M., Kaminski, N. E., Schatz, A. R., Gopher, A., Almog, S., Martin, B. R., Compton, D. R., Pertwee, R. G., Griffin, G., Bayewitch, M., Barg, J., & Vogel, Z. (1995). Identification of an endogenous 2-

monoglyceride, present in canine gut, that binds to cannabinoid receptors. *Biochemical Pharmacology*, *50*(1), 83–90. https://doi.org/10.1016/0006-2952(95)00109-D

Mechoulam, R., & Gaoni, Y. (1965). A Total Synthesis of dl-Δ1-Tetrahydrocannabinol, the Active Constituent of Hashish. *Journal of the American Chemical Society*, *87*(14), 3273–3275. https://doi.org/10.1021/JA01092A065/ASSET/JA01092A065.FP.PNG_V03

Mei, J., Li, Y., Niu, L., Liang, R., Tang, M., Cai, Q., Xu, J., Zhang, D., Yin, X., Liu, X., Shen, Y., Liu, J., Xu, M., Xia, P., Ling, J., Wu, Y., Liang, J., Zhang, J., & Yu, P. (2024). SGLT2 inhibitors: a novel therapy for cognitive impairment via multifaceted effects on the nervous system. *Translational Neurodegeneration 2024 13:1*, *13*(1), 1–16. https://doi.org/10.1186/S40035-024-00431-Y

Mergenthaler, P., Lindauer, U., Dienel, G. A., & Meisel, A. (2013). Sugar for the brain: the role of glucose in physiological and pathological brain function. *Trends in Neurosciences*, *36*(10), 587. https://doi.org/10.1016/J.TINS.2013.07.001

Metna-Laurent, M., & Marsicano, G. (2015). Rising stars: Modulation of brain functions by astroglial type-1 cannabinoid receptors. *GLIA*. https://doi.org/10.1002/glia.22773

Metna-Laurent, M., Mondésir, M., Grel, A., Vallée, M., & Piazza, P. V. (2017). Cannabinoid-Induced Tetrad in Mice. *Current Protocols in Neuroscience*, *80*, 9.59.1-9.59.10. https://doi.org/10.1002/CPNS.31

Miederer, I., Uebbing, K., Röhrich, J., Maus, S., Bausbacher, N., Krauter, K., Weyer-Elberich, V., Lutz, B., Schreckenberger, M., & Urban, R. (2017). Effects of tetrahydrocannabinol on glucose uptake in the rat brain. *Neuropharmacology*, *117*, 273–281. https://doi.org/10.1016/J.NEUROPHARM.2017.02.011

Miguel-Quesada, C., Zaforas, M., Herrera-Pérez, S., Lines, J., Fernández-López, E., Alonso-Calviño, E., Ardaya, M., Soria, F. N., Araque, A., Aguilar, J., & Rosa, J. M. (2023). Astrocytes adjust the dynamic range of cortical network activity to control modality-specific sensory information processing. *Cell Reports*, *42*(8). https://doi.org/10.1016/J.CELREP.2023.112950

Miller, R. H., & Raff, M. C. (1984). Fibrous and protoplasmic astrocytes are biochemically and developmentally distinct. *The Journal of Neuroscience : The Official Journal of the Society for Neuroscience*, *4*(2), 585–592. https://doi.org/10.1523/JNEUROSCI.04-02-00585.1984

Min, R., & Nevian, T. (2012). Astrocyte signaling controls spike timing-dependent depression at neocortical synapses. *Nature Neuroscience*, *15*(5), 746–753. https://doi.org/10.1038/nn.3075

Miraucourt, L. S., Tsui, J., Gobert, D., Desjardins, J.-F., Schohl, A., Sild, M., Spratt, P., Castonguay, A., De Koninck, Y., Marsh-Armstrong, N., Wiseman, P. W., & Ruthazer, E. S. (2016). Endocannabinoid signaling enhances visual responses through modulation of intracellular chloride levels in retinal ganglion cells. *ELife*, *5*. https://doi.org/10.7554/ELIFE.15932

Moldrich, G., & Wenger, T. (2000). Localization of the CB1 cannabinoid receptor in the rat brain. An immunohistochemical study. *Peptides*, *21*(11), 1735–1742. https://doi.org/10.1016/S0196-9781(00)00324-7

Moore, R. A., Fisher, E., Finn, D. P., Finnerup, N. B., Gilron, I., Haroutounian, S., Krane, E., Rice, A. S. C., Rowbotham, M., Wallace, M., & Eccleston, C. (2021). Cannabinoids, cannabis, and cannabis-based medicines for pain management: an overview of systematic reviews. *Pain*, *162*(Suppl 1), S67–S79. https://doi.org/10.1097/J.PAIN.0000000000001941

Morales, P., & Jagerovic, N. (2020). Novel approaches and current challenges with targeting the endocannabinoid system. *Expert Opinion on Drug Discovery*, *15*(8), 917–930. https://doi.org/10.1080/17460441.2020.1752178

Morales, P., & Reggio, P. H. (2021). Emerging Roles of Cannabinoids and Synthetic Cannabinoids in Clinical Experimental Models. In *Advances in Experimental Medicine and Biology* (Vol. 1264, pp. 47–65). Springer. https://doi.org/10.1007/978-3-030-57369-0_4

Morant-Ferrando, B., Jimenez-Blasco, D., Alonso-Batan, P., Agulla, J., Lapresa, R., Garcia-Rodriguez, D., Yunta-Sanchez, S., Lopez-Fabuel, I., Fernandez, E., Carmeliet, P., Almeida, A., Garcia-Macia, M., & Bolaños, J. P. (2023). Fatty acid oxidation organizes mitochondrial supercomplexes to sustain astrocytic ROS and cognition. *Nature Metabolism 2023 5:8*, *5*(8), 1290–1302. https://doi.org/10.1038/s42255-023-00835-6

Morris, M. E., & Felmlee, M. A. (2008). Overview of the proton-coupled MCT (SLC16A) family of transporters: characterization, function and role in the transport of the drug of

abuse gamma-hydroxybutyric acid. *The AAPS Journal.*., *10*(2), 311–321. https://doi.org/10.1208/S12248-008-9035-6

Munro, S., Thomas, K. L., & Abu-Shaar, M. (1993). Molecular characterization of a peripheral receptor for cannabinoids. *Nature*, *365*(6441), 61–65. https://doi.org/10.1038/365061A0

Murat, C. D. B., & García-Cáceres, C. (2021). Astrocyte Gliotransmission in the Regulation of Systemic Metabolism. *Metabolites*, *11*(11), 732. https://doi.org/10.3390/METABO11110732

Murataeva, N., Straiker, A., & MacKie, K. (2014). Parsing the players: 2-arachidonoylglycerol synthesis and degradation in the CNS. In *British Journal of Pharmacology* (Vol. 171, Issue 6, pp. 1379–1391). Nature Publishing Group. https://doi.org/10.1111/bph.12411

Nadeau, O. W., Fontes, J. D., & Carlson, G. M. (2018). The regulation of glycogenolysis in the brain. *The Journal of Biological Chemistry*, *293*(19), 7099–7107. https://doi.org/10.1074/JBC.R117.803023

Nagamatsu, S., Kornhauser, J. M., Burant, C. F., Seino, S., Mayo, K. E., & Bell, G. I. (1992). Glucose transporter expression in brain. cDNA sequence of mouse GLUT3, the brain facilitative glucose transporter isoform, and identification of sites of expression by in situ hybridization. *Journal of Biological Chemistry*, *267*(1), 467–472. https://doi.org/10.1016/S0021-9258(18)48518-3

Nasu, Y., Aggarwal, A., Le, G. N. T., Vo, C. T., Kambe, Y., Wang, X., Beinlich, F. R. M., Lee, A. B., Ram, T. R., Wang, F., Gorzo, K. A., Kamijo, Y., Boisvert, M., Nishinami, S., Kawamura, G., Ozawa, T., Toda, H., Gordon, G. R., Ge, S., … Campbell, R. E. (2023). Lactate biosensors for spectrally and spatially multiplexed fluorescence imaging. *Nature Communications 2023 14:1*, *14*(1), 1–17. https://doi.org/10.1038/s41467-023-42230-5

Navarrete, M., & Araque, A. (2008). Endocannabinoids Mediate Neuron-Astrocyte Communication. *Neuron*, *57*(6), 883–893. https://doi.org/10.1016/j.neuron.2008.01.029

Navarrete, M., & Araque, A. (2010). Endocannabinoids potentiate synaptic transmission through stimulation of astrocytes. *Neuron*, *68*(1), 113–126. https://doi.org/10.1016/j.neuron.2010.08.043

Navarrete, M., Díez, A., & Araque, A. (2014). Astrocytes in endocannabinoid signalling. In *Philosophical Transactions of the Royal Society B: Biological Sciences* (Vol. 369, Issue 1654, p. 20130599). Royal Society of London. https://doi.org/10.1098/rstb.2013.0599

Navarrete, M., Perea, G., de Sevilla, D. F., Gómez-Gonzalo, M., Núñez, A., Martín, E. D., & Araque, A. (2012). Astrocytes mediate in vivo cholinergic-induced synaptic plasticity. *PLoS Biology*, *10*(2). https://doi.org/10.1371/JOURNAL.PBIO.1001259

Neal, E. S., Xu, W., & Borges, K. (2024). Metabolic aspects of genetic ion channel epilepsies. *Journal of Neurochemistry*, *168*(12), 3911–3935. https://doi.org/10.1111/JNC.15938

Nehlig, A. (2004). Brain uptake and metabolism of ketone bodies in animal models. *Prostaglandins Leukotrienes and Essential Fatty Acids*, *70*(3), 265–275. https://doi.org/10.1016/j.plefa.2003.07.006

Newman, L. A., Korol, D. L., & Gold, P. E. (2011). Lactate produced by glycogenolysis in astrocytes regulates memory processing. *PloS One*, *6*(12). https://doi.org/10.1371/JOURNAL.PONE.0028427

Newton, A. C. (2018). Protein kinase C: perfectly balanced. *Critical Reviews in Biochemistry and Molecular Biology*, *53*(2), 208–230. https://doi.org/10.1080/10409238.2018.1442408

Nguyen, V. H., Verdurand, M., Dedeurwaerdere, S., Wang, H., Zahra, D., Gregoire, M. C., & Zavitsanou, K. (2012). Increased brain metabolism after acute administration of the synthetic cannabinoid HU210: a small animal PET imaging study with 18F-FDG. *Brain Research Bulletin*, *87*(2–3), 172–179. https://doi.org/10.1016/J.BRAINRESBULL.2011.11.011

Nikas, S. P., Ji, L., Liu, Y., Georgiadis, M. O., Dopeshwarkar, A., Straiker, A., Kudalkar, S., Sadybekov, A. V., Dvorakova, M., Katritch, V., Mackie, K., Marnett, L., & Makriyannis, A. (2024). Chiral Me-2-arachidonoyl Glycerols: The First Potent Endocannabinoid Glyceride Templates with Stability to COX-2. *ACS Medicinal Chemistry Letters*, *15*(6), 965–971. https://doi.org/10.1021/ACSMEDCHEMLETT.4C00175/SUPPL_FILE/ML4C00175_SI_001.PDF

Nolfi-Donegan, D., Braganza, A., & Shiva, S. (2020). Mitochondrial electron transport chain: Oxidative phosphorylation, oxidant production, and methods of measurement. *Redox Biology*, *37*, 101674. https://doi.org/10.1016/J.REDOX.2020.101674

Oberheim, N. A., Goldman, S. A., & Nedergaard, M. (2012). Heterogeneity of Astrocytic Form and Function. *Methods in Molecular Biology (Clifton, N.J.)*, *814*, 23. https://doi.org/10.1007/978-1-61779-452-0_3

O'dea, M. R., Hasel, | Philip, Hasel, P., & O', M. R. (2025). Are we there yet? Exploring astrocyte heterogeneity one cell at a time. *Glia*, *73*(3), 619–631. https://doi.org/10.1002/GLIA.24621

Ohno-Shosaku, T., Maejima, T., & Kano, M. (2001). Endogenous cannabinoids mediate retrograde signals from depolarized postsynaptic neurons to presynaptic terminals. *Neuron*, *29*(3), 729–738. https://doi.org/10.1016/S0896-6273(01)00247-1

Oliveira da Cruz, J. F., Robin, L. M., Drago, F., Marsicano, G., & Metna-Laurent, M. (2016). Astroglial type-1 cannabinoid receptor (CB1): A new player in the tripartite synapse. In *Neuroscience* (Vol. 323, pp. 35–42). Elsevier Ltd. https://doi.org/10.1016/j.neuroscience.2015.05.002

Ozaita, A., Puighermanal, E., & Maldonado, R. (2007). Regulation of PI3K/Akt/GSK-3 pathway by cannabinoids in the brain. *Journal of Neurochemistry*, *102*(4), 1105–1114. https://doi.org/10.1111/J.1471-4159.2007.04642.X

Pacher, P., Bátkai, S., & Kunos, G. (2006). The endocannabinoid system as an emerging target of pharmacotherapy. In *Pharmacological Reviews* (Vol. 58, Issue 3, pp. 389–462). Pharmacol Rev. https://doi.org/10.1124/pr.58.3.2

Pajarillo, E., Rizor, A., Lee, J., Aschner, M., & Lee, E. (2019). The role of astrocytic glutamate transporters GLT-1 and GLAST in neurological disorders: Potential targets for neurotherapeutics. *Neuropharmacology*, *161*. https://doi.org/10.1016/J.NEUROPHARM.2019.03.002

Panatier, A., Vallée, J., Haber, M., Murai, K. K., Lacaille, J. C., & Robitaille, R. (2011). Astrocytes are endogenous regulators of basal transmission at central synapses. *Cell*, *146*(5), 785–798. https://doi.org/10.1016/J.CELL.2011.07.022

Partanen, J., & Achim, K. (2022a). Neurons gating behavior—developmental, molecular and functional features of neurons in the Substantia Nigra pars reticulata. *Frontiers in Neuroscience*, *16*, 976209. https://doi.org/10.3389/FNINS.2022.976209/BIBTEX

Partanen, J., & Achim, K. (2022b). Neurons gating behavior—developmental, molecular and functional features of neurons in the Substantia Nigra pars reticulata. *Frontiers in Neuroscience*, *16*, 976209. https://doi.org/10.3389/FNINS.2022.976209/BIBTEX

Patra, K. C., & Hay, N. (2014). The pentose phosphate pathway and cancer. *Trends in Biochemical Sciences*, *39*(8), 347. https://doi.org/10.1016/J.TIBS.2014.06.005

Pearson-Leary, J., & McNay, E. C. (2016). Novel Roles for the Insulin-Regulated Glucose Transporter-4 in Hippocampally Dependent Memory. *Journal of Neuroscience*, *36*(47), 11851–11864. https://doi.org/10.1523/JNEUROSCI.1700-16.2016

Pellerin, L., Bouzier-Sore, A. K., Aubert, A., Serres, S., Merle, M., Costalat, R., & Magistretti, P. J. (2007). Activity-dependent regulation of energy metabolism by astrocytes: An update. In *GLIA*. https://doi.org/10.1002/glia.20528

Pelligrino, D. A., Vetri, F., & Xu, H. L. (2011). Purinergic mechanisms in gliovascular coupling. *Seminars in Cell & Developmental Biology*, *22*(2), 229. https://doi.org/10.1016/J.SEMCDB.2011.02.010

Perea, G., Gómez, R., Mederos, S., Covelo, A., Ballesteros, J. J., Schlosser, L., Hernández-Vivanco, A., Martín-Fernández, M., Quintana, R., Rayan, A., Díez, A., Fuenzalida, M., Agarwal, A., Bergles, D. E., Bettler, B., Manahan-Vaughan, D., Martín, E. D., Kirchhoff, F., & Araque, A. (2016). Activity-dependent switch of GABAergic inhibition into glutamatergic excitation in astrocyte-neuron networks. *ELife*, *5*(DECEMBER2016), e20362. https://doi.org/10.7554/ELIFE.20362

Perea, G., Navarrete, M., & Araque, A. (2009). Tripartite synapses: astrocytes process and control synaptic information. *Trends in Neurosciences*, *32*(8), 421–431. https://doi.org/10.1016/J.TINS.2009.05.001

Pertwee, R. (2010). Receptors and Channels Targeted by Synthetic Cannabinoid Receptor Agonists and Antagonists. *Current Medicinal Chemistry*. https://doi.org/10.2174/092986710790980050

Pertwee, R. G. (2008). The diverse CB 1 and CB 2 receptor pharmacology of three plant cannabinoids: Δ 9-tetrahydrocannabinol, cannabidiol and Δ 9-tetrahydrocannabivarin. In *British Journal of Pharmacology* (Vol. 153, Issue 2, pp. 199–215). Wiley-Blackwell. https://doi.org/10.1038/sj.bjp.0707442

Pfrieger, F. W. (2003). Role of cholesterol in synapse formation and function. *Biochimica et Biophysica Acta - Biomembranes*, *1610*(2), 271–280. https://doi.org/10.1016/S0005-2736(03)00024-5

Pierre, K., & Pellerin, L. (2005). Monocarboxylate transporters in the central nervous system: distribution, regulation and function. *Journal of Neurochemistry*, *94*(1), 1–14. https://doi.org/10.1111/J.1471-4159.2005.03168.X

Piette, C., Cui, Y., Gervasi, N., & Venance, L. (2020). Lights on Endocannabinoid-Mediated Synaptic Potentiation. *Frontiers in Molecular Neuroscience*, *13*, 559023. https://doi.org/10.3389/FNMOL.2020.00132/XML

Piomelli, D. (2003). The molecular logic of endocannabinoid signalling. *Nature Reviews Neuroscience*, *4*(11), 873–884. https://doi.org/10.1038/nrn1247

Porter, A. C., Sauer, J. M., Knierman, M. D., Becker, G. W., Berna, M. J., Bao, J., Nomikos, G. G., Carter, P., Bymaster, F. P., Leese, A. B., & Felder, C. C. (2002). Characterization of a novel endocannabinoid, virodhamine, with antagonist activity at the CB1 receptor. *The Journal of Pharmacology and Experimental Therapeutics*, *301*(3), 1020–1024. https://doi.org/10.1124/JPET.301.3.1020

Pragallapati, S., & Manyam, R. (2019). Glucose transporter 1 in health and disease. *Journal of Oral and Maxillofacial Pathology : JOMFP*, *23*(3), 443. https://doi.org/10.4103/JOMFP.JOMFP_22_18

Przybyla, J. A., & Watts, V. J. (2010). Ligand-induced regulation and localization of cannabinoid CB1 and dopamine D2L receptor heterodimers. *Journal of Pharmacology and Experimental Therapeutics*, *332*(3), 710–719. https://doi.org/10.1124/jpet.109.162701

Pulido, C., & Ryan, T. A. (2021). Synaptic vesicle pools are a major hidden resting metabolic burden of nerve terminals. *Science Advances*, *7*(49). https://doi.org/10.1126/SCIADV.ABI9027

Rae, C. D., Baur, J. A., Borges, K., Dienel, G., Díaz-García, C. M., Douglass, S. R., Drew, K., Duarte, J. M. N., Duran, J., Kann, O., Kristian, T., Lee-Liu, D., Lindquist, B. E., McNay, E. C., Robinson, M. B., Rothman, D. L., Rowlands, B. D., Ryan, T. A., Scafidi, J., … McKenna, M. C. (2024). Brain energy metabolism: A roadmap for future research. *Journal of Neurochemistry*, *168*(5), 910–954. https://doi.org/10.1111/JNC.16032

Ranganathan, M., & D'Souza, D. C. (2006). The acute effects of cannabinoids on memory in humans: A review. In *Psychopharmacology* (Vol. 188, Issue 4, pp. 425–444). Psychopharmacology (Berl). https://doi.org/10.1007/s00213-006-0508-y

Rangaraju, V., Calloway, N., & Ryan, T. A. (2014). Activity-driven local ATP synthesis is required for synaptic function. *Cell*, *156*(4), 825–835. https://doi.org/10.1016/j.cell.2013.12.042

Rezende, B., Alencar, A. K. N., de Bem, G. F., Fontes-Dantas, F. L., & Montes, G. C. (2023). Endocannabinoid System: Chemical Characteristics and Biological Activity. *Pharmaceuticals*, *16*(2), 148. https://doi.org/10.3390/PH16020148

Robbe, D., Kopf, M., Remaury, A., Bockaert, J., & Manzoni, O. J. (2002). Endogenous cannabinoids mediate long-term synaptic depression in the nucleus accumbens. *Proceedings of the National Academy of Sciences of the United States of America*, *99*(12), 8384–8388. https://doi.org/10.1073/pnas.122149199

Robin, L. M., Oliveira da Cruz, J. F., Langlais, V. C., Martin-Fernandez, M., Metna-Laurent, M., Busquets-Garcia, A., Bellocchio, L., Soria-Gomez, E., Papouin, T., Varilh, M., Sherwood, M. W., Belluomo, I., Balcells, G., Matias, I., Bosier, B., Drago, F., Van Eeckhaut, A., Smolders, I., Georges, F., … Marsicano, G. (2018). Astroglial CB1 Receptors Determine Synaptic D-Serine Availability to Enable Recognition Memory. *Neuron*, *98*(5), 935-944.e5. https://doi.org/10.1016/j.neuron.2018.04.034

Rocha, G. S., Freire, M. A. M., Britto, A. M., Paiva, K. M., Oliveira, R. F., Fonseca, I. A. T., Araújo, D. P., Oliveira, L. C., Guzen, F. P., Morais, P. L. A. G., & Cavalcanti, J. R. L. P. (2023). Basal ganglia for beginners: the basic concepts you need to know and their role in movement control. *Frontiers in Systems Neuroscience*, *17*, 1242929. https://doi.org/10.3389/FNSYS.2023.1242929/BIBTEX

Rock, E. M., & Parker, L. A. (2021). Constituents of Cannabis Sativa. In *Advances in Experimental Medicine and Biology* (Vol. 1264, pp. 1–13). Springer. https://doi.org/10.1007/978-3-030-57369-0_1

Rose, C. R., Felix, L., Zeug, A., Dietrich, D., Reiner, A., & Henneberger, C. (2018). Astroglial Glutamate Signaling and Uptake in the Hippocampus. *Frontiers in Molecular Neuroscience, 10*. https://doi.org/10.3389/FNMOL.2017.00451

Rose, J., Brian, C., Pappa, A., Panayiotidis, M. I., & Franco, R. (2020). Mitochondrial Metabolism in Astrocytes Regulates Brain Bioenergetics, Neurotransmission and Redox Balance. *Frontiers in Neuroscience*, *14*. https://doi.org/10.3389/FNINS.2020.536682

Rozenfeld, R., & Devi, L. A. (2008). Regulation of CB1 cannabinoid receptor trafficking by the adaptor protein AP-3. *FASEB Journal : Official Publication of the Federation of American Societies for Experimental Biology*, *22*(7), 2311–2322. https://doi.org/10.1096/FJ.07-102731

Rupareliya, V. P., Singh, A. A., Butt, A. M., A, H., & Kumar, H. (2023). The "molecular soldiers" of the CNS: Astrocytes, a comprehensive review on their roles and molecular signatures. *European Journal of Pharmacology*, *959*, 176048. https://doi.org/10.1016/J.EJPHAR.2023.176048

Saito, E. R., Warren, C. E., Hanegan, C. M., Larsen, J. G., du Randt, J. D., Cannon, M., Saito, J. Y., Campbell, R. J., Kemberling, C. M., Miller, G. S., Edwards, J. G., & Bikman, B. T. (2022). A Novel Ketone-Supplemented Diet Improves Recognition Memory and Hippocampal Mitochondrial Efficiency in Healthy Adult Mice. *Metabolites*, *12*(11). https://doi.org/10.3390/METABO12111019

San Martín, A., Ceballo, S., Ruminot, I., Lerchundi, R., Frommer, W. B., & Barros, L. F. (2013). A Genetically Encoded FRET Lactate Sensor and Its Use To Detect the Warburg Effect in Single Cancer Cells. *PLOS ONE*, *8*(2), e57712. https://doi.org/10.1371/JOURNAL.PONE.0057712

Sánchez, M. G., Ruiz-Llorente, L., Sánchez, A. M., & Díaz-Laviada, I. (2003). Activation of phosphoinositide 3-kinase/PKB pathway by CB1 and CB2 cannabinoid receptors expressed in prostate PC-3 cells. Involvement in Raf-1 stimulation and NGF induction. *Cellular Signalling*, *15*(9), 851–859. https://doi.org/10.1016/S0898-6568(03)00036-6

Savtchouk, I., & Volterra, A. (2018). Gliotransmission: Beyond Black-and-White. *The Journal of Neuroscience*, *38*(1), 14. https://doi.org/10.1523/JNEUROSCI.0017-17.2017

Scheyer, A., Yasmin, F., Naskar, S., & Patel, S. (2022). Endocannabinoids at the synapse and beyond: implications for neuropsychiatric disease pathophysiology and treatment. *Neuropsychopharmacology*, *48*(1), 37. https://doi.org/10.1038/S41386-022-01438-7

Schlosburg, J. E., Blankman, J. L., Long, J. Z., Nomura, D. K., Pan, B., Kinsey, S. G., Nguyen, P. T., Ramesh, D., Booker, L., Burston, J. J., Thomas, E. A., Selley, D. E., Sim-Selley, L.

J., Liu, Q. S., Lichtman, A. H., & Cravatt, B. F. (2010). Chronic monoacylglycerol lipase blockade causes functional antagonism of the endocannabinoid system. *Nature Neuroscience*, *13*(9), 1113–1119. https://doi.org/10.1038/NN.2616

Schousboe, A. (2020). Astrocytic Metabolism Focusing on Glutamate Homeostasis: A Short Review Dedicated to Vittorio Gallo. *Neurochemical Research*, *45*(3), 522–525. https://doi.org/10.1007/S11064-019-02888-0/METRICS

Schousboe, A., Scafidi, S., Bak, L. K., Waagepetersen, H. S., & McKenna, M. C. (2014). Glutamate Metabolism in the Brain Focusing on Astrocytes. *Advances in Neurobiology*, *11*, 13. https://doi.org/10.1007/978-3-319-08894-5_2

Semenza, G. L., Jiang, B. H., Leung, S. W., Passantino, R., Concordat, J. P., Maire, P., & Giallongo, A. (1996). Hypoxia response elements in the aldolase A, enolase 1, and lactate dehydrogenase a gene promoters contain essential binding sites for hypoxia-inducible factor 1. *Journal of Biological Chemistry*, *271*(51), 32529–32537. https://doi.org/10.1074/jbc.271.51.32529

Serrat, R., Covelo, A., Kouskoff, V., Delcasso, S., Ruiz-Calvo, A., Chenouard, N., Stella, C., Blancard, C., Salin, B., Julio-Kalajzić, F., Cannich, A., Massa, F., Varilh, M., Deforges, S., Robin, L. M., De Stefani, D., Busquets-Garcia, A., Gambino, F., Beyeler, A., … Marsicano, G. (2021). Astroglial ER-mitochondria calcium transfer mediates endocannabinoid-dependent synaptic integration. *Cell Reports*, *37*(12). https://doi.org/10.1016/J.CELREP.2021.110133

Shonesy, B. C., Winder, D. G., Patel, S., & Colbran, R. J. (2015). The initiation of synaptic 2-AG mobilization requires both an increased supply of diacylglycerol precursor and increased postsynaptic calcium. *Neuropharmacology*, *91*, 57–62. https://doi.org/10.1016/j.neuropharm.2014.11.026

Simankowicz, P., & Stępniewska, J. (2025). The Role of Endocannabinoids in Physiological Processes and Disease Pathology: A Comprehensive Review. *Journal of Clinical Medicine*, *14*(8), 2851. https://doi.org/10.3390/JCM14082851/S1

Simon, G. M., & Cravatt, B. F. (2010). Characterization of mice lacking candidate N-acyl ethanolamine biosynthetic enzymes provides evidence for multiple pathways that contribute to endocannabinoid production in vivo. *Molecular BioSystems*, *6*(8), 1411–1418. https://doi.org/10.1039/c000237b

Simpson, E. H., Akam, T., Patriarchi, T., Blanco-Pozo, M., Burgeno, L. M., Mohebi, A., Cragg, S. J., & Walton, M. E. (2024). Lights, fiber, action! A primer on in vivo fiber photometry. *Neuron*, *112*(5), 718–739. https://doi.org/10.1016/J.NEURON.2023.11.016

Simpson, I. A., Carruthers, A., & Vannucci, S. J. (2007). Supply and demand in cerebral energy metabolism: the role of nutrient transporters. *Journal of Cerebral Blood Flow and Metabolism : Official Journal of the International Society of Cerebral Blood Flow and Metabolism*, *27*(11), 1766–1791. https://doi.org/10.1038/SJ.JCBFM.9600521

Soria-Gómez, E., Bellocchio, L., Reguero, L., Lepousez, G., Martin, C., Bendahmane, M., Ruehle, S., Remmers, F., Desprez, T., Matias, I., Wiesner, T., Cannich, A., Nissant, A., Wadleigh, A., Pape, H. C., Chiarlone, A. P., Quarta, C., Verrier, D., Vincent, P., … Marsicano, G. (2014). The endocannabinoid system controls food intake via olfactory processes. *Nature Neuroscience*, *17*(3), 407–415. https://doi.org/10.1038/NN.3647

Soria-Gómez, E., Busquets-Garcia, A., Hu, F., Mehidi, A., Cannich, A., Roux, L., Louit, I., Alonso, L., Wiesner, T., Georges, F., Verrier, D., Vincent, P., Ferreira, G., Luo, M., & Marsicano, G. (2015). Habenular CB1 Receptors Control the Expression of Aversive Memories. *Neuron*, *88*(2), 306–313. https://doi.org/10.1016/J.NEURON.2015.08.035

Soria-Gomez, E., Pagano Zottola, A. C., Mariani, Y., Desprez, T., Barresi, M., Bonilla-del Río, I., Muguruza, C., Le Bon-Jego, M., Julio-Kalajzić, F., Flynn, R., Terral, G., Fernández-Moncada, I., Robin, L. M., Oliveira da Cruz, J. F., Corinti, S., Amer, Y. O., Goncalves, J., Varilh, M., Cannich, A., … Bellocchio, L. (2021). Subcellular specificity of cannabinoid effects in striatonigral circuits. *Neuron*, *109*(9), 1513-1526.e11. https://doi.org/10.1016/j.neuron.2021.03.007

Sotelo-Hitschfeld, T., Niemeyer, M. I., Mächler, P., Ruminot, I., Lerchundi, R., Wyss, M. T., Stobart, J., Fernández-Moncada, I., Valdebenito, R., Garrido-Gerter, P., Contreras-Baeza, Y., Schneider, B. L., Aebischer, P., Lengacher, S., Martín, A. S., Le Douce, J., Bonvento, G., Magistretti, P. J., Sepúlveda, F. V., … Felipe Barros, L. (2015). Channel-mediated lactate release by K^+-stimulated astrocytes. *The Journal of Neuroscience : The Official Journal of the Society for Neuroscience*, *35*(10), 4168–4178. https://doi.org/10.1523/JNEUROSCI.5036-14.2015

Stella, N. (2023). THC and CBD: Similarities and differences between siblings. *Neuron*, *111*(3), 302–327. https://doi.org/10.1016/J.NEURON.2022.12.022

Suárez, L. E., Markello, R. D., Betzel, R. F., & Misic, B. (2020). Linking Structure and Function in Macroscale Brain Networks. *Trends in Cognitive Sciences*, *24*(4), 302–315. https://doi.org/10.1016/J.TICS.2020.01.008

Sunahara, R. K., Dessauer, C. W., & Gilman, A. G. (1996). Complexity and diversity of mammalian adenylyl cyclases. In *Annual Review of Pharmacology and Toxicology* (Vol. 36, pp. 461–480). Annual Reviews Inc. https://doi.org/10.1146/annurev.pa.36.040196.002333

Suzuki, A., Stern, S. A., Bozdagi, O., Huntley, G. W., Walker, R. H., Magistretti, P. J., & Alberini, C. M. (2011). Astrocyte-neuron lactate transport is required for long-term memory formation. *Cell*, *144*(5), 810. https://doi.org/10.1016/J.CELL.2011.02.018

Szrok-Jurga, S., Turyn, J., Hebanowska, A., Swierczynski, J., Czumaj, A., Sledzinski, T., & Stelmanska, E. (2023). The Role of Acyl-CoA β-Oxidation in Brain Metabolism and Neurodegenerative Diseases. *International Journal of Molecular Sciences*, *24*(18), 13977. https://doi.org/10.3390/IJMS241813977

Tadi, M., Allaman, I., Lengacher, S., Grenningloh, G., & Magistretti, P. J. (2015). Learning-Induced Gene Expression in the Hippocampus Reveals a Role of Neuron -Astrocyte Metabolic Coupling in Long Term Memory. *PloS One*, *10*(10). https://doi.org/10.1371/JOURNAL.PONE.0141568

Takata, N., Mishima, T., Hisatsune, C., Nagai, T., Ebisui, E., Mikoshiba, K., & Hirase, H. (2011). Astrocyte calcium signaling transforms cholinergic modulation to cortical plasticity in vivo. *The Journal of Neuroscience : The Official Journal of the Society for Neuroscience*, *31*(49), 18155–18165. https://doi.org/10.1523/JNEUROSCI.5289-11.2011

Tanimura, A., Yamazaki, M., Hashimotodani, Y., Uchigashima, M., Kawata, S., Abe, M., Kita, Y., Hashimoto, K., Shimizu, T., Watanabe, M., Sakimura, K., & Kano, M. (2010). The Endocannabinoid 2-Arachidonoylglycerol Produced by Diacylglycerol Lipase α Mediates Retrograde Suppression of Synaptic Transmission. *Neuron*, *65*(3), 320–327. https://doi.org/10.1016/j.neuron.2010.01.021

Tanner, L. B., Goglia, A. G., Wei, M. H., Sehgal, T., Parsons, L. R., Park, J. O., White, E., Toettcher, J. E., & Rabinowitz, J. D. (2018). Four key steps control glycolytic flux in mammalian cells. *Cell Systems*, *7*(1), 49. https://doi.org/10.1016/J.CELS.2018.06.003

TeSlaa, T., Ralser, M., Fan, J., & Rabinowitz, J. D. (2023). The pentose phosphate pathway in health and disease. *Nature Metabolism*, *5*(8), 1275. https://doi.org/10.1038/S42255-023-00863-2

Theparambil, S. M., Kopach, O., Braga, A., Nizari, S., Hosford, P. S., Sagi-Kiss, V., Hadjihambi, A., Konstantinou, C., Esteras, N., Gutierrez Del Arroyo, A., Ackland, G. L., Teschemacher, A. G., Dale, N., Eckle, T., Andrikopoulos, P., Rusakov, D. A., Kasparov, S., & Gourine, A. V. (2024). Adenosine signalling to astrocytes coordinates brain metabolism and function. *Nature 2024 632:8023*, *632*(8023), 139–146. https://doi.org/10.1038/s41586-024-07611-w

Thibault, K., Carrel, D., Bonnard, D., Gallatz, K., Simon, A., Biard, M., Pezet, S., Palkovits, M., & Lenkei, Z. (2013). Activation-dependent subcellular distribution patterns of CB1 cannabinoid receptors in the rat forebrain. *Cerebral Cortex (New York, N.Y. : 1991)*, *23*(11), 2581–2591. https://doi.org/10.1093/CERCOR/BHS240

Thomas, A., Baillie, G. L., Phillips, A. M., Razdan, R. K., Ross, R. A., & Pertwee, R. G. (2007). Cannabidiol displays unexpectedly high potency as an antagonist of CB1 and CB2 receptor agonists in vitro. *British Journal of Pharmacology*, *150*(5), 613–623. https://doi.org/10.1038/SJ.BJP.0707133

Tsuboi, K., Ikematsu, N., Uyama, T., G. Deutsch, D., Tokumura, A., & Ueda, N. (2013). Biosynthetic Pathways of Bioactive N-Acylethanolamines in Brain. *CNS & Neurological Disorders - Drug Targets*, *12*(1), 7–16. https://doi.org/10.2174/1871527311312010005

Tsuboi, K., Sun, Y. X., Okamoto, Y., Araki, N., Tonai, T., & Ueda, N. (2005). Molecular characterization of N-acylethanolamine-hydrolyzing acid amidase, a novel member of the choloylglycine hydrolase family with structural and functional similarity to acid ceramidase. *Journal of Biological Chemistry*, *280*(12), 11082–11092. https://doi.org/10.1074/jbc.M413473200

Tu, D., Gao, Y., Yang, R., Guan, T., Hong, J. S., & Gao, H. M. (2019). The pentose phosphate pathway regulates chronic neuroinflammation and dopaminergic neurodegeneration. *Journal of Neuroinflammation*, *16*(1), 255. https://doi.org/10.1186/S12974-019-1659-1

Turcotte, C., Chouinard, F., Lefebvre, J. S., & Flamand, N. (2015). Regulation of inflammation by cannabinoids, the endocannabinoids 2-arachidonoyl-glycerol and arachidonoyl-

ethanolamide, and their metabolites. *Journal of Leukocyte Biology*, *97*(6), 1049–1070. https://doi.org/10.1189/jlb.3ru0115-021r

Turu, G., & Hunyady, L. (2010). Signal transduction of the CB1 cannabinoid receptor. In *Journal of Molecular Endocrinology* (Vol. 44, Issue 2, pp. 75–85). J Mol Endocrinol. https://doi.org/10.1677/JME-08-0190

Twitchell, W., Brown, S., & Mackie, K. (1997). Cannabinoids inhibit n- and p/q-type calcium channels in cultured rat hippocampal neurons. *Journal of Neurophysiology*, *78*(1), 43–50. https://doi.org/10.1152/JN.1997.78.1.43/ASSET/IMAGES/LARGE/JNP.JY12F4.JPEG

Ueno, M., Chiba, Y., Murakami, R., Miyai, Y., Matsumoto, K., Wakamatsu, K., Takebayashi, G., Uemura, N., & Yanase, K. (2023). Distribution of Monocarboxylate Transporters in Brain and Choroid Plexus Epithelium. *Pharmaceutics*, *15*(8). https://doi.org/10.3390/PHARMACEUTICS15082062

Upadhyay, G., Fihurka, O., Habecker, C., Patel, P., & Sanchez-Ramos, J. (2023). Measurement of Δ9THC and metabolites in the brain and peripheral tissues after intranasal instillation of a nanoformulation. *Journal of Cannabis Research*, *5*(1), 3. https://doi.org/10.1186/S42238-022-00171-8

Urquhart, P., Nicolaou, A., & Woodward, D. F. (2015). Endocannabinoids and their oxygenation by cyclo-oxygenases, lipoxygenases and other oxygenases. In *Biochimica et Biophysica Acta - Molecular and Cell Biology of Lipids* (Vol. 1851, Issue 4, pp. 366–376). Elsevier B.V. https://doi.org/10.1016/j.bbalip.2014.12.015

Vaccari-Cardoso, B., Antipina, M., Teschemacher, A. G., & Kasparov, S. (2022). Lactate-Mediated Signaling in the Brain-An Update. *Brain Sciences*, *13*(1). https://doi.org/10.3390/BRAINSCI13010049

Valles, S. L., Singh, S. K., Campos-Campos, J., Colmena, C., Campo-Palacio, I., Alvarez-Gamez, K., Caballero, O., & Jorda, A. (2023). Functions of Astrocytes under Normal Conditions and after a Brain Disease. *International Journal of Molecular Sciences*, *24*(9), 8434. https://doi.org/10.3390/IJMS24098434

Van Hall, G., Strømstad, M., Rasmussen, P., Jans, Ø., Zaar, M., Gam, C., Quistorff, B., Secher, N. H., & Nielsen, H. B. (2009). Blood lactate is an important energy source for the human brain. *Journal of Cerebral Blood Flow and Metabolism : Official Journal of the*

International Society of Cerebral Blood Flow and Metabolism, *29*(6), 1121–1129. https://doi.org/10.1038/JCBFM.2009.35

Verkhratsky, A., & Nedergaard, M. (2018). Physiology of astroglia. *Physiological Reviews*, *98*(1), 239–389. https://doi.org/10.1152/physrev.00042.2016

Verkhratsky, A., Parpura, V., Li, B., & Scuderi, C. (2021). Astrocytes: The Housekeepers and Guardians of the CNS. *Advances in Neurobiology*, *26*, 21. https://doi.org/10.1007/978-3-030-77375-5_2

Vicente-Gutierrez, C., Bonora, N., Bobo-Jimenez, V., Jimenez-Blasco, D., Lopez-Fabuel, I., Fernandez, E., Josephine, C., Bonvento, G., Enriquez, J. A., Almeida, A., & Bolaños, J. P. (2019). Astrocytic mitochondrial ROS modulate brain metabolism and mouse behaviour. *Nature Metabolism*, *1*(2), 201–211. https://doi.org/10.1038/S42255-018-0031-6

Vijay, N., & Morris, M. E. (2014). Role of Monocarboxylate Transporters in Drug Delivery to the Brain. *Current Pharmaceutical Design*, *20*(10), 1487. https://doi.org/10.2174/13816128113199990462

Volkow, N. D., Swanson, J. M., Evins, A. E., DeLisi, L. E., Meier, M. H., Gonzalez, R., Bloomfield, M. A. P., Curran, H. V., & Baler, R. (2016). Effects of Cannabis Use on Human Behavior, Including Cognition, Motivation, and Psychosis: A Review. *JAMA Psychiatry*, *73*(3), 292–297. https://doi.org/10.1001/JAMAPSYCHIATRY.2015.3278

Wang, H., Liu, S., Sun, Y., Chen, C., Hu, Z., Li, Q., Long, J., Yan, Q., Liang, J., Lin, Y., Yang, S., Lin, M., Liu, X., Wang, H., Yu, J., Yi, F., Tan, Y., Yang, Y., Chen, N., & Ai, Q. (2024). Target modulation of glycolytic pathways as a new strategy for the treatment of neuroinflammatory diseases. *Ageing Research Reviews*, *101*, 102472. https://doi.org/10.1016/J.ARR.2024.102472

Wang, T., & Zhang, Y. (2024). Mechanisms and therapeutic targets of carbon monoxide poisoning: A focus on reactive oxygen species. *Chemico-Biological Interactions*, *403*, 111223. https://doi.org/10.1016/J.CBI.2024.111223

Weber, B., & Barros, L. F. (2015). The Astrocyte: Powerhouse and Recycling Center. *Cold Spring Harbor Perspectives in Biology*, *7*(12). https://doi.org/10.1101/CSHPERSPECT.A020396

Westlake, T. M., Howlett, A. C., Bonner, T. I., Matsuda, L. A., & Herkenham, M. (1994). Cannabinoid receptor binding and messenger RNA expression in human brain: An in vitro receptor autoradiography and in situ hybridization histochemistry study of normal aged and Alzheimer's brains. *Neuroscience*, *63*(3), 637–652. https://doi.org/10.1016/0306-4522(94)90511-8

Whitlow, C. T., Freedland, C. S., & Porrino, L. J. (2002). Metabolic mapping of the time-dependent effects of delta 9-tetrahydrocannabinol administration in the rat. *Psychopharmacology*, *161*(2), 129–136. https://doi.org/10.1007/S00213-002-1001-X

Wilson, R. I., & Nicoll, R. A. (2001). Endogenous cannabinoids mediate retrograde signalling at hippocampal synapses. *Nature*, *410*(6828), 588–592. https://doi.org/10.1038/35069076

Won, W., Bhalla, M., Lee, J.-H., & Lee, C. J. (2025). Astrocytes as Key Regulators of Neural Signaling in Health and Disease. *Annual Review of Neuroscience*, *48*(Volume 48, 2025), 251–276. https://doi.org/10.1146/ANNUREV-NEURO-112723-035356

Woodward, D. F., Liang, Y., & Krauss, A. H. P. (2008). Prostamides (prostaglandin-ethanolamides) and their pharmacology. In *British Journal of Pharmacology* (Vol. 153, Issue 3, pp. 410–419). Br J Pharmacol. https://doi.org/10.1038/sj.bjp.0707434

Wright, E. M., & Loo, D. D. F. (2020). Active Glucose Transport 2020 and Beyond. *Function*, *2*(1), zqaa047. https://doi.org/10.1093/FUNCTION/ZQAA047

Wu, A., Lee, D., & Xiong, W. C. (2023). Lactate Metabolism, Signaling, and Function in Brain Development, Synaptic Plasticity, Angiogenesis, and Neurodegenerative Diseases. *International Journal of Molecular Sciences 2023, Vol. 24, Page 13398*, *24*(17), 13398. https://doi.org/10.3390/IJMS241713398

Xie, X., Li, Y., Xu, S., Zhou, P., Yang, L., Xu, Y., Qiu, Y., Yang, Y., & Li, Y. (2022). Genetic Blockade of NAAA Cell-specifically Regulates Fatty Acid Ethanolamides (FAEs) Metabolism and Inflammatory Responses. *Frontiers in Pharmacology*, *12*, 817603. https://doi.org/10.3389/FPHAR.2021.817603/FULL

Xu, T. R., Ward, R. J., Pediani, J. D., & Milligan, G. (2011). The orexin OX 1 receptor exists predominantly as a homodimer in the basal state: Potential regulation of receptor organization by both agonist and antagonist ligands. *Biochemical Journal*, *439*(1), 171–183. https://doi.org/10.1042/BJ20110230

Yang, D., Wang, X., Zhang, L., Fang, Y., Zheng, Q., Liu, X., Yu, W., Chen, S., Ying, J., & Hua, F. (2022). Lipid metabolism and storage in neuroglia: role in brain development and neurodegenerative diseases. *Cell & Bioscience 2022 12:1*, *12*(1), 1–16. https://doi.org/10.1186/S13578-022-00828-0

Yang, J., Chen, J., Liu, Y., Chen, K. H., Baraban, J. M., & Qiu, Z. (2023). Ventral tegmental area astrocytes modulate cocaine reward by tonically releasing GABA. *Neuron*, *111*(7), 1104-1117.e6. https://doi.org/10.1016/J.NEURON.2022.12.033

Yang, J., Ruchti, E., Petit, J. M., Jourdain, P., Grenningloh, G., Allaman, I., & Magistretti, P. J. (2014). Lactate promotes plasticity gene expression by potentiating NMDA signaling in neurons. *Proceedings of the National Academy of Sciences of the United States of America*, *111*(33), 12228–12233. https://doi.org/10.1073/PNAS.1322912111

Yeh, T. H., Lee, D. Y., Gianino, S. M., & Gutmann, D. H. (2009). Microarray analyses reveal regional astrocyte heterogeneity with implications for neurofibromatosis type 1 (NF1)-regulated glial proliferation. *Glia*, *57*(11), 1239–1249. https://doi.org/10.1002/GLIA.20845

Zapata, A., & Lupica, C. R. (2021). Lateral habenula cannabinoid CB1 receptor involvement in drug-associated impulsive behavior. *Neuropharmacology*, *192*, 108604. https://doi.org/10.1016/J.NEUROPHARM.2021.108604

Zhang, J., & Liu, Q. (2015). Cholesterol metabolism and homeostasis in the brain. *Protein & Cell*, *6*(4), 254. https://doi.org/10.1007/S13238-014-0131-3

Zhang, S., Lachance, B. B., Mattson, M. P., & Jia, X. (2021). Glucose metabolic crosstalk and regulation in brain function and diseases. *Progress in Neurobiology*, *204*, 102089. https://doi.org/10.1016/J.PNEUROBIO.2021.102089

Zhang, X., Alshakhshir, N., & Zhao, L. (2021). Glycolytic Metabolism, Brain Resilience, and Alzheimer's Disease. *Frontiers in Neuroscience*, *15*, 662242. https://doi.org/10.3389/FNINS.2021.662242

Zhang, Y. M., Qi, Y. B., Gao, Y. N., Chen, W. G., Zhou, T., Zang, Y., & Li, J. (2023). Astrocyte metabolism and signaling pathways in the CNS. *Frontiers in Neuroscience*, *17*, 1217451. https://doi.org/10.3389/FNINS.2023.1217451/BIBTEX

Zhang, Y., Xue, Y., Meng, S., Luo, Y., Liang, J., Li, J., Ai, S., Sun, C., Shen, H., Zhu, W., Wu, P., Lu, L., & Shi, J. (2016). Inhibition of Lactate Transport Erases Drug Memory and Prevents Drug Relapse. *Biological Psychiatry*, *79*(11), 928–939. https://doi.org/10.1016/J.BIOPSYCH.2015.07.007

Zhou, F. M., & Lee, C. R. (2011). Intrinsic and integrative properties of substantia nigra pars reticulata neurons. *Neuroscience*, *198*, 69. https://doi.org/10.1016/J.NEUROSCIENCE.2011.07.061

Zhou, J., Gu, J., Qian, Q., Zhang, Y., Huang, T., Li, X., Liu, Z., Shao, Q., Liang, Y., Qiao, L., Xu, X., Chen, Q., Xu, Z., Li, Y., Gao, J., Pan, Y., Wang, Y., O'Connor, R., Hippen, K. L., … Blazar, B. R. (2024). Lactate supports Treg function and immune balance via MGAT1 effects on N-glycosylation in the mitochondria. *The Journal of Clinical Investigation*, *134*(20), e175897. https://doi.org/10.1172/JCI175897

Zhou, Z., Ikegaya, Y., & Koyama, R. (2019). The Astrocytic cAMP Pathway in Health and Disease. *International Journal of Molecular Sciences*, *20*(3), 779. https://doi.org/10.3390/IJMS20030779

Zielke, H. R., Zielke, C. L., & Baab, P. J. (2009). Direct measurement of oxidative metabolism in the living brain by microdialysis: a review. *Journal of Neurochemistry*, *109*(SUPPL. 1), 24–29. https://doi.org/10.1111/J.1471-4159.2009.05941.X

Zimmer, T. S., Orr, A. L., & Orr, A. G. (2024). Astrocytes in selective vulnerability to neurodegenerative disease. *Trends in Neurosciences*, *47*(4), 289–302. https://doi.org/10.1016/J.TINS.2024.02.008

Zuend, M., Saab, A. S., Wyss, M. T., Ferrari, K. D., Hösli, L., Looser, Z. J., Stobart, J. L., Duran, J., Guinovart, J. J., Barros, L. F., & Weber, B. (2020). Arousal-induced cortical activity triggers lactate release from astrocytes. *Nature Metabolism*, *2*(2), 179–191. https://doi.org/10.1038/S42255-020-0170-4